ABSTRACT

Title of Dissertation: STRUCTURE-GUIDED ENGINEERING OF A MULTIMERIC BACTERIOPHAGE-ENCODED ENDOLYSIN PLYC

Xiaoran Shang, Doctor of Philosophy, 2019

Dissertation directed by: Associate Professor Daniel C. Nelson
Institute for Bioscience and Biotechnology Research and Department of Veterinary Medicine

Emerging antibiotic resistance has become a global health threat. One alternative to antibiotics is bacteriophage-encoded endolysins. Endolysins are peptidoglycan hydrolases produced at the end of the bacteriophage replication cycle resulting in bacterial cell lysis and progeny bacteriophage release. Endolysins are also capable of destroying the Gram-positive bacterial peptidoglycan when applied externally as recombinant proteins. These enzymes typically consist of an enzymatically active domain (EAD) and a separate cell wall binding domain (CBD). Studies have shown therapeutic efficacy of endolysins *in vitro* and *in vivo*, with no resistance developed to date. An endolysin from the streptococcal C1 phage, known as PlyC, has the highest activity of any endolysin reported. It also has a unique multimeric structure consisting of one activity subunit (PlyCA) harboring two synergistically acting catalytic domains, GyH and CHAP, and eight identical binding subunits (PlyCB) forming an

octameric ring. Groups A, C, and E streptococci as well as *Streptococcus uberis* are sensitive to the lytic activities of PlyC. In order to harness the potent activity of PlyC for use against other bacteria, we sought to change/extend the host range of PlyC by engineering PlyCB and PlyCA, respectively. We first used a structure-guided mutagenesis method to obtain the single PlyCB monomer subunit, $PlyCB_{K40A\ E43A}$ (PlyCBm), aiming to study the binding mechanism of PlyCB. Via fluorescence microscopy and binding assays, we determined that PlyCBm retained the host range of the octamer with a much lower binding affinity, which suggests the PlyCB octamer binds concurrently to a specific epitope on the bacterial surface resulting in a tight, stable interaction. Thus, it is not feasible to change/extend the PlyC host range via engineering PlyCB. Next, we proposed a novel design to engineer PlyCA. We successfully created two chimeric endolysins, ClyX-1 and ClyX-2, possessing the synergistic activity of the GyH and CHAP catalytic domains, but extended the host range to include, *Streptococcus pneumoniae*, Group B streptococci, *Streptococcus mutans*, and *Enterococcus faecalis*, all strains previously insensitive to PlyC. Finally, we tested a novel hypothesis that a positively charged catalytic domain could display lytic activity in a CBD-independent manner resulting in a broad host range. Using the PlyC CHAP domain as a model, we converted the net surface charge of the CHAP domain from negative three to positive one through positive seven. Notwithstanding the range of charges, our mutant CHAP domains did not show lytic activity in a CBD-independent manner, suggesting that other factors, like surface charge distribution, need to be considered in such a way of engineering.

STRUCTURE-GUIDED ENGINEERING OF A MULTIMERIC BACTERIOPHAGE-ENCODED ENDOLYSIN PLYC

by

Xiaoran Shang

Dissertation submitted to the Faculty of the Graduate School of the
University of Maryland, College Park, in partial fulfillment
of the requirements for the degree of
[Doctor of Philosophy]
[2019]

Advisory Committee:
Associate Professor Daniel Nelson, Chair
Professor Kevin McIver, Dean's Rep
Associate Professor Georgiy (George) Belov
Associate Professor Nicole LaRonde
NIST Research Biologist Zvi Kelman

Acknowledgments

First, I would like to express my deepest gratefulness to my mentor, Dr. Daniel Nelson, for offering me the opportunity to study in his laboratory. His support, guidance, wisdom, and generosity have encouraged me during my graduate training. His curiosity and attitude to science inspired me to move forward in my scientific career. The experience in the Nelson lab has been a life-treasure for me. For all that, I am everlastingly grateful.

I would like to thank my graduate committee, Dr. Kelvin McIver, Dr. Georgiy Belov, Dr. Nicole LaRonde, and Dr. Zvi Kelman, for their wise insights and consistent guidance.

Additionally, I would like to thank our collaborators, Dr. Hongping Wei and group, Dr. Krystyna Dąbrowska and group, and Dr. Osnat Herzberg and group for the opportunity to be involved in their research.

I would like to thank my labmates, past and present, Sara, Harley, Irina, Daniel, Adit, Hang, Niels, Heng, Yan, and Sarah for their generous assistance and the fellows and friends in the IBBR/MOCB department.

Finally, I would like to thank my family, my parents, Chunning and Yanyan, and my husband, Chuan, for their unconditional love, support, and encouragement.

Table of Contents

List of Tables

List of Figures

List of Abbreviations

AA	Amino acid
AMPs	Antimicrobial peptides
BLI	Bio-layer interferometry
BHI	Brain heart infusion
CBD	Cell-wall binding domain
CFU	Colony forming units
CD	Circular dichroism
CDC	Center for Disease Control and Prevention
CHAP	Cysteine, histidine-dependent amidohydrolase/peptidase
DNA	Deoxyribonucleic acid
EAD/ECD	Enzymatically active domain/Enzymatically catalytic domain
ETDA	Ethylenediaminetetraacetic acid
FDA	United States Food and Drug Administration
GAS	Group A Streptococcus
GBS	Group B Streptococcus
GCS	Group C Streptococcus
GES	Group E Streptococcus
GFP	Green fluorescent protein
GyH	Glycosol hydrolase
LB	Luria-Beterani
MBEC	Minimum biofilm elimination concentration
MDR	Multidrug resistance
MIC	Minimum inhibitory concentration
MRSA	Methicillin-resistant *Staphylococcus aureus*
NAG	N-acetylglucosamine
NAM	N-acetylmuramic acid
NCBI	National Center for Biotechnology Information
NIST	National Institute of Standards and Technology
OD	Optical density
PBS	Phosphate buffered saline
PBP	Penicillin-binding protein
PCR	Polymerase chain reaction
PDB	Protein data bank
PG	Peptidoglycan
PI	Propidium iodide
SDM	Site-directed mutagenesis
SDS	Sodium dodecyl sulfate
SDS-PAGE	Sodium dodecyl sulfate polyacrylamide gel electrophoresis
SEC	Size-exclusion chromatography
SOE PCR	Gene splicing by overlap extension polymerase chain reaction
SPR	Surface plasmon resonance
THY	Todd-Hewitt broth supplemented with 1% [wt/vol] yeast extract

TSB	Tryptic soy broth
VISA	Vancomycin-intermediate *Staphylococcus aureus*
V_{max}	Maximum velocity
WHO	World Health Organization
WT	Wild-type
XDR	Extensively drug-resistant

Chapter 1:
Introduction and Literature Review

1.1 Streptococcal Infectious Diseases

The *Streptococcus* genus consists of a diverse collection of Gram-positive bacteria that is significant in human medicine and the animal industry. Various species of streptococci are important members of the commensal microflora on the mucosal surfaces of human and animals, although some can cause severe infectious diseases ranging from acute to chronic (Facklam, 2002; Mitchell, 2003; Patterson, 1996). In humans, streptococcal infections cause diseases varying from dental caries and pharyngitis to life-threatening necrotizing fasciitis and meningitis. In animals, the infections cause equine strangles in horses, swine lymphadenitis in pigs, and bovine mastitis in dairy cows. Due to the resistance to conventional antibiotics and the lack of vaccines, infections of streptococci show an increased rate of morbidity, mortality, and treatment cost, leading to a tremendous burden in both public health and economy (Pfoh et al., 2008).

Group A Streptococcus

Streptococcus pyogenes, also known as group A streptococcus (GAS), is a human pathogen that infects over ~800 million people a year (Carapetis et al., 2005). It usually colonizes the epithelial surfaces of the throat and skin causing mild superficial diseases including pharyngitis, scarlet fever, and impetigo. Pharyngitis,

also known as “strep throat” or a sore throat, is one of the most common childhood diseases, but it is able to infect people of all ages with over ~600 million cases per year (Carapetis et al., 2005). Scarlet fever can develop with GAS pharyngitis due to the pyrogenic exotoxin SpeA (Shulman & Tanz, 2010). GAS can also cause impetigo, a skin infection, affecting people living in a tropical and subtropical area with poor hygiene habits (Cole & Gazewood, 2007). These mild infections are not life-threatening, but without the proper treatment, they may lead to autoimmune-related post-infection sequelae, such as rheumatic fever/heart disease, acute glomerulonephritis, and reactive arthritis. Acute rheumatic heart disease affects 2.4 million children aged from 5 to 14 years old, and about 15.6 million of all one year-olds, with 233,000 deaths each year, which is the greatest burden of GAS infections (Carapetis et al., 2005; Walker et al., 2014). Besides the local infections and post-infectious diseases, GAS is capable of infecting soft tissues, joints, or the lower respiratory track, resulting in severe and potentially invasive fatal diseases such as necrotizing fasciitis and streptococcal toxic shock syndrome (STSS) (Cunningham, 2000; Parks et al., 2015). The morbidity and mortality rates of invasive GAS infections are unexpectedly high, and 8-23% of patients die within a week of infection. On a global scale, GAS is related to 500, 000 deaths per year and, therefore, is rated as the ninth leading pathogen of human mortality (Carapetis et al., 2005).

As a well-adapted human pathogen, GAS develops complex virulence mechanisms for different stages of infection. The initial attachment and invasion require a range of molecules on the surface of GAS including the hyaluronic acid capsule, lipoteichoic acid, fibronectin-binding proteins (FBP), and the M-protein

(Mitchell, 2003; Walker et al., 2014). To avoid the host defense, the M-protein is able to bind the innate immune complement–control proteins to change the complement pathway, while C5a peptidase displayed on the surface of GAS destroys the C5a thereby preventing neutrophil recruitment (Mitchell, 2003; Walker et al., 2014). In the meantime, GAS secretes toxins and tissue-degrading enzymes, such as hemolysins, streptokinase, hyaluronidase, and superantigens, to cause tissue damage and toxic-shock syndrome. Among these virulence factors, the M-protein has been studied comprehensively for its function and structure as a model for other bacterial surface proteins as well as a possible candidate for GAS vaccines development (Fischetti, 1991). To regulate the virulence factors in various niches, GAS exploits global regulatory circuits. One such pathway is controlled by the *mga* gene, which positively regulates itself and serves as a protein to bind to the promoter of the genes that it regulates, including M-protein (Ring et al., 2000), C5a peptidase (*scpA*), M-like proteins (*mrp*, *enn*, and *fcR*), serum opacity factor (*sof*), and secreted inhibitor of complement (Cunningham, 2000). Further studies discovered the Mga pathway is related to carbohydrate uptake by GAS and the sugar acts as a signal for the phosphorylation of Mga (McIver et al., 1995). In summary, the various virulence factors of GAS enable it as the most "versatile" of the streptococcal pathogens.

Group B streptococcus

Streptococcus agalactiae, or group B streptococcus (GBS), colonizes the human gastrointestinal (GI) track where it co-exists as a commensal. However, it is an important causative agent of invasive infections in three populations: infants,

pregnant women, and non-pregnant immunocompromised adults. GBS is the main cause of neonatal sepsis, pneumonia, and meningitis in West Europe and the United State (Schuchat, 2001). Two types of GBS infections are found in early infancy. The early-onset disease occurs in the first week of life due to perinatal transmission during labor and delivery (Katz & Bowes, 1988). The late-onset disease occurs between 1 week and 3 months of age, and the reason for that is less well understood. The acute GBS infections in newborns can lead to death, disability, and sometimes severe chronic sequelae, such as neurologic damage (Pearlman, 2003). GBS infections in pregnant women range from mild urinary tract infection to life-threatening sepsis and meningitis. In the US, about half of maternal GBS infections could cause fetal death, neonatal infection, neonatal death, or pregnancy loss (Phares et al., 2008). Besides the infants and pregnant women, the older adults, especially those with diabetes, malignancy, and other cause of immunodeficiency are in the danger of GBS invasive infections. Recently, the risk of infections in older people is increasing in nursing home residents, and in the US, over three-quarters of GBS infectious cases occur in the elderly and causes 90% of GBS death (Verani & Schrag, 2010).

Like GAS, GBS expresses a variety of virulence factors to survive in the host. The polysaccharide capsule is important for protecting GBS from the innate complement pathway. A range of GBS surface proteins, such as laminin-binding proteins, fibrinogen-binding proteins, and fibronectin-binding proteins, enable the organisms to attach to human laminin and escape opsonophagocytosis (Li et al., 1997; Schubert et al., 2002; Spellerberg et al., 1999). The hemolysin, CylE, is the key factor

causing damage of lung epithelial and endothelial cells, brain epithelial cells, and macrophages (Ring et al., 2000).

Streptococcus pneumoniae

S. pneumoniae are usually considered normal flora when the colonize the mucosal surfaces of the human upper respiratory tract. Approximately 25-60% of children and <10% of adults are asymptomatic carriers of *S. pneumoniae* in the nose (Abdullahi et al., 2012; Nunes et al., 2005; Yahiaoui et al., 2016). However, pneumococci can cause mild to severe diseases, such as otitis media (middle-ear infection), pneumonia (lung infection), bacteremia (blood infection), and meningitis (brain infection), when they invade the sterile sites. According to Center for Disease Control, up to 1 million children below 5 years old die yearly due to pneumococcal infections, and about 5% of those that get pneumococcal infections die from the disease in the US. In 2017, the World Health Organization listed pneumococcus as the fourth leading pathogen of human mortality, only after HIV, *Mycobacterium tuberculosis*, and *Plasmodium falciparum* (Carapetis et al., 2005).

S. pneumoniae produce various virulence factors to survive in different host environments. Like other pathogens, the polysaccharide capsule is the main virulence factor mediating attachment and anti-phagocytosis properties. In addition to the capsule, pneumococci possess other virulence factors, including pneumolysin, phosphorylcholine, and choline-binding proteins. The pneumolysin is a type of pore-forming protein involved in a range of activities. Pneumolysin actives the complement pathway to stimulate the productions of inflammatory mediators

(Cockeran et al., 2002). In addition, it causes damage to the ependymal cilia of the brain, inducing the program cell death of the brain cells (Braun et al., 2002; Hirst et al., 2000). Phosphorylcholine binds to the platelet-activating factor (PAF) receptor. PAF, by its name, can induce platelet aggregation, but several studies indicate that PAF is also a G-protein involved in signaling in a variety of cell types and tissues (Cundell et al., 1995; Ishii et al., 2002; Tuomanen et al., 1985). The choline-binding proteins (Cbp) include key proteins unique to *S. pneumoniae*. For example, the autolysin LytA is essential for cell division and surface protein A (PspA) is important for escape of the innate immune system (Hammerschmidt et al., 1997).

Streptococcus mutans

S. mutans belongs to the viridans streptococci and naturally colonizes the human oral cavity. Although the bacteria possess low virulence, it is the main factor of dental caries. With dissemination into the bloodstream, it may cause bacteremia and infective endocarditis (Parks et al., 2015). *S. mutans* with other oral bacteria, such as *S. sanguis*, *S. mitis*, and *S. salivarius*, attach to the surface of the teeth to form a biofilm known as "plaque". When the sugar level increases in the oral cavity, *S. mutans* consumes the additional sugar generating an acid environment and, therefore leads to the decay of tooth enamel (Nomura et al., 2017). Dental caries is a prevalent chronic disease in the US with 3,000,000 cases per year. The annual cost in the US for dental infections is about 24 billion dollars, and 90% of these are related to the rebuilding of teeth. Not only dental caries, but also dental treatment and daily oral care practices may allow *S. mutans* to transmit into the bloodstream. Thus, bacteremia

may happen in people with vulnerable immune systems, such as patients following chemotherapy or transplant surgeries (Parks et al., 2015). Infective endocarditis is due to the adherence of bacteria to damage heart valves. In the US, about 15,000 new cases of infective endocarditis are reported each year with a 15% to 20% mortality rate (Nakano et al., 2007).

To survive in the oral cavity, *S. mutans* expresses several adhesins, such as streptococcal protein antigen P (SpaP), on the bacterial surface. These adhesins bind to salivary agglutinin glycoprotein to start the initial attachment of a biofilm on the surface of the tooth. Genome analysis of *S. mutans* reveals numerous genes for transport and metabolism of various sugars. The fermentation of the sugars produces lactic acid, which creates an acid environment and causes tooth decay. The ATPase of *S. mutans* is capable of maintaining neutral intracellular pH and thus, allows *S. mutans* to become acid tolerant (Mitchell, 2003). These key virulence factors make *S. mutans* the leading pathogen in the oral cavity.

Other streptococci

Streptococci are not only human pathogens, but some of them also cause disease in animals. Group C streptococci, group E streptococci, *S. uberis*, and *S. suis* are related to essential diseases in cattle, pigs, horses, and sheep. The infections of the livestock usually lead to a significant economic loss in the US. Among these, *S. suis* is a zoonotic organism, which transmits from animal to human. This infection mostly occurs on pig farmers and abattoir workers due to exposure to the ill pigs or pig meat (Hardie & Whiley, 1997b).

To summarize, different groups of streptococci possess unique virulence factors that enable them to be versatile pathogens for humans and animals.

1.2 Antibiotics and Resistance

The discovery and application of antibiotics have transformed modern medicine and saved millions of lives. Since the 1940s to 1990s, the development of antibiotics from natural products and synthetic chemicals has propelled the battle with pathogenic bacteria, and the results have been revolutionary (Andersson & Hughes, 2010). However, the overuse and misuse of antibiotics in recent years have increased the frequency of resistance gene transmission between both pathogens and commensal organisms (Kohanski et al., 2010). Compounding the situation, development of new antibiotics in the last few decades has slowed down due to rapid loss of efficacy and market failure due to limited profit motive. These circumstances created the "post-antibiotic" era and provoke the need for new, novel antibacterial approaches.

Antibiotics Discovery and Resistance Development

One day in 1928, a scientist had been cultivating *Staphylococcus spp.* in a petri dish when he left for a two-week vacation. After the vacation, he found the petri dish was contaminated by a *Penicillium* mold, and interestingly, no bacteria grew close to the mold. This scientist was Alexander Fleming and he eventually discovered penicillin from the *Penicillium* mold, thereby founding the field of classical antibiotics. He devoted his life trying to cultivate penicillin from the mold and use as

an antimicrobial agent. With many attempts and failures, the chemists Howard Florey and Ernest Chain from Oxford University, fulfilled the goal of the large-scale production of penicillin in 1940. The first use of penicillin was in 1942. John Fulton, a friend of Howard Florey, used 5.5 grams of crude penicillin saved the life of Anne Miller from septicemia. In 1943, streptomycin, the first aminoglycoside antibiotic, was discovered by Albert Schatz and Selman Waksman. Streptomycin was used in many cases with Gram-negative bacterial infections and was an active drug against *Mycobacterium tuberculosis*.

The use of penicillin and streptomycin in controlling bacterial infections during World War II propelled the golden era of antibiotic development. Numerous antibiotics containing different chemical groups/classes were discovered between the 1950s and 1970s including tetracycline (1950), chloramphenicol (1951), erythromycin (1953), vancomycin (1972), and carbapenems (1976). After the 1980s, pharmaceutical companies started to investigate synthetic antibiotic compounds based on previously discovered classes. In the last 30 years, only three antibiotics with a novel mode of action were introduced to the market (Linezolid, Daptomycin, and Ceftaroline).

The race between the development of antibiotic resistance and new antibiotics has never stopped. The first clinical resistance to penicillin was observed in 1945, only 3 years after its first, although resistance in the laboratory had been noted as early as 1940. Similarly, resistance to tetracycline was detected in the laboratory even before it reached the market. In general, resistance to new antibiotics was continuously noted within several years after the drugs reached the market (Table 1-

1). Moreover, emerging bacterial pathogens have evolved the ability of multi-resistance, such as multidrug-resistant *Acinetobacter*, multidrug-resistant *Pseudomonas aeruginosa*, and so on (Davies & Di Girolamo, 2010). Although low in frequency, clinical resistance now has been documented for every "last-resort" antibiotic on the market.

Table 1-1. Antibiotic resistance development: A timeline of key events.

Adapted from (Ventola, 2015).

Antibiotic	Introduced	Resistance Observed	Organism
Penicillin	1942	1945	*Staphylococcus*
		1965	*Pneumococcus*
Streptomycin	1943	1958	*Gonococcus*
Tetracycline	1950	1959	*Shigella*
Erythromycin	1953	1968	*Streptococcus*
Methicillin	1960	1962	*Staphylococcus*
Gentamicin	1967	1979	*Enterococcus*
Vancomycin	1972	1988	*Enterococcus*
		2002	*Staphylococcus*
Imipenem	1985	1998	*Enterobacteriaceae*
Ceftazidime	1985	1987	*Enterobacteriaceae*
Levofloxacin	1996	1996	*Pneumococcus*
Linezolid	2000	2001	*Staphylococcus*
Daptomycin	2003	2005	*Staphylococcus*
Ceftaroline	2010	2011	*Staphylococcus*

Antibiotic Mechanisms of Action

Antibiotics are classified into five categories based on the mechanism of action. Most current used antibiotics are bactericidal resulting in bacterial death. These antibiotics target essential processes or structures of bacteria, such as cell wall synthesis, protein synthesis, or nucleic acid synthesis (Kapoor et al., 2017; Kohanski et al., 2010).

The largest class of antibiotics inhibit cell wall synthesis leading to improper cell division, autolysin activity, and SOS response (Kapoor et al., 2017). These antibiotics can function in two ways. In one mechanism, they act as analogs which bind to the proteins necessary for cell wall synthesis. The most famous antibiotic, penicillin, belongs to this mechanism as the β-lactam moiety binds to penicillin-binding proteins inhibiting the normal function of these proteins in the bacterial cell wall. The second mechanism hinders cell wall synthesis by binding to the precursor peptidoglycan subunit. Vancomycin, a large drug molecule vancomycin, uses this mechanism by binding a D-alanyl subunit in the cell wall and preventing transpeptidation.

The second large class of antibiotics includes inhibitors of protein biosynthesis. Aminoglycosides (e.g., tetracycline, gentamicin, streptomycin, and kanamycin) interact with the 16S rRNA of the 30S subunit resulting misreading and premature termination of the translation of mRNA. Chloramphenicol (e.g., erythromycin, azithromycin) interacts with the 23S rRNA of the 50S subunit resulting in the inhibition of binding t-RNA. Antibiotics in this class must pass the cytoplasmic membrane and, in this process, they need energy generated from oxygen and active proton motive force. Thus, this group of antibiotics works poorly for anaerobic

bacteria. However, they may be used together with the cell wall targeting drugs to facilitate the entry, displaying synergism.

The third group of antibiotics inhibits the synthesis of DNA or RNA. Fluoroquinolones and trimethoprim-sulfamethoxazole are drugs that block DNA synthesis via interfering with DNA gyrase/topoisomerase IV (e.g., ciprofloxacin, levofloxacin). Rifampicins block RNA synthesis via binding the DNA-dependent RNA polymerase.

The fourth antibiotic class disturbs cell membrane permeability, preventing the growth of bacterial cells. Examples include colistin, daptomycin, and ionophores. The last category includes drugs that interfere with bacterial metabolism. Isoniazid and sulfonamides inhibit the normal function of certain essential energy pathways.

It is notable that antibiotics can be more effective in a combination treatment due to either an additive effect or a synergistic effect (Kohanski et al., 2010). As mentioned above, the protein synthesis inhibitors display synergism with cell wall synthesis inhibitors. However, the combination can also be antagonistic, meaning the effect of the two drugs is less than the effect of the single-drug treatment. This effect can be observed from the combination of a DNA synthesis inhibitor and a protein synthesis inhibitor due to the non-structured RNA from DNA synthesis inhibitor slowing the function of protein synthesis inhibitor. Further studies of the synergy or antagonism effect will provide more insight into the cell death mechanism and could be used to slow down the process of antibiotic resistance development.

Mechanisms of Antibiotics Resistance

Although there are five categories of antibiotics focusing on different mechanisms of action, bacteria have adopted many ways to develop resistance. Some bacteria are naturally resistant to certain antibiotics. Others can survive via genetic mutations through antibiotic selection, and these advantageous mutations can be passed through different generations and even transferred to other organisms via horizontal gene transfer (Blair et al., 2015; Munita & Arias, 2016).

The intrinsic resistance of a bacterial species is the ability to prevent the entry or function of specific antibiotic due to inherent structural or functional properties. One simple example is the aminoglycoside group. The aminoglycosides need to pass the bacterial membrane and enter the cytosol with the help of the energy-dependent bacterial transport system facilitated by oxygen and proton force. Thus, this group of drug works better on aerobic bacteria than anaerobic bacteria. The other example is the biocide triclosan. This drug displays broad efficacy against Gram-positive and most Gram-negative bacteria, but it cannot prevent the growth of *Pseudomonas* due to an insensitive allele of the target of the drug. Some drugs are only effective against Gram-positive but not Gram-negative organisms, such as the lipopeptide daptomycin or the glycopeptide vancomycin. These restrictions are due to the primary difference between the Gram-positive and Gram-negative cell wall compositions (Blair et al., 2015).

In addition to intrinsic resistance, bacteria also develop mutational resistance in four aspects: (i) target modification, (ii) antibiotic inactivation, (iii) activation of efflux pumps, (iv) changes in the metabolic pathway (Munita & Arias, 2016). In the

first group, bacteria modify the antibiotic target site resulting in the improper binding. One example is the penicillin-binding protein 2a (PBP2a) transpeptidase of methicillin-resistant *Staphylococcus aureus*. The *mecA* gene encodes the PBP2a instead of PBP, inhibiting the binding of β-lactams. To cooperate with the change of PBP2a, the peptidoglycan of *S. aureus* changes in composition and structure, which involved several additional genes (Tenover, 2006). The second primary resistance mechanism requires the production of enzymes that degrade the drug, such as hydrolysis, group transfer, or a redox mechanism (Bonnet, 2004; Bush et al., 1995; Kotra & Mobashery, 1999; Poole, 2004). The most well-known enzyme is the β-lactamase family, which can cleave the ring of β-lactams. Other hydrolytic enzymes include esterases in macrolide resistance, transferases in aminoglycosides, and virginiamycin M in streptogramin. The efflux pumps can be found in both Gram-positive and Gram-negative organisms and are used to pump the antibiotics out of the cytoplasm. This mechanism is well known for the multidrug-resistance (MDR) efflux pumps (Blair et al., 2015). The resistance nodulation division (RND) pump is found in Gram-negative bacteria and is one of the best-characterized efflux transporter. One example of the RND pump is the AcrB in *E. coli.* Once *E. coli* infects, the *acrB* genes encounter the small molecules, such as indole and bile, to overexpress the AcrB pump. The structure of AcrB pump consists of two distinct pockets that can accommodate different substrates (Eicher et al., 2012; Hung et al., 2013; Vargiu & Nikaido, 2012). The last mechanism is due to global cell adaptations, which change important metabolic pathways via modulation of the network during infection.

The gain of foreign DNA material via horizontal gene transfer (HGT) is another vital factor of bacterial evolution and resistance. The simplest type of HGT is via transformation by incorporation of DNA in the environment by naturally competent bacteria. However, this method is not responsible for clinically relevant antibiotic resistance. In contrast, conjugation is the most relevant form of HGT clinically. In conjugations, many bacterial surface components, like pili, can make cell-to-cell contact allowing exchange of DNA, and this contact occurs at high rates in the gastrointestinal tract (GI) of a human. In another method, lysogenic bacteriophages can also be carriers of resistant genes and spread these genes via transduction (Munita & Arias, 2016).

Antibiotics Resistant Streptococci

Antibiotics are still an effective treatment for streptococcal infectious diseases due to the fact that streptococci remain susceptible to common antibiotics (Cattoir, 2016). However, in the past 15 years, the rate of streptococcal antibiotic failure has increased to 40% in some regions of the world (Brook, 2013). *S. pneumoniae* are associated with a rising rate of resistance to penicillin and are possibly resistant to other new antibiotics. One remarkable capability of *S. pneumoniae* is the ability to uptake and incorporate exogenous DNA (natural competence) from other pneumococci. Group A streptococci, group B streptococci, and viridans group members are also pathogens with a high rate of resistance development as genes related to resistance have been noted in these species via meta-gene analysis (Cattoir,

2016). In 2013, antibiotic-resistant *S. pneumoniae* infections were reported as one of the serious threats in a CDC annual report (Figure 1.1).

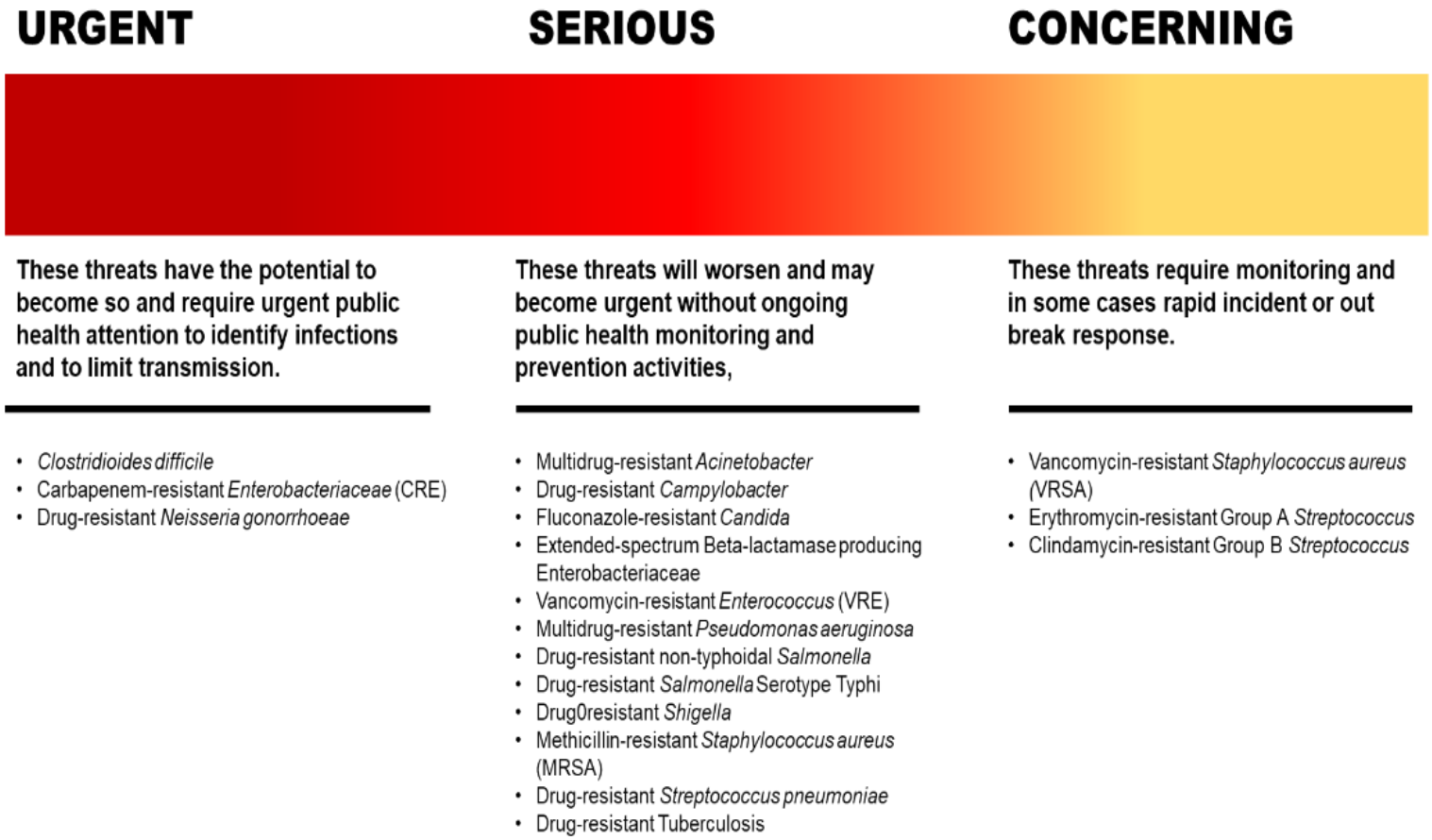

Figure 1.1 Antibiotic resistance threats. The figure was adapted from data released by the CDC in 2013.

1.3 Alternative Antimicrobial: Bacteriophage-Derived Endolysins

Widespread distribution of antibiotic-resistance genes in bacteria has led us to enter the post-antibiotic era. Bacterial infectious diseases that were once treatable through the use of antibiotics are becoming deadly again (Brown & Wright, 2016). Moreover, the overuse of broad-spectrum antibiotics accelerates the dispersal of resistance genes not only to pathogens, but also to commensal organisms (Nelson et al., 2012). Thus, the development of alternative antimicrobial agents is one of the highest global priorities in biological, pharmaceutical, and medical investigations (Veiga-Crespo et al., 2007). One alternative to antibiotics is the use of endolysins, which are bacteriophage-derived peptidoglycan hydrolases, and alternately termed phage lysins or enzybiotics.

History

Bacteriophage (phage) are viruses that infect bacteria. They were discovered independently by Frederick Twort and Félix d'Hérelle in 1915 and 1917, respectively, and are considered as the most abundant microbial agents on the earth (Summers, 2011). Not long after d'Hérelle's discovery, phage were studied as a treatment of bacterial infectious diseases due to their potent bactericidal capacity. The first reported case of phage application was in 1921 from Richard Bruynoghe and Joseph Maisin, who used phage to treat a staphylococcal skin infection (Hermoso et al., 2007). Several companies started the commercialization of phage in the 1930s in the US, France, and the region of the former Soviet Union now known as Georgia. With the discoveries and industrial manufacturing of antibiotics in the 1940s, the use

of phage as antimicrobial treatments was abandoned in the US and western Europe, leaving the former Soviet Union and eastern Europe to continue actively studying and using phage (Sulakvelidze et al., 2001). However, over 60 years later, there is renewed interest in phage as potential therapies for the management of bacterial pathogens that have emerged resistance to clinically approved antibiotics. A few human phage therapy studies have been performed in Poland, Georgia, and Russia, including studies on *Shigella* phage against bacterial dysentery in 1968, *Staphylococcus* phage against lung and pleural infections in 1982, *E. coli* phage against recurrent subphrenic abscess in 1994, and a phage cocktail therapy against various infections in 1987 (Sulakvelidze et al., 2001). In the meantime, the application of phage has grown to more areas, such as agriculture, aquaculture, and wastewater treatment (Goodridge, 2004; Withey et al., 2005). Moreover, in August 2006, the US Food and Drug Administration (FDA) approved the use of a cocktail phage therapy containing six individual, purified phage against *Listeria monocytogenes* for decontamination of ready-to-eat meat and poultry products. This action indicates that the FDA is open to consideration of using phage as an antimicrobial for bacterial infectious diseases in humans.

However, there are still several concerns using the whole phage for therapeutic application. First, phage usually have a relatively narrow host range. Phage often show strain specificity, thus necessitating various phage just to cover all strains within a single bacterial species. Second, the lifestyles of phage are unpredictable under different physiological conditions. Phage have two distinct life cycles, lytic and lysogenic. When phage therapy is considered, it is important to select strictly lytic

phage to assure bacterial killing. Third, bacteria can evolve resistance towards phage that targets every stage of the phage infection process. The surface proteins of bacteria may be mutated to prevent phage attachment. The injected phage DNA may either be degraded via a variety of restriction-modification systems or the CRISPR-Cas system. Alternately, the infected bacterium may commit cell death through the abortive infection system to limit the viral propagation and spread through the clonal bacterial population (Dy et al., 2014). Fourth, the administration of phage is more complicated than that of chemical drugs. Due to the self-replication, the pharmacokinetics is of phage therapy is hard to measure which, results in additoinal problems associated with the regulation of phage therapies. Thus, the use of phage-produced molecules or enzymes that are capable of direclty killing bacteria would have inherent advantages over whole phage therapy.

One of the most promising phage molecules is a class of cell wall hydrolases termed as endolysins. Endolysins are produced at the end of the phage replication cycle resulting in cell lysis and progeny phage release. During this cycle, phage also produce another protein called holin, which accumulates until it reaches a critical mass and forms pores in the cytoplasmic membrane, allowing the endolysins to gain access to the cell wall (Fischetti et al., 2006). However, endolysins are also capable of destroying the Gram-positive bacterial peptidoglycan when applied exogenously, resulting in "lysis from without" (Figure 1-2). Several phage endolysins had been purified and used as a laboratory tool for cell wall extractions before the 1990s. However, when antibiotic resistance became a serious problem, scientists proposed that endolysins could be a potential antimicrobial alternative (Fischetti, 2018).

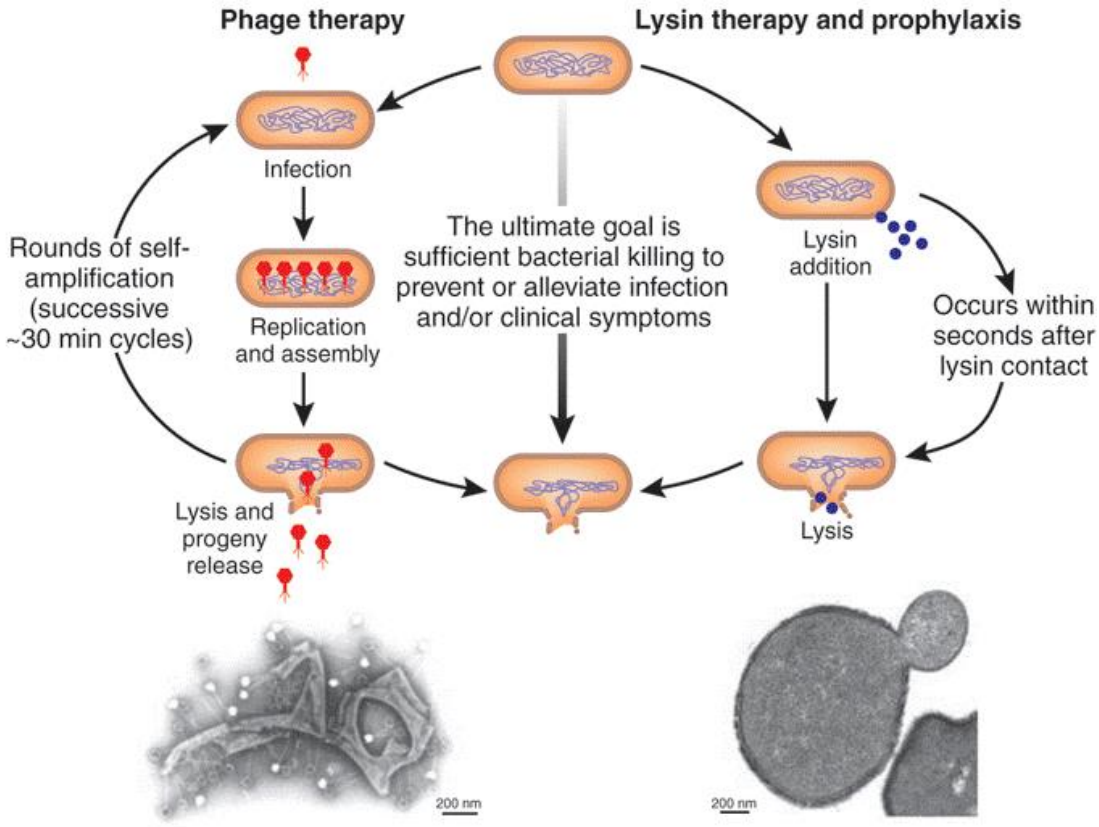

Figure 1-2. Comparison of phage therapy and endolysin therapy. Phage therapy (on the left) applies lytic phage (in red) to lyse the bacteria, which usually occurs over 30 min. The electron microscope picture shows the phage particles adhering to the debris of a lysed streptococcal cell. In comparison, endolysin therapy includes the use of recombination endolysins (in blue) applied outside the bacteria, resulting in osmotic lysis within a few minutes. The electron microscope picture shows a cross-section of *Bacillus anthracis* treated with the purified PlyG displaying an externalized osmotic lysis. Figure adapted from (Fischetti et al., 2006)

Through the past 20 years of study, the efficacy of endolysins has been validated both *in vitro* and *in vivo* against a variety of Gram-positive pathogens, and few endolysins have entered human clinical trials.

Domain Architecture of Endolysins

Endolysins usually consist of two components: the conserved enzymatically catalytic domains (ECD)/enzymatically active domains (EAD) and a cell wall binding domain (CBD). Depending on the different origins of endolysins, they can adopt different modular structures (Figure 1-3).

Endolysins derived from phage that infect Gram-positive bacteria have a very similar modular structure with one or more N-terminal EADs and a C-terminal CBD (Fischetti, 2010; Loessner, 2005; Oliveira et al., 2012; Schmelcher et al., 2012). The EADs possess the hydrolytic activity of the enzyme, and the CBDs possess the binding activity to carbohydrates on the surface of the peptidoglycan (PG). In some cases, the endolysins contain two EADs connecting to each other at the N-termini. However, the presence of more than one EAD in endolysins does not ensure higher activity since the EAD(s) in the middle are usually silence (Becker et al., 2009). Whereas many EADs require the presence of the CBD for binding and subsequent activity, some EADs can bind the bacterial surface independently of the CBD such as T4 lysozyme (Matthews & Remington, 1974). One unique example of endolysins derived from phage infecting Gram-positive bacteria is the streptococcal C1 phage endolysin, PlyC. This endolysin is composed of nine subunits in a 114 kDa holoenzyme and will be discussed in a later section (Nelson et al., 2006).

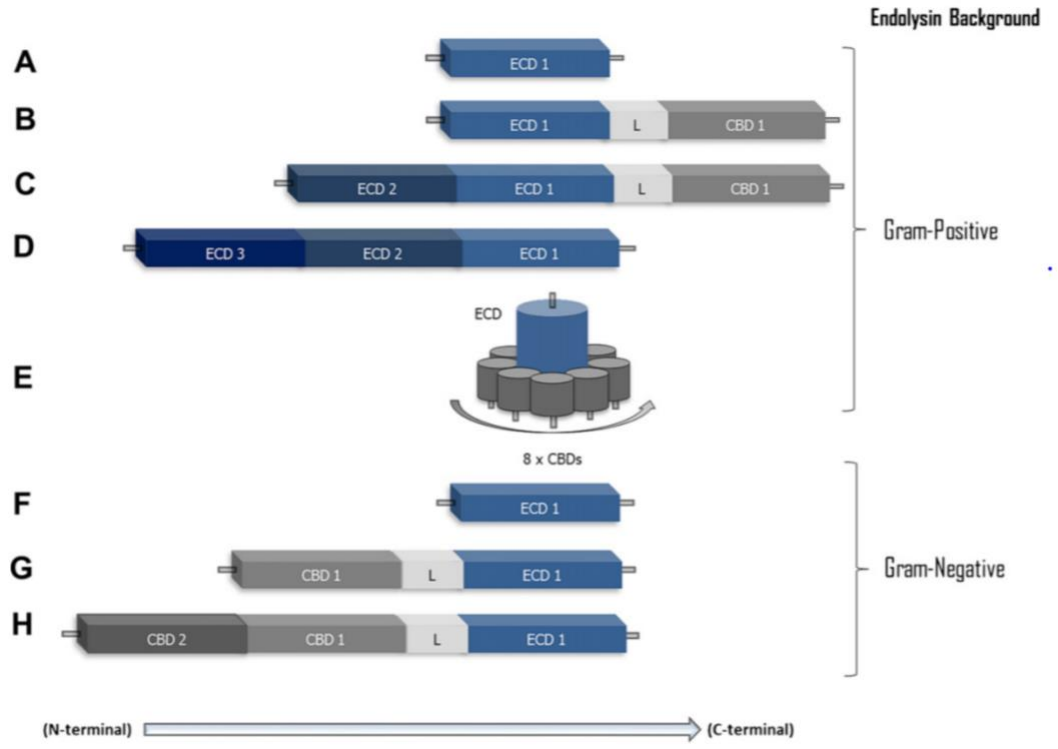

Figure 1-3. Modular Architectures of Gram-positive and Gram-negative endolysins. The endolysins derived from phage that infect Gram-positive bacteria display five possible structures: **(A)** Single globular enzymatically catalytic domain (ECD)/enzymatically active domain (EAD). **(B)** On N-terminal ECD/EAD and one C-terminal CBD. **(C)** Two N-terminal ECDs/EADs and one C-terminal CBD. **(D)** Three ECDs/EADs. **(E)** Multimeric structure with one ECD/EAD and eight CBDs. The endolysins derived from phage that infect Gram-negative bacteria display three possible structures: **(F)** Single globular ECD/EAD. **(G)** One N-terminal CBD and one C-terminal ECD/EAD. (**H)** Two N-terminal CBDs and one N-terminal ECD/EAD. Figure adapted from (Oliveira et al., 2013).

Endolysins derived from phage that infect Gram-negative bacteria are simple in structure comprising of a single globular EAD, since the peptidoglycan of Gram-negative bacteria, contained between the inner and outer membranes, is thin and lacks carbohydrates or other surface moieties associated with the Gram-positive peptidoglycan (Oliveira et al., 2013). Notwithstanding, some exceptions exist. For example, some of these endolysins may possess a modular structure with an N-terminal CBD and C-terminal EAD, such as KZ144 of phage phiKZ (Briers et al., 2007). However, the CBDs of endolysins targeting Gram-negative bacteria directly bind to PG, not to the surface carbohydrates (Briers et al., 2007).

Bacteriolytic Mechanism

The PG layers of Gram-positive and Gram-negative organisms are different in both thickness and composition. The PG of Gram-positive bacteria is about 20-80 nm thick and is the core element of the bacterial surface. In contrast, the PG of Gram-negative bacteria is 5 to 10 nm and the PG is shielded from the external environment by the protective outer membrane, which contains teichoic acids and surface proteins (Schleifer & Kandler, 1972). The sugar backbone of PG is conserved in all bacteria and consists of N-acetylmuramic acid (MurNAc) and N-acetylglucosamine (GlcNAc) connected by β-1,4 glycosidic bonds. The differences between organisms is in the composition of the short stem tetrapeptide and the crossbridge (Meroueh et al., 2006). An L-lysine type (Lys-type) PG is typical for most Gram-positive organisms, while a *meso*-2,6-diaminopimelic acid type (mDAP-type) is observed in all Gram-negative organisms, as well as the Gram-positive *Bacillus* and *Listeria* spp. The mDAP-type

PG consists of simple peptide stems directly linked to each other via an amide bond. However, in the Lys-type PG, the peptide stems are connected by crossbridges consisting of different amino acids in different species, such as a pentaglycine crossbridge in staphylococci or a dialanine crossbridge in streptococci (Figure1-4) (Schleifer & Kandler, 1972).

Although the types of PG are different, the covalent bonds in the PG are conserved. Thus, because endolysins are PG hydrolases, their EADs target a limited number of chemical bonds and can, therefore, be classified into five enzymatic groups: N-acetylmuramidases, lytic transglycosylases, N-acetyl-β-D-glucosaminidases, N-acetylmuramoyl-L-alanine amidases, and endopeptidases (Borysowski et al., 2006). Among the five groups, N-acetylmuramidases and lytic transglycosylases cleave the N-acetylmuramoyl-β-1,4-N-acetylglucosamine bond (Figure 1-4, label 2,3). N-acetyl-β-D-glucosaminidases cleave the sugar backbones at the N-acetylglucosaminyl-β-1,4-N-acetylmuramic acid bond (Figure 1-4, label 1). N-acetylmuramoyl-L-alanine amidases release the peptide stem from sugar backbone via cleaving between MurNAc and L-alanine (Figure 1-4, label 4). Endopeptidases cleave the bond between two amino acids that occur either in the peptide stems or in the crossbridges (Figure 1-4, label 5,6,7,8). The cysteine, histidine-dependent amidohydrolase/peptidase (CHAP) domain is the most common EAD observed in endolysins. CHAP domains can either be an L-alanine amidase or an endopeptidase. The first reported CHAP displaying both amidase and endopeptidase activity is as the EAD of a staphylococcal endolysin, PlyGRCS (Linden et al., 2015).

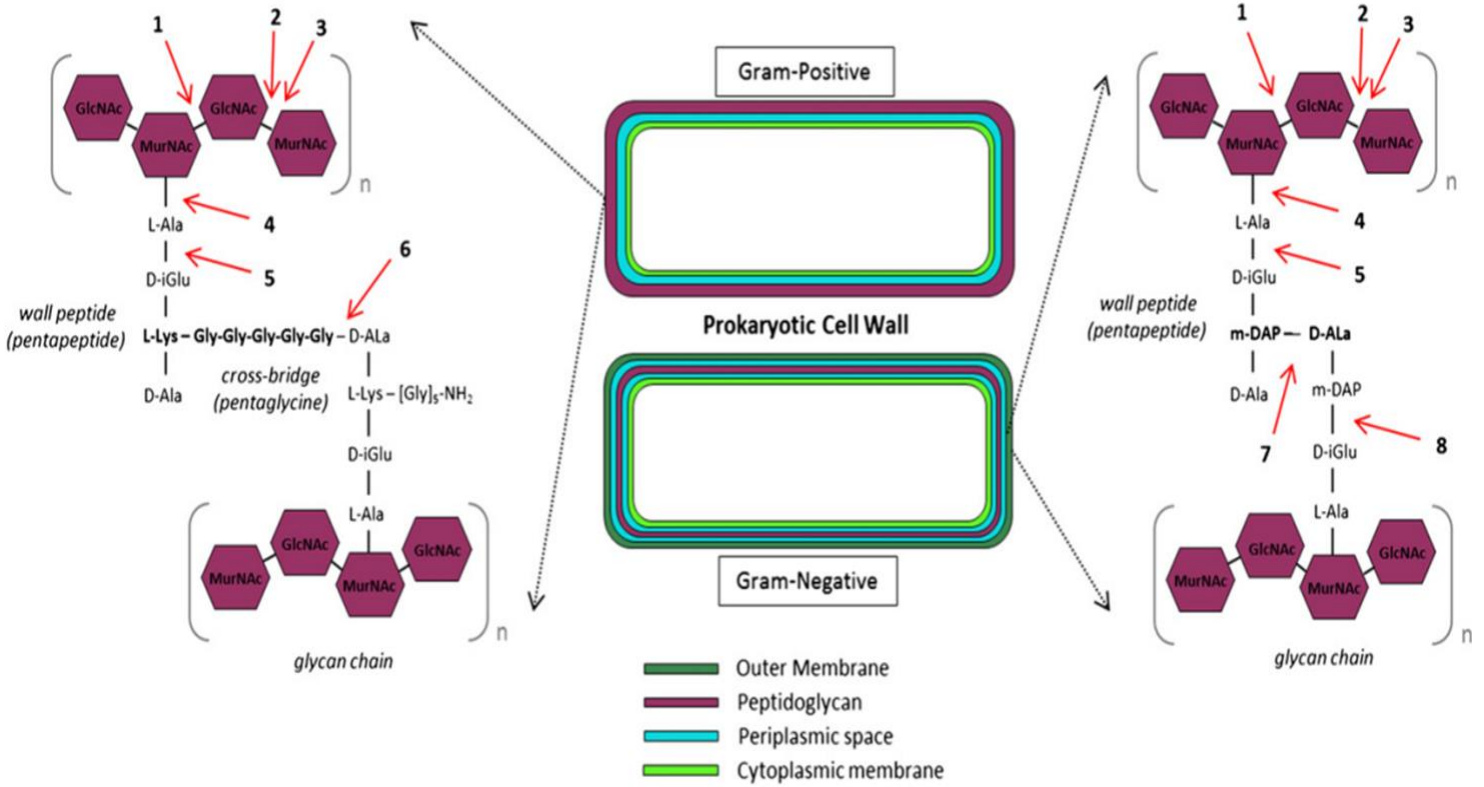

Figure 1-4 Schematic figure of DAP-type and Lys-type peptidoglycan structure and cleavage site of endolysins. 1) N-acetyl-β-D-glucosaminidase; 2) N-acetyl-β-D-muramidase; 3) lytic transglycosylase; 4) N-acetylmuramoyl-L-alanine amidase; 5) L-alanoyl-D-glutamate endopeptidase; 6) D-alanyl-glycyl endopeptidase; 7) D-alanine-D-meso-DAP endopeptidase and 8) D-glutamyl-m-DAP endopeptidase. Adapted from (Oliveira et al., 2013).

Cell Wall Binding Domains

The cell wall binding domains (CBDs) possess no enzymatic activity but rather function to bind a specific substrate, usually a carbohydrate or teichoic acid, attached to the host PG (Fischetti, 2008). Thus, the specificity of the endolysin is often dictated by the specificity of the CBD. Unlike the EADs, the CBDs are divergent since they have been evolving over millions of years to recognize many different ligands on the cell wall. Researchers are interested in studying the binding affinity and binding ligands for CBDs. Unfortunately, few ligands for CBDs have been precisely identified, and without the known ligands, the study of affinity is complicated.

Although the CBDs are diverse, some common domain motifs have been identified: (i) The LysM (Lysin Motif) is considered to bind the broadest range of receptors and may bind specifically to GlcNAc residues in the sugar backbone of the PG (Buist et al., 2008; Garvey & Santi, 1986; Ohnuma et al., 2008; Visweswaran et al., 2011). One notable LysM domain is the CBD of the endolysin from phage Lb338-1 infecting *Lactobacillus* (Oliveira et al., 2013). (ii) Another common motif is the PG binding domain (Peptidoglycan Binding Domain), which targets the D-Asn residue in PG crossbridges in both Gram-positive and Gram-negative organisms. Examples include the LcLys and LyLys2 of *Lactobacillus casei* phage, PVP-SE1 of *Salmonella* phage, and KZ144 and EL188 of *Pseudomonas* phage (Briers et al., 2007; Regulski et al., 2013; Walmagh et al., 2012). (iii) Less common CBD motifs include FOG (Friend of GATA-zinc finger protein), SLAP (SRC-like Adapter Protein), and SPOR (Sporulation Related Domain) (Oliveira et al., 2013). (iv) The Choline-Binding

Modules are CBDs that specifically target and bind choline-containing teichoic acids in the cell wall of *S. pneumoniae* (Hermoso et al., 2007). The CBDs in this group usually consist of different repeats of choline-binding modules that display various binding affinities (Garcia et al., 1987). (v) CWH (Clostridial Hydrophobic with Conserved Tryptophan W) is the family of CBDs that target the cell wall of *Clostridium acetibutylicum* (Sullivan et al., 2007). (vi) Lastly, SH3 (SRC Homology 3- domain) binds to proline-rich ligands and is the family most associated with staphylococcal endolysins (Buist et al., 2008; Grundling et al., 2006; Mayer et al., 1988).

Antimicrobial Potential (Bacterial resistance, Safety, Immunogenicity, Synergy, Biofilm)

One advantage of endolysins over traditional antibiotics is the near-species specificity displayed by these enzymes. The overuse and misuse of broad-range antibiotics usually disturb the normal flora resulting in the growth of opportunistic pathogens, such as *Clostridium difficile* in the GI tract. Moreover, these practices accelerate the horizontal gene transfer of resistance within the bacterial community consisting of both pathogens and commensal organisms (Nelson et al., 2012). To date, there are not any reports of strains developing resistance to endolysins. One likely explanation is the coevolution of bacteriophage and bacteria has led to the endolysins binding to and cleaving essential and highly conserved targets in the PG (Fischetti, 2005). The other explanation is the highly lytic efficacy of endolysins applied from without, killing bacteria within seconds or minutes, thereby not allowing

time for selective pressure to generate resistance mechanisms. Several studies have attempted to address the lack of resistance to endolysins. In one study, *S. pneumoniae* cells were continuously treated with increasing concentrations of the Pal endolysin, but no resistant strains were detected (Loeffler et al., 2001). In the other studies, the PlyG endolysin and chemical mutagens were added to *Bacillus anthracis* culture in order to accelerate evolution of PlyG-resistant strains. However, these organisms remained fully sensitive to PlyG while they generated 1,000-10,000-fold increases in streptomycin resistance under the same conditions (Schuch et al., 2002). Another study using an engineered endolysin, ClyS, against MRSA found that the MIC was unchanged after repeated treatment of the endolysin (Pastagia et al., 2011). Despite these encouraging results, it is important to note that there are reports of resistance to non-endolysin PG hydrolases, specifically lysozyme and bacteriocins. Resistance against human lysozyme has been linked to secondary changes of the cell wall, such as O-acetylation and N-deacetylation of the PG (DeHart et al., 1995; Grundling et al., 2006; Sugai et al., 1997). Notably, endolysins that utilize the EADs with lysozyme-like activity are quite rare. In a second example, *S. aureus* generates resistance to lysostaphin, a bacteriocin, by changing the constituents of the crossbridge, the target of this enzyme (DeHart et al., 1995).

Preclinical safety and toxicity profiles on mammalian cells and tissues are critically necessary for future translational development of endolysins. According to clinicaltrails.gov, there are at least three endolysin-based therapies in Phase 2 clinical trials. SAL200, a pharmaceutical composition containing the SAL-1 endolysin specific for *S. aureus*, displayed no signs of toxicity in the central nervous and

respiratory system of rodents and dogs (Jun et al., 2014). Similarly, there were no signs of abnormalities or adverse events in monkeys (Jun et al., 2016). In a Phase 1 human trial, again, no adverse events were detected using SAL200 (Jun et al., 2017). Another safety trial was recently completed by the Dabrowska group in Poland (Harhala et al., 2018). In this study, the authors were able to show that two pneumococcal endolysins, Cpl-1 and Pal, are overall safe in terms of immune responses, microbiome changes, and inflammatory response. Although more studies are anticipated to emphasize the safety of endolysins, the proteinaceous nature of these enzymes implies a noncorrosive and biodegradable nature, which is another advantage compared to chemical antimicrobials (Nelson et al., 2012).

The immune response is a considerable part of the safety issue, but in this section, we only focus on the antibodies that are generated against the endolysins. Specific serum antibodies against PlyG, PlyC, and Pal were raised and mixed *in vitro* with these endolysins and it was found that the killing of bacterial targets was slowed, but not terminated (Fischetti, 2005; Loeffler & Fischetti, 2003). In another study, mice were injected with Cpl-1 three times a week for four weeks resulting in positive IgG production against Cpl-1. However, when *S. pneumoniae* was given intravenously to immunized and naïve mice followed by Cpl-1 treatment, there was no significant difference between the two groups regarding the reduction of bacteria (Loeffler & Fischetti, 2003). Similarly, multiple enzymes have been shown to display the same efficacy in the presence or absence of high titer antibodies (Fischetti, 2010; Jado et al., 2003; Rashel et al., 2007). Taken together, the data suggest that specific

antibodies are developed to endolysins *in vivo* but they do not neutralize their hydrolytic activity.

Like antibiotics, the synergy effect has been noted for multiple PG hydrolases in combination with other PG hydrolases or antibiotics. The pneumococcal endolysin Cpl-1 displayed synergy with either the Pal pneumococcal endolysin or traditional antibiotics like penicillin (Djurkovic et al., 2005; Jado et al., 2003; Loeffler & Fischetti, 2003). The *S. aureus* endolysin, LysK, displayed synergy with the bacteriocin lysostaphin in a checkerboard assay (Becker et al., 2008), even on strains normally resistant to lysostaphin. To conclude, most synergy effects were observed between the endolysins targeting different bonds in PG and the combined use of endolysins with antibiotics may slow down the development of resistance.

A biofilm is a growth phenotype of a bacterial community that grows as a thick mat on a solid or liquid surface in order to protect the community from environmental stress, such as antimicrobials or limited nutritional sources. Several studies have described the effectiveness of endolysins at dispersing the biofilm and killing the bacteria (Kokai-Kun et al., 2009; O'Flaherty et al., 2005; Sass & Bierbaum, 2007; Shen et al., 2013; Son et al., 2010; Walencka et al., 2005; Wu et al., 2003; Yang et al., 2016). The endolysins Φ11, SAL-2, PlyGRCS, LysK, and lysostaphin have all been shown to eliminate static staphylococcal biofilms. PlyC can eliminate both static and dynamic *S. pyogenes* biofilms. An engineered endolysin, ClyR, can eliminate a *S. mutans* biofilm under both physiological and cariogenic conditions. These results suggest that endolysins are a potential new weapon for eliminating biofilms.

Endolysins-Related Applications (Medicine, Food Safety, Disinfectant)

Although phage therapy was used to treat bacterial infections in the 1920s before the discovery of antibiotics and the phage endolysins have been studied, purified, and used a laboratory tools for cell wall extraction since the 1970s, it was not until the 2000s when researchers started to investigate the use of endolysins as antimicrobials. The first study supporting this role and showing *in vivo* efficacy was done at Rockefeller University by Nelson *et al.* (Nelson et al., 2001). It was discovered that oral administration of a streptococcal phage endolysin, later named PlyC, could prevent and treat upper respiratory colonization in mice by *S. pyogenes*. Later, more endolysins were tested *in vivo* to validate these enzymes as candidate therapeutics for the treatment of bacterial infections. Nasopharyngeal colonization of mice by *S. pneumoniae* could be eliminated by a single dose of the specific enzyme Pal within 5 h (Loeffler et al., 2001). In another study, a different *S. pneumoniae* endolysin, Cpl-1, was proven to be effective both in a mucosal colonization model and in a systemic bacteremia model (Loeffler et al., 2003). One endolysin targeting group B streptococci, PlyGBS, could significantly reduce bacteria in a vaginal and oropharyngeal colonization model (Cheng et al., 2005).

The use of endolysins was expanded to include bacterial infection caused by bacteria other than streptococci. PlyG, an endolysin from γ-phage of *Bacillus anthracis*, displayed the ability to protect 70-80% of infected mice when injected with *B. anthracis* spores (Schuch et al., 2002). By 2000, methicillin-resistant *S. aureus* (MRSA) had become an emerging public health threat and several studies focused on endolysins targeting both planktonic cell and biofilms of *S. aureus*. The first anti-

MRSA study was done with MV-L, endolysin from the ΦMR11 phage (Rashel et al., 2007). *In vivo*, this enzyme was shown to reduce MRSA nasal colonization by 3 logs and protect 100% of mice in an intraperitoneal model. More *staphylococcal* endolysins, such as LysK and LysGH15, were then shown to be effective against MRSA *in vivo* (Fenton et al., 2010; Gu et al., 2011). Recently, two drugs compositions containing endolysins are in Phase 2 clinical trials against staphylococcal infections (SAL200 and CF-301).

In addition to directly killing bacteria as antimicrobials, the CBDs of endolysins can be fused to the Fc region of human IgG to create a targeted immunotherapeutic. One study by Raz et al. created a "lysibody" by fusing the CBDs of endolysins targeting MRSA to the Fc region of human IgG. These lysibodies induced the fixation of complement on the surface of the staphylococci and promoted phagocytosis by macrophages and neutrophils (Raz et al., 2017). This was the first published study to exploit the high binding affinity of CBDs to eliminate bacterial infections. This approach provides another possibility of using endolysins as anti-infection therapeutics.

Endolysins can also be used for detection and control of foodborne pathogens. As stated above, the CBDs of endolysins are specific for their targets with high affinity. These advantages have made CBDs good candidates for detection tools. One example is the use of *Listeria* phage endolysin CBDs. Kretzer et al. took advantage of these features designing a CBD-based magnetic separation tool for detection of *Listeria* (Kretzer et al., 2007). This method was better than the conventional plating method in both accuracy and efficacy. Purified endolysins can also be used as

biopreservatives. Obeso et al. showed an endolysin (LysH5) effectively killed *S. aureus* in cow milk with a reduction of 8 log units compared to the control (Obeso et al., 2008). Additional endolysins and engineered endolysins, such as B30, Ply700, λSA2E-Lyso-SH3b, have likewise shown antimicrobial activity in milk or milk products (Celia et al., 2008; Mayer et al., 2011; Schmelcher et al., 2015). Moreover, the *Listeria* phage endolysins Ply118, Ply511, and PlyP35 are promising agents to decrease the number of bacteria on solid surface of food products (Zhang et al., 2012). An alternative approach to control foodborne pathogens is the production of endolysins by recombinant starter organisms. Engineered probiotics can harbor endolysin genes on interest, and under certain circumstances the probiotics can be triggered to produce endolysins targeting pathogens. This application has been used in the food fermentation process (Rodriguez-Rubio et al., 2012). Although there are still limitations of endolysin applications in food safety due to the complex matrix of food products and limited accessibility, these studies are still valuable for further endolysins development.

Another use of endolysins is for the decontamination of environmental pathogens. The chemical disinfectants have drawbacks of being toxic and/or corrosive due to reactive chemical groups. Endolysins do not depend upon the chemically toxic reactive groups, and as proteins, they are biodegradable and non-corrosive. Research done by Hoopes et al. demonstrated the potential of a streptococcal endolysin, PlyC, to be used as a disinfectant against *Streptococcus equi*, which is transmitted through the shedding of live bacteria by horses and drainage onto surfaces in stalls or barns. PlyC was found more active than commercial

disinfectants with 1 μg of PlyC able to sterile 10^8 CFU/ml *S. equi* within 30 min (Hoopes et al., 2009). Because an endolysin disinfectant is considered a "green" disinfectant, it could have applications in nursing homes, surgical suites, meat-packing facilities, and child care settings.

1.4 PlyC, A Unique Multimeric Streptococcal Endolysin

PlyC, an endolysin derived from streptococcal C1 phage, is an evolutionary outlier of all discovered endolysins due to its unique molecular structure and noteworthy lytic activity (Nelson et al., 2003). First discovered in 1957, lysates of the C1 phage containing PlyC were capable of lysis of Group A, Group C, and Group E streptococci (Krause, 1957). During the past 50 years, the studies of the genomics, methods of purification, protein structure, *in vivo* and *in vitro* anti-streptococcal efficacy have demonstrated PlyC as one of the most potent endolysins (Fischetti et al., 1985; Nelson et al., 2001; Wheeler et al., 1980).

Unique High Bactericidal Activity

Since the discovery of PlyC, it has been used as a laboratory tool for isolating peptidoglycan-associated proteins and extracting DNA from GAS (Fischetti, 2018). The first study of PlyC, then called the C1 lysin, focusing on anti-streptococcal activity was published in 2001 by Nelson et al. In this study, both *in vitro* and *in vivo* activity were assessed (Nelson et al., 2001). For the *in vitro* study, PlyC was diluted to from 1,000 U to 10 U and challenged with 10^6 CFU/ml of GAS. 1,000 U of PlyC

completely sterilized cultures in 5s, whereas 100 U of PlyC could reduce the bacterial viability by 3 logs in 5 s, 4 logs in 1 min, and 6 logs in 10 min (Figure 1-5 B). The killing mechanism of PlyC is via the disruption of PG resulting in the osmotic lysis of the bacterial cells (Figure 1-5 A).

The lytic profile of PlyC was also analyzed *in vitro*. Representative streptococcal strains were exposed to 250 U of the purified PlyC. As expected, PlyC displayed lytic activity against all GAS strains tested, consisting of the serological grouping strain, an M protein-negative strain, 8 unique M protein types, and an A-variant strain. Also, PlyC was also effective against GCS, and GES (Nelson et al., 2001).

For the *in vivo* study, a murine model was used. In the first experiment, 1,000 U of PlyC or buffer was premixed with GAS *in vitro* and then orally and nasally administered to 5 mice. None of the PlyC-treated mice were colonized after 24 h. In the second experiment, 21 mice were pretreated orally with 250 U PlyC before challenge with 10^7 GAS to confirm the prevention ability of PlyC. In these two experiments, PlyC showed a protective effect against bacterial infection. In the third experiment, 9 mice were heavily colonized by GAS for 4 days. With 500 U of PlyC, the bacteria from all treated mice were eradicated after 24 h (Figure 1-5 C).

A

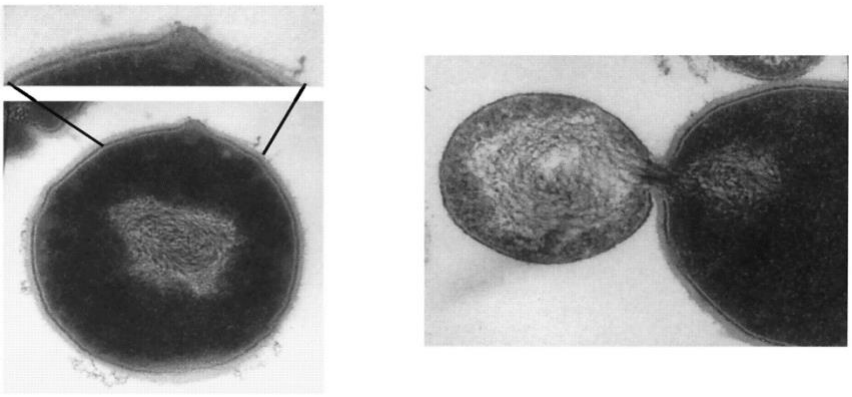

B

Lysin units	Starting count	5 sec	30 sec	60 sec	5 min	10 min
1,000	5×10^6	0	0	0	0	0
100	8.6×10^6	1,530	1,196	771	64	6
10	9.8×10^6	>3,000	>3,000	>3,000	>3,000	>3,000

Indicated numbers are cfus.

C

Mouse	Strep (10^7) ↓	Day 1	Day 2	Day 3	Day 4	Lysin ↓	Postlysin treatment: Day 4, 2 hr	Day 5, 24 hr	Day 6, 48 hr
1		>300	>300	>300	>300		0	0	200*
2		>300	>300	>300	>300		0	50*	0
3		>300	>300	>300	>300		0	0	0
4		>300	>300	>300	>300		0	0	0
5		>300	>300	>300	>300		0	Dead	Dead
6		>300	>300	>300	>300		0	n.d.	0
7		>300	>300	>300	>300		0	n.d.	0
8		>300	>300	>300	>300		0	n.d.	0
9		>300	>300	>300	>300		0	n.d.	0
Total colonized		9/9	9/9	9/9	9/9		0/9	2/5	2/9

n.d., no data collected; indicated numbers are cfus..
*Isolated streptococci remained sensitive to lysin treatment *in vitro*.

Figure 1-5. *In vitro* and *in vivo* efficacy of PlyC against GAS. (A) Thin-section electron micrograph of PlyC-treated GAS for 15 s. (B) *In vitro* analysis of PlyC against GAS. (C) *In vivo* analysis of PlyC elimination of GAS. Taken from (Nelson et al., 2001).

Unique Multimeric Structure

In 2001, PlyC was shown to be a potential antimicrobial agent based on the *in vitro* and *in vivo* studies, but little was known about the enzyme itself. In 2006, Nelson et al. dissected the catalytic domain and cell binding domain of PlyC, and first proposed a multimeric structural model (Nelson et al., 2006). Unlike other endolysins derived from phage infecting Gram-positive bacteria, PlyC was shown to be encoded by two genes, *plyCB* and *plyCA.* The gene of *plyCB* encodes a 72 aa protein product with the molecular mass of ~8 kDa, and the gene of *plyCA* encodes a 465 aa protein product with a molecular mass of ~50 kDa. Interestingly, a simple 1:1 heterodimer model of PlyCA and PlyCB does not rationalize the ~114 kDa mass of the native PlyC as determined by dynamic light scattering. In contrast, 8 PlyCB/1 PlyCA or 2 PlyCB/2 PlyCA stoichiometric models would fit the observed mass of PlyC. The polypeptide-extinction coefficient was then calculated to further validate the model, and confirmed a stoichiometric assumption of the 8:1 holoenzyme model.

Pfam database analysis revealed a putative C-terminal CHAP domain of PlyCA, indicating that PlyCA would contain the potential catalytic domain. Alignment of PlyCA against known members of the CHAP family suggested that Cys-333 and His-420 were the putative active-site residues. Thus, site-directed mutagenesis of cysteine to serine (C333S) and histidine to alanine (H420A) were made and the mutants PlyC (PlyCA) C333S and PlyC (PlyCA) H420A were shown to have significantly reduced lytic activity, about 1% activity compared to wide-type PlyC (PlyCA) (Figure 1-6A). As controls, the mutations of other cysteine residues did not affect the activity.

Therefore, these results confirmed that Cys-333 and His-420 are the active sites and the CHAP domain in PlyCA serves the role as the EAD in the native PlyC.

PlyCA alone cannot lyse the bacteria cell (<1% WT activity), so PlyCB was hypothesized to act as the CBD of the native PlyC that brings PlyCA to the cell surface. To validate this, PlyC (PlyCA) C333S and PlyCB were purified and fluorescently labeled, added to bacteria, and observed for cell binding via fluorescence microscopy. Purified PlyCB self-assembled into an octamer with a mass of 64 kDa based on analytical gel fitration. The microscope pictures confirmed the hypothesis that PlyCB is the CBD. Both PlyC (PlyCA) C333S and PlyCB could decorate the surface of *S. pyogenes* cell walls (Figure 1-6 B and C), but no other bacteria were sensitive to PlyC (Figure 1-6 D).

The crystal structure of PlyC was solved by McGowan in 2012 (McGowan et al., 2012). This structure confirmed the hypothesis that PlyC contains nine subunits, eight PlyCB monomers for each PlyCA (Figure 1-7 A). In addition to a previously known CHAP domain, a glycoside hydrolase domain (GyH) was revealed as a second catalytic domain in PlyCA, and furthermore, it is shown to work synergistically/cooperatively with the CHAP domain to achieve the unusually high activity noted for PlyC. A docking domain of PlyCA between the two EADs (yellow in Figure 1-7A) forms an antiparallel bundle of three α-helices, which interacts with the N-terminus of the eight PlyCB subunits to form the PlyC holoenzyme. Eight PlyCB monomers arrange into an octameric ring with a diameter of 80 Å and a height of 20 Å (Figure 1-7 B).

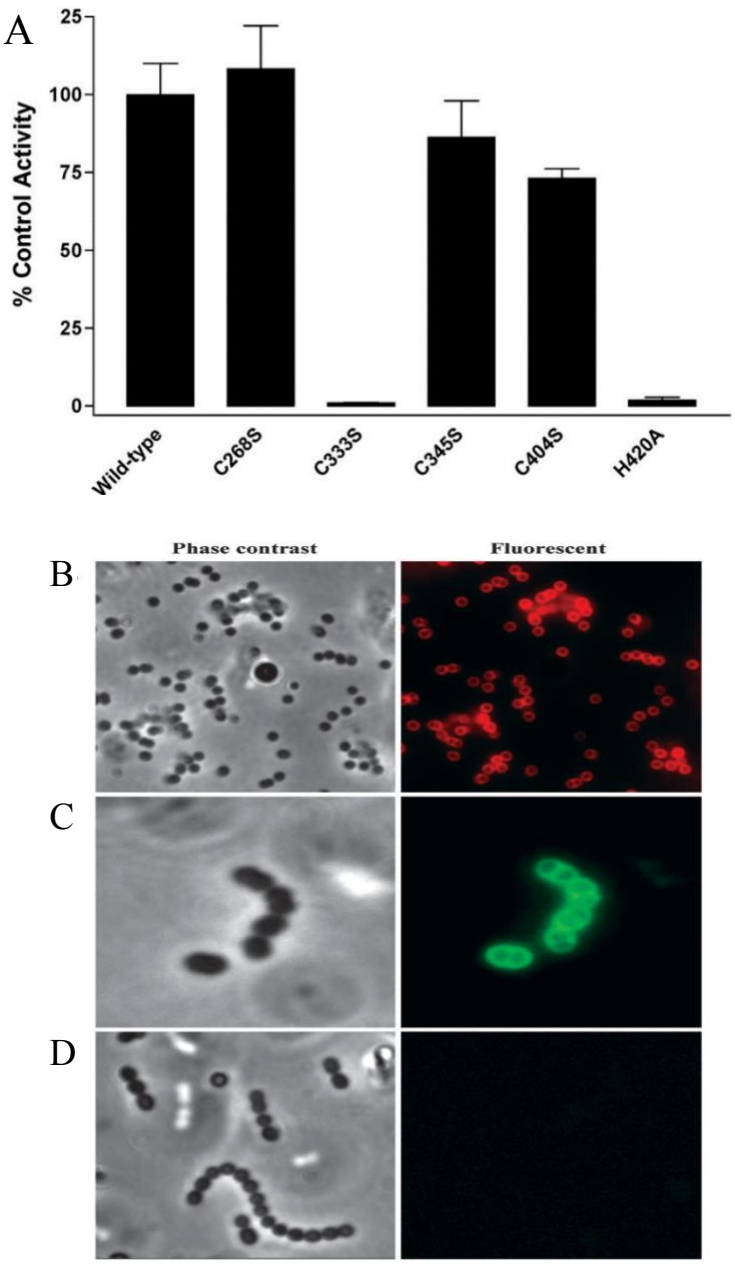

Figure 1-6. PlyCA contains the catalytic domain and PlyCB contains the cell wall binding domain. (A) PlyCA mutants C333S and H420A displayed no activity. (B) PlyC (PlyCA) C333S conjugated to AlexaFluor-568 specifically labels *S. pyogenes*. (C) PlyCB conjugated to AlexaFluor-488 specifically labels *S. pyogenes*. (D) Fluorescent PlyCB cannot label strains insensitive to PlyC. Taken from (Nelson et al., 2006).

Each PlyCB monomer contains a four-stranded β-sheet in the middle of a short α-helix at each side (Figure 1-8 A). It displays no significant sequence similarity to any other protein and, thus, presents a rare example of a CBD. The oligomerization of PlyCB is mediated through strand/helix hydrogen bonding interactions at each surface (Figure 1-8 C). Mutational data reveals that each PlyCB monomer contains potential binding sites for cell wall components (Figure 1-8 A and B). Modulation of the PlyCB CBD may lead to enhancement of binding properties and subsequent activity. Specifically, it is unknown whether all eight PlyCB monomers participate in binding or whether the presence of all eight merely increased the avidity of the interaction. Importantly, point mutagenesis has shown that the key residues involved in binding are on the monomer surface rather than at the monomer/monomer junction, which interacts through intersubunit hydrogen bonds (Figure 1-8 A and C).

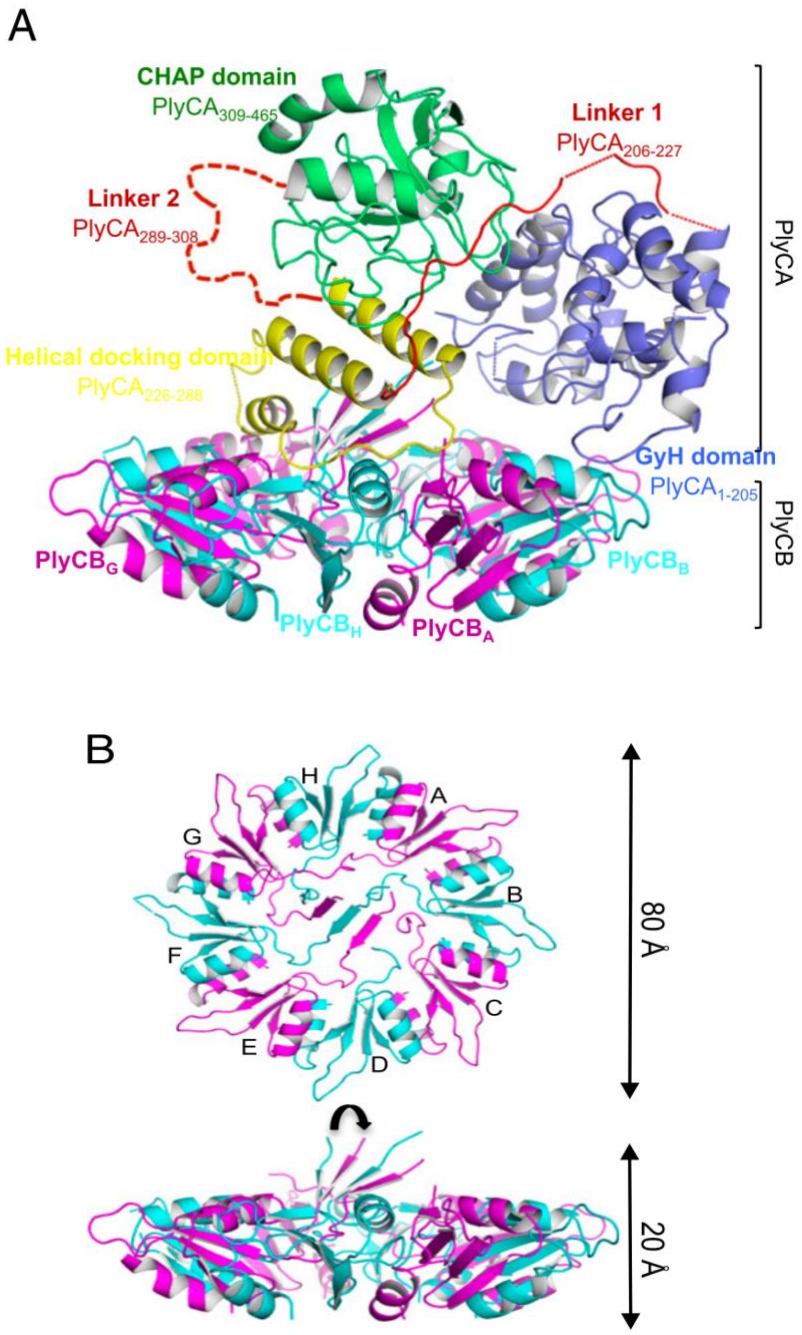

Figure 1-7 Structure of PlyC. (A) The 3.3Å X-ray crystal structure of PlyC consists of eight PlyCB subunits for each PlyCA. The PlyCB monomers are colored alternately and labeled as monomers A-H. The PlyCA subunit is colored by domains as indicated. (B) PlyCB alone colored alternately by monomers. (PlyCB PDB: 4F87, PlyC PDB: 4F88) Taken from (McGowan et al., 2012).

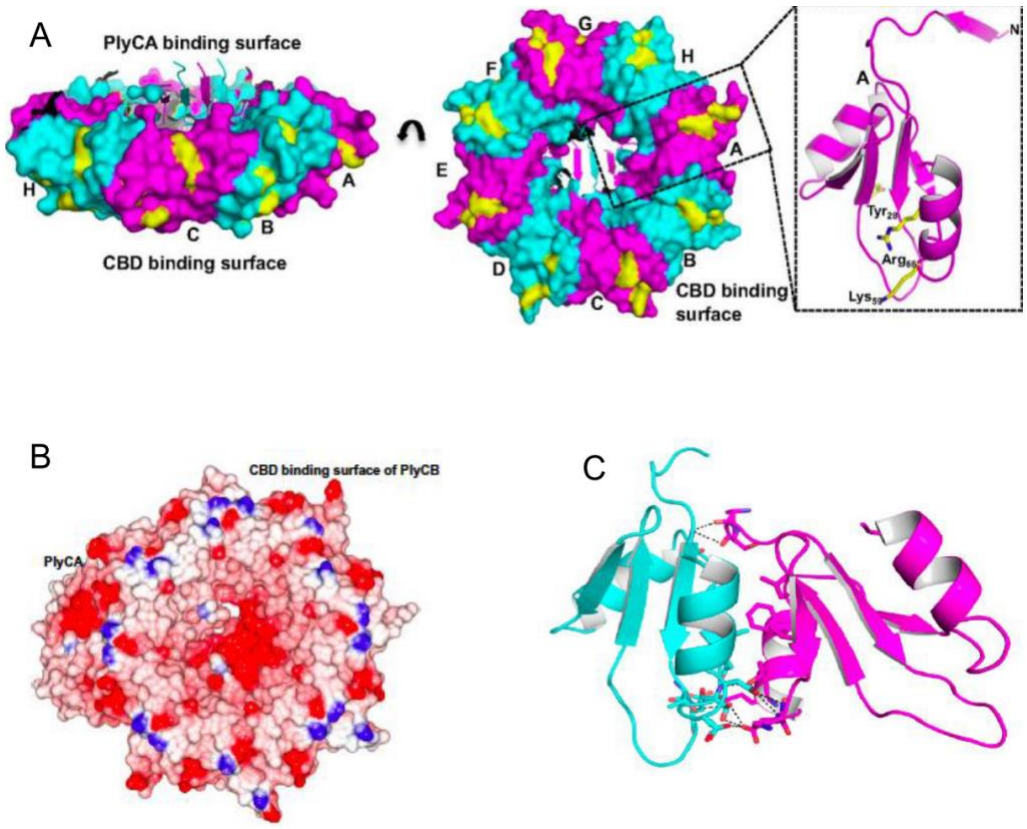

Figure 1-8. PlyCB dissection. (A) PlyCB has eight cell-wall binding grooves. The cell-wall-binding surface of PlyCB alone shows the residues involved in cell wall binding in yellow. Cartoon depiction of PlyCB monomer A shows cell wall binding residues in yellow sticks as indicated. (B) The electrostatic surface potential of PlyCB. Lys and Arg residues were assigned a single positive charge, and Asp and Glu residues were assigned a single negative charge. Blue color indicates positive potential charge, and red color indicates negative potential charge. The binding grooves are positively charged. (C) The 1.4Å X-ray crystal structure of PlyCB monomer/monomer interface. The interaction is mediated by 12 H-bonds. (PlyCB PDB: 4F87) Taken from (McGowan et al., 2012).

1.5 Engineering of Bacteriophage Endolysins

Bacteriophage optimize endolysins for lytic activity through coevolution with bacterial hosts to ensure phage survival. When applied as recombinant proteins exogenously, endolysins are being used for a different purpose, and therefore, lose this evolutionary pressure. Thus, there exists an engineering potential for endolysins to modify their function to increase activity, alter host range, or overcome complex extracellular environments (Sao-Jose, 2018). As a growing amount of research focuses on the modular designs and crystal structures of endolysins, structure-based rational engineering, such as domain swapping, structure-guided mutagenesis, and chimeragenesis, has produced endolysins with desirable properties for specific applications.

Increasing the Lytic Spectrum and Activity

Chimeragenesis is a potential engineering approach that has been successfully exploited by nature, such as the pneumococcal endolysin Pal, whose two domains indicate homology to different phage species (Sheehan et al., 1997). Chimeragenesis by scientists via domain swapping, later, proved the capability to create engineered endolysins possessing higher activity or an expanded lytic spectrum. Several examples of endolysin engineering are noted below.

Two *Listeria monocytogenes* phage endolysins, Ply118 and PlyPSA, were used for domain shifting to generate fusions with improved capacity (Schmelcher et al., 2011). One of the fusions (EAD118_III_CBDPSA) displayed a 3-fold increase in activity against *Listeria* serovars that were naturally targeted by the parental PlyPSA.

The other chimeric endolysin, PL3, combined the EAD of Pal, a pneumococcal endolysin, and the CBD of LytA, a pneumococcal autolysin, exhibited higher activity and stability than the parental enzymes (Blazquez et al., 2016). Another example is the chimeric pneumococcal endolysin Cpl-711, which is the combination of the EAD from Cpl-7 and the CBD from Cpl-1 (Diez-Martinez et al., 2015). Although both parental enzymes are specific for pneumococci, Cpl-711 showed significant improvement in killing and antibiofilm activity *in vitro* and in a mouse model compared to the parental enzymes.

In some cases, chimeric endolysins may keep the parental activity, but with an expansion of the lytic spectrum. For example, domain swapping between an EAD of the streptococcal prophage λSA2 and the SH3b-type CBD of either LysK or lysostaphin created two new chimeras. LysK and lysostaphin both target staphylococci whereas λSA2 targets streptococci. Both new chimeras (λSA2-E-Lyso-SH3b and λSA2-E-LysK-SH3b) showed 5-fold increased anti-staphylococcal activity when compared to the parental λSA2 endolysin while retaining impressive anti-streptococcal activity (Becker et al., 2009). In another example, the CBD of PlySs2 is recognized as having a broad host spectrum binding domain. Yang et al. fused the CHAP domain of PlyC to the CBD from PlySs2, creating a chimeric enzyme ClyR. This enzyme displayed antibacterial efficacy towards streptococcal, enterococcal, and staphylococcal species similar to PlySs2, but also had activity against species that PlySs2 does not work on, such as *S. mutans* (Yang et al., 2015).

Many EADs require the presence of the CBD for binding and subsequent activity. For example, PlyCA displays no activity without PlyCB, however, some

EADs can bind the bacterial surface independently of CBD. One example is staphylococcal endolysin LysK. The LysK EAD, a cysteine-histidine amidohydrolase/peptidase domain (CHAP), displays higher lytic activity against live clinical staphylococcal isolates than the full-length LysK (Horgan et al., 2009). The other example is the clostridial endolysin CD27L, where deletion of the CBD not only increases lytic activity against *Clostridium difficile* stains compared to full-length CD27L, but the host range is extended to include *listerial* strains that are not sensitive to CD27L (Mayer et al., 2011). These cases indicate that the modular design of endolysins active against Gram-positive organisms are similar but are not necessarily limited to one model and domain deletions are a method to increase lytic spectrum and activity. As mentioned above, not all EADs display activity in the absence of the CBDs, thus, there remains a good bit to be learned about the molecular interaction between EADs and CBDs. A study by Low et al. showed that a net positive charge of an EAD enables it to function independently of its CBD, presumably through ionic interactions with the bacterial surface, which typically has a net negative charge due to surface carbohydrates (Low et al., 2011). This conceptual understanding was then applied to endolysin engineering studies for increasing EAD activity and expansion of host range. For example, the EAD of the *B. subtilis* phage endolysin, XlyA, has a net charge of Z=-3 at neutral pH. Site-directed mutagenesis of five non-cationic residues to lysine (K) produced a shift in net charge from Z=-3 to Z=+3, and the mutated XlyA EAD was able to lyse *B. subtilis* cells at a rate nearly identical to that of full-length XlyA. Currently, it is unknown if this principle applies to all EADs with a net negative charge. However, using this principle to delete a CBD

to make a smaller enzyme may also serve to increase the efficacy where size may be a limiting factor. For example, the S-layer of *B. anthracis* acts as a molecular sieve, and the positively charged EAD from PlyL was shown to display higher lytic activity than the full-length PlyL. Additionally, change of the net charge of the CBD could also enhance the lytic activity of the enzyme. Cpl-7 is a pneumococcal endolysin but presents much lower bacteriolytic activity when compared to other pneumococcal enzymes, such as Cpl-1 and Pal (Diez-Martinez et al., 2013). After Low et al. 's study, Díez-Martínez et al. found that the CBD of Cpl-7 possesses a negative charge at neutral pH. Moreover, they changed the net charge of the CBD from -14.93 to +3 via site-directed mutagenesis of 13 non-structural amino acids. The new mutant was called Cpl-7S, and it displayed improved bactericidal activity against pneumococcal and non-pneumococcal species when compared to its parental enzyme (Diez-Martinez et al., 2013).

Improving the Stability

A crucial property for development of endolysins as therapeutic agents is the shelf-life relating to its intrinsic thermal stability. Many naturally thermostable endolysins have been discovered, such as the Ph2119 endolysin, which retains 87% of its activity after 6 h of incubation at 95°C (Plotka et al., 2014), a *Salmonella* phage endolysin, Lys68, which is not completely inactivated until it is exposed to 100°C for 39 min (Oliveira et al., 2014), a *Clostridium* endolysin, LysCPS2, which retains 30% of its lytic activity after 10 min of incubation at 95°C (Ha et al., 2018), and a *Bacillus* endolysin, PlyG, which retains 50% of lytic activity after being heated to 80°C

(Heselpoth et al., 2015). However, most endolysins are easily denatured at mesophilic temperatures. One way to engineer stability to an endolysin is via chimeragenesis to increase thermostability. For example, the chimera containing the EAD of the thermostable endolysin PlyGVE2 and the CBD of PlyCP26F not only retains the host range of PlyCP26F towards to *C. perfringens*, but also preserved more than 57% of its lytic activity after incubation for 30 min at 55°C, comparing to the total loss of activity for the parental endolysin PlyCP26F under the same conditions (Swift et al., 2015).

In addition to chimeragenesis, random mutagenesis with selective pressure is another method used by bioengineers to integrate thermostability into endolysins. One example is the multimeric domain endolysin, PlyC. A heating experiment ranging from 37°C-100°C demonstrated that PlyC irreversibly denatured at 42°C. Interestingly, the T_G of PlyCB is 75°C, whereas the T_G of one of the catalytic domains, CHAP, in PlyCA is around 39.1°C, suggesting that this domain is the most heat-susceptible structural element. A study done by Heselpoth et al. used a random mutagenesis method based on the error-prone PCR, followed by a selective screening for the mutants with enhanced thermostability. The 29C3 mutant displayed more than a 2-fold increase in stability at 45°C (Heselpoth & Nelson, 2012). In a parallel study, the Heselpoth took advantage of bioinformatic tools to predict the mutation and one of the mutants, PlyC (PlyCA)T406R, illustrated a 16-fold increase in stability and an increased denaturation temperature by 2.2°C compared to the WT PlyC (Heselpoth et al., 2015).

Another important consideration for therapeutic development of endolysins is their half-life in the bloodstream. Research done by Resch et al. aimed to increase the half-life of the endolysin, Cpl-1 (Resch et al., 2011). They discovered that the dimerization of a Cpl-1 mutant (Cpl-$1^{C45S, D324C}$) via the disulfide bonding displayed a 10-fold decrease in plasma clearance in mice compared to native Cpl-1, while doubling the lytic activity of Cpl-1 at the same time. This method worked because the size of the dimeric endolysin is 74kDa, while proteins below 45-50kDa tend to be cleared from plasma by renal filtration. The same result can be achieved via the addition of non-immunogenic polymers to the endolysins. One example is the addition of conjugated poly-L-lysine polycationic polymers to lysostaphin, which resulted in reductions of immunogenicity, proteolysis, and instability (Veronese & Mero, 2008; Walsh et al., 2003).

Reducing the Resistance Possibility

In the previous section, bacterial resistance to endolysins has been thoroughly discussed. Endolysins specifically cleave the essential bonds in the PG within seconds, and several studies support that repeated exposure of bacteria to endolysins does not affect the MIC. These facts support that emergence of resistance to endolysins should be rare. Moreover, a great number of phage endolysins possess dual lytic domains, which are predicted to be more difficult to develop resistance (Fischetti, 2005). With the inspiration of the dual lytic domains, the Donovan laboratory has taken a more advanced step to create three lytic domains in one endolysin, aiming to further reduce the resistance possibility (Becker et al., 2009). In this study, they engineered triple-

lytic-domain constructs using the enzymes LysK and lysostaphin; two PG hydrolases well-known to be active against several MRSA strains. The authors created fusions of the two lytic domains of LysK and the lytic domain of lysostaphin, in two combinations that were capable of cleaving three different. LysK-Lyso, two lytic domains of LysK to the N-terminal of lysostaphin, and Lyso-LysK, two lytic domains of LysK in the middle of lysostaphin, were created. In an assay to evaluate the resistant development *in vitro* against *S. aureus* strain Newman, the parental enzyme's MIC increased 42-fold and 585-fold, respectively. In contrast, LysK-lyso and lyso-LysK yielded only 8-fold and 2-fold increases in MIC, respectively.

Enhancing the Activity against Gram-Negative Bacteria

Due to the protection of the outer membrane of Gram-negative bacteria, native endolysins cannot cleave the peptidoglycan "from without" unless there is a disruption and/or translocation of the outer membrane. Concerning protein engineering strategies, two principal methods have been applied to improve outer membrane penetration by endolysins.

One engineering method is to provide the enzyme with a binding capacity for the receptor on the outer membrane. The first successful engineering effort to create an endolysin active against a Gram-negative organism was done by Lukacik et al., who creating an engineered T4 lysozyme that killed *E. coli* via fusion of the N-terminal binding domain of pesticin (Lukacik et al., 2012). Pesticin is a bacteriocin produced by *Yersinia pestis* that specifically binds to the outer membrane transporter FyuA. FyuA is a major virulence factor in some pathogenic *E. coli* strains. The engineered

T4 lysozyme with an N-terminal FyuA binding domain could bind to FyuA, was transported across the outer membrane to the periplasmic space, and resulted in cleaves of the PG by the T4 lysozyme.

An alternative method is to arm the endolysin with membrane-penetrating peptides that can disrupt the lipopolysaccharides (LPS) and some phospholipids. These studies were done extensively by Briers and Lavigne, and the engineered endolysins were called "Artilysin®", for artificial lysin (Briers & Lavigne, 2015). The most successful examples have fused the endolysin from *Pseudomonas fluoresens* and *Salmonella enterica*, OBPgp279 and PVP-SE1gp146, with a polycationic nonapeptides to the N-terminus (Briers et al., 2014). Both artilysins displayed improved antibacterial effects against *P. aeruginosa* and expanded efficacy against *A. baumanni*. Further refinements to adjust the flexibility of the artilysins via increasing linker length between the peptide and enzyme resulted in even higher activity. Remarkably, several follow-on studies suggested that artilysins also displayed potent bactericidal activity against multidrug-resistant strains and bacterial persisters (Gerstmans et al., 2016).

1.6 Purpose of Research

Given the unique structure and high activity of PlyC, there is much interest in understanding the mechanism that governs this enzyme as well as approaches that can be used to modify its properties and activity. With a long-term goal of exploiting the specialties of PlyC on more bacterial species as a new antimicrobial agent, custom engineering methods based on its structure should be developed. This dissertation

focuses on engineering methods for PlyC as well as the outcomes that can then be further applied. A structure-guided, site-directed mutagenesis method is applied to create monomeric PlyCB in order to understand the binding mechanism and creating a specific CBD for chimeragenesis (Chapter II). A novel design strategy to apply the synergy of the PlyCA dual lytic domains led to several potent engineered endolysins active against other streptococci (Chapter III). Finally, a hypothesis of the role of protein net charge has been tested using the negatively charged PlyCA CHAP domain as a model (Chapter IV). Taken together, the bioengineering strategies contained in this dissertation provide a better understanding of the PlyC mechanism of action while at the same time suggests several strategies for improving or expanding the lytic properties of PlyC.

Chapter 2: Structure-Guided Mutagenesis of PlyCB – Dissecting the Binding Mechanism

2.1 Abstract

Bacteriophage endolysins are murein hydrolases produced at the end of the phage replication cycle and have been studied as novel antibacterial therapeutic agents. PlyC, an endolysin from the C1 streptococcal bacteriophage, possesses the most potent activity towards specific streptococcal hosts. Structural and biochemical studies reveal the molecular basis behind this potency: PlyC is a holoenzyme consisting of one enzymatically active domain (PlyCA) and eight identical cell binding domains (PlyCB) that self-assemble into an octamer, which represents a unique structural arrangement not seen in any other endolysin. Despite detailed structural information, there remain questions on the binding mechanism of the PlyCB octamer and how it affects the lytic activity. Here, we demonstrate that the native PlyCB octamer can be engineered to a PlyCB monomer (PlyCBm) through structure-guided mutagenesis that breaks hydrogen bonds between PlyCB octamer subunits. Tandem duplication of the PlyCB monomer (PlyCB2m) is then created to further analyze the binding. Gel-filtration and protein cross-linking confirm the mass of PlyCBm and PlyCB2m, and fluorescence microscopy validates that they retain the same binding capability to streptococci as the PlyCB octamer. In addition, the comparison of EC_{50} among PlyCBm, PlyCB2m, and PlyCB octamer suggests a concurrent binding model for the PlyCB octamer. The PlyCBm/PlyCB2m-derived chimeras provide a rationale to further study the relations between binding affinities

and lytic activities. Finally, the observations that PlyCBm translocates epithelial membranes and, with an enzymatically active domain, kills intracellular *S. pyogenes* D471, suggest PlyCBm possesses multiple functions that can be exploited for further bioengineering studies.

2.2 Introduction

The development of alternative antimicrobial agents is one of the highest global priorities in biological, pharmaceutical, and medical investigations due to the ever-growing concern of antibiotic resistance (Brown & Wright, 2016). One class of alternative antimicrobial agents that has attracted increasing attention is endolysins, also termed phage lysins or enzybiotics, which are bacteriophage-encoded peptidoglycan hydrolases (Fischetti, 2008). They are produced at the end of the phage replication cycle resulting in bacterial cell lysis and new phage release. In addition, these enzymes are also capable of destroying the Gram-positive bacterial peptidoglycan (PG) when applied extrinsically as recombinant proteins (Fischetti et al., 2006). As antimicrobial agents, endolysins feature a defined host spectrum and kill bacteria regardless of their antibiotic sensitivity (Fischetti, 2008).

The structure of endolysins that act on Gram-positive organisms mostly features a similar modular design with an enzymatically active domain (EAD) at the N-terminus fused via a short linker to a cell-binding domain (CBD) at the C-terminus (Fischetti, 2005; Loessner, 2005). The CBD binds to distinct epitopes on the bacterial cell wall, faciliating hydrolysis of the PG bonds by the EAD.

The streptococcal phage C1 endolysin, known as PlyC, possesses the highest activity of any endolysin reported to date and it is a rare example of a multimeric endolysin (McGowan et al., 2012; Nelson et al., 2001; Nelson et al., 2006). Biochemical and biophysical characterization of PlyC reveal that it is a holoenzyme composed of nine proteins: eight 8 kDa PlyC cell binding domain subunits (PlyCB) and one 50 kDa enzymatically active subunit (PlyCA) (Nelson et al., 2006). PlyCB and PlyCA are encoded by two separate genes, *plycB* and *plycA*, respectively, which is a distinctive feature that separates PlyC from all other endolysins. Furthermore, PlyCA contains two catalytic domains, CHAP and GyH, which work synergistically to achieve the noted high rate of bacteriolytic activity. The eight PlyCB subunits self-assemble in an octameric ring-shaped structure that interacts with PlyCA via unique protein-protein interaction (McGowan et al., 2012). Like CBDs of other endolysins, the PlyCB octamer defines the host range of PlyC to groups A, C, E streptococci and *Streptococcus uberis*, which cause diseases in both human and animals (Nelson et al., 2006). In addition to binding the surface of streptococcal cells, PlyCB is also capable of binding to phosphatidylserine on the plasma membrane of eukaryotic cells and mediates PlyC internalization, allowing activity of the holoenzyme against intracellular streptococci (Shen et al., 2016). These features make PlyCB an exceptional example of an endolysin CBD.

Despite substantial study on PlyC, many questions remain on the binding mechanism and binding epitopes of PlyCB. The streptococcal binding site of PlyCB is found on each subunit, and there are thus eight binding sites on the PlyCB octamer. Point mutagenesis has shown that the key residues involved in binding are on the

monomer surface rather than at the monomer/monomer junction, which interacts through inter-subunit hydrogen bonds. However, it is unknown whether all eight PlyCB monomers participate in binding. Concurrent binding may lead to enhancement of binding properties and subsequent activities, whereas a consecutive interaction may result in a more fleeting binding (McGowan et al., 2012).

Here, the PlyCB monomer (PlyCBm) and a duplication of the PlyCB monomer (PlyCB2m) were created via structure-guided mutagenesis to study the binding mechanism of the PlyCB octamer. In addition, these two new CBDs were engineered with an N-terminal EAD to evaluate lytic activity on extracellular and intracellular bacteria *in vitro*. The different properties observed for the PlyCBm/PlyCB2m derived chimeras suggested a rationale for optimizing the endolysin activity.

2.3 Materials and Methods

Bacterial Strains and Growth Conditions

Bacterial strains used in this study are listed in Appendix B. *Streptococcus pyogenes* strain D471 was the primary strain for the cell wall binding assay and the turbidity reduction assay, although additional strains were tested as indicated. All strains were stored at -80°C and grown at 37°C. Streptococci were grown in liquid THY medium (Todd-Hewitt broth, supplemented with 1% (wt/vol) yeast extract); staphylococci were grown in TSB medium (trypticase soy broth); and bacilli were grown in BHI medium (brain heart infusion). *Escherichia coli* strains DH5α and BL21 (DE3), containing the constructs, were grown in LB medium (Luria broth) with

kanamycin (50 µg/ml) or carbenicillin (50 µg/ml) in a shaking incubator unless otherwise stated. All chemicals and culture media were acquired from Sigma unless otherwise stated.

PlyCB Octamer Interactions

PyMOL was used to perform the PlyCB structural representations including the H-bonds and the suggested mutations (The PyMOL Molecular Graphics System, Version 2.0 Schrödinger, and LLC). The residues involved in H-bond formation at the interfaces of the PlyCB octameric ring were identified through PDBePISA (Protein Interfaces, Surfaces, and Assemblies) (Krissinel & Henrick, 2007). The 1.4-Å resolution crystal structure of PlyCB (Protein Data Bank ID 4F87) was used for both the PyMOL offline package and the PDBePISA online server.

Cloning and Site-Directed Mutagenesis

The plasmids and primers used in this work are listed in Appendix A. The constructs for pBAD24::*plyCB*, pBAD24::*plyC*, and pBAD24::*plyC*Δ*GyH* were previously described (McGowan et al., 2012; Nelson et al., 2012). An N-terminal His-tag was added to *plyCB* following standard DNA manipulation and cloning procedures (Sambrook, 1989). Plasmids harboring the *plyCB* mutants were constructed by mutagenesis using the QuikChange II Site-Directed Mutagenesis Kit (Agilent Technologies) with phosphorylated primers. The double CBD (PlyCB2m) construct was made via insertion an additional CBD gene downstream of the pBAD24::*plyCBm-N-6His* via XbaI/SalI sites. The quadruple CBD (PlyCB4m)

construct was made via insertion an additional double CBD gene downstream of the pBAD24::*plyCB2m-N-6His* via SalI/PstI sites.

To create a series of PlyCBm/PlyCB2m chimeric proteins, the DNA sequences of the GyH domain ($PlyCA_{1-205}$), CHAP domain ($PlyCA_{309-465}$), and PlyCA subunit were amplified by PCR from pBAD24::*plyC* (McGowan et al., 2012). Likewise, the $CHAP_{LysK}$ domain with linker sequence (1-197aa) and $CHAP_{PlySs2}$ domain with linker sequence (1-161aa) were amplified by PCR from pBAD24::*lysK* and pBAD24::*plySs2*, respectively, which in turn had been chemically synthesized by GenArt ThermoFisher. The $Amidase_{PlyG}$ domain with linker sequence (1-172aa) was amplified by PCR from pBAD24::*plyG* and the $Amidase_{pal}$ domain with linker sequence (1-149aa) was amplified by PCR from pBAD24::*pal*. All of the amplified DNA sequences of the EADs contained first 20 nucleotides of *plyCBm/PlyCB2m* at their 3'ends. Similarly, the DNA sequences of *plyCBm/plyCB2m* were amplified with the last 20 nucleotides of each EAD at the 5' ends. The resulting PCR fragments were joined and amplified by PCR-based Gene Splicing by Overlap Extension PCR (SOE PCR) (Horton et al., 1990; Pease, 1990) before insertion into NdeI/BamHI sites of a pET28a vector. All plasmids encoding recombinant proteins were verified by DNA sequencing before being transformed into the expression strain *E. coli* BL21 (DE3).

Protein Expression and Purification

For overproduction of different constructs, *E. coli* BL21 (DE3) cells were grown in baffled Erlenmeyer flasks at 37°C until the OD_{600} reached 0.6-0.8. Protein expression was induced at 18°C for 20 h with 0.25% L-arabinose for pBAD24

constructs or 0.1 mM isopropyl β-D-thiogalactoside (IPTG) for pET28a (+) constructs. The cells were harvested at 5,000 rpm for 15 min at 4°C and resuspended in PBS, pH 7.4, supplemented with 1 mM phenylmethanesulfonyl fluoride (PMSF) and 10 mM imidazole. The bacteria were sonicated on ice for 15 min, with the insoluble cellular debris subsequently pelleted at 12,000 rpm for 1 h at 4°C. The soluble lysate was applied to a nickel-nitrilotriacetic acid (Ni-NTA) column (Qiagen). Protein samples were eluted from the column using a step gradient consisting of imidazole concentrations ranging from 20 mM to 500 mM in PBS, pH 7.4. The elution fractions were subjected to 7.5% SDS-PAGE before being dialyzed against PBS, pH 7.4, overnight at 4°C. The protein concentrations were determined spectrophotometrically (NanoDrop 2000c) using the theoretical molar absorption coefficient at 280 nm. Purified proteins were stored at 4°C in PBS.

Protein Mass Analysis

PlyCB WT and mutants were characterized for proper folding and mass estimation by analytical gel filtration as previously described (Nelson, D. et al., 2006). Briefly, 500 µl of 2 mg/ml of each sample was subjected to analytical gel filtration on a Superose 12 column (GE Healthcare) calibrated with gel filtration standards (Bio-Rad). The cross-linking experiment was performed using bis(sulfosuccinimidyl) (BS^3) (ThermoFisher) per the manufacturer's instructions. A fresh stock of BS^3 was made in 20 mM sodium phosphate buffer, pH 7.4, then added to 100 µg of purified protein to reach a final concentration of 5 mM/10 mM. The reaction was allowed to react for 1 hour at room temperature and quenched by the

addition of Tris buffer (final concentration of 50mM) for 15 min at room temperature. The crosslinked protein samples were analyzed by 7.5% SDS-PAGE in reduced sample buffer.

Fluorescent Labeling of Proteins

Purified PlyCB, PlyCBm, PlyCB2m, or PlyCB R66E were reacted with the carboxylic acid, succinimidyl ester of AlexaFluor® 555 (Molecular Probes) according to the manufacturer's instructions. Briefly, 1 mg of proteins was mixed with 10 µl of AlexaFluor® 555 dye (2.0 mg/ml in DMSO), then incubated at room temperature for 1 hour with constant stirring. Unreacted dye was removed from the labeled protein by application to a 5 ml HiTrap desalting column (GE Healthcare) equilibrated with PBS.

Cell Wall Binding Assays and Fluorescence Microscopy

Overnight cultures of bacteria were pelleted (5,000 rpm, 10 min, 4°C), washed, and resuspended with PBS, pH 7.4. 100 µl of each bacterial culture was incubated at room temperature with either 10 µg of AlexaFluor® labeled PlyCB or PlyCBm/PlyCB2m containing the 6xHis tag for 10 min. The samples containing PlyCBm/PlyCB2m were washed with PBS and incubated for another 10 min at room temperature with 1 µl of AlexaFluor® 488 conjugated His-tag monoclonal antibody (Invitrogen). Both samples were rewashed with PBS before being visualized via fluorescence and bright field microscopy. Negative controls, bacteria only, and bacteria with unlabeled proteins, were applied. An Eclipse 80i epifluorescent

microscope workstation (Nikon) with X-Cite 120 illuminator (EXFO) and Retiga 2000R CCD camera was used. NIS-Elements software (Nikon) was used for image analysis.

Effective Concentration (EC_{50}) of PlyCB, PlyCBm, PlyCB2m

The EC_{50} was quantified using a whole bacterial ELISA as previously described (Elder et al.), with minor modifications. An overnight *S. pyogenes* D471 culture was treated with 0.4% formalin (υ/υ) for 4 hours at room temperature. Then, the bacterial cells were washed three times and resuspended with PBS, pH 7.4, containing 0.05% (υ/υ) Tween 20 (PBST) to reach a final OD_{600}=1. 100 µl of the bacterial suspension was added to a black 96-well plate with clear bottom coated with poly-D-lysine (Corning Incorporated) and incubated overnight at 4°C. Next morning, plates were centrifuged (4,000 rpm, 10 min, 4°C), and washed three times with PBST. Bacterial adherence was confirmed by scanning with an inverted light microscope, and nearly confluent coverage of all wells was considered satisfactory. The bacteria-coated wells were received 100 µl of serial diluted AlexaFluor® 555 labeled PlyCB WT, PlyCBm, or PlyCB2m, and incubated for 1 h at room temperature covering by aluminum foil. The plate was then washed three times with PBST. Controls included the flowing: *(i)* wells with PBST only, *(ii)* wells with serial diluted unlabeled proteins, *(iii)* wells with bacteria only, *(iv)* wells with serial diluted AlexaFluor® labeled proteins and *(v)* wells with bacteria and AlexaFluor® labeled PlyCB R66E, a mutant known to lack the ability to bind the streptococcal surface. The binding was quantified through fluorescence reading at excitation wavelength

555 and emission wavelength 580 via a SpectraMax M5 Multi-Mode Microplate Reader (Molecular Devices). The fraction bound was calculated using the fluorescence reading of protein-bacteria complexes over the saturated binding signal. EC_{50} was the concentration achieving 50% of binding (fraction bound=0.5). All tests were performed in triplicate.

Turbidity Reduction Assay

Turbidity reduction assays were performed as previously described (Nelson, D. C. et al., 2012). Briefly, overnight bacterial cells (stationary phase) were centrifuged (4,000 rpm, 5 min, 4°C), washed and resuspended in PBS, pH 7.4, and mixed 1:1 (υ/υ) with endolysin to a final OD_{600}=1 in a standard 96-well titration plate (ThermoFisher). OD_{600} readings were taken every 15 sec for 20 min at 37°C on a SpectraMax 190 spectrophotometer (Molecular Devices). The OD_{600} reduction curve and V_{max}, the slope of the linear portion, was used to represent the endolysins activity. All tests were performed in triplicate.

Epithelial Cell Culture and Confocal Microscopy

Human alveolar epithelial A549 cells (Human Lung Carcinoma cell line, CCL-185) were cultured in F-12K medium supplemented with 10% fetal bovine serum (FBS) at 37ºC, 5% CO_2, and 95% relative humidity. The second or third generation of cells was seeded onto 12 mm^2 coverslips in 24-well tissue culture plates. When reaching 80% confluence, cells were washed twice with PBS before incubation with 20 µg/ml AlexaFluor® labeled PlyCB or PlyCBm in serum-free

medium for 30 min. The cells were again washed three times with PBS, fixed by 4% paraformaldehyde, and mounted with ProLong® Gold Antifade Reagent with 4',6-diamidino-2-phenylindole (DAPI) on glass slides for microscopic examination using an inverted scanning confocal microscope with Argon laser excitation (Carl Zeiss LSM 710). Images and Z-stacks were obtained with a Plan Apochromat 100×/1.4 objective lens and analyzed with the Zen 2010 digital imaging software (Carl Zeiss).

Streptococci/Epithelial Cell Co-culture Assay

The co-culture assay was conducted as previously described (Shen et al., 2016). Briefly, lung epithelial cells A549 were grown to 80% confluent monolayers in 24-well tissue culture plates. An overnight culture of *S.pyogenes* D471 was washed in sterile PBS, pH 7.4, and then, resuspended in serum-free media and incubated with epithelial cells at a multiplicity of infection of 100 bacterial cells per one epithelial cell for 2 h. 10 μg/ml penicillin and 200 μg/ml gentamicin were added to the co-culture for 1 hour to kill non-adherent and adherent bacteria. Different amounts of endolysins were added to the post-antibiotic treated co-culture and incubated for two hours. Epithelial cells were detached by 100 μl of a 0.25% trypsin/0.02% EDTA solution before being lysed by 400 μl of a 0.025% Triton X-100 solution in PBS. The lysed cells in solution were serially diluted in PBS and plated on blood agar plates for enumeration of CFUs. The experiment was conducted in triplicate.

2.4 Results

Prediction of Monomeric Mutations via PlyCB Octamer Interactions

PlyCB, the cell wall binding domain of PlyC, consists of eight identical subunits forming a self-assembling octameric ring. The binding site of each PlyCB subunit is lined by residues $Tyr_{28,}$ Lys_{59}, and Arg_{66} (Fig 2-1 A) (McGowan et al., 2012). The interactions between any two PlyCB octamers are mediated by 15 hydrogen bonds (H-bonds) and 3 van der Waals forces in the strand/helix interfaces (Fig 2-1 B) (McGowan et al., 2012). In this study, Protein Interfaces, Surfaces and Assemblies (PDEePISA) was applied to the 1.4-Å resolution structure of PlyCB (Protein Data Bank ID 4F87) for the identification of the residues involved in the H-bonds (Krissinel & Henrick, 2007) (Table 2-1). Two H-bonds are formed between the backbone of Val10 and Ser11 in the chain A with Gly15 in the chain B at both N-termini. The other 13 H-bonds are formed between the side chains of residues 40-44 in chain A with residues 20-21 and 56-61 in chain B (Fig. 2-1 B, 2-1 C, Table 2-1). Among the residues in this section, five are polar amino acids with charged side chains and participate in up to 11 H-bonds (Table 2-1).

To create a PlyCB monomer, we hypothesized that mutation of the polar amino acids to a non-polar amino acid (i.e. alanine) would prevent the formation of H-bonds, and as such, formation of the octamer. Therefore, three residues (Lys40, Asp41, and Glu43) that were not involved in the bacterial binding sites and did not otherwise play an evident structural role, were selected for site-directed mutagenesis (Fig 2-1 A and 2-1 C)

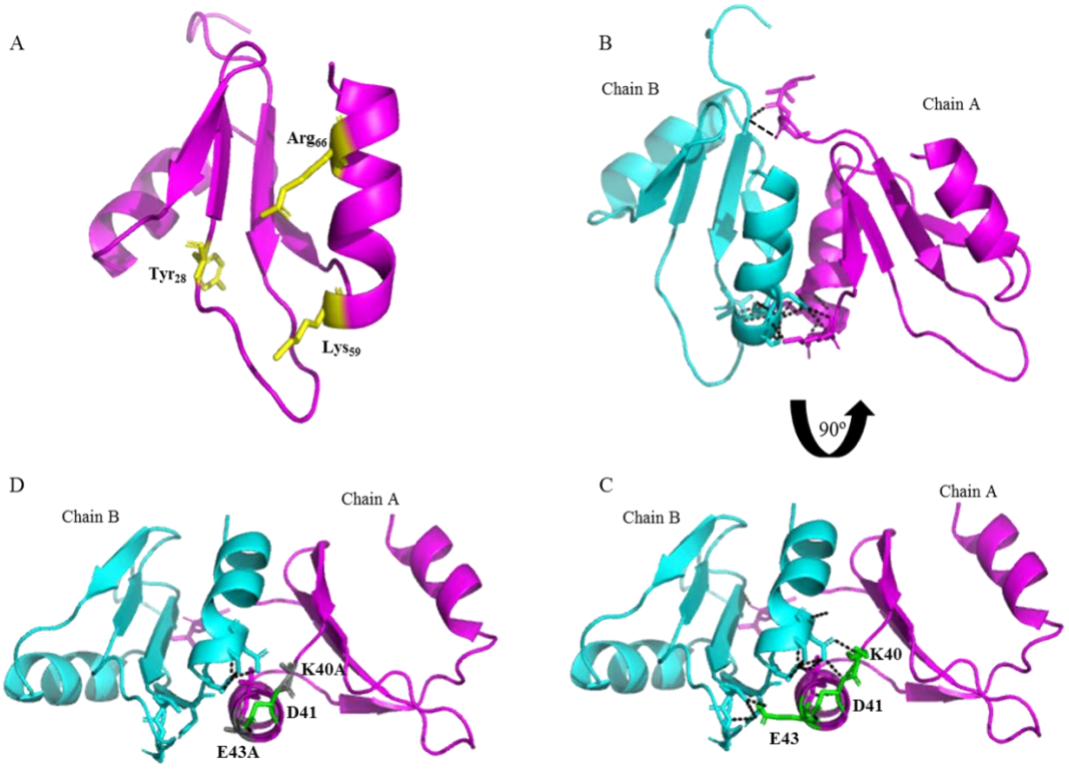

Figure 2-1. Cartoon models of PlyCB monomer and PlyCB octamer interactions. **(A)** The 1.4 Å X-ray crystal structure of the PlyCB monomer, containing four β-sheets and two α-helicies. The residues involved in the binding site of each PlyCB monomer to the bacterial surface are indicated in yellow. **(B)** The 1.4 Å X-ray crystal structure of PlyCB interactions between chain A (magenta) and chain B (cyan). The interactions are mediated through 15 H-bonds indicated as black dash lines. **(C)** Altered orientation of PlyCB chain A and chain B interactions. Thirteen H-bonds (black dash lines) are formed between the side chains of residues 40-44 in chain A with residues 20-21/56-61 in chain B. The residues that are collectively involved in 11 H-bonds are labeled in green. **(D)** Mutagenesis of residues K40 and E41 (grey) to alanine diminishes the H-bonds formed in this area. (PlyCB PDB: 4F87)

Table 2-1. Residues forming H-bonds in PlyCB chain A and chain B

Chain A		Chain B		Distance
Residue	Position	Residue	position	
Val	10	Gly	15	2.96 Å
Ser	11	Gly	15	3.42 Å
Lys	40	Asp	61	2.81 Å
		Asp	61	3.33 Å
Asp	41	Asp	61	3.1 Å
		Ser	58	2.68 Å
		Ser	60	2.87Å
Glu	43	Asn	56	3.55 Å
		Thr	20	2.6 Å
		Thr	20	3.32 Å
		Asp	21	2.79 Å
		Asn	56	2.9 Å
Thr	44	Ser	58	3.05 Å
		Asp	61	2.63 Å
		Ser	58	2.95 Å

PlyCB$_{K40A:E43A}$ is a Monomer

A total of seven PlyCB mutants, K40A, D41A, E43A, K40A:D41A, K40A:E43A, D41A:E43A, and K40A:D41A:E43A were made. All expressed as soluble proteins indicating them to be ~8 kDa PlyCB monomers on SDS-PAGE analysis (Fig. 2-2 A). Mutants were then applied to analytical gel filtration using a Superose 12 column with a broad fractionation range between 1,000 Da and 300,000 Da for proper folding and size prediction. The triple mutation, K40A:D41A:E43A, was eluted from the void volume suggesting that the protein was either aggregated or in a non-globular shape (data not shown). Five of the other six mutants were eluted in the same fraction, between the 158 kDa and 44 kDa molecular mass standards, which is the same elution profile noted for the WT PlyCB octamer. In contrast, the double mutation, K40A:E43A, was eluted in a late fraction, smaller than the 17kDa molecular mass standard, indicating that PlyCB$_{K40A:E43A}$ is a potential monomeric cell binding domain at ~8 kDa (Fig. 2-2 B). The computational model via PyMOL implied these two mutations dramatically diminished the formation of H-bonds in this region of the structure (Fig 2-1 D). To further authenticate the mass of PlyCB$_{K40A:E43A,}$ we used a non-cleavable cross-linker, bis(sulfosuccinimidyl) (BS^3), which reacts with primary amines and the ε amine of lysine. SDS-PAGE analysis of the cross-linked PlyCB WT with 5 mM BS^3 showed different oligomeric PlyCB monomers, and an increasing amount of 10 mM BS^3 produced octameric PlyCB as well as oligomers of PlyCB octamers (Fig. 2-2 C). Compared to PlyCB WT, PlyCB$_{K40A:E43A}$ remained steady at the mass of ~8 kDa in the presence of 10 mM BS^3, confirming that it is a PlyCB monomer. Hence, it was named PlyCBm (Fig. 2-2 C).

In order to understand the binding mechanism of PlyCB, the tandem duplicate of PlyCBm, called PlyCB2m, and quadruple PlyCBm, called PlyCB4m, were constructed aiming to compare the binding affinity of different PlyCB oligomers. No protein expression was observed for PlyCB4m and, therefore, it was excluded from further study (data not shown). Analytical gel filtration of purified PlyCB2m showed the expected double monomer mass of ~16 kDa (Fig. 2-2 D).

PlyCBm and PlyCB2m Retain the PlyCB Octamer's Binding Ranges

After the mass of PlyCBm and PlyCB2m was confirmed, we sought to know whether they retained the ability to bind the streptococcal surface, which would indicate both proper folding and that a single site is sufficient for binding. Both PlyCBm and PlyCB2m bound the surface of *S. pyogenes* D471 in the same manner as the WT PlyCB octamer as viewed by fluorescent microscopy (Fig. 2-3 A-C). Moreover, both PlyCBm and PlyCB2m bound to other streptococcal strains sensitive to PlyC, including group C streptococci (*S. dysagalactiae subs. equisimilis*, *S. equi*, *S. equi subs. zooepidemicus*), group E streptococci, and *S. uberis*, but not non-host bacteria (Table 2-2).

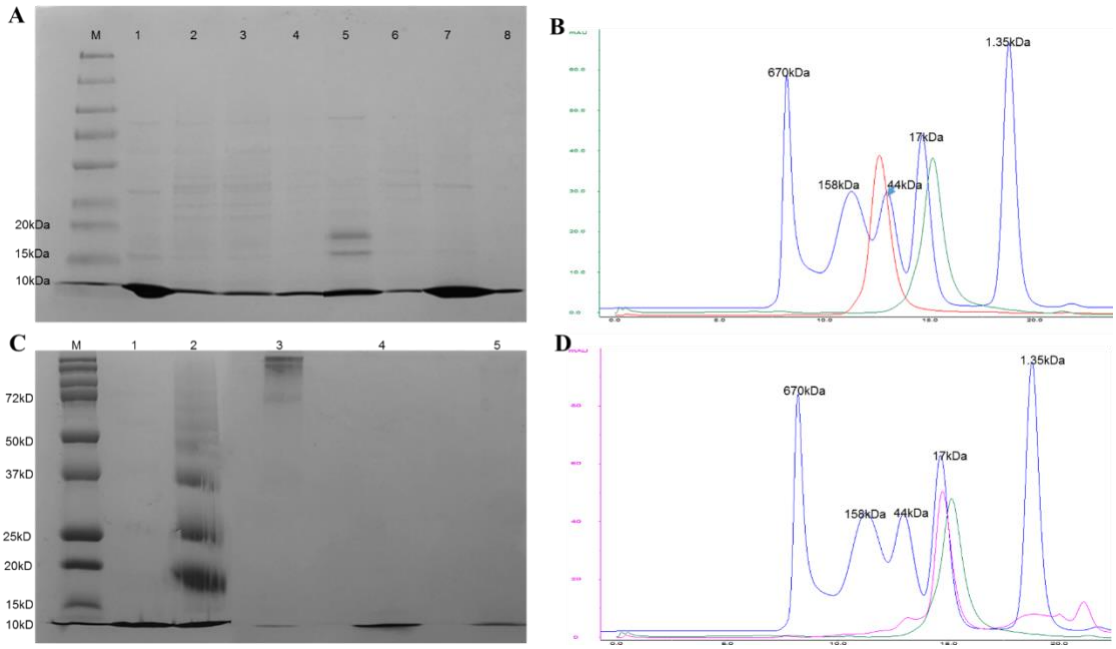

Figure 2-2. Elucidation of the mass of PlyCBm and PlyCB2m. (A) 7.5% SDS-PAGE indicates ~8 kDa bands for PlyCB WT and various PlyCB mutants. The lanes correspond to: (M) BioRad protein marker, (1) PlyCB WT, (2) PlyCB K40A, (3) PlyCB D41A, (4) PlyCB E43A, (5) PlyCB K40A:D41A, (6) PlyCB K40A:E43A, (7) PlyCB D41A:K43A, (8) PlyCB K40A:D41A:K43A. **(B)** Analytical gel filtration of PlyCB WT and PlyCB K40A:E43A (PlyCBm) using a Superose 12 column. BioRad standard indicated as the blue curve; PlyCB WT octamer is indicated as the red curve; PlyCBm is indicated as the green curve. **(C)** Cross-linking of PlyCB WT and PlyCBm. 7.5% SDS-PAGE shows both PlyCB WT and PlyCBm at ~8 kDa without bis(sulfosuccinimidyl) (BS^3) crosslinker. At the presence of 5 mM/10 mM of BS^3, PlyCB WT forms oligomers, while PlyCBm is still a monomer. The lanes correspond to: (M) BioRad protein marker, (1) PlyCB WT, (2) PlyCB WT with 5 mM of BS^3, (3) PlyCB WT with 10 mM of BS^3, (4) PlyCBm, (5) PlyCBm with 10 mM of BS^3 **(D)** Analytical gel filtration of PlyCBm and PlyCB2m using a Superose 12 column. BioRad standards indicated as the blue curve; PlyCB K40A:E43A (PlyCBm) is indicated as the green curve; PlyCB2m is indicated as the pink curve.

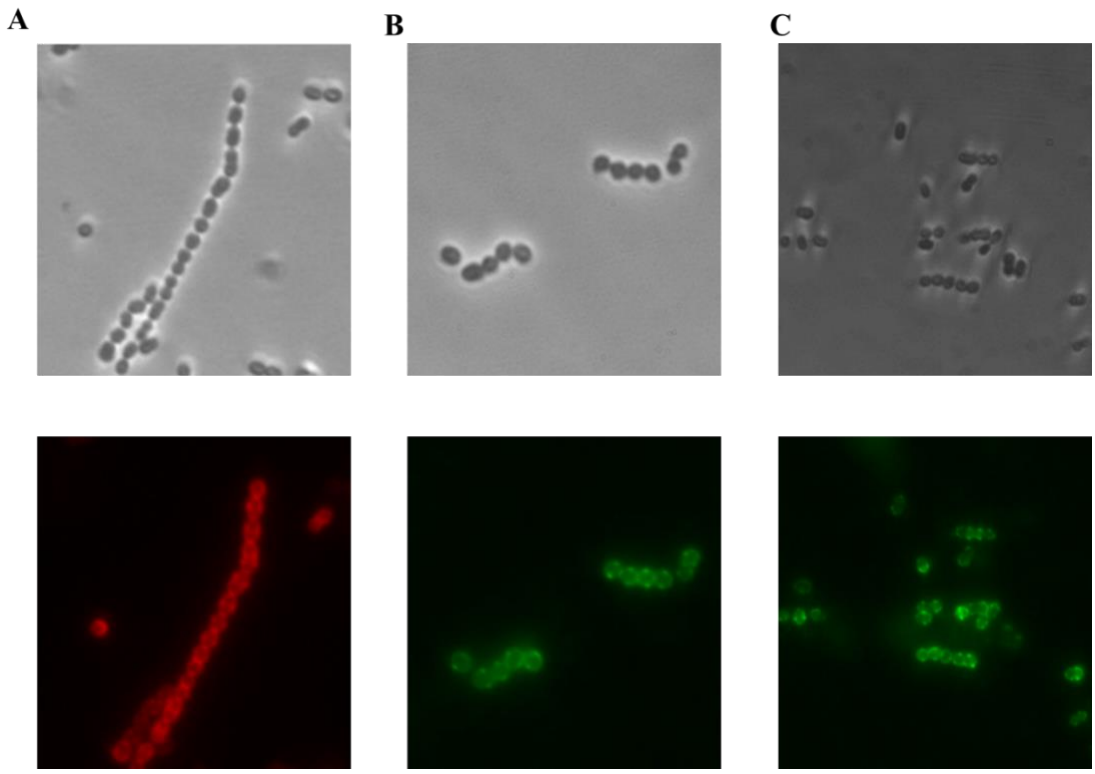

Figure 2-3. Binding of PlyCB octamer, PlyCBm, and PlyCB2m to the surface of *S. pyogenes* D471. Images represent the bright field (top panel) and fluorescent field (bottom panel). **(A)** AlexaFluor® 555-labeled PlyCB octamer. **(B)** PlyCBm with AlexaFluor® 488 conjugated His-tag monoclonal antibody. **(C)** PlyCB2m with AlexaFluor® 488 conjugated His-tag monoclonal antibody.

Table 2-2. Binding of CBDs to different Gram-positive bacteria.

Bacteria	Strain[1]	Binding of CBD[2]		
		PlyCB octamer	PlyCBm	PlyCB2m
S. pyogenes	D471	+	+	+
S. agalactiae	A909	-	-	-
S. dysagalactiae subs.equisimilis	ATCC 21597	+	+	+
S. equi	ATCC 9528	+	+	+
S. equi subs.zooepidemicus	ATCC 700400	+	+	+
Group E streptococci	K131	+	+	+
S. uberis	BAA-854	+	+	+
S. pneumoniae	TIGR4	-	-	-
S. mitis	ATCC J22	-	-	-
S. mutans	ATCC 25175	-	-	-
S. oralis	ATCC PK34	-	-	-
S. rattus	BHT	-	-	-
S. sobrinus	ATCC 6715	-	-	-
B. cereus	ATCC 4342	-	-	-
S. aureus	NRS385	-	-	-

[1]See Appendix B for the source of species and strains.

[2] +, binding; -, no binding.

EC_{50} Suggests PlyCB Octamer Binds Concurrently

It is unknown whether all eight subunits of PlyCB bind to the bacterial surface at the same time (i.e. concurrent model) or one after another in a rolling manner (i.e. consecutive model) (McGowan et al., 2012). Because a single PlyCBm containing one binding site was capable of binding, we assessed the binding pattern of the PlyCBm versus the PlyCB octamer. A whole cell bacterial ELISA was conducted and the effective concentration of the CBD that gives half-maximal binding (EC_{50}) was used to represent the binding avidity. The EC_{50} values for PlyCBm, PlyCB2m, and PlyCB were 120, 570, and 900 nM, respectively (Fig. 2-4). In contrast, PlyCB R66E, a known PlyCB mutant that abolishes binding, acted as a negative control, and showed no detectable binding. The data, taken together, supports a concurrent model and suggests all eight PlyCB subunits simultaneously participate in binding the streptococcal surface.

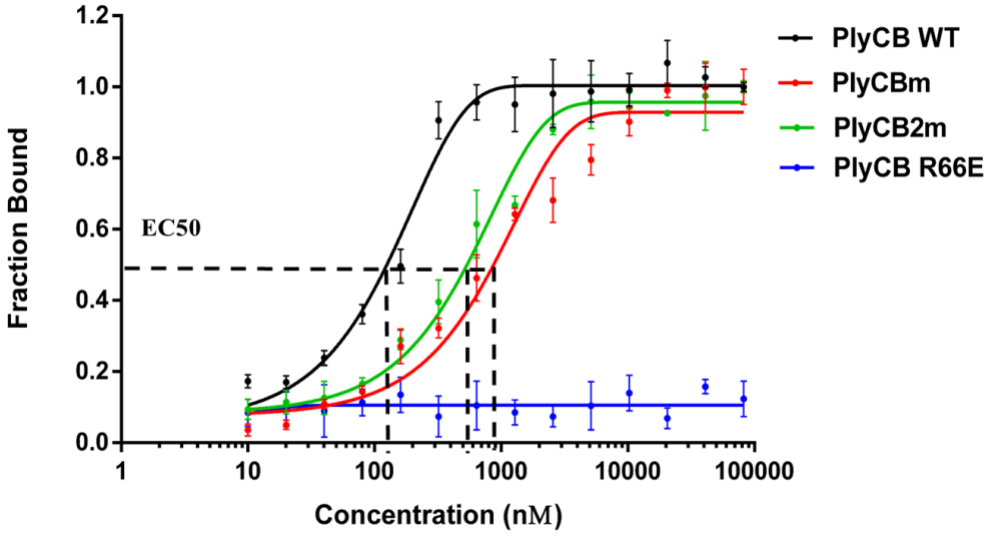

Figure 2-4. EC_{50} of PlyCB WT, PlyCBm and PlyCB2m. Various amounts of AlexaFluor® 555 labeled proteins were incubated with *S. pyogenes* D471 at room temperature for 1 hour to make a saturation binding curve using a nonlinear fit analysis. The fraction bound represents the percentage of binding. EC_{50} is the effective concentration of each CBD at 50% maximal binding. Error bars represent the standard deviation, and all tests were conducted in triplicate.

Binding Affinity Affects Lytic Activity

We next sought to determine whether the differences in binding affinity affected the lytic activity of PlyC. The EC_{50} data indicated that the PlyCB octamer displayed a very tight, stable interaction between the PlyC holoenzyme and cell wall. However, strong binding does not necessarily correlate with an increase of lytic activity as tight binding may decrease the turnover rate of the endolysin. Notably, Schmelcher et al. demonstrated that the increased binding affinity of Ply500 CBD tandem repeats targeting *Listeria* reduces the lytic activity of Ply500 in physiological condition (Schmelcher et al., 2011). To test this hypothesis, PlyCBm-derived chimeras were made with the parental EADs: CHAP_CBm (i.e. the PlyCA CHAP domain fused to the PlyCBm), GyH_CBm (i.e. the PlyCA GyH domain fused to PlyCBm), and PlyCA_CBm (full-length PlyCA fused to PlyCBm). Lytic activity of all chimeras was then determined against *S. pyogenes* D471 via the turbidity reduction assay. No protein expression was observed for PlyCA_CBm, hence it was excluded from further testing. 10 μM of CHAP_CBm displayed moderate activity corresponded to a 50% decreases in OD_{600} in 20 min, whereas GyH_CBm only caused ~15% decreases in OD_{600} and was not considered further (Fig. 2-5 A). The endolysin PlyCΔGyH, containing the PlyCA CHAP domain in contaxt of the full PlyCB octamer (McGowan et al., 2012) was used here to demonstrate the effect of the binding affinity on activity. When tested at equimolar concentrations and under physiological condition (PBS, pH 7.4), CHAP_CBm displayed ~40% of the PlyCΔGyH activity (Fig. 2-5 B), indicating that the tighter binding provided by the PlyCB octamer promoted the lytic activity. To validate the observation, we reasoned

that a chimera of the PlyCA CHAP domain with PlyCB2m (i.e. CHAP_CB2m) should exhibit stronger activity than CHAP_CBm. As shown in Fig. 2-5 B, the two cell wall binding sites of CHAP_CB2m helped the increase of activity to ~60% of PlyCΔGyH. The data suggests that increasing the binding affinity by increasing the number of PlyCB subunits increases the lytic activity of chimeras containing the PlyCA CHAP domain as an EAD.

Different Enzymatically Active Domains Affect Lytic Activity

We next sought to evaluate different EADs with PlyCBm since catalytic efficiency of the EAD may also play a role in the lytic activity. Notably, such chimeragenesis approaches have demonstrated a range of activities, with some greater than that displayed by the parental enzymes (Blazquez et al., 2016; Diez-Martinez et al., 2015; Schmelcher et al., 2011; Vazquez et al., 2017; Yang et al., 2016; Yang et al., 2015). Thus, other two CHAP domain EADs, $CHAP_{LysK}$ from LysK and $CHAP_{PlySs2}$ from PlySs2, and two amidase EADs from PlyG and Pal, were selected to make $CHAP_{LysK}$_CBm, $CHAP_{PlySs2}$_CBm, $Amidase_{PlyG}$_CBm, and $Amidase_{Pal}$_CBm. All chimeras were expressed as soluble proteins, purified to homogeneity, and the lytic activities were assessed by turbidity reduction. When tested at equal concentrations using stationary phase *S. pyogenes* D471, $CHAP_{PlySs2}$_CBm, $Amidase_{PlyG}$_CBm, and $Amidase_{Pal}$_CBm only displayed ~20%, ~50%, and ~25% of the CHAP_CBm activity, respectively (Fig. 2-6 A). However, $CHAP_{LysK}$_CBm with the EAD from a staphylococcal endolysin, LysK, displayed nearly twice the lytic activity of CHAP_CBm (Fig. 2-6 A). Furthermore, the activity of $CHAP_{LysK}$_CBm

was comparable to the activity of PlyCΔGyH (Fig. 2-6 B), which contained the PlyCA CHAP in context of the full PlyCB octamer. Taken together, the data suggests the catalytic efficiency of the EAD is just as important in determining overall activity as binding affinity of the CBD for a given endolysin. It should, therefore, be possible to "tune" a chimeric endolysin to produce optimal activity by proper selection of the EAD and evaluation of CBD repeats.

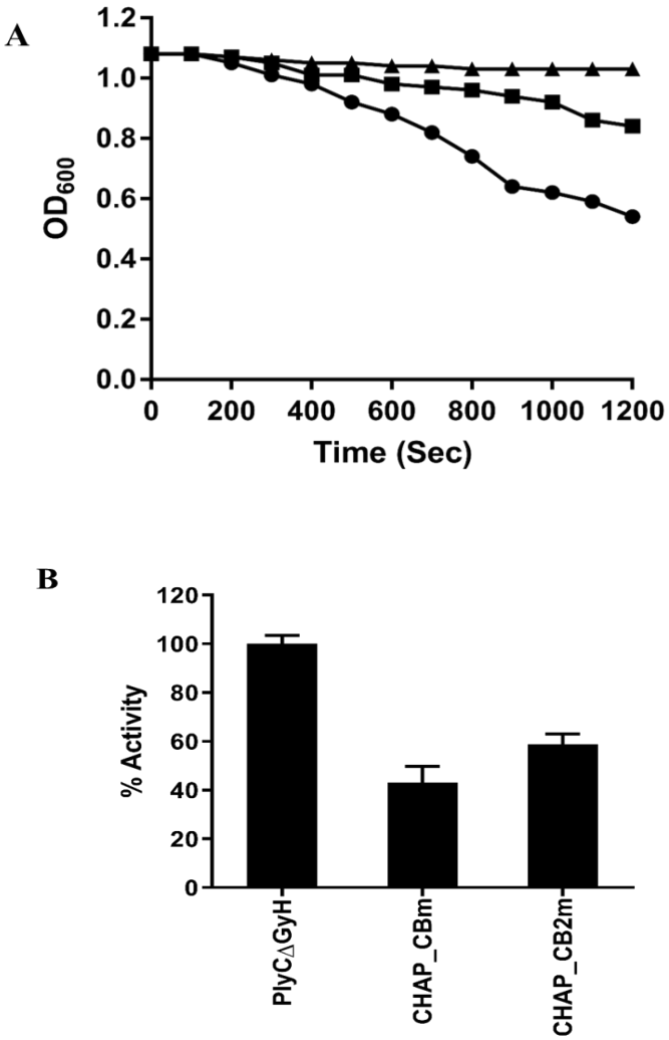

Figure 2-5. Lytic activity of PlyCBm/PlyCB2m-derived chimeras against stationary phase *S. pyogenes* D471. 10 µM of each enzyme was added to bacteria and the decrease of OD_{600} was followed for 20 min to allow for calculation of V_{max} as described in Methods. **(A)** OD_{600} curves of PBS (triangles), CHAP_CBm (circles), and GyH_CBm (squares). **(B)** Effect of binding affinity on lytic activity. The lytic activities, based on V_{max} of each enzyme, were normalized to 100% V_{max} of PlyCΔGyH. Error bars represent the standard deviation, and all tests were conducted in triplicate.

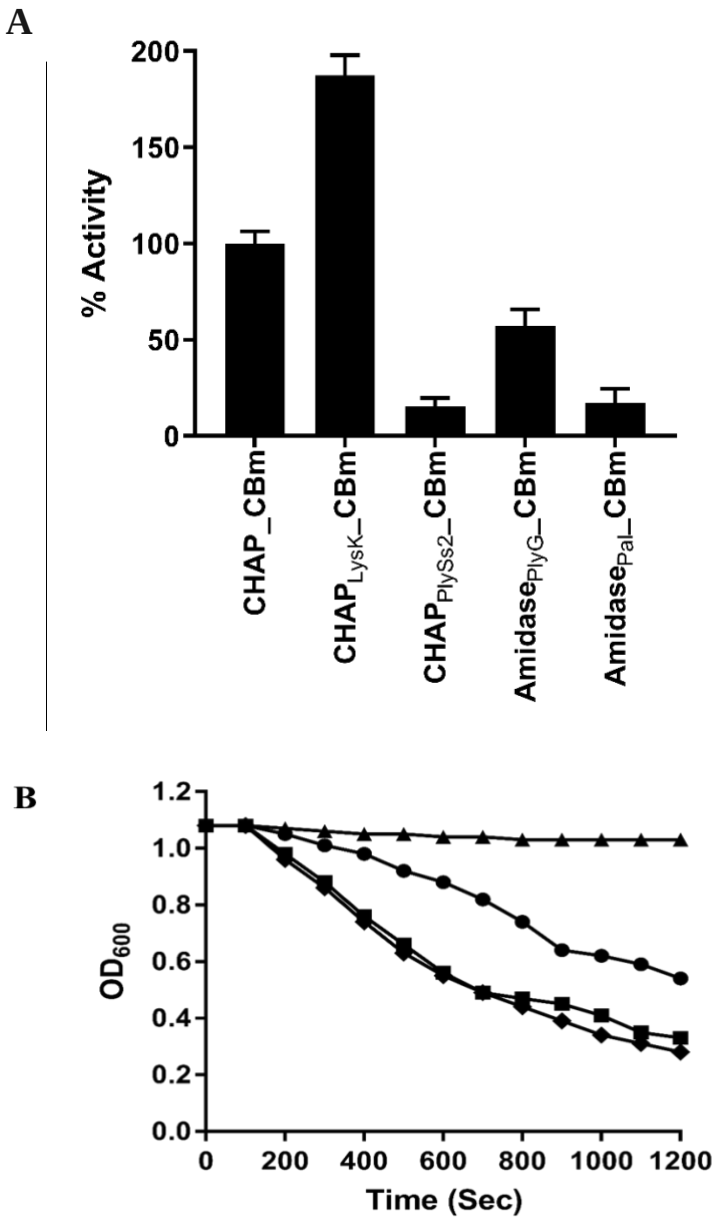

Figure 2-6. Effect of EADs on lytic activity. 10 µM of each enzyme was added to stationary phase *S. pyogenes* D471. The OD_{600} was followed for 20 min and the V_{max} was calculated as described in Methods. **(A)** The % lytic activities of each enzyme were normalized to 100% V_{max} of CHAP_CBm. **(B)** OD_{600} curves of PBS (triangles), CHAP_CBm (circles), $CHAP_{LysK}$_CBm (squares), and PlyCΔGyH (diamonds). Error bars represent the standard deviation and all tests were conducted in triplicate.

PlyCBm Mediates Epithelial Cell Internalization, and CHAP_CBm Can Kill Internalized *S. pyogenes* D471

In addition to the streptococcal binding properties of PlyCB, our laboratory has recently shown that the key residues R29, K59, and R66 on PlyCB subunits form a pocket that binds phosphatidylserine on the eukaryotic membrane, which mediates internalization of PlyC and subsequent eliminating intracellular streptococci (Shen et al., 2016). As R29, K59, and R66 were not affected by mutations to create PlyCBm, we hypothesized that PlyCBm should retain the membrane translocation characteristics of the PlyCB octamer. At a concentration of 5 μg/ml, fluorescently labeled PlyCB octamers and PlyCBm were internalized by human A549 epithelial cells within 30 min (Fig. 2-7 A). Both the internalized PlyCB octamer and PlyCBm were found in vesicle-like structures and diffused in the cells indicating they internalized via a similar mechanism.

Next, we determined whether a chimera of PlyCBm with an EAD could kill the intracellular *S. pyogenes* D471. A co-culture model of human epithelial cells and *S. pyogenes* D471 was conducted to address the killing by CHAP_CBm. Treatment with 2 mg/ml CHAP_CBm reduced intracellular colonization by 50% within 2 hours, and lower concentrations resulted in a dose-response (Fig. 2-7 B). These data indicated that PlyCBm was able to cross the plasma membrane and eliminate the internalized *S.pyogenes* D471 with an EAD.

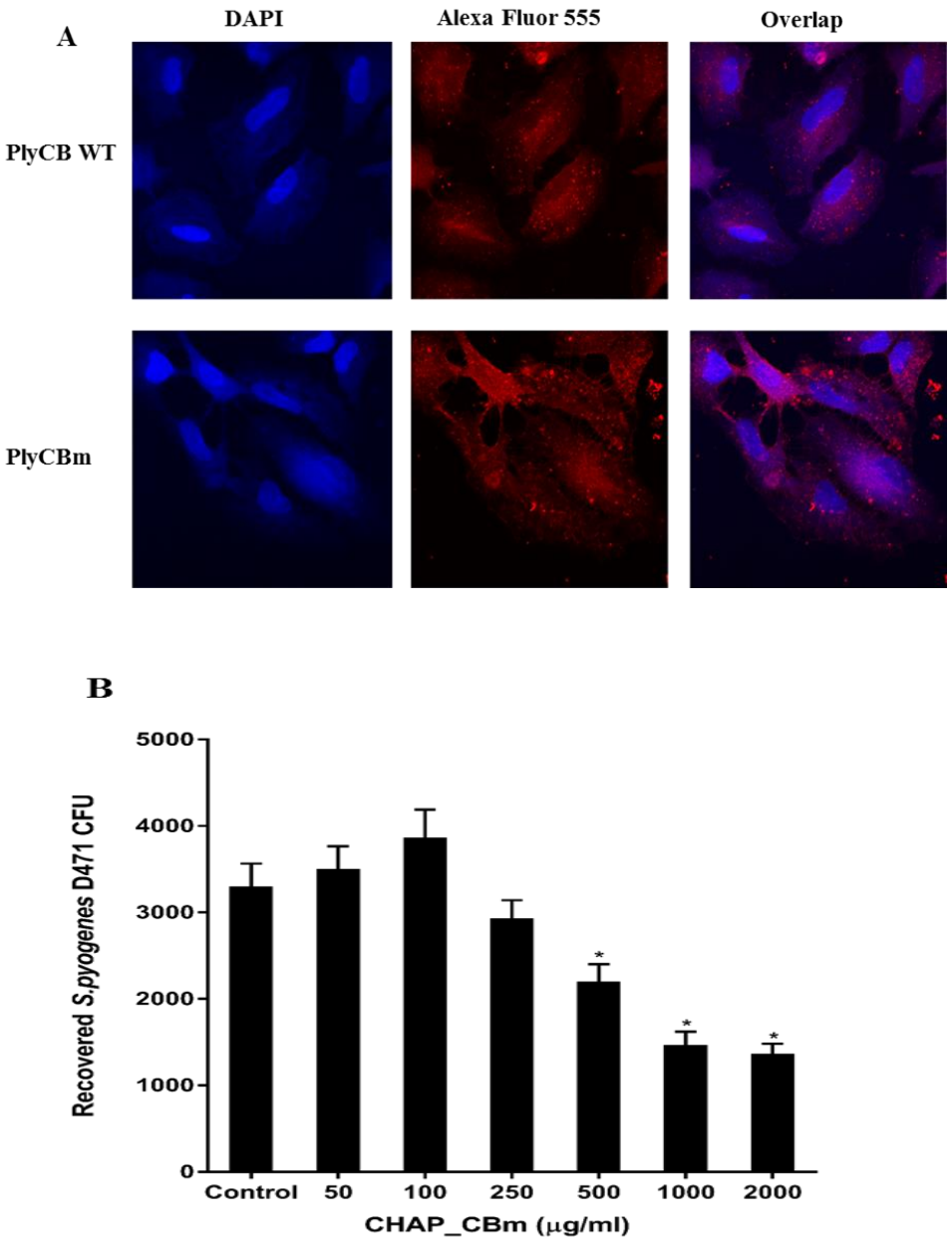

Figure 2-7. Internalization of PlyCBm. (A) Confocal microscopy of internalized PlyCB octamers and PlyCBm at 100x. DAPI stains A549 epithelial cells nucleus; PlyCB octamer and PlyCBm are labeled with AlexaFluor® 555. **(B)** CHAP_CBm eliminates intracellular *S. pyogenes* D471 in a dose-dependent manner. The tests were conducted in triplicate, with means and standard deviations displayed. Statistical analysis using Student's t-test is reported as *: $p < 0.005$.

2.5 Discussion

The PlyC cell binding domain (PlyCB) displays high specificity against groups A, C, and E streptococci in addition to *S. uberis*, yet it also mediates the internalization of PlyC to eliminate intracellular streptococci. These features endorse the use of PlyC as a novel antibacterial therapeutic agent. Moreover, the molecular basis for PlyCB is interesting from the perspective of understanding the binding mechanism and for the development of PlyCB-derived chimeras. Here we show computational analysis of the inter-subunit interactions of the PlyCB octamer following by site-directed mutagenesis that a PlyCB monomer (PlyCBm) can be created, as well as the tandem duplication of PlyCB monomer (PlyCB2m). With the essential binding residues intact on each PlyCB subunit, PlyCBm and PlyCB2m retain the same binding ability and host range as the PlyCB octamer. In addition, the chimeras created with PlyCBm/PlyCB2m hint at the relationship between binding affinity and activity, as well as prove that PlyCBm can contribute to further chimeragenesis that is specific for both streptococci and intracellular delivery.

As a cell binding domain, PlyCB shares no sequence similarity to any other proteins and thus represents a rare example of CBD (McGowan et al., 2012). While some multimeric endolysins have recently been described, they contain a second CBD as the result of an alternate start codon within the endolysin gene rather than being product of a second gene. Furthermore, no described endolysin contains an octameric CBD. Whether all eight PlyCB monomers participate in binding or whether the presence of all eight merely increases the avidity for the bacterial surface has never been addressed. The EC_{50} data show that PlyCBm and PlyCB2m bind less

tightly than the PlyCB octamer, implying that more than two binding sites, and possibly all eight, are concurrently involved in epitope binding on bacterial cell wall. Although the EC_{50} of PlyCBm and PlyCB2m is relatively high, they are still within the nanomolar range, which is comparable to the affinity of an antibody-antigen complex (Lopez & Garcia, 2004; Schmelcher et al., 2010). It is worthy to note that CBDs with such high specificities and binding affinities have been applied as biosensor tools to detect *Listeria* cells, *Bacillus cereus* cells, and *Staphylococcus aureus* cells (Kong et al., 2017; Kong et al., 2015; Tolba et al., 2010; Walcher et al., 2010; Yu et al., 2016). In comparison with the PlyCB octamer, the monomeric structure of PlyCBm is easier to engineer as a biosensor tool to diagnosis streptococci.

The goal of endolysin engineering is to be able to fine tune the interplay between on and off rates for both the EAD and CBD. If the on rate or off rate is too slow, the catalytic efficiency decreases. Until recently, chimeragenesis has been the only method employed for endolysin engineering. While this approach does allow selection of different EAD and CBD combinations to optimize activity, it does not inherently provide the ability to modulate the binding ability of either domain. For the first time, the creation of monomeric PlyCB as well as the ability to add tandem PlyCB monomer repeats allows for a method to "tune" the binding, and subsequently the activity, of an engineered endolysin.

The tuning concept is further supported through the change of EADs. When $CHAP_{LysK}$ replaced the PlyC CHAP domain in the chimera, the activity doubled. $CHAP_{LysK}$ is an EAD of LysK endolysin targeting staphylococcal pathogens.

Although the endopeptidase cleavage site for $CHAP_{LysK}$ is reported between D-alanine and the first glycine in the pentaglycine cross-bridge of staphylococci, a bond not present in the streptococcal PG, $CHAP_{LysK}$ can nonetheless lyse streptococci in a moderate to weak manner without the CBD (Becker et al., 2009; Fenton et al., 2010; O'Mahony & Coffey, 2011). CHAP from PlyC and $CHAP_{LysK}$ belong to the same cysteine, histidine-dependent amidohydrolases/peptidases family (CHAP). One theory for the doubling of activity with $CHAP_{LysK}$ compared to the PlyC CHAP may be the positive charged carried by $CHAP_{LysK}$ (pI=9.08) in contrast to the negative surface charge for the CHAP from PlyC (pI=4.03), as a number of studies have reported (Low et al., 2011 Osterman, & Liddington, 2011; Mayer et al., 2011 Narbad, & Meijers, 2011). The difference in enzymatic activity between CHAP_CBm and $CHAP_{LysK}$_CBm hints that a more catalytically active EAD can facilitate a CBD with a lower binding affinity to improve total activity. On the other hand, the observation that PlyCΔGyH shows similar activity as $CHAP_{LysK}$_CBm suggested that a less active EAD can be facilitated by a CBD with high binding affinity to improve bactericidal efficacy. Accordingly, we infer that the efficiency of the endolysins depend on the balance between binding affinities of CBDs and enzymatic activities of EADs. Furthermore, these observations provide a way to optimize the endolysin through chimeragenesis: a less active EAD needs a tighter binding CBD to ensure hydrolysis thoroughly; a more active EAD needs a less tight binding CBD to increase the turnover rates.

It is anticipated that PlyCBm inherits the capability of internalization via the interaction of a cationic binding groove with plasma membranes. We speculate that

the lower killing efficiency of CHAP_CBm compared to PlyC in the mammalian cells is because PlyC is the most active endolysin described to date. However, the instance that CHAP_CBm kills the internalized *S.pyogenes* D471 proves the possibility that PlyCBm can work as an intracellular cargo for delivery into mammalian cells.

This study, through a monomerized CBD to confirm the binding mechanism of the PlyCB octamer, suggests a rationale to optimize the activities of endolysin. Finally, the creation of PlyCBm as the dual functional CBD, streptococci recognition and cell penetration, provide more possibilities to further antimicrobial development and bioengineering studies.

Chapter 3: A Novel Design to Exploit the Synergy of the PlyC Catalytic Domains

3.1 Abstract

Bacteriophage-derived endolysins have great potential as alternative antimicrobial agents for Gram-positive bacterial infectious diseases as they are peptidoglycan hydrolases that can destroy susceptible bacteria when applied exogenously. Due to the modular structure of endolysins, engineering methods can be used to improve their properties or change their host range via manipulation of the functional domains. The multimeric endolysin, PlyC, has potent activity on groups A, C, and E streptococci, as well as *Streptococcus uberis*, but is devoid of activity on other streptococci such as *S. agalactiae* (i.e., group B strep), *S. mutans*, or *S. pneumoniae*. PlyCA, the enzymatically active domain of PlyC, consists of two catalytic domains, GyH, a glycosyl hydrolase, and CHAP, a cysteine, histidine-dependent amidohydrolase/peptidase. Notably, GyH and CHAP have been shown to work synergistically to achieve lytic rates ~100 fold higher than comparable single catalytic domain endolysins. In this work, we provide a new design of chimeric endolysins to take advantage of the synergistic effects of PlyCA. ClyX-1 was created via fusing the pneumococcal Cpl-1 cell binding domain (CBD) in between the GyH and CHAP catalytic domains of PlyCA. This chimera displayed ~100 fold increase in activity *in vitro* against *S. pneumoniae* and dramatically improved activity *in vivo* compared to the parental Cpl-1 enzyme. ClyX-2 was then created using a similar strategy by fusing the broad host range PlySs2 CBD between GyH and CHAP

catalytic domains. ClyX-2 not only demonstrated wild-type PlyC activities on groups A, C and E streptococci but now included high levels of activity against *S. mutans* and *S. agalactiae*. Moreover, this design format (i.e., CBD in the middle of two catalytic domains) can also be applied to other enzymes in order to achieve improved activity. CHAP or GH25 catalytic domains were added to the C-terminus of full-length Cpl-1 and PlySs2, respectively, and displayed synergistic effects. To date, with the exception of PlyC, two catalytic domains in one endolysin have not shown synergism, even in enzymes that naturally contained two catalytic domains. Our work suggests a novel design for adopting the synergy of two catalytic domains for increased lytic activity.

3.2 Introduction

The *Streptococcus* is a genus of Gram-positive bacteria consisting of diverse species widely distributed across the normal flora of human and animals (Pouliot et al., 2015). Although some streptococci cause no harm or are carried asymptomatically, most species are highly virulent and known to cause significant diseases. *Streptococcus mutans, Streptococcus pyogenes* (GAS), *Streptococcus agalactiae* (GBS), and *Streptococcus pneumoniae* are particularly notable as causative agents of serious acute infections in human, ranging from dental caries and pharyngitis to life-threatening conditions such as necrotizing fasciitis and meningitis (Mitchell, 2003). As animal pathogens, group C streptococci (GCS), group E streptococci (Oliveira, L. M. et al.), *Streptococcus uberis*, and *Streptococcus suis* infect major livestock (i.e., cattle, pigs, and horses) leading to considerable economic

loss to farmers (Hardie & Whiley, 1997a). Due to the widespread distribution of antibiotic-resistance genes and the overuse of broad-spectrum antibiotics, streptococci that used to sensitive to conventional antibiotics have started developing resistant phenotypes (Brown & Wright, 2016; Macris et al., 1998). In a report published by the Centers for Disease Control (CDC 2013), drug-resistant *Streptococcus pneumoniae* has been labeled as a "serious" public health threat and erythromycin-resistant GAS and clindamycin-resistant GBS as "concerning" public health threats. The emergence of resistant streptococci calls for the need to source alternative antimicrobial agents.

Bacteriophage-encoded endolysins, one of the alternative treatments, have gained attention and been extensively studied (Fischetti, 2005; Loessner, 2005). Endolysins, also known as phage lysins or enzybiotics, are peptidoglycan (PG) hydrolases produced at the end of the phage replication cycle resulting in cell lysis and new phage release. When applied exogenously, these enzymes are capable of destroying the Gram-positive bacterial PG rapidly and specifically (Loeffler et al., 2003; Royet & Dziarski, 2007; Schuch et al., 2002). Endolysins derived from phage that infect Gram-positive hosts have modular structures with the enzymatically-active domain(s) (EADs) at the N-terminus and a cell-binding domain (CBD) at the C-terminus. The EADs are capable of cleaving specific covalent bonds in the PG network to damage the intrinsic structural integrity. The CBDs possess no enzymatic activity but rather function to bind a specific substrate, usually a carbohydrate or teichoic acid, attached to the host PG (Fischetti, 2005).

Several streptococcal endolysins have been discovered and investigated for enzymatic activity, structure-related characteristics, and *in vivo* safety and efficiency.

PlyC, an endolysin from streptococcal C1 phage, displays the most remarkable activity, ~100 fold that of the other endolysins. Unlike other endolysins, PlyC is the only multimeric structured endolysin consisting of nine subunits — eight CBDs (PlyCB) to one EAD (PlyCA) encoding from two genes. Previous research has shown that PlyCB is specific for GAS, GCS, GES, and *Streptococcus uberis*, limiting the PlyC activity against these species. Moreover, the high activity of PlyC is due to synergistic activity of two catalytic domains, an N-terminal glycoside hydrolase (GyH) and a C-terminal cysteine, histidine-dependent amidohydrolase/peptidase (CHAP), that are positioned such that their catalytic active sites face each other forming a central binding grove (McGowan et al., 2012; Nelson et al., 2001; Nelson et al., 2006). Cpl-1, derived from the streptococcal Cp-1 phage, is another well-studied streptococcal endolysin whose CBD contains six repeated choline binding domains that specifically binds to the choline on the teichoic acid of pneumococci (Garcia et al., 1987). This enzyme has been validated to efficiently protect rats from pneumococcal-induced endocarditis and meningitis (Entenza et al., 2005; Grandgirard et al., 2008; Loeffler et al., 2001). Another streptococcal endolysin possessing broad host range is known as PlySs2, derived from *Streptococcus suis* phage. It displays lytic activity against multiple species of different bacterial pathogens, including methicillin-resistant *Staphylococcus aureus* (MRSA) (Gilmer et al., 2013 & Fischetti, 2013). Due to the potent efficacy against MRSA, PlySs2 (CF-301) is being developed by the ContraFect Corporation and has shown improved results in *S. aureus* bacteremia compared to antibiotics alone (Schuch et al., 2014).

As a growing amount of research focuses on the modular design and crystal structures of endolysins, structure-based rational engineering has produced endolysins with desirable properties for specific applications (Broendum et al., 2018; Sao-Jose, 2018). Chimeragenesis is a potential engineering approach that has been successfully exploited by nature, such as pneumococcal endolysin Pal, whose EAD and CBD indicate homology to different phage species (Sheehan et al., 1997; Garcia, 1997). Engineering chimeras through domains shuffling have also been shown to be useful for extending specificity and increasing activity. For example, one streptococcal chimera, ClyR, is the combination of the PlyCA CHAP as and EAD and the PlySs2 CBD, retains the host range of PlySs2 with extension to *Streptococcus mutans* (Yang et al., 2015). The other example is the pneumococcal chimera, Cpl-711, the combination of the Cpl-7 EAD and Cpl-1 CBD, displays much higher activity and stability than the parental enzymes (Diez-Martinez et al., 2015).

Given the unique structure and high activity of PlyC, there is much interest in creating PlyCA chimeras with different CBDs to take advantage of the synergistic effects of the EADs and to expand its host range. Here, we provide modular designs that use both EAD domains of PlyCA with either a choline specific CBD from Cpl-1 or a broad host CBD from PlySs2. By doing so, we were able to create ClyX-1 and ClyX-2 with a design that contains the two PlyCA EADs on each side of the Cpl-1 CBD or PlySs2 CBD, respectively, to preserve the distance/positioning of the EADs and maintain synergy. We then applied this design rule (i.e. EAD-CBD-EAD) to other EADs and assessed whether the chimeras possessed additive or synergistic activities.

3.3 Materials and Methods

Bacterial Strains and Growth Conditions

The bacterial strains in this study were stored at -80°C as frozen stock in 20% glycerol, and are described in Appendix B. Streptococcal strains were cultivated in Todd Hewitt broth supplemented with 1% (wt/vol) yeast extract without shaking. *Bacillus* strains were grown in brain heart infusion broth. All other bacterial strains including staphylococci and enterococci were cultured in tryptic soy broth (TSB). *E. coli* strains DH5α and BL21(DE3) were cultured in Luria-Bertani (LB) broth supplemented with 50 µg/mL carbenicillin or kanamycin as needed. All media were purchased from Fisher Scientific, Hampton, NH. Unless otherwise stated, bacterial strains were propagated at 37°C and shaken at 200 rpm.

Cloning of Chimeric Proteins

The plasmids and primers used in this study are listed in Appendix A. The plasmid constructs for pBAD24::*plyC*, pBAD24::*plyCA*, pBAD24::*plyC*Δ*GyH*, and pBAD24::*plyC*Δ*CHAP* were cloned as previously described (McGowan et al., 2012; Nelson et al., 2006). The sequence of endolysins Cpl-1 and PlySs2 were previoulsy published (Garcia et al., 1987; Gilmer et al., 2013). Cpl-1 was cloned into pBAD24, and PlySs2 were codon-optimized for expression in *E. coli* and chemically synthesized by Thermo Fisher (Waltham, MA). Primers were designed with 20 amino acid overlap at each end of the connected pieces. First, each part of the chimera was individually amplified through PCR to equip with the overlapping sequences. Then, the resulting PCR fragments were fused and amplified again by PCR-based Gene

Splicing by Overlap Extension PCR (SOE PCR) (Horton et al., 1990; Pease, 1990). For constructions contain three gene pieces (*clyX-1, clyX-1 Linkers, clyX-2)*, another round of SOE PCR was performed. Final recombinant gene products were inserted via NdeI/BamHI sites into pET28a vector and cultured on LB plates supplemented with 50 µg/mL kanamycin. The resistant colonies were again picked and verified by DNA sequencing before being transformed into the expression strain BL21 (DE3).

Expression and Purification of Chimeric Proteins

E. coli BL21 (DE3) cells containing the recombinant genes were grown overnight in LB broth with carbenicillin or kanamycin (50µg/mL). The next day, the culture was 1:100 diluted into a 1.5 L of fresh sterile LB broth supplemented with carbenicillin or kanamycin (50µg/mL). The culture was shaken at 200 rpm at 37°C for 3.5 h to reach OD_{600}=0.8. Proteins were induced using 0.25% (wt/vol) of L-arabinose for pBAD24 constructs or 0.1 mM isopropyl β-D-thiogalactoside (IPTG) for pET28a (+) constructs at 18°C for another 20 h. The next morning, the cells were pelleted at 5000 rpm for 15 min at 4°C and stored at -80°C overnight before sonication. The frozen pellets were thawed in lysis buffer (PBS, pH 7.4, supplemented with 1 mM phenylmethanesulfonyl fluoride (PMSF) and 10 mM imidazole) with shaking until dissolved completely. Sonication was then applied to lyse cells on ice for 15 min. The cell debris was removed via centrifugation at 12,000 rpm for 1 h at 4°C. The soluble portion containing recombinant proteins was passed through a nickel-nitrilotriacetic acid (Ni-NTA) column (Qiagen) and fractions were collected from eluted buffers (PBS, pH 7.4, supplemented with 20, 50, 100, 250, and

500 mM imidazole). Purified proteins were verified by SDS-PAGE analysis with Coomassie stain and the fractions containing recombinant proteins were dialyzed against PBS, pH 7.4, overnight at 4°C. The proteins were concentrated to the desired concentration and sterilized through the 0.2 µm filter before being stored at -80°C for further analysis. For the *in vivo* murine model, the endotoxin was removed via EndoTrap®HD kit (Hyglos, GmbH) and determined by the EndoLISA®ELISA assay (Hyglos, GmbH).

Bacteriolytic Assay

The bacteriolytic assay was adapted from a turbidity reduction assay as previously described (Nelson et al., 2012). An overnight bacterial culture (stationary phase) was harvested at 5,000 for 10 min at 4°C, washed twice and resuspended in PBS buffer, pH 7.4. In a standard 96-well titration plate (Thermo Fisher), the resuspended bacterial solution was mixed 1:1 (υ/υ) with endolysin to a final OD_{600} between 0. 8 to 1.0. In each run, PBS was included as a negative control. Spectrophotometric readings (OD_{600}) were taken every 15 s over 10 min on a SpectraMax 190 spectrophotometer (Molecular Devices). V_{max} was calculated as the slope of the linear portion and represented the endolysins activity. All experiments were conducted in triplicate to obtain the standard deviation.

In Vitro Characterization of ClyX-1

The optimal biochemical conditions for ClyX-1 against stationary phase *S. pneumoniae* TIGR 4 were determined using the turbidity reduction assay described

above. For temperature stability, ClyX-1 was incubated at indicated temperatures (4°C, 16°C, 25°C, 37°C, 45°C, 55°C, or 65°C) for 30 min, recovered on ice for 5 min, and subjected to the spectrophotometric analysis. For optimal pH condition, pneumococci (TIGR 4) were suspended in 40 mM boric acid/phosphoric acid (BP) buffer, pH 3-10, and were challenged against ClyX-1.

Bactericidal Assay

Overnight bacterial cells were diluted 2x in rich media to generate a final concentration of 5.0 x 10^6 CFU/ml. 100 µl of the diluted bacterial culture was added into a standard 96-well titration plate (Thermo Fisher) in triplicate and mixed with 100 µl of sterile-filtered enzymes. Plates were sealed and incubated at 37°C for 5-60 min. After incubation, bacterial cells were serially diluted in 10-fold increments into sterile PBS and plated on THY/TSB agar. Log killing was calculated as follows: -log [(CFU under enzyme treatment)/ (CFU under PBS treatment)].

Dimerization of ClyX-1

The dimerization of ClyX-1 was based on the size change in the presence of choline monitored by the analytical gel filtration on a Superose 12 column (GE Healthcare). Briefly, 500 µl of 1 mg/ml ClyX-1 was injected in the sample loop. PBS and PBS with 50 mM choline were used as the elution buffer separately to determine the change of protein mass. The standard protein mass curve was obtained through gel filtration standards (BioRad).

MIC Analysis

The minimal inhibitory concentrations (MICs) of enzymes and antibiotics were determined in a standard 96-well titration plate (Thermo Fisher) in triplicate as described previously (Wiegand et al., 2008). Briefly, overnight pneumococcal cultures were diluted with 2x THY to obtain a final concentration of 1 x 10^7 CFU/ml, and other bacterial species were diluted 2-fold in medium to 1 x 10^5 CFU/ml. 100 µl of the diluted bacterial culture was placed into each well, mixing with the serial 2-fold diluted 100 µl of enzymes/antibiotics. PBS buffer was used as a negative control. The plates were sealed with parafilm and statically incubated at 37°C for 24 h. The MIC was defined as the lowest concentration of treatment that inhibited visible growth of the bacterium.

Peptidoglycan Purification and Digestion by PlyC

The purification of the *S. pyogenes* D471 peptidoglycan was carried based on a previously described protocol with minor modifications (Pritchard et al., 2004). Briefly, an overnight bacterial culture was pelleted at 5,000 rpm for 15 min in a centrifuge and resuspended in 25 ml of PBS per liter of cells. French Press using a cellular pressure of 15,000 p.s.i was applied twice to lyse the cells. The unbroken cells were removed at 5,000 rpm for 5 min. The supernatant was again subjected to centrifugation at 20,000 rpm for 45 min at 4°C to pellet cell walls. The pelleted cell walls were rinsed and resuspended in PBS buffer supplemented with 0.2% (wt/vol) benzonase and proteinase K for 7 h. After incubation, the samples were boiled at

100°C in 4% (wt/vol) SDS for 30 min, washed at least 3 times and resuspended in MiliQ water.

50 µg of PlyC in PBS buffer, pH 7.4, was added to *S. pyogenes* D471 cell wall suspensions (OD_{600}=1.0, PBS buffer, pH 7.4) in a final volume of 500 µl. After digestion at 37°C for 16 h, the reaction mixture was clarified by centrifugation (13,000 rpm, 5 min), and the supernatant was ultrafiltered using a 5000-MW cutoff Vivaspin. The flow-through was aliquoted and prepared for mass spectrometry analysis.

In Vivo Mouse Infection Models

All mouse infection experiments were carried out in an ABSL-2 lab, and all experimental methods were carried out following the regulations and guidelines set forth by the Animal Experiments Committee of Wuhan Institute of Virology, Chinese Academy of Sciences. All experimental protocols were approved by the Animal Experiments Committee of Wuhan Institute of Virology, Chinese Academy of Sciences (WIVA17201602). Animals were randomized and cared in individually ventilated cages following a set of animal welfare and ethical criteria during the experiment and euthanized at the end of observation.

In the mouse systemic infection model, female BALB/c mice (6-8 weeks old) were injected intraperitoneally with *S. pneumoniae* NS26 at a single dose of 2.95×10^7 CFU/mouse and divided randomly into multiple groups. Bacterial burden in blood and organs in mice 1 h post-infected were confirmed by plating on THY agar as described previously. One hour post-infection, these groups intraperitoneally received

a single dose of 20, 40, or 80 μg/mouse of PlyCpl-1 (n=10); 20, 40, or 80 μg/mouse of Cpl-1 (n=10); 100 μg/mouse of penicillin G (n=10); or an equal volume of PBS buffer (n=10). The survival data for all groups were recorded for 10 days.

3.4 Results

Design and Engineer Specific Host Chimeras Containing PlyCA

With the aim of creating endolysins that possess highly active PlyCA but work against non-PlyC sensitive species, we chose to incorporate a specific-binding CBD. Thus, the Cpl-1 CBD, which is strictly dependent on the presence of choline residues in the teichoic acid of pneumococci strains, was chosen as the bacterial recognition domain. Figure 3-1 displays a schematic representation of the three engineered chimeric proteins (PlyCA_Cpl-1 CBD, ClyX-1, ClyX-1 linkers) and their parental proteins (PlyCA and Cpl-1).

PlyCA_Cpl-1 CBD contains full-length PlyCA at the N-termini and the full length of Cpl-1 CBD at the C-termini. The structure follows the typical native endolysins and the chimeric endolysins module, which is N-terminal EADs and C-terminal CBDs. ClyX-1 contains the Cpl-1 CBD in the middle of PlyCA, substituting for the docking domain, which does not affect activity (McGowan et al., 2012), and ClyX-1-linkers is similar to ClyX-1 but with two extra native linkers in the PlyCA.

ClyX-1 and ClyX-1 linkers expressed as soluble enzymes and were purified to homogeneity based on SDS-PAGE analysis. No protein expression was observed for PlyCA_Cpl-1 CBD, and therefore, was excluded from further characterization.

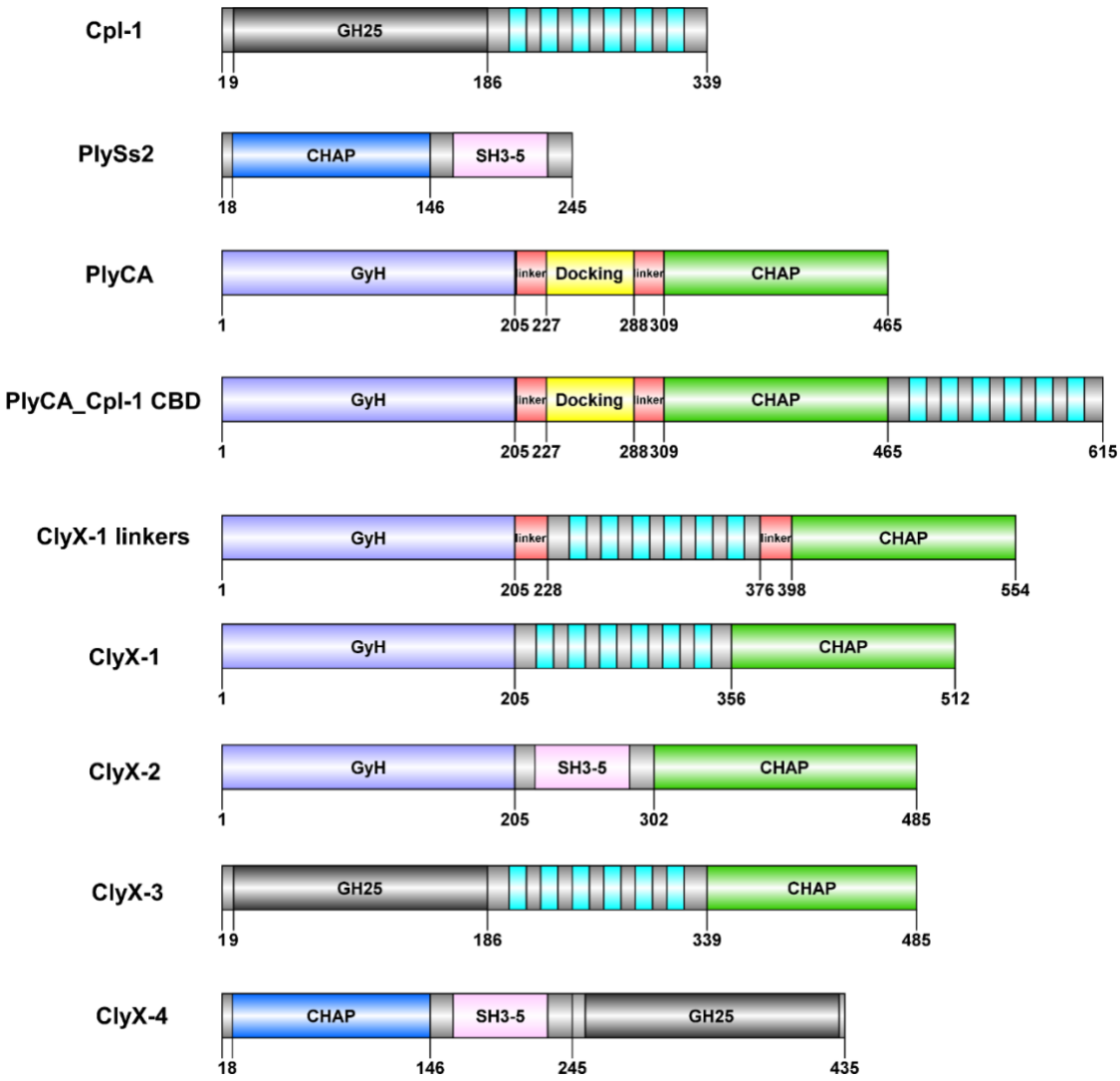

Figure 3-1. Schematic of the constructs. Cpl-1 and PlySs2 are the full length endolysins derived from phage Cp-1 and *S. suis* phage respectively. The GH25 and CHAP domains are the EADs; the cyan rectangles indicate the choline binding repeats in Cpl-1 and the SH3-5 domain is the CBD of PlySs2. The PlyCA is the EAD of PlyC composing N' terminal GyH domain and C' terminal CHAP domain. The PlyCA_Cpl-1 CBD, ClyX-1 linkers, ClyX-1, ClyX-2, ClyX-3, and ClyX-4 are chimeric endolysins by shuffling the different EADs and CBDs from Cpl-1, PlySs2, and PlyCA.

In Vitro Characterization of ClyX-1

The bacteriolytic capacity of ClyX-1 and ClyX-1 with linkers were analyzed via the turbidity reduction assay against an overnight culture of *S. pneumoniae* ATCC TIGR 4. Both enzymes-induced lysis of the bacterial peptidoglycan caused a decrease in OD from 1.0 to 0.2 (80%) within the first 2 min of the turbidity assay at 5 µg/ml (Figure 3-2 a). The result was not surprising since the linkers were the only difference between these two enzymes, and it is plausible that the unstructured regions of the PlyCA GyH, PlyCA CHAP, and Cpl-1 CBD provide sufficient flexibility for enzymatical activity without the additional linkers. Therefore, we only focused on ClyX-1 for the remainder of the experiments. The high lytic activity noted by turbidity reduction correlated well with the data for bacterial survival treatment. ClyX-1 nearly sterilized the culture after just 5 min, causing a decrease in TIGR 4 viability of ~6 logs at as low as 0.5 µg/ml (Figure 3-2 b). Next, the stability of ClyX-1 at different temperatures and pH was surveyed to determine the optimal conditions. ClyX-1 was stable at lower temperatures and displayed highest activity at 37°C, however, the activity rapidly dropped above 45°C (Figure 3-2 c). These observations were consistent with the known Tm values of Cpl-1 (42.9°C) and PlyCA (46.2°C) (Heselpoth et al., 2015 & Nelson, 2015; Sanz et al., 1993 Usobiaga, & Menendez, 1993). The optimal pH is and ClyX-1 completely lost activity at pH values above 8 and below 4 due to protein precipitation (Figure 3-2 d). These observations were compatible with previous studies of Cpl-1 (Garcia et al., 1987; Loeffler et al., 2003). The antimicrobial spectrum of ClyX-1 was tested *in vitro* via turbidity reduction assay on a variety of *S. pneumoniae* strains and other streptococci. All tested strains

of pneumococci were susceptible to ClyX-1 including the 14 most frequent serotypes, mutants that have a non-functional LytA autolysin (Lyt 4.4), and strains that lack capsule (R36A and R6) (Figure 3-2 e). The variations in activity on these different serotypes may be due to accessibility of the peptidoglycan. The killing spectrum of ClyX-1 was specific for pneumococci, as no other streptococcal strains tested were lysed. Collectively, our data suggests the Cpl-1 CBD provides the specificity of ClyX-1 and it retains a host range limited to pneumococci.

The Cpl-1 CBD is known to dimerize in the presence of choline and Cpl-1 is suspected to dimerize on the pneumococcal surface upon binding choline containing teichoic acids. We, therefore, wondered if ClyX-1 was able to form dimers in the presence of choline, especially since ClyX-1 contains the Cpl-1 CBD in the middle of the polypeptide rather than on the C-terminus, as it is located in Cpl-1. We analyzed ClyX-1 by analytical gel filtration in the absence or presence of 50 mM choline (Figure 3-2 f). In PBS, ClyX-1 eluted ~57 kDa based on protein standards, whereas the presence of choline shifted the elution curve to ~114 kDa, indicating that ClyX-1 possesses the ability to form choline-dependent dimers (Figure 3-2 f).

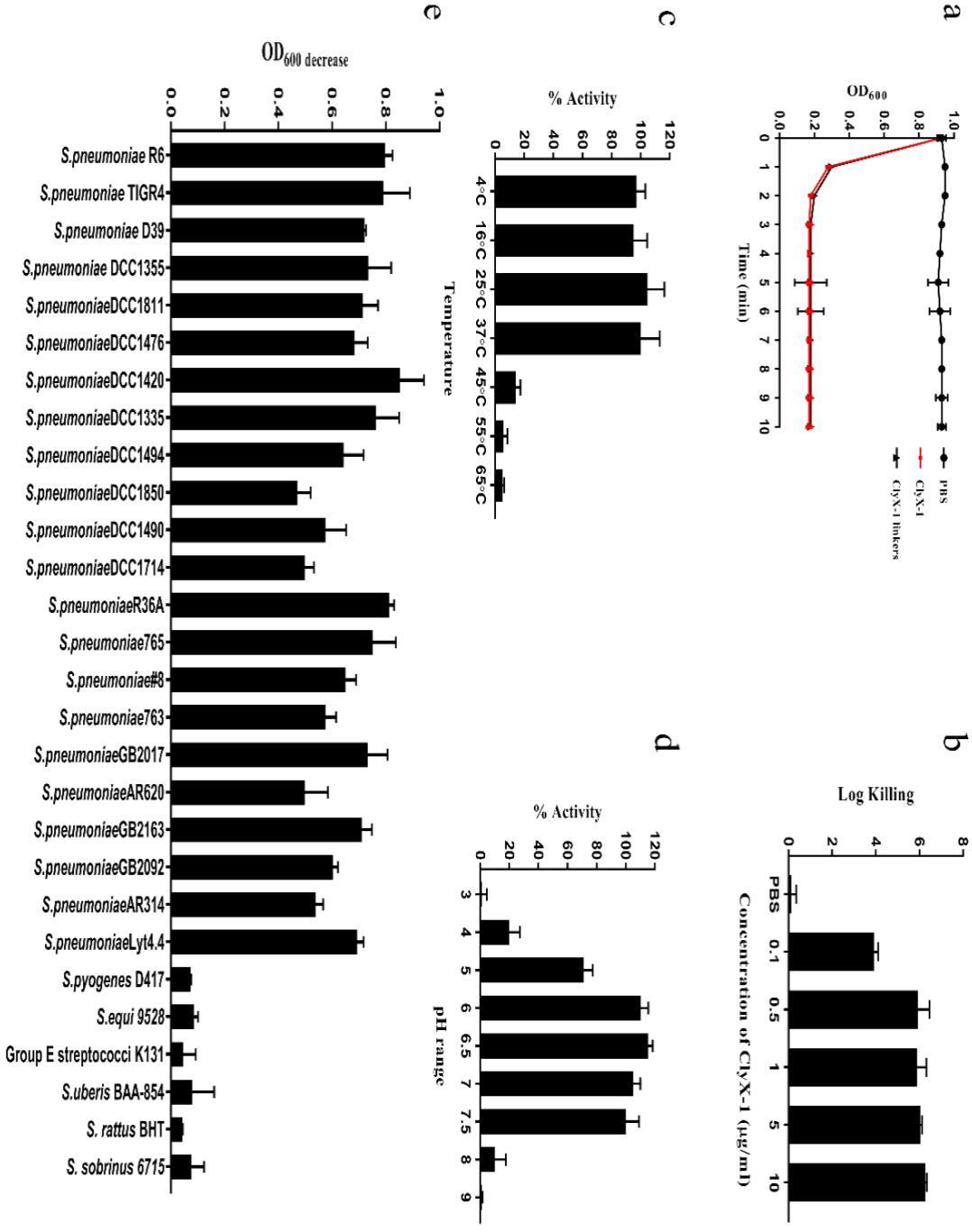
a
OD600
Time (min)
PBS
ClyX-1
ClyX-1 linkers
b
Log Killing
PBS
0.1
0.5
1
5
10
Concentration of ClyX-1 (μg/ml)
c
% Activity
4°C
16°C
25°C
37°C
45°C
55°C
65°C
Temperature
d
% Activity
pH range
e
OD600 decrease
S.pneumoniae R6
S.pneumoniae TIGR4
S.pneumoniae D39
S.pneumoniae DCC1355
S.pneumoniaeDCC1811
S.pneumoniaeDCC1476
S.pneumoniaeDCC1420
S.pneumoniaeDCC1335
S.pneumoniaeDCC1494
S.pneumoniaeDCC1850
S.pneumoniaeDCC1490
S.pneumoniaeDCC1714
S.pneumoniaeR36A
S.pneumoniae765
S.pneumoniae#8
S.pneumoniae763
S.pneumoniaeGB2017
S.pneumoniaeAR620
S.pneumoniaeGB2163
S.pneumoniaeGB2092
S.pneumoniaeAR314
S.pneumoniaeLyt4.4
S.pyogenes D417
S.equi 9528
Group E streptococci K131
S.uberis BAA-854
S. rattus BHT
S. sobrinus 6715

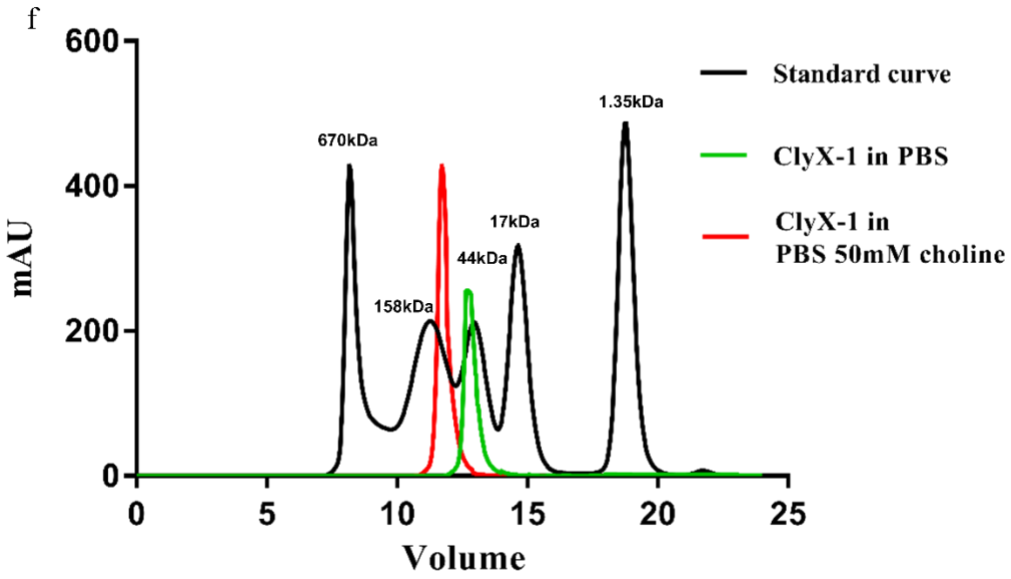

Figure 3-2. Characterization of ClyX-1. (a) Bacteriolytic effects of 5 µl/ml ClyX-1 and ClyX-1 with linkers against stationary phase *S. pneumoniae* TIGR 4. (b) Bactericidal effects of ClyX-1 against stationary phase *S. pneumoniae* R6. Different concentrations of ClyX-1 were mixed with 10^6 colony forming units for 5 min. Log killing was determined through the comparisons of PBS treatment and ClyX-1 treatment. (c)-(d) Biochemical characterization of ClyX-1. The effects of temperature stability (c) and pH (d) were evaluated. 5 µl/ml of ClyX-1 was assayed for lytic activity via turbidity reduction assay against stationary phase *S. pneumoniae* TIGR 4 cells for 10 min. Values were presented as a percentage of lytic activity in relation to activity observed for pH 7 and 37ºC. (e) The host range of ClyX-1. Multiple strains of streptococci were tested for susceptibility. The bacterial cells were washed twice and resuspended in PBS to a final OD_{600} of 0.9-1.0. The changes of OD_{600} were presented after treating with 5 µg/ml of ClyX-1 for 10 min. All experiments were done in triplicate, and the error bars represent the standard deviations. (f) Gel filtration shows dimerization of ClyX-1 in the presence of choline.

ClyX-1 is More Active than Parental Enzymes *in vitro* and *in vivo*

After demonstrating the extremely high activity of ClyX-1, we compared its efficacy with Cpl-1 both *in vitro* and *in vivo*. Bactericidal assays were repeated using ClyX-1, Cpl-1, and PlyCA at different concentrations (0.5 µg/ml to 50 µg/ml) on *S. pneumoniae* D39 (Figure 3-3 a). ClyX-1 sterilized the bacteria within 5 min at even the lowest concentration (0.5 µg/ml), while Cpl-1 also sterilized the culture, required a concentration of 50 µg/ml and only reduced < 1 log at 0.5 µg/ml. PlyCA displayed no bactericidal activity against pneumococci, which supports previous reports that that PlyCA has negligible inherent lytic activity in the absence of the PlyC CBD (PlyCB) (McGowan et al., 2012).

To further evaluate the activity of ClyX-1, a MIC test was performed against eight common serotypes of pneumococci including two penicillin-resistant strains and one capsule-free mutant (Table 3-1). Penicillin and levofloxacin were tested as standards to benchmark the antimicrobial activity. All of the strains were sensitive to levofloxacin (MIC<=2). Only the two penicillin-resistant strains indicated MICs larger than 2 µg/ml. The Cpl-1 MICs for all strains was between 16 µg/ml and 32 µg/ml, comparable to MICs for this enzyme reported in the literature (Djurkovic et al., 2005). The MICs of ClyX-1 were lower than that of Cpl-1 and even levofloxacin, ranging from 0.13 µg/ml to 0.5 µg/ml. As expected, penicillin-resistance had no affect the MICs of ClyX-1.

To validate the *in vitro* bactericidal activity of ClyX-1, we used a mouse systemic infection model to test the *in vivo* efficacy of the enzyme. Mice were challenged to lethal dose of 2.95×10^7 CFU, which proved lethal in 2 days for control

mice. One hour after infection, the mice were intraperitoneally injected with a single dose containing different amounts of either ClyX-1 or Cpl-1 ranging from 20 μg/mouse to 80 μg/mouse. The antibiotic control was penicillin G at 100 μg/mouse, and the negative control was as PBS, pH 7.4 buffer. The mice were observed and survival data was recorded. All the mice treated with PBS buffer died within the first two days. ClyX-1 treatment resulted in rescuing 80%, 40% and 30% of the mice responding to the doses of 80 μg, 40 μg, and 20μg, respectively. The highest amount of Cpl-1, 80 μg, resulted in rescuing only 20% of the mice, and the mice treated with 20 μg of Cpl-1 all died by day 5 (Figure 3-3 b). These observations suggest that ClyX-1 is much more active than Cpl-1 *in vitro* and *in vivo*.

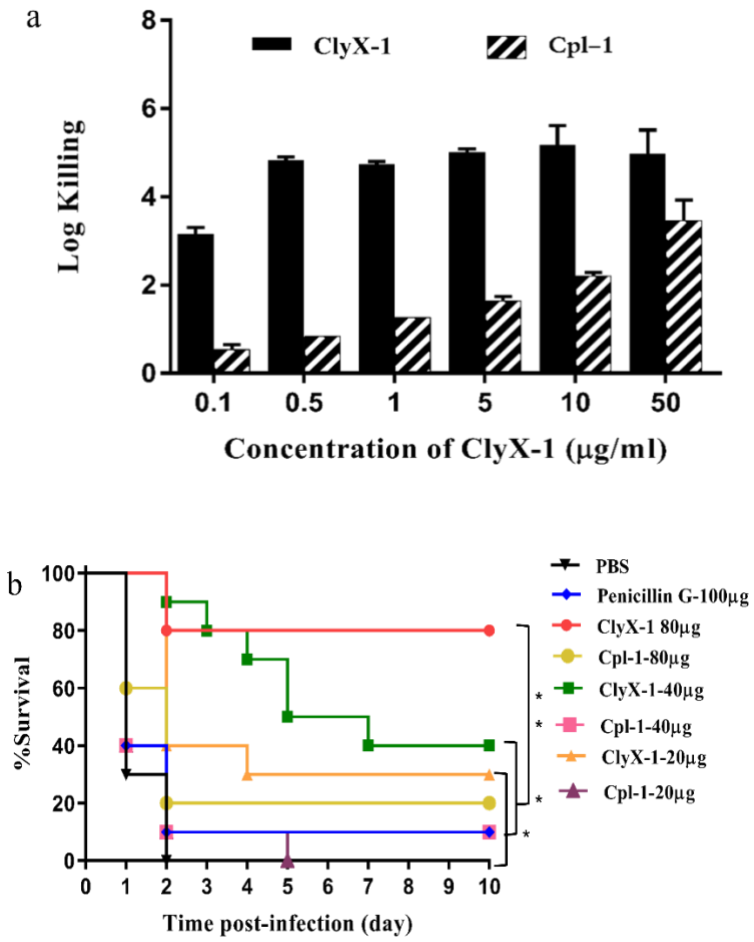

Figure 3-3. Comparisons of bactericidal activity of ClyX-1 and Cpl-1 *in vitro* and *in vivo*. (a) Different concentrations of ClyX-1 and Cpl-1 were mixed with 10^6 overnight *S. pneumoniae* D39 culture for 5 min. The cells were then serial diluted and plated on the THY plates. Log killing was determined through comparison of PBS treatment and enzyme treatment. The experiments were repeated for three times, and the error bars represent standard deviation. (b) Female BALB/c mice were injected intraperitoneally with pneumococcal strain *Spn* NS26 at a single lethal dose of 2.95 X 10^7 CFU/mouse. One hour after the infections, different concentrations of endolysins, antibiotics, and PBS were injected to mice intraperitoneally. The mice were monitored for 10 days for survival and the data were represented as the percentage of survival. The data was plotted as Kaplan-Meier survival curves and analyzed via the Log-rank (Mantel-Cox) test (*P<0.001; **P<0.0001).

Table 3-1. MICs of endolysins and antibiotics for pneumococcal strains

Strain[1]	Serotype	MIC (μg/ml) of:							
		Penicillin	Levofloxacin	Cpl-1	ClyX-1	GyH_Cpl-1 CBD	Cpl-1 CBD_CHAP	Combination[2]	ClyX-3
D39	2	0.06	0.5	16	0.13	32	16	16	4
TIGR 4	4	0.06	0.5	16	0.13	32	16	16	2
DCC1335	9V (Sp9-3)	4	2	32	0.5	128	16	32	16
DCC1490	14	0.03	1	32	0.5	32	32	32	8
DCC1476	15	0.5	2	32	0.5	64	32	32	16
DCC1355	19	0.06	0.5	16	0.25	32	16	16	8
DCC1420	23F (Sp23-1)	2	2	32	0.5	64	16	32	8
R6	capsule free	0.06	0.5	16	0.13	32	16	16	2

[1]See Appendix B for the source of species and strains.

[2]Combination treatment is GyH_Cpl-1 CBD and Cpl-1 CBD_CHAP are mixed in an amount ratio 1:1.

The High Activity of ClyX-1 is due to the Synergistic Effects of GyH and CHAP Domains

The bactericidal assays suggest ClyX-1 is several hundred times more potent than Cpl-1 (compare 0.1 µg/ml ClyX-1 to 50 µg/ml Cpl-1 in Figure 3-3 a) and the MIC assay suggests ClyX-1 is 64-128 times more potent than Cpl-1 (compare MICs of 0.13 to 0.5 µg/ml for ClyX-1 to 16-32 µg/ml for Cpl-1 in Table 3-1), suggesting the EADs of ClyX-1 retain the synergy seen in PlyC. To confirm the synergy of GyH and CHAP domains in ClyX-1, we examined the activity of each domain separately. First, we made the constructs of GyH_Cpl-1 CBD (ClyX-$1_{1\text{-}356}$) and Cpl-1 CBD_CHAP (ClyX-$1_{205\text{-}512}$), each of which consists of the Cpl-1 CBD and a functional EAD from ClyX-1. Next, we analyzed the lytic activity via turbidity reduction assay and MIC assay for ClyX-1, GyH_Cpl-1 CBD (ClyX-$1_{1\text{-}356}$), Cpl-1 CBD_CHAP (ClyX-$1_{205\text{-}512}$), and the combination of the GyH_Cpl-1 CBD and Cpl-1 CBD_CHAP constructs. Neither GyH_Cpl-1 alone, Cpl-1_CHAP alone, or the combination of both in a 1:1 ratio attained 20% of the ClyX-1 lytic activity (Figure 3-4). Consistent with these results, the MIC values showed all constructs performing similar to, or worse than, the parental Cpl-1 (Table 3-1). Thus, we suggest that the GyH and CHAP domains in ClyX-1 recapitulate the synergism due to positioning of the catalytic domains as seen in PlyC.

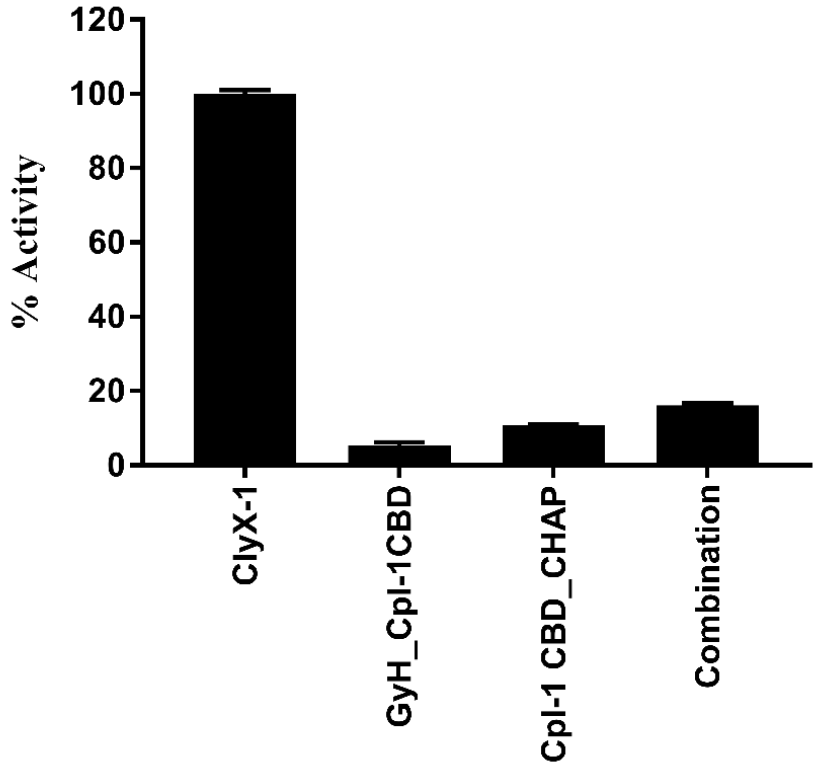

Figure 3-4. GyH and CHAP domains in ClyX-1 show synergy. The constructs of GyH_Cpl-1 CBD (ClyX-$1_{1\text{-}356}$) and Cpl-1 CBD_CHAP (ClyX-1 $_{205\text{-}512}$) were cloned and expressed for the synergy test. 5 µg/ml of each enzyme was used for the lytic activity via turbidity reduction assay against stationary phase *S. pneumoniae* R6 cells for 10 min. For the combination group, 2.5 µg/ml of GyH_Cpl-1 CBD (ClyX-$1_{1\text{-}356}$) and Cpl-1 CBD_CHAP (ClyX-1 $_{205\text{-}512}$) were used. Values are presented as the percentage of lytic activity in relation to the highest activity observed. All experiments were done in triplicate, and the error bars represent the standard deviations.

Design and Engineer a Broad Host Range Chimera Containing PlyCA

We next explored whether a different CBD can replace the Cpl-1 CBD in the ClyX-1 construct and likewise display synergistic activity, but on a new bacterial target. We, therefore, selected the PlySs2 CBD, which belongs to the SH3-5 domain family and is known to have a broad host range against most streptococci and enterococci. The new construct, termed ClyX-2 (Figure 3-1), was expressed as a soluble protein, purified, and its host spectrum was analyzed via the turbidity reduction assay. ClyX-2 was able to lyse every streptococcal species tested, including GAS, GBS, GCS, GES, *S. uberis*, and *S. mutans*, as well as *Enterococcus faecalis*, and select strains of *Staphylococcus aureus* (Figure 3-5 a). This host range overlaps the known host range of PlySs2, although *S. mutans* activity had not previously been associated with PlySs2. Next, the bactericidal efficacy of ClyX-2 and PlySs2 were compared via a log killing experiment (Figure 3-5 b). On all bacterial species tested, 100 μg/ml of ClyX-2 caused a ~6 log reduction in CFUs while the same amount of PlySs2 only caused a ~4 log reduction. Decreasing the amount of ClyX-2 to 5 μg/ml resulted in a similar log reduction as that of PlySs2 at 100 μg/ml. It should be noted that due to the mass differences between ClyX-2 and PlySs2 (i.e. ClyX-2 is ~51 kDa and PlySs2 is ~ 26 kDa), the molarity of the PlySs2 is twice as that of ClyX-2, suggesting ClyX-2 possesses synergy between the EADs that equates to ~40 times the potency of parental PlySs2 (see Figure 3-5 b for a comparison of mass concentration and molar concentration). In a similar manner, the MICs of ClyX-2 were lower than that of PlySs2 (range 4x to 64x lower), especially for GAS (2 μg/ml vs. 128 μg/ml) and GCS (4 μg/ml vs. > 512 μg/ml) (Table 3-2). Notably, *S. aureus* was the only

strain that showed low MICs for PlySs2 than ClyX-2. However, despite PlySs2's notable activity on staphylococcal strains, the PlySs2 CBD used in construction of ClyX-2, does not, in fact, bind the staphylococcal surface (Huang et al., 2015; Wei, 2015) . The binding activity of PlySs2 for the staphylococcal surface is thought to be mediated by its EAD. These results provide a second example demonstrating the engineering platform that a CBD can be placed in the middle of the PlyCA GyH and CHAP domains, maintain the synergy between these catalytic domains, and redirect the lytic actions of the chimera toward the host range of the CBD.

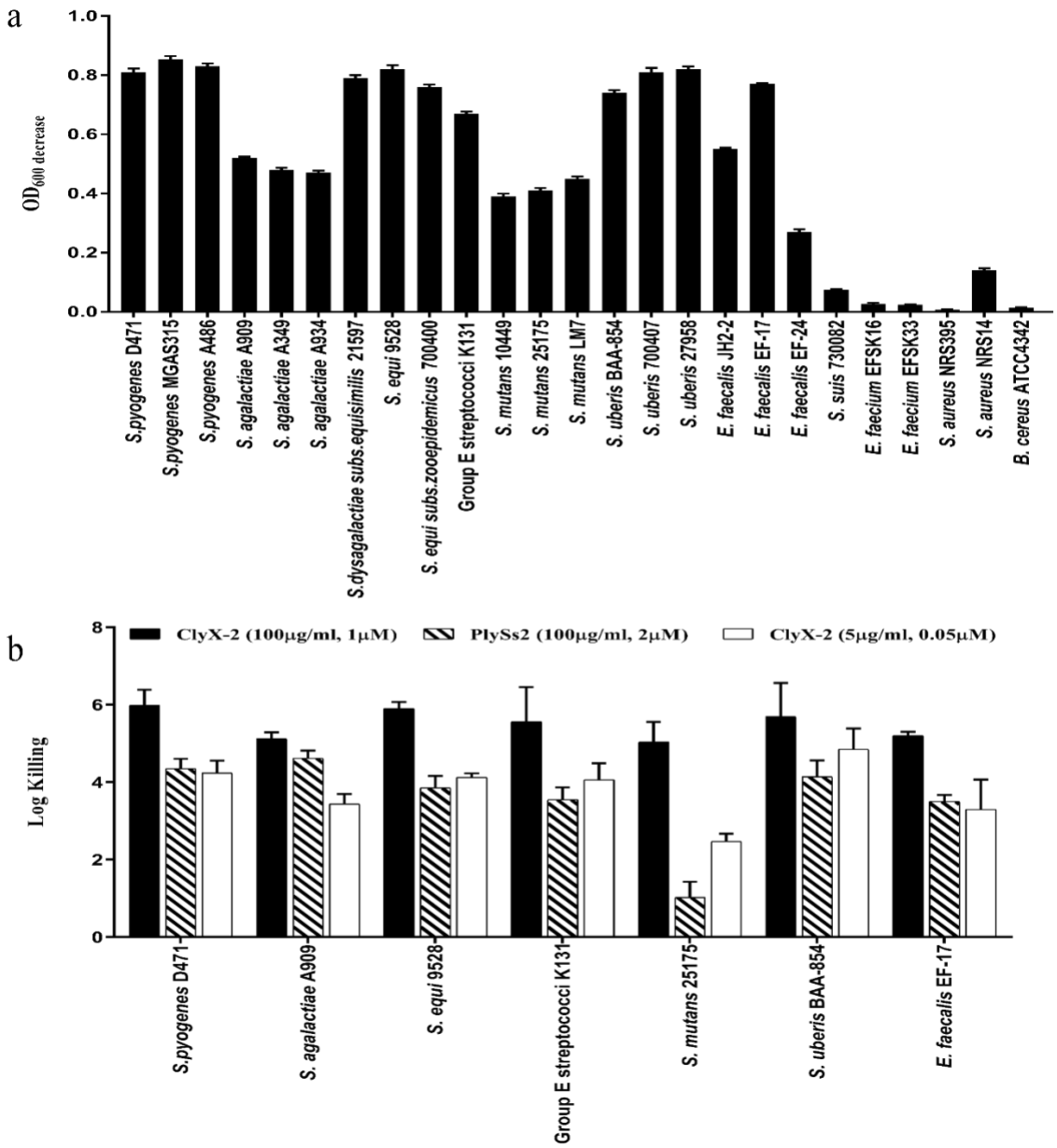

Figure 3-5. Lytic profile and bactericidal activity of ClyX-2. (a) Host range of ClyX-2. Different bacterial strains were used to test susceptibility via a turbidity reduction assay. The values were presented as the decrease OD_{600} in 10 min with 25 μg/ml of ClyX-2. (b) Bactericidal activity of ClyX-2. PlySs2 and ClyX-2 were mixed with 10^6 CFUs for 1 h after which surviving colonies were plated. Log killing was determined through comparison of PBS treatment and ClyX-1 treatment. All experiments were done in triplicate, and the error bars represent the standard deviations.

Table 3-2. MICs of endolysins and antibiotics for other streptococci stains

Species[1]	Strain[1]	MIC (μg/ml) of:		
		PlySs2	**ClyX-2**	**ClyX-4**
S. pyogenes (GAS)	D471	128	2	32
	MGAS315	128	2	32
	A486	128	2	32
S. agalactiae (GBS)	A909	128	32	64
	A349	256	32	128
S. equi (GCS)	9528	>512	4	256
GES	K131	>512	64	256
S. mutans	10449	>512	128	256
	25175	>512	128	256
S. uberis	BAA-854	>512	64	256
	700407	>512	64	256
E. faecalis	JH2-2	512	64	256
	EF-17	512	64	256
S. suis	730082	256	>512	64
S. aureus	NRS395	32	>512	>512

[1]See Appendix B for the source of species and strains.

Determine the Cleavage Specificity of PlyCA GyH and PlyCA CHAP

In order to exploit the synergy between the PlyCA GyH and CHAP domains for bioengineering purposes, the bonds cleaved by these EADs must be present in the peptidoglycan being targeted. If one of the two EADs is "silent" because the bond it cleaves is not present in the peptidoglycan, synergy will be lost. Therefore, we need to ascertain exactly which peptidoglycan bonds are cleaved by GyH and CHAP.

The PlyCA GyH domain was first characterized as a glycosyl hydrolyse due to its ability to generate reducing sugars during peptidoglycan digestion, however, it was never biochemically determined the glycosyl hydrolase activity was an N-acetylmuramidase activity or an N-acetylglucosaminidase (McGowan et al., 2012). Recently, a DALI search identified that the closest homolog to the PlyCA GyH is an N-acetylglucosaminidase domain from the glycosyl hydrolase 73 family (GH73), but again, experimental evidence is lacking (Abdul Rahman et al., 2015). The PlyCA CHAP was first characterized as an "amidase" because digestion of peptidoglycan by CHAP yields a free N-terminus, and more specifically, an N-terminal alanine residue (Fischetti VA, 1972; McGowan et al., 2012). However, the streptococcal peptidoglycan often possesses a cross-bridge consisting of two alanine residues, so it is not clear whether the CHAP domain acts as an N-acetylmuramoyl-L-alanine amidase or as an endopeptidase acting on the cross-bridge.

To further determine the specific cleavage sites, PlyC digested *S. pyogens* D471 peptidoglycan was analyzed via mass spectrometry (MS). Surprisingly, a muropeptide with an *m/z* value of 1079.5 corresponding to the size of O-acetylated N-acetylmuramic acid (NAM) and N-acetylglucosamine (NAG) with A_4QK (Figure 3-

6) was the most abundant species after digestion, suggesting that CHAP is not an amidase cleaving between NAM and L-alanine of the stem peptide. Moreover, these results confirmed that the PlyC GyH is a glucosaminidase due to the cleavage of the O-acetylated NAM, but left four possible cut sites for the CHAP domain (Figure 3-7). Through the comparison of the MS data and the host range of PlyC, ClyX-1, and ClyX-2, all the bacterial strains that were sensitive to these enzymes contain the D-ala and L-ala in the PG structure. Thus, we suggest that CHAP is an endopeptidase cutting the bonds between D-ala and L-ala which is only in streptococcal PG structure (Figure 3-7 a).

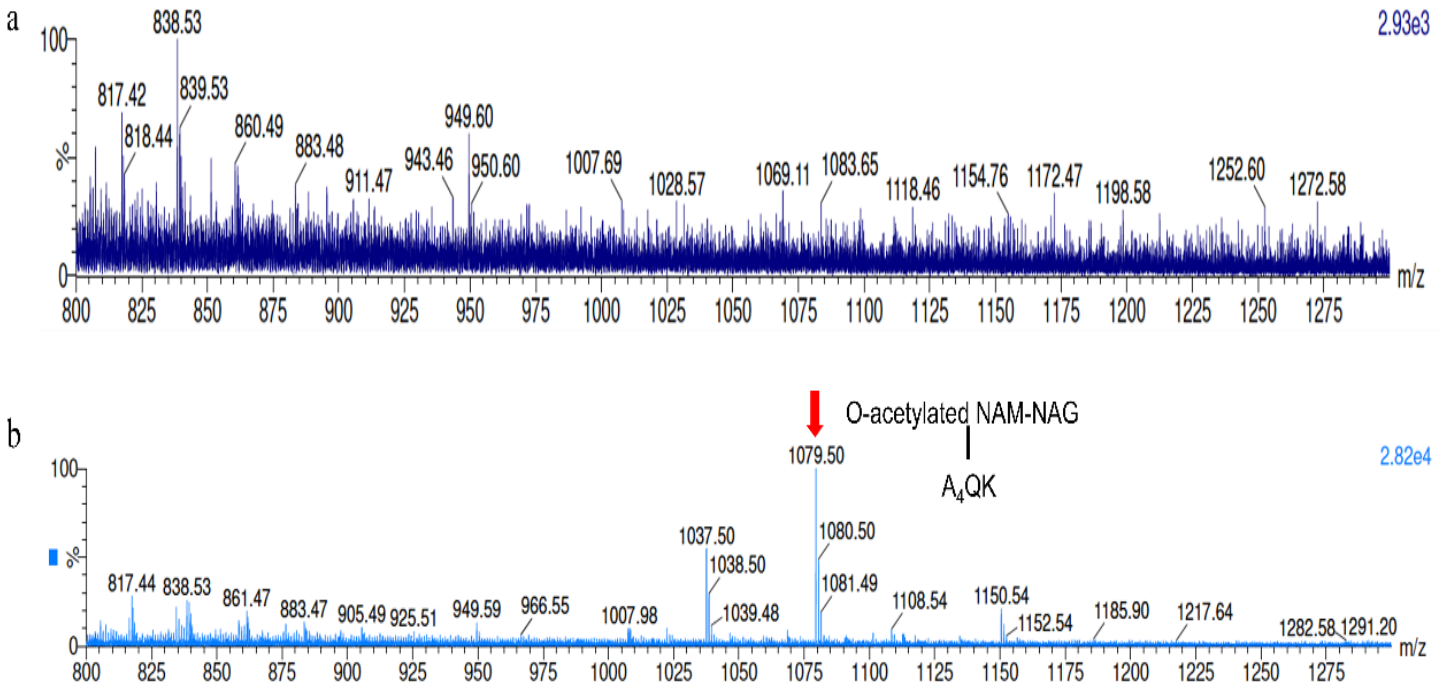

Figure 3-6. The cleavage specificity of PlyCA GyH and PlyCA CHAP. The peptidoglycan of *S. pyogenes* D471 was extracted. The purified peptidoglycan was incubated with 50µg of PlyC for 16 hours at 37°C. The reaction mixture was clarified by centrifugation (13,000rpm, 5min) and the supernatant was ultrafiltered using a 5000-MW cutoff Vivaspin. (a) MS analysis of undigested peptidoglycan (b) PlyC-digested peptidoglycan.The dominant peak of 1079.50 is the mass of O-acetylated NAM-NAG with four alanine, one glutamine and one lysine.

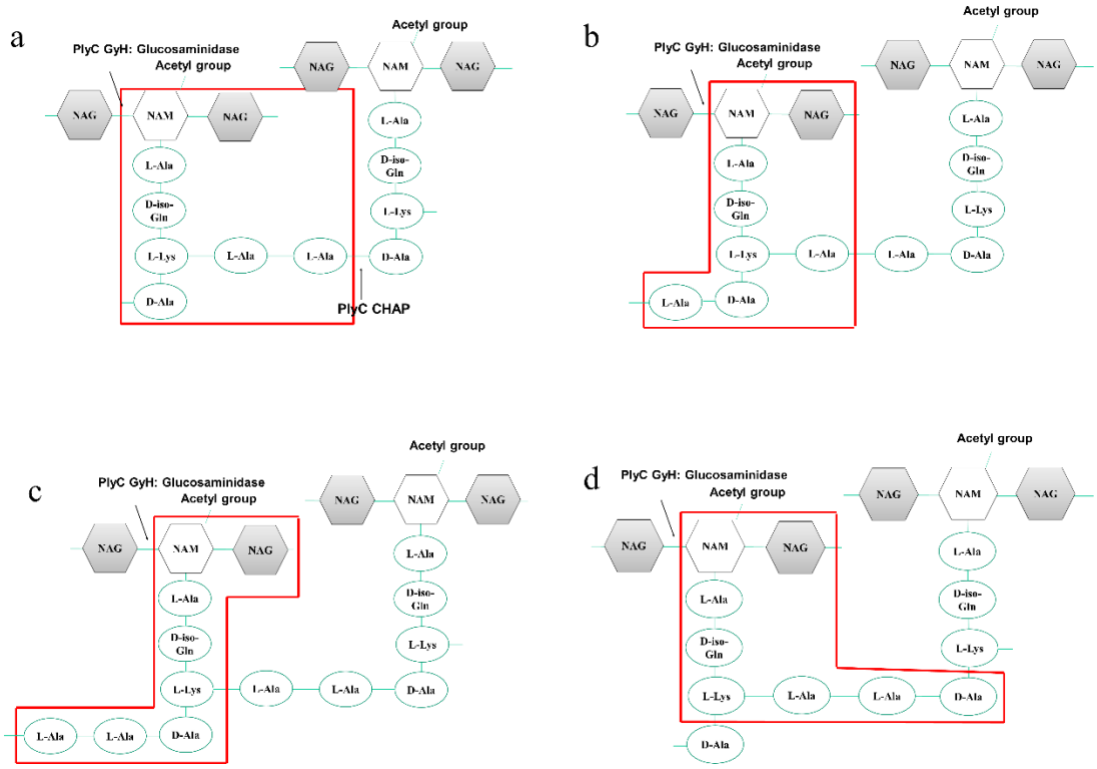

Figure 3-7. Four structures for the muropeptide. These four scenarios correspond to the peak 1079.5, which is represented O-acetylated NAM and NAG with A_4QK. The bacteria that are sensitive to ClyX-1 and ClyX-2 possess the D-Alanyl-L-Alanine bonds in the peptide stem. Supplementing with the host specificity information, CHAP domain in PlyC (PlyCA) suggests a function of D-Alanyl-L-Alanine endopeptidase, which is in figure (a).

Apply the Design Rationale to Add a C-terminal EAD

We next asked whether the design rationale, i.e. two EADs at each side of the CBD, could be used to engineer non-PlyCA based endolysins for increased activity. Toward this end, we created the ClyX-3, the full-length Cpl-1 endolysin with an additional C-terminal PlyC CHAP domain, and ClyX-4, the full-length PlySs2 endolysin, with an additional C-terminal Cpl-1 EAD (a GH25 family member) (Figure 3-1). These constructs were successfully expressed and purified as soluble proteins. We found that ClyX-3 was capable of reducing ~4 logs of the tested pneumococcal strains, whereas Cpl-1 only caused ~2 logs reduction (Figure 3-8 a). Similarly, the ClyX-4 was more active than PlySs2 against GAS, GBS, GCS, *S. uberis, S. suis,* and *S. mutants* (Figure 3-8 b). These results conclude that addition of the C-terminal EAD can augment the activity of the endolysin. Via further analysis of the MICs, we noticed that although the activity of ClyX-3 and ClyX-4 were better than parental endolysins (2-4X low MICs), they were still less active compared to ClyX-1 and ClyX-2 possessing the synergy activity (Table 3-1 and Table 3-2). These observations suggest that the effects of the two EADs in ClyX-3 and ClyX-4 may be more additive than synergistic, further underscoring the unique spatial arrangement of opposing catalytic active sites in the PlyC GyH and CHAP domains.

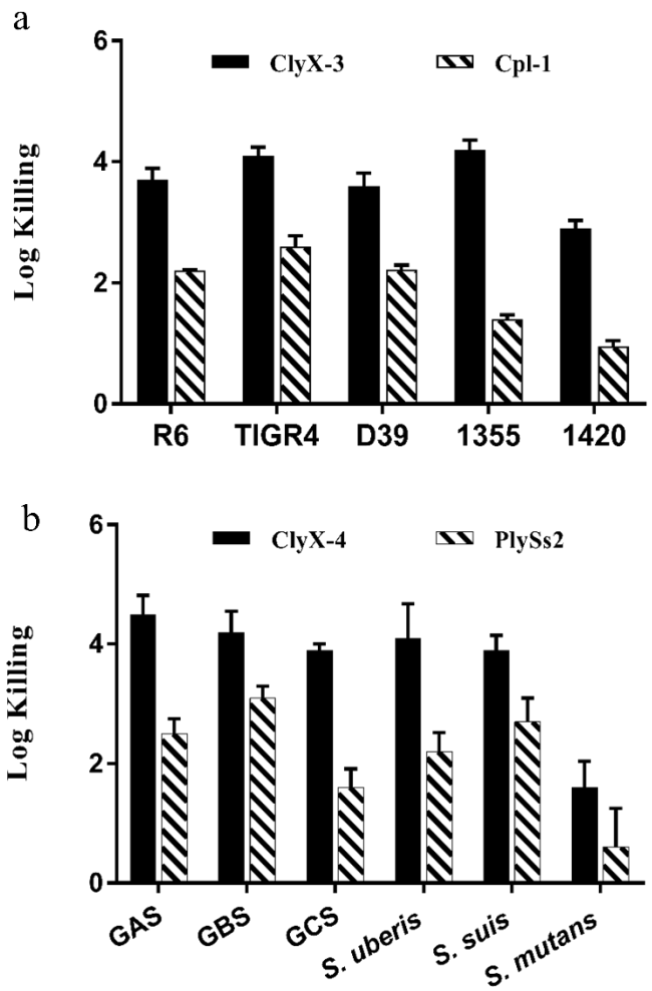

Figure 3-8. Bactericidal activity of ClyX-3 and ClyX-4. (a) Bactericidal effects of ClyX-3 against five strains of stationary phase *S. pneumoniae*. 5 µg/ml of enzymes were mixed with 10^6 CFUs for 5 min and survivors were serial diluted and plated. Log killing was determined through the comparison of PBS treatment and enzyme treatment. (b) Bactericidal effects of ClyX-4 against stationary phase streptococci. 50 µg/ml of enzymes were mixed with 10^6 CFUs for 1 h and survivors were serial diluted and plated. Log killing was determined through the comparison of PBS treatment and enzyme treatment. The experiments were repeated for three times, and the error bars represent standard deviations.

3.5 Discussion

Although PlyC has a multimeric structure, it is not the only endolysin that harbors two catalytic domains. Several examples of dual catalytic domains include: *Staphylococcus* phage K endolysin, LysK, contains N-terminal CHAP and amidase domains (Becker et al., 2009); the GBS endolysin B30 (also known as PlyGBS) has both N-terminal N-acetylmuramidase and D-alanyl-L-alanyl endopeptidase domains (Pritchard et al., 2004); the streptococcal λsa2 phage endolysin consists of a centrally located CBD separating an N-terminal D-glutaminyl-L-lysine endopeptidase domain and a C-terminal N-acetylglucosaminidase domain (Pritchard et al., 2007). However, in virtually every example, the second catalytic domains in these endolysins were found to be silent in enzymatic activity (Becker et al., 2009; Donovan & Foster-Frey, 2008; Donovan et al., 2006). It is unknown why these enzymes possess silent catalytic domains. Toward this end, PlyC is the only known endolysin with two confirmed, enzymatically active domains that furthermore display synergy due to the spatial arrangement of the opposing GyH and CHAP catalytic domains [McGowan et al., 2012).

Engineering endolysins to possess multiple EADs is not a new concept. Becker et al. has created a series of chimeric endolysins containing two, and even three, unique catalytic domains that cleave separate bonds in the peptidoglycan (Becker et al., 2016). While these enzymes were more refractory to development of resistance, the addition of a second or third EAD did not yield an additive effect, much less a synergistic effect. It should be noted that all constructs contained EADs in a linear fashion, beginning at the N-terminus (i.e. the CBD was always at the C-

terminal end), so it is unknown if any of these constructs may have performed better with a centrally located CBD as we have proposed for our engineering studies with PlyCA.

We assume that taking advantage of known synergistic catalytic domains, the PlyC GyH and CHAP, was just a starting point for engineering highly active endolysins. Due to the success of the domain swapping methods, our initial approach was to add a CBD to the C-terminus of PlyCA. However, none of the constructs were expressed. Indeed, PlyCA itself is very difficult to express in the absence of co-expression of PlyCB. Further examination of the PlyCA structure suggested the docking domain, linking GyH and CHAP with the octameric PlyCB, may not be required. We, therefore, decided to try adding a CBD, in the case of ClyX-1 it was the Cpl-1 CBD, to the middle position of the docking domain. Previous studies suggested the importance of the linker between EADs and CBDs (Schmelcher et al., 2011) and in the case of PlyCA, we expected the linkers would be exceptionally important to provide both spacing and flexibility to the EADs. However, to our surprise, the linkers turned out to be dispensible for activity (Figure 3-2 a), at least in the case of ClyX-1. Perhaps the Cpl-1 CBD, which contains six repeated choline binding modules, imparts greater flexibility than CBDs that lack such repeats. Nonetheless, the role of linkers for other engineered enzymes will need to be empirically determined for each system. Another unanticipated result was the ability of ClyX-1 to dimerize in the presence of choline (Figure 3-2 f). Although the CBDs of most pneumococcal endolysins form dimers in the presence of choline, it is not known if this process occurs on the bacterial surface or whether it is an absolute requirement

for lytic activity. Nonetheless, the ability of ClyX-1 to form dimers, given the central rather than terminal location of the Cpl-1 CBD, further suggests a degree of flexibility in this domain. In a similar manner, the SH3-5 domain (i.e. broad host spectrum CBD of PlySs2), was also able to properly fold and function as a binding domain despite the central location in ClyX-2 rather than the C-terminal location in the parental PlySs2.

We propose this design idea for a broad application. Through the successful engineered examples, ClyX-1 and ClyX-2, we show that a central CBD could provide not only binding specificity but also required distance for the two EADs to reach their separate substrates. The two EADs, Cpl-1 EAD (GH25) and PlyC CHAP, did not show a synergistic or additive effect when mixed. However, being cloned in one endolysin, ClyX-3, they displayed increased enzymatic activity. ClyX-4 performed similarly in that cloning the two EADs, PlySs2 CHAP and Cpl-2 EAD (GH25) as into one protein, they displayed increased activity. Nonetheless, the activity of ClyX-3 and ClyX-4 were less than that of ClyX-1 and ClyX-2 since the GyH and CHAP together were known to show the most potent activity. To summarize, the achievement of these two chimeric endolysins suggests that the CBD in the middle of two EADs is a feasible method to engineer endolysins.

The engineered endolysins, specifically ClyX-2, only worked on streptococci, but not on staphylococci or other species. One explanation is the binding specificity. The endolysins harboring SH3-5 binding domain were supposed to lysis the staphylococcal cells. However, research has proved that the CBD of PlySs2 could not bind to the staphylococci, while in the context of the full-length endolysin, the

dynamic of the protein leads to the binding and lysis of staphylococcal cells (Huang et al., 2015). The other explanation is cutting specificity. The GyH domain is a glucosaminidase cutting the β-(1,4) glycosidic bond between NAG and NAM. This bond is in all of the bacterial species, making the GyH domain a universal EAD. However, the CHAP domain is a D-alanyl-L-alanine endopeptidase. This is not the first EAD reported as the D-alanyl-L-alanine endopeptidase. Other endolysins possessing this enzymatic activity include include PlyB30/PlyGBS (Pritchard et al., 2004), PlyPy (Lood et al., 2014), and the bacterium-produced bacteriocin, zoocin A (Gargis et al., 2009). This may explain why ClyX-2 is not active against *Staphylococcus aureus* and *Streptococcus suis*, which has peptidoglycan crossbridges that contains either give glycines or a direct cross-link to the ε-amino group of the lysine in the stem peptide, respectively (Schleifer & Kandler, 1972). Furthermore, it is not surprising that the host range of ClyX-2 is similar to the host ranges of PlyGBS and PlyPy. ClyX-2 has activity against other strains that contain D-Ala-L-Ala bonds, including *S. mutans* and *E. faecalis*, but not *E. feacium*.

In conclusion, we proposed a novel design to harness the potent efficacy of PlyC towards streptococcal species insensitive to PlyC. We confirmed that ClyX-1 and ClyX-2 displayed dramatically improved bacteriolytic and bactericidal activity compared to the parental CBD donors, due to the synergy effects of the GyH and CHAP domains. By applying the idea to design two EADs endolysins, we created ClyX-3 and ClyX-4 in which the two EADs functioned in an additive manner.

Chapter 4:
Contributions of Net Charge on the PlyC Endolysin CHAP Domain

4.1 Abstract

Bacteriophage endolysins, enzymes that degrade the bacterial peptidoglycan (PG), have gained increasing interest as alternative antimicrobial agents due to their ability to kill antibiotic resistant pathogens efficiently when applied externally as purified proteins. Classical endolysins consist of an N-terminal enzymatically-active domain (EAD) cleaving covalent bonds in PG, and a C-terminal cell-binding domain (CBD) that recognizes specific ligands on the surface of the PG. Although CBDs are essential for the EADs to access the peptidoglycan substrates, some EADs have activity in the absence of CBDs and a few display better activities profiles or an extended host spectrum. A current hypothesis suggests a net positive charge on the EAD enables it to reach the negatively charged bacterial surface via ionic interactions in the absence of a CBD. Here, we used the PlyC CHAP domain as a model EAD to further test the hypothesis. We mutated negatively charged surface amino acids of the CHAP domain that are not involved in structured regions to neutral or positively charged amino acids in order to increase the net charge from negative three to positive one through positive seven. The seven mutant candidates were successfully express and purified as soluble proteins. However, none of the mutants were as active

as WT CHAP. The analysis of electrostatic surface potential implied that the surface charge distribution may affect the activity of the positively charged EAD. Thus, we suggest that while charge should continue to be considered for future engineering efforts, it should not be the sole focus of such engineering efforts.

4.2 Introduction

Bacteriophage endolysins are peptidoglycan (PG) hydrolases produced by phage at the end of a lytic cycle (Fischetti, 2011). With the help of holins, pore-forming proteins, endolysins can pass the cytoplasmic membrane reaching and degrading the PG layer of the cell wall resulting in the lysis of the bacteria and the release of new progeny virions (Young, 1992). These enzymes are also capable of destroying the Gram-positive bacterial PG from outside the cell as recombinant proteins (Fischetti et al., 2006). Due to the protection of the outer membrane (OM), the exogenously added endolysins usually cannot access the PG of Gram-negative bacteria. However, engineered endolysins with cationic or membrane-disrupting peptides have been reported to successfully kill Gram-negative bacteria from without (Briers et al., 2014). Consequently, endolysins are novel antimicrobial agents and can be used to treat antibiotic-resistant bacterial infections because their mode of action is not inhibited by traditional resistance mechanisms (Fischetti et al., 2006).

Endolysins derived from phages that infect Gram-positive hosts have very similar modular structures with one or more N-terminal enzymatically-active domains (EADs) and a C-terminal cell wall binding domain (CBD) (Oliveira et al., 2013). The EADs that cleave covalent bonds in the PG are conserved into five mechanistic classes: muramidases, glucosaminidases, N-acetylmuramyl-L-alanine amidases,

endopeptidase, and lytic transglycosylases. In contrast, the CBDs possess no enzymatic activity but rather function to bind to the specific ligands on the cell wall, which are usually a carbohydrate or teichoic acid moiety. Thus, the endolysin host range is often dictated by the specificity of the CBD, which is either broad-spectrum, targeting molecules harbored by a bacterial genus or multiple genera, or narrow-spectrum, targeting molecules shared by a single species or serovar (Broendum et al., 2018a; Nelson et al., 2012). The CBDs have been shown to be essential for function of EADs in a number of modular endolysins, including PlyGRCS (Linden et al., 2015), PlySs2 (Huang et al., 2015), PlyB (Porter et al., 2007), Cpl-1 (Sanz et al., 1992), and PlyB30 (Donovan et al., 2006).

Whereas many EADs require the presence of the CBD for binding and subsequent activity, some EADs can bind the bacterial surface independently of the CBD, and a few even have increased enzymatic activity compared to the full-length endolysin. One example is the staphylococcal phage endolysin, LysK. The LysK EAD, a cysteine-histidine amidohydrolase/endopeptidase (CHAP) domain, alone displays higher lytic activity against staphylococci than the full-length LysK (Horgan et al., 2009). Similarly, when the Group B streptococcal phage endolysin, PlyGBS, was truncated to the EAD, a ~20 fold increase in specific activities was noted compared to PlyGBS (Cheng & Fischetti, 2007). Moreover, without the constraining binding properties of the CBD, some EADs from the modular endolysins showed an extended host range compared with the full-length endolysins. Examples include the EAD of the *Bacillus anthracis* phage endolysin, PlyL (Low et al., 2011) and the EAD of the *Clostridium difficile* phage endolysin, CD27L (Mayer et al., 2011).

The reason why some EADs can target and lyse the PG in the absence of CBDs whereas the presence of CBDs is an absolute requirement for activity in other endolysins was unknown. Then, a ground-breaking study by Low et al. suggested that a net positive charge of an EAD enables it to function independently of its CBD, presumably through ionic interactions with the bacterial surface, which typically has a net negative charge due to surface carbohydrates (Low et al., 2011). This conceptual understanding was then applied by the authors to endolysin bioengineering studies for increasing activity of EADs and expansion of host range. For example, the EAD of a *B. subtilis* phage endolysin, XlyA, had a net charge (Z) of negative three at neutral pH. Site-directed mutagenesis of five non-cationic residues to lysine (K) produced a shift in net charge from Z=-3 to Z=+3, and the mutated XlyA EAD alone was able to lyse *B. subtilis* cells at a rate nearly identical to that of full-length XlyA. In a separate study, addition of a simple positively-charged peptide enhanced the lytic activity of the λSa2lys endolysin (Rodriguez-Rubio et al., 2016), suggesting the positive charges may increase the avidity of the enzyme for the bacterial surface.

In the present work, we sought to validate the Low's hypothesis. The model EAD for this study is the CHAP domain from the PlyC endolysin (McGowan et al., 2012). This EAD possesses potent catalytic activity, is amenable to engineering (i.e., has been subjected to mutational analysis to improve thermostability (Heselpoth et al., 2015)), and has been used as the EAD in chimeragenesis projects incorporating different CBDs (i.e., ClyR (Yang et al., 2015) and ClyJ (Yang et al., 2019)). The homolog of the PlyC CHAP domain via a DALI search is the LysK CHAP domain, which is known to harbor improved activity compared to full-length LysK. The net

charge of the LysK CHAP is Z=+1, whereas the net charge of the PlyC CHAP is Z=-3. Therefore, the PlyC CHAP is a good candidate to test Low's hypothesis that conversion of the net charge on an EAD will enable it to display lytic activity in the absence of a CBD.

4.3 Material and Method

Bacterial Strains and Culture Conditions

Streptococcus pyogenes D471 was cultured from a -80°C frozen stock and grown in Todd Hewitt broth supplemented with 1% yeast extract (THY) without shaking at 37°C. *E. coli* strains DH5α and BL21 (DE3) were grown in Luria-Bertani (LB) broth. When needed, kanamycin (50 μg/ml) was added to the media. All bacterial cultures were grown at 37°C in a shaking incubator unless otherwise stated.

In silico Modeling of PlyC CHAP Mutants

The crystal structure of the PlyCA CHAP was obtained from the original 3.3-Å crystal structure of PlyC (Protein Data Bank ID 4F88). The XlyA and XlyA+5K structures were obtained from published data (Protein Data Bank ID 3RDR and ID 3HMB, respectively). The strategy used to change the net surface charge (Z) of the CHAP domain was to substitute negatively charged amino acids, aspartic acid (D) and glutamic acid (E), that are surface exposed and not involved in structured regions (i.e. α-helix or β-sheet) to neutral (alanine (A)) or positively charged (lysine (K)) amino acids to increase the Z score from negative three to positive one through positive seven at pH 7.4. The net surface charges were calculated from the online

protein calculator (http://protcalc.sourceforge.net). PyMOL (The PyMOL Molecular Graphics System, Version 1.7.4 Schrödinger, LLC) was used to identify surface amino acids and a library of CHAP mutant candidates was established following the outlined strategy. Before further validation, the CHAP mutant candidates had their side-chain orientation optimized using the FoldX 3.0 Repair PBD command (Guerois et al., 2002). The resulting coordinates were then processed by FoldX 3.0 for calculating the free energy change of the mutants ($\Delta\Delta G_{FoldX}$). The desirable mutants possessed $\Delta\Delta G_{FoldX} < 0$ kcal/mol ($\Delta\Delta G_{FoldX} = \Delta G_{mut} - \Delta G_{WT}$) and the mutants with the largest negative $\Delta\Delta G_{FoldX}$ were then picked for experimental study. The electrostatic surface potential was imaged using CCP4MG (McNicholas et al., 2011).

Cloning and Site-directed Mutagenesis

The primers used in this study are listed in Table 2. The WT gene of PlyCA CHAP domain was amplified from pBAD24::*plyC* (Nelson et al., 2006) and cloned via NdeI and BamHI sites into pET28a, as the template for the mutagenesis. The Change-IT™ Multiple Mutation Site-Directed Mutagenesis Kit from Affymetrix was used to generate all mutants. Each mutation was designed to be in the middle of a 30 nucleotide phosphorylated forward primer and the mutagenesis followed instructions provided by the manufacturer of the kit. The resulting mutants were confirmed by sequencing (Macrogen, USA) before being transformed into *E. coli* BL21 (DE3) for protein expression.

Protein Expression and Purification

The overnight cultures of *E. coli* BL21 (DE3) harboring the WT PlyCA CHAP domain or mutants were sub-cultured 1:100 into a 1.5 L LB supplemented with kanamycin in a 4 L baffled Erlenmeyer flask at 37°C in a shaking incubator. The culture was induced at mid-log phase (about 4 h) with 1 mM isopropyl β-D-1-thiogalactopyranoside (IPTG) at incubated at 18°C overnight. The next morning, *E. coli* BL21 (DE3) bacterial cells were harvested at 5,000 rpm, resuspended in PBS, pH 7.4, sonicated, and clarified via centrifugation at 12,000 rpm at 4°C. The soluble portion of the cell lysate was applied to a Ni-NTA resin column (Thermo Fisher). The 6X His-tagged protein was washed and eluted using a gradient of imidazole from 20 mM to 500 mM in PBS buffer, pH 7.4. The protein purity was assessed on a 7.5% SDS-PAGE gel before dialysis to remove the imidazole. The 6x His-tag was removed using the Thrombin Cleavage Capture Kit (EMD Millipore) according to the protocol provided by the manufacturer.

Table 4-1. Primers information

Plasmid	Template	Primer	Sequence*
CHAP D311K	pET28a::*chap*	XS3	5’-ATGGGGTCTAAAAG AGTTGCAGCAAAC-3’
CHAP D355K	pET28a::*chap*	XS4	5’-TCATACTCAACAGGTAAAC CAATGCTACCGTTA-3’
CHAP D363K	pET28a::*chap*	XS5	5’-CTACCGTTAATTGGTAAAG GTATGAACGCTCAT-3’
CHAP D429K	pET28a::*chap*	XS6	5’-ATTGAAAGCTGGTCAAAAA CTACCGTTACAGTC-3’
CHAP D429A	pET28a::*chap*	XS8	5’-ATTGAAAGCTGGTCAGCGA CTACCGTTACAGTC-3’
CHAP D450K	pET28a::*chap*	XS7	5’-ATACGCAGCACCTATAAAC TTAACACATTCCTA-3’

*The underlined nucleotides represent the mutations.

In Vitro Endolysin Activity

The activities of the PlyC CHAP domain and its mutants were evaluated via a spectrophotometric-based turbidity reduction assay as described previously (Nelson et al., 2012). An overnight culture of *S. pyogenes* D471 was harvested at 4,500 rpm for 10 min, washed twice and resuspended in PBS, pH 7.4 buffer to reach an OD_{600} = 2.0. In a flat-bottom 96-well plate (Fisher Science), bacterial cells were mixed 1:1 with equimolar amounts of the PlyC CHAP domain or its mutants and the OD_{600} was monitored every 15 sec for 1 hour at 37°C using a SpectraMax 190 spectrophotometer (Molecular Devices). Each assay was conducted in triplicate.

4.4 Results

Library of PlyC CHAP Mutants

The PlyC CHAP domain (C-terminal of PlyCA, amino acid 309-465) was isolated from the PlyC holoenzyme crystal structure and edited in PyMOL (atomic coordinates were only available for amino acid 310-464). Five surface and unstructured residues, Asp-311, Asp-355, Asp-363, Asp-429, and Asp-450, were selected for mutagenesis (Figure 4-1). Through different combinations of point mutations incorporating either a neutral charge (i.e. alanine) or a positive charge (i.e. lysine) in place of each aspartic acid residue, a library of 192 mutant candidates harboring a surface net charge from positive one to positive seven was generated.

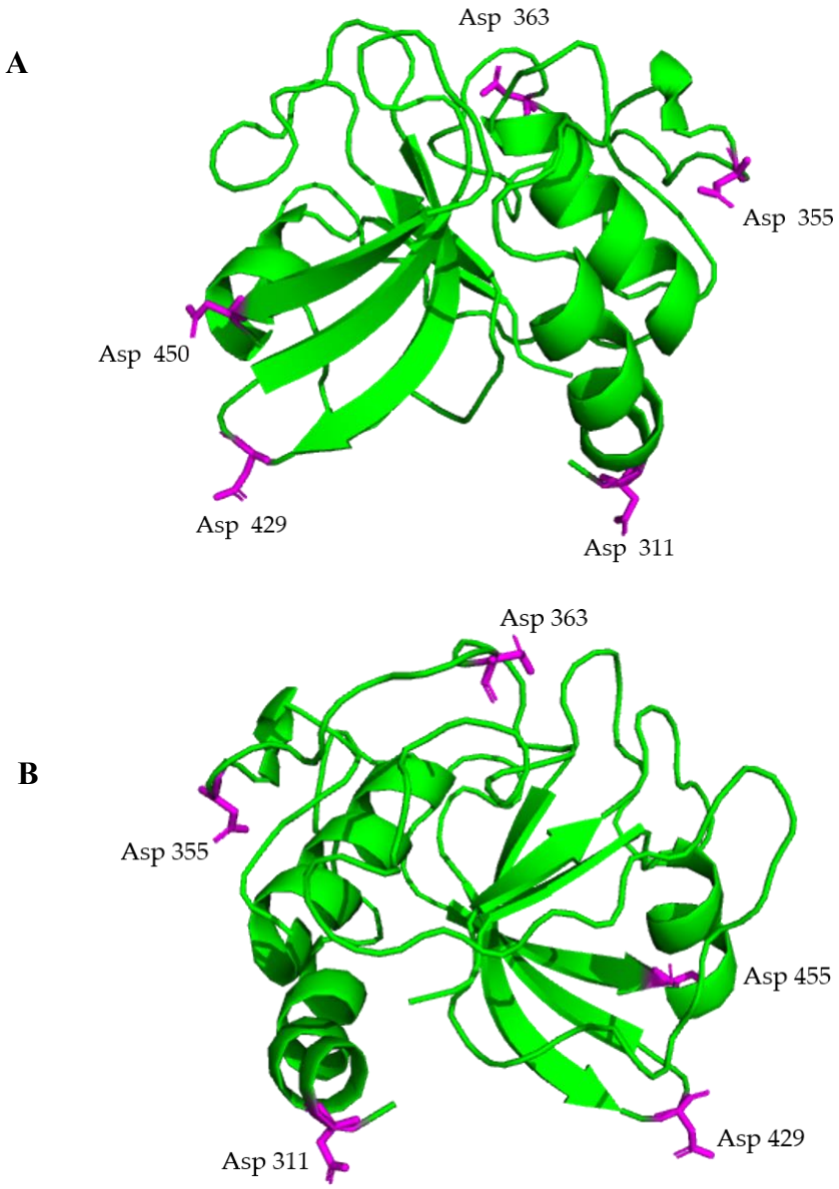

Figure 4-1. Mutation sites of PlyC CHAP. (a) 3.3 Å resolution of PlyC CHAP crystal structure. The magenta-colored amino acids represent the mutation site. (b) 180° horizontal rotation of (a). The mutation sites are solvent exposed, not structured in α-helix or β-sheets, and form no interactions with other residues. (PlyC PDB: 4F88)

Prediction of the Properly Folded PlyC CHAP Mutants via $\Delta\Delta G_{FoldX}$

FoldX is a computational biology tool developed for rapid evaluation of the effect of mutations on stability, folding, and dynamics of proteins (Schymkowitz, 2005). FoldX was used to narrow down the mutants via the free energy change of proteins ($\Delta\Delta G_{FoldX} = \Delta G_{mut} - \Delta G_{WT}$). A negative $\Delta\Delta G_{FoldX}$ ($\Delta\Delta G_{FoldX} < 0$) suggests the mutation is more stable than the wild-type (WT) protein and should fold properly. However, 79% of the mutants were predicted to have positive $\Delta\Delta G_{FoldX}$, meaning the mutations had destabilizing effects (Figure 4-2). At each charge category (Z=+1 to Z=+7), only the mutants possessing the largest predicted negative $\Delta\Delta G_{FoldX}$ were chosen to be made (Table 4-2). Notably, the selected +6 charged and +7 charged CHAP mutants contained either neutral or positive $\Delta\Delta G_{Foldx}$, probably due to the high number of required mutations (Table 4-2).

Protein Solubility and Purity

All the chosen mutants were expressed and purified by nickel affinity chromatography. The 6x His-tag at the N-terminus of each protein, which might affect the net surface charge in solution, was cleaved by thrombin before further purification. The SDS-PAGE gel after His-tag removal suggested that the PlyC CHAP mutants were pure and as soluble as the WT CHAP (Figure 4-3).

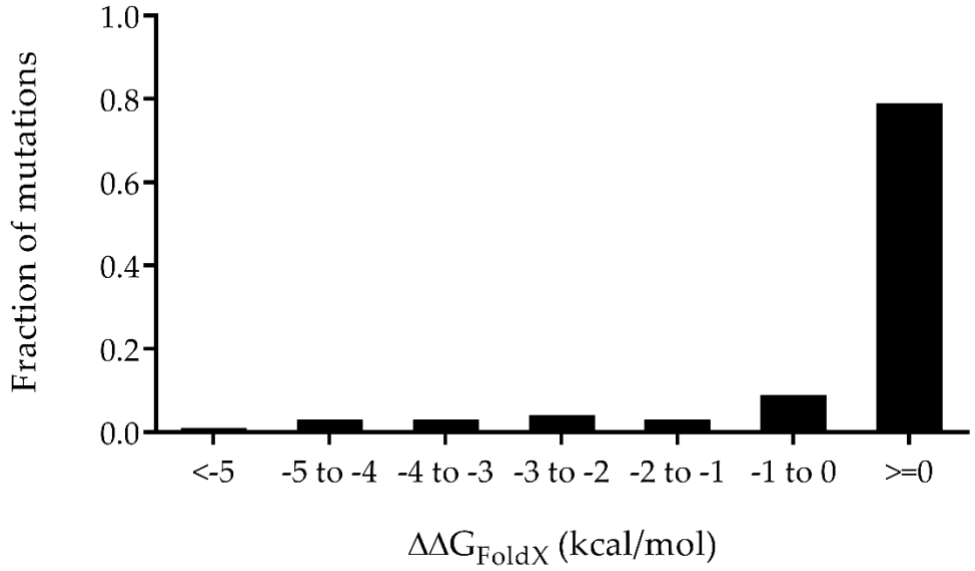

Figure 4-2. **Distribution of the predicted change in folding free energy ($\Delta\Delta G_{foldX}$) for all 192 possible CHAP mutants calculated with FoldX3.0.** Mutations with $\Delta\Delta G_{foldX}<0$ are expected to retain the same folding as wild type.

Table 4-2. PlyC CHAP WT and selective mutants

	PI (Isoelectric point)	Net Charge Z at pH 7.4	Point Mutations	$\Delta\Delta G_{FoldX} = \Delta G_{Mut} - \Delta G_{WT}$
CHAP WT	6.11	-3	NA	0
CHAP +1	7.89	+1	D311K:D355K	-5.32
CHAP +2	8.29	+2	D311K:D355K: D429A	-4.61
CHAP +3	8.59	+3	D311K:D355K: D363K	-4.32
CHAP +4	8.88	+4	D311K:D355K: D363K:D429A	-4.13
CHAP +5	9.11	+5	D311K:D355K: D363K:D429K	-2.49
CHAP +6	9.3	+6	D311K:D355K: D363K:D429A: D450K	0.01
CHAP +7	9.43	+7	D311K:D355K: D363K:D429K: D450K	1.11

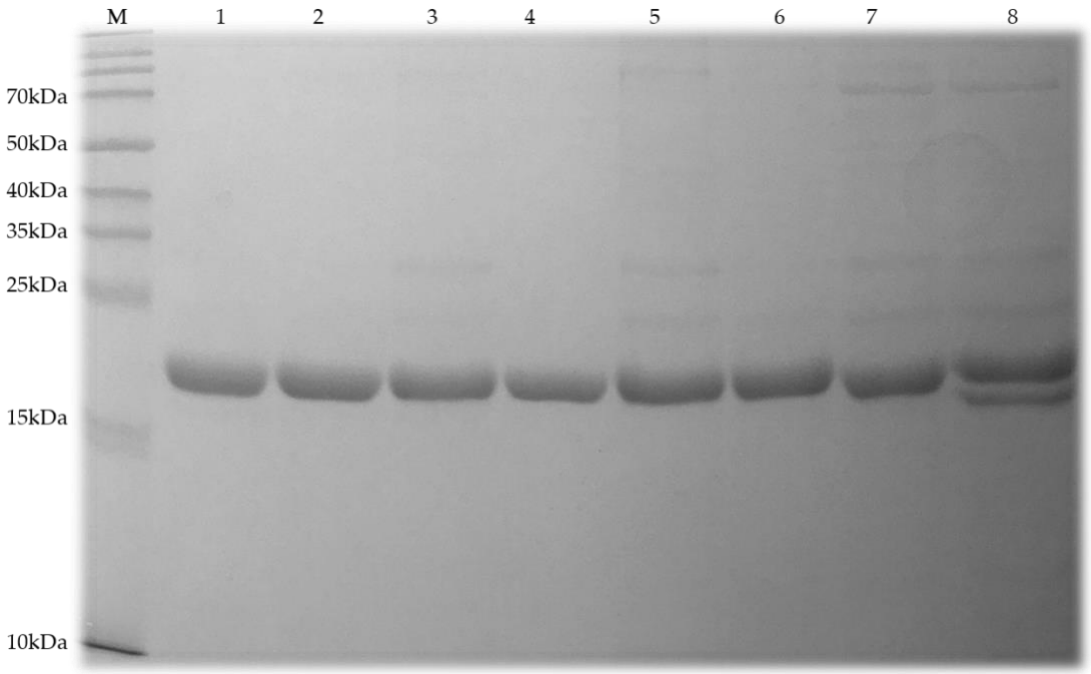

Figure 4-3. The SDS-PAGE analysis of the PlyC CHAP WT and mutants. The solubility and purity of each enzyme after the His-tag cleavage were accessed via on a 7.5% SDS-PAGE gel. The lanes correlate to: (M) biorad molecular protein marker, (1) PlyC CHAP WT, (2) PlyC CHAP +1, (3) PlyC CHAP +2, (4) PlyC CHAP +3, (5) PlyC CHAP +4, (6) PlyC CHAP +5, (7) PlyC CHAP +6 and, (8) PlyC CHAP +7.

In Vitro PlyC CHAP Mutants' Activity

PlyC is one of the most potent endolysins studied to date (Nelson et al., 2001) and the PlyC CHAP domain requires the CBD for full activity. However, despite the Z=-1 charge, the PlyC CHAP domain does retain a very small (<1% of PlyC), but measurable and reproducible lytic activity against sensitive streptococcal species (McGowan et al., 2012). A turbidity reduction assay was used to benchmark the lytic activity of the PlyC CHAP mutants to WT PlyC CHAP. However, none of the CHAP mutants displayed increased lytic activity compared with WT using *Streptococcus pyogenes* D471 as host over a broad concentration range (Figure 4-4). Nonetheless, the data has several interesting aspects. First, the CHAP mutants with a net positive one and positive two surface charges (CHAP+1 and CHAP+2) showed the same lytic activity as WT, which suggested that the positive charge alone does not affect lytic activity. Second, in the low concentration range (< 16 μg/ml), the CHAP mutants with positive three to seven surface charges (CHAP+3 to CHAP+7) were virtually devoid of lytic activity, but as the concentration increased, they had similar lytic activity as WT and CHAP+1 and CHAP+2. The activity noted for CHAP WT compared to the full PlyC holoenzyme is consistent with previous data (McGowan et al., 2012), and presumably represents activity resulting from random collisions of CHAP with the cell wall in the absence of the PlyC CBD.

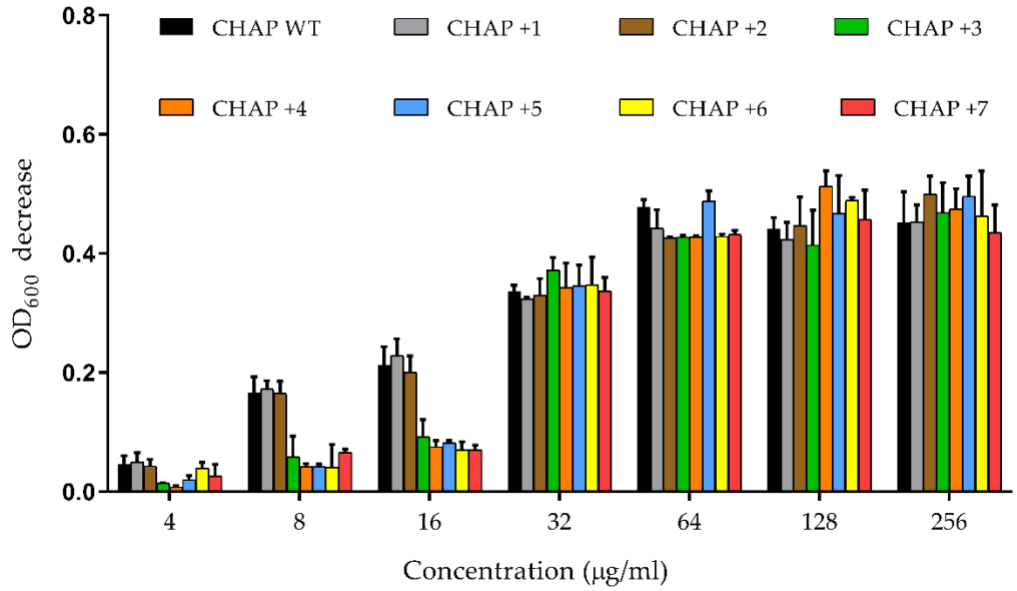

Figure 4-4. *In vitro* lytic activity against *S. pyogenes* D471. The different concentrations of enzymes were added to the overnight washed bacterial culture. The OD_{600} was recorded every 15 sec for 1 hour. The OD_{600} decrease was represented as the enzymes activity. The experiment was conducted on triplicates, and the error bars represent the standard deviation.

Analysis of PlyC CHAP Electrostatic Surface Potential

The surface charge distributions were then examined through CCP4MG software (McNicholas et al., 2011). The active site residues (C333 and H420) of PlyC CHAP are in a neutral groove, which remains unchanged in CHAP mutants. Although the increased positive charge indicates increased positive electrostatic potential in the CHAP mutants, the regions accumulating the positive surface potential is evenly distributed on the PlyC CHAP surface (Figure 4-5A). Low et. al did not imply the relationship between the relative position of the active site and the positive charge distribution (Low et al., 2011). However, when we examined the surface potential of their mutants, XlyA vs. XlyA+5K, we did notice the mutations resulted in an accumulation of positive surface potential near the active site (negative groove in Figure 4-5B). Thus, simple conversion of the charge on the EAD may not adequate to create a CBD-independent lytic activity.

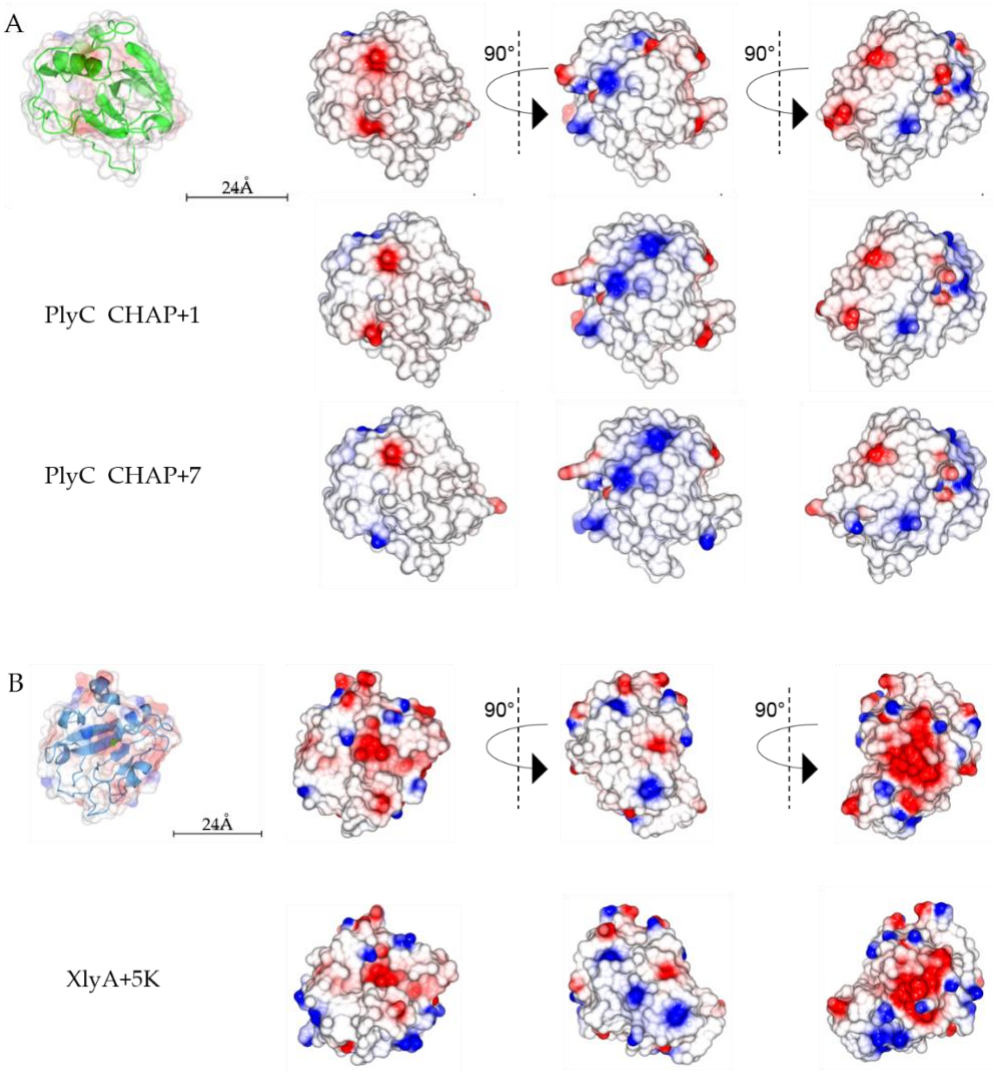

Figure 5. CCP4MG generated electrostatic surface potential maps of PlyC CHAP and XlyA and their mutants. Surfaces are color-coded according to electrostatic potential (calculated by the Poisson-Boltzmann solver within CCP4MG). The color of the surface represents the electrostatic potential at the protein surface, going from blue (potential of +10kT/e) to red (potential of -10kT/e). (A) Electrostatic surface potential of PlyC CHAP WT (PDB: 4F88), CHAP +1, and CHAP +7 in different orientations. The active site of PlyC CHAP is in a neutral groove. (B) Electrostatic surface potential of XlyA and XlyA+5K in different orientations. The active site of XlyA is in a negative groove. (XlyA PDB: 3RDR; XlyA PDB: 3HMB)

4.5 Discussion

Bacteriophage endolysins have been studied for over 50 years and used as tools in the laboratory to lyse Gram-positive bacterial cells. Their function of lysis from without was not appreciated as an alternative to antibiotics until the widespread emergence of antibiotic resistance. Fischetti's group was the first to report the use of a purified endolysin *in vivo* to control a Gram-positive bacterial infection (Nelson et al., 2001). In this study, an endolysin derived from the streptococci C1 phage, PlyC, protected mice from oral colonization *S. pyogenes* as well as eliminated the bacteria in pre-colonized mice within 2 hours. This was the first evidence that endolysins had the therapeutic potential as antimicrobials. Later, more endolysins were characterized *in vitro* and studied *in vivo* via various animal models. An *S. pneumoniae* phage endolysin, Cpl-1, was validated to effectively kill bacteria and protect mice in both a nasal model (Loeffler et al., 2001) and pneumococcal bacteremia models (Jado et al., 2003; Loeffler et al., 2003). In addition to the mouse models, Cpl-1 showed efficacy in an *S. pneumoniae*-induced endocarditis rat model (Entenza et al., 2005) and in an infant rat model of pneumococcal meningitis (Grandgirard et al., 2008). Endolysins have also been validated against other bacterial species. The first *in vivo* anti-staphylococcal investigation was the use of the MV-L endolysin that successfully reduced 3 logs of methicillin-resistant *Staphylococcus aureus* (MRSA) in a nasal colonization model and protect all the mice in an intraperitoneal model (Rashel et al., 2007). Other anti-staphylococcal endolysins, LysGH15, CHAPK, and an engineered endolysin ClyS, all displayed potent bacteriolytic properties against MRSA in animal studies (Cheng, M. et al., 2018; Daniel et al., 2010; Fenton et al., 2010; Gu et al.,

2011). In other animal models, the PlyGBS endolysin reduced Group B streptococci by 3 logs in a murine vaginal model (Cheng et al., 2005) and the PlyG endolysin provided protection for 13 out of 19 mice in a *B. anthracis*-induced intraperitoneal mouse model (Schuch et al., 2002). Most recently, the Ply6A3 endolysin derived from an *Acinetobacter baumannii* phage, demonstrated a 70% rescue rate of the mice in a lethal *A. baumannii* sepsis model (Wu et al., 2018). These *in vivo* studies have led to several endolysin in human clinical trials. SAL200 is a pharmaceutical composition consisting of the SAL-1 endolysin that is bacteriolytic to *S. aureus*. It has successfully passed Phase I clinical trials with no serious safety concerns and entered Phase II clinical trials (Jun et al., 2016). Another pharmaceutical product, CF-301 contains the PlySs2 endolysin, which also targets staphylococci and has likewise passed Phase I trials for the safety and tolerability (Abdelkader et al., 2019). Another endolysin product, known as Gladskin, contains the Staphefekt SA.100 endolysin and is currently commercialized as a skin care product for atopic dermatitis (Totte et al., 2017).

Bacteriophage have optimized endolysins for lytic activity through coevolution with bacterial hosts to ensure their survival. When applied as recombinant proteins exogenously, endolysins are not being used for their intended purpose and lose this evolutionary pressure. Therefore, these enzymes have the engineering potential to be further modified to increase activity, alter host range, or overcome complex extracellular environments (Schmelcher et al., 2012). As a growing amount of research focuses on the modular design and crystal structures of endolysins, structure-based rational engineering approaches, such as structure-guided site-directed

mutagenesis and chimeragenesis, have produced engineered endolysins with desirable properties for specific applications. The site-directed mutagenesis of PlyC CHAP Thr406 to arginine was shown to stabilize PlyC with a 16 fold increase of half-life at 45°C (Heselpoth et al., 2015). In another study, site-directed mutagenesis was applied to convert the negatively charged CBD of Cpl-7 from -14.93 to +3.0 at the neutral pH, resulting in the improvement of the lytic activity *in vitro* and *in vivo* compared to the native Cpl-7 endolysin (Diez-Martinez et al., 2013). Chimeragenesis is a method to exchange the endolysin's functional modules for better activities and expanded host range. This engineering approach has been exploited by nature itself, such as the pneumococcal endolysin Pal whose two domains indicate homology to different phage species (Sheehan et al., 1997). Some well-studied chimeolysins that harbor extended host ranges include λSA2-E-Lyso-SH3b (Becker et al., 2009), λSA2-E-LysK-SH3b (Schmelcher et al., 2012), ClyR (Yang et al., 2016; Yang et al., 2015), and, ClyS (Daniel et al., 2010). Others possessing superior activity than their parental enzymes include Cpl-711 (Diez-Martinez et al., 2015), Csl2 (Vazquez et al., 2017), and PL3 (Blazquez et al., 2016).

The ultimate goal of this study is to create an engineered endolysin that is simple (i.e., one catalytic domain) and works on a very broad host range (i.e., does not require a CBD, meaning the EAD alone defines host range). Toward this end, we sought to engineer the PlyC CHAP domain to be such an enzyme using engineering principles guided by the findings of Low et al. Toward this, we successfully made a range of positively charged CHAP mutants. The crystal structure of PlyC provided a model for selecting the potential point mutations. The computational tool, FoldX,

helped narrow down the candidates from a total of 192 to 40. The ones that are most stable among the 40 candidates were used for cloning, protein expression, and purification. The achievement of this experimental design suggests that computational tools, like FoldX, can be used in the upstream evaluation providing a rationale for the random mutations. Our results indicated that none of the positively charged CHAP mutants displayed similar or higher lytic activity than WT CHAP. Thus, at least for the PlyC CHAP, the hypothesis developed by Low et al. is not supported.

In summary, our research tested a novel method to fine-turn the lytic activity and the host range. Although the computational model led us to engineer the PlyCA CHAP with positive charge successfully, the engineered enzymes did not display improved activity. We suggest that while the positive charge should continue to be acknowledged for future engineering efforts, it should not be the sole focus and other characteristics related to positive charge (i.e., charge distribution/electrostatics surface potential) should be taken into consideration.

Chapter 5:
Discussion and Future Directions

5.1 Summary of the dissertation

The *Streptococcus* is a genus of bacteria causing several diseases from mild superficial infections to life-threatening conditions in both humans and animals. Although it is one of the few bacterial genera that is still sensitive to antibiotics, the emergence of resistant species has been noticed recent years, such as drug-resistant *Streptococcus pneumoniae*, erythromycin-resistant Group A streptococcus, and clindamycin-resistant Group B streptococcus. In addition, *streptococci* show a propensity to colonize as intracellular pathogens or to form biofilms, which result in antibiotic evasion.

Endolysins are the PG hydrolases produced at the end of the phage replication cycle. They can lyse the Gram-positive bacterial PG from outside leading to the osmotic lysis of bacteria. The antimicrobial efficacy of these enzymes has been addressed *in vitro* and *in vivo* against varieties of Gram-positive pathogens, especially the antibiotic-resistant species. The data suggest a broad use of these enzymes in medication, food safety, and disinfection. Compared to antibiotics, the resistance to endolysins is unlikely to develop based on several studies and the killing of endolysins is much more specific to their target species due to the cell binding domain (CBD). Furthermore, endolysins have been reported to clear intracellular bacteria (Shen et al., 2016) as well as to disrupt biofilms (Donlan, 2008; O'Flaherty et al., 2005; Sass & Bierbaum, 2007; Shen et al., 2013; Son et al., 2010).

PlyC, an endolysin from streptococcal C1 phage, is the most potent endolysin to date targeting GAS, GCS, GES, and *S. uberis*. Such high bactericidal activity is related to its unique structure. Unlike typical modular endolysins that contain two domains on one polypeptide, PlyC is a holoenzyme composed of eight cell binding domain subunits (PlyCB) and one enzymatically-active domain (PlyCA) interacting via protein-protein interactions to create a holoenzyme. The eight PlyCB subunits form an octamer and provide the binding specificity, and the PlyCA consists of two catalytic domains, a glycosyl hydrolase domain (GyH) and a cysteine, histidine-dependent amidohydrolase/peptidase (CHAP) domain. As much as the structural and biological data indicate the unique properties of PlyC, many questions remain. When it comes to application, PlyC is limited to some species of streptococci due to the host specificity of PlyCB. It is hard to change this specificity since it is not clear how PlyCB binds its substrate. Alternatively, if different CBDs can substitute PlyCB to allow PlyCA to retain activity, then the host range may be dramatically expanded. Rationale-based engineer techniques, such as chimeragenesis (Blazquez et al., 2016; Diez-Martinez et al., 2015; Pastagia et al., 2011; Yang et al., 2015) and site-directed mutagenesis (Diez-Martinez et al., 2013; Low et al., 2011), have been shown to effectively arm the endolysins with enhanced activity and expanded host spectrum.

In this dissertation, tailored engineering methods have been applied either to study the binding mechanism of PlyCB (Chapter 2) or to expand the host range of PlyCA (Chapter 3 and 4). The thesis aimed to overcome the host limitation of PlyC that could eventually be applied to more species as a new antimicrobial agent. First, the binding mechanism of PlyCB was addressed: whether all eight PlyCB monomers

participate in binding or whether the presence of all eight merely increased the avidity of the interactions. The site-directed mutagenesis was used to dissociate PlyCB octamer, and the binding affinity was assessed to learn the binding mechanism (Chapter 2). Second, a variety of CBDs were added to PlyCA in different forms to create specific/expanded host ranges different than observed for PlyC (Chapter 3). Third, a hypothesis that the positive protein net charge could expand the host spectrum was tested by converting the net charge of the CHAP domain from a negative charge to positive charge (Chapter 4).

The crystal structure reveals that the oligomerization of PlyCB is mediated through strand/helix hydrogen bonding interactions at each interface. Ccomputational analysis determined the important residues, Lys40, Asp41, and Glu43, are involved in monomer/monomer interactions. Site-directed mutagenesis of Lys40 and Glu43 to alanine decreases the number of monomer/monomer hydrogen bonds from 12 to only 2, which creates the PlyCB monomer (PlyCBm). Then, the PlyCBm was validated via analytical gel filtration and cross-linking. As expected, the PlyCBm retains the binding specificity of the PlyCB octamer to GAS, GCG, GES, and *S. uberis*. However, the binding affinity of the octamer is much higher than the monomer, which suggests that the octamer binds on the bacterial surface concurrently. Next, the relation of lytic activity and the binding affinity was assessed via chimeric endolysins containing PlyCBm and PlyCB2m. The results indicate that both the affinity, and subsequently the lytic activity, can be tuned to an idealized optimal through engineering efforts and modulation of the number of PlyCB monomers.

Direct substitution of PlyCB with other CBDs was applied to change the host range of PlyC aiming to exploit the synergistic bactericidal effect of PlyCA towards other bacteria. The synergy does not remain in the traditional domain swapping by the addition of a CBD at the C-terminus of PlyCA. Thus, a novel design that replaces the docking domain of PlyCA with a CBD created ClyX-1. The host range of ClyX-1 and ClyX-2 depends on the nature of their CBD, and their activities are 20-100 fold increased over the CBD donor parental enzymes. Moreover, this design can be applied to engineer two functional EADs in one endolysin. ClyX-3 and ClyX-4 are the engineered endolysins with an additional EAD targeting different bonds in PG at the C-terminus. The activity evaluations of ClyX-3 and ClyX-4 suggest that the two EADs separated by the CBD function normally to improve the lytic activity. This design can be further applied to create two EAD endolysins targeting other bacterial species.

Site-directed mutagenesis of CHAP to convert the net charge is a method adapted from Low's research (Low et al., 2011). Theoretically, a positively charged EAD displays the bactericidal activity in a CBD-independent manner due to the physical attraction of the positive charge and the negative charge on the bacterial surface. Five surface unstructured amino acids of CHAP, D311, D355, D363, D429, and D450, were mutated to alanine or lysine in different combinations to convert the charge of CHAP from negative three to positive one through positive seven. Computational screening of the mutants using the FoldX algorithm can effectively identify the ones with correct folding. Even though the CHAP mutants with the net charge from positive one through positive seven were expressed and purified

successfully, their activity did not show a CBD-independent manner suggesting other factors, such as the surface electrostatic potential of the EAD, may be involved in this method for refining the host range.

5.2 Discussion

Before the studies mentioned in Chapter 2 to Chapter 4, there is no published research involving host range modification of PlyC. Although it is the most potent endolysin to date, the complex holoenzyme structure is a hurdle to further engineering. One reason for that is PlyC is encoded by two separate genes. The addition of different genes to either the end of *plyCA* or *plyCB* leads to expression and/or folding issues. The other reason is that the PlyCB subunits form an octamer as the cell binding domain and interact with PlyCA via protein-protein interaction. The widely applied method to change/expand the host range of an endolysin is via domain swapping. This method is more suitable for a traditional structured endolysin encoded by one gene with the monomeric architecture of an N-terminal EAD linked to a C-terminal CBD. The specificity of monomeric CBDs is dependent on the different substrates, usually carbohydrates, on the surface of the bacterial PG. It is unknown how the PlyCB octamer binds to the surface of the bacteria. Is the specificity due to the oligomerization or the different substrates on the bacterial surface? Thus, the first aim of this thesis is to understand the binding mechanism of PlyCB.

The PlyCBm obtained from mutagenesis retained the same host range as that of the PlyCB octamer. Based on the fluorescence protein bacterial cell binding assay, both fluorescently-labeled PlyCBm and the PlyCB octamer similarly decorated the

cell wall, suggesting that they recognized the same ligand on the bacterial surface. Thus, the specificity of PlyCB to GAS, GCS, GES, and *S. uberis* is not due to the oligomerization of the CBD but to the specific ligand binding. The binding affinity is important to understand the binding mechanism of the PlyCB octamer. A concurrent binding indicates a higher affinity of the octamer, while the consecutive interaction indicates the similar affinity of monomer and octamer. Two label-free technologies, surface plasmon resonance (SPR) and bio-layer interferometry (BLI), are commonly used to measure the biomolecular interactions (Douzi, 2017; Shah & Duncan, 2014). However, both systems measure the wavelength before and after the proteins binding to the immobilized ligands, and the wavelength shifts represent the amount of binding. The size of the bacteria is about 10^2 times larger than the size of the CBDs. The wavelength shift is hard to detect when CBDs bind to the bacteria immobilized on the surface. Therefore, the fluorescence labeling binding assay was adopted for quantitative measurement. Although the results from this assay were preliminary and not precise for the affinity, they implied that the binding of PlyCB is concurrent.

The PlyCBm is a good tool to study the relation of binding affinity and bactericidal activity. The previous study indicated that the increased binding affinity decreases the lytic activity under physiological condition but increases the lytic activity under high salt concentration (Schmelcher et al., 2011). The chimeric endolysin containing the PlyCA CHAP and PlyCBm (CHAP_CBm) was created to compare the activity with PlyCΔGyH (PlyCA CHAP and PlyCB octamer). PlyCΔGyH displayed higher lytic activity compared that of CHAP_CBm, indicating that in our case, the higher binding affinity results in higher lytic activity. This is

supported by the chimeric endolysin containing the PlyCA CHAP and PlyCB2m, which displayed better activity than that of CHAP_PlyCBm, indicating that PlyCA CHAP favors a tighter binding. Interestingly, changing the EAD from PlyC CHAP to the LysK CHAP with PlyCBm and PlyCB2m enhanced the lytic activity even further, implying that the different EADs prefer the CBD with different binding affinity.

Even though PlyCBm provides limited use in the chimeragenesis application, since it keeps the same host range and contains low binding affinity, PlyCBm is nonetheless suitable for other applications due to its simple structure. The PlyCB octamer and PlyCBm have a moonlight function, which is to enter the mammalian cell via endocytosis by the interaction of PlyCB and phosphatidylserine (Shen et al., 2016). Thus, the PlyCBm can be an intracellular peptide fused with endolysins targeting intracellular bacterial pathogens. The other application of PlyCBm is to use as a tool to diagnose GAS, GCS, GES, and *S. uberis.* Although the binding affinity of PlyCBm and bacteria is low, the effective concentration of 50% PlyCBm is in a nanomolar range which is similar or even better than the binding affinity of antibodies (Fischetti, 2010).

Changing/expanding the host range from the perspective of PlyCB is not feasible since the PlyCB octamer and PlyCB bind to the specific epitope on the surface of GAS, GCS, GES, and *S. uberis*. Thus, the fusion of a different CBD to PlyCA is the second aim. Direct addition of a CBD to the N-terminal or C-terminal PlyCA resulted in an unexpressed protein. The results are similar to the overexpression of PlyCA only. The PlyCA in a previous study was overexpressed with the PlyCB mutant that cannot form the holoenzyme, and only then was it able to be purified using

ammonium sulfate precipitation. One explanation is the gene composition of PlyC. PlyC is encoded by an operon. The first ORF is *plyCB*; the second ORF is a putative endonuclease gene called *lil* for lysin intergenic locus; the third ORF is *plyCA.* The *lil* is not translated in the expression of PlyC, but Δ*lil* construct ablates enzyme activity (Nelson et al., 2006). Thus, the function of *lil* remains unknown but may relate to the eight PlyCB monomers to one PlyCA ratio. Surprisingly, when the docking domain in PlyCA was replaced with a CBD, the expression issues were solved, and the protein was easily overexpressed. This result may indicate that the *lil* responds to the region of the *plyCA* docking gene resulting in the production of eight PlyCB for one PlyCA.

The central CBD provides both length and flexibility for the GyH and CHAP domains to perform synergistically. The goal is to translate the endolysin as an antimicrobial agent. The mouse pneumococcal infection model showed that a low dose of ClyX-1 protected 80% mice. Although 20 μg of ClyX-1 only protected 30% mice, the same amount of Cpl-1 treated mice died in the first five days. So far, the doses of ClyX-1 in this study were the lowest amount compared to the amount of endolysin used in other pneumococcal mouse infection models. Furthermore, the MICs indicated that ClyX-1 was efficient for the penicillin-resistant strains. Thus, these data suggest that ClyX-1 is a novel candidate for resistant pneumococcal infections.

At present, the engineered endolysins do not work on any bacterial species other than streptococci. One explanation is the CBDs we used do not bind to other bacterial species. The other explanation is that the GyH and CHAP domains only cut the bonds involved in the streptococcal PG. To test the second hypothesis, we ran the mass

spectrophotometry for the digested PG. The results reveal that GyH is glycosaminidase that cuts the sugar backbone, while the CHAP is an endopeptidase cutting D-Ala-L-Ala bonds in the cross-bridge only in the streptococcal PG and several enterococcal PG. Thus, the synergy of GyH and CHAP cannot be applied to any other species due to the specificity of the CHAP.

The failure of creating the CBD-independent CHAP does not indicate the method on conversion of EADs surface net charge will not work. Using the CHAP domain for this study was far from ideal. With GyH domain in PlyCA, they display a synergic effect. However, any one of the domains possesses very low enzymatic activity (McGowan et al., 2012). One reason to use the PlyCA CHAP domain is the easy accessibility of the clone for expressing. The other reason to use is that the homolog of CHAP from LysK shows activity in a CBD-independent manner. Moreover, the surface net charge of the PlyCA CHAP is negative three while that of the LysK CHAP is positive one. Thus, we believed changing the net negative charge to positive will arm the PlyCA CHAP as a CBD-independent enzyme. The deficiency of the study is that we neglected the importance of surface charge distribution. Therefore, in the future application, we will add more criteria for selecting the point-mutations.

5.3 Future Directions

Further Application: analysis of ClyX-1 and ClyX-2

Although we assessed the bactericidal activity of ClyX-1 and ClyX-2 in Chapter 2, these two chimeric endolysins can be applied to many fields. *S. pneumoniae* forms a biofilm during different infection states, such as otitis media, chronic rhinosinusitis, and pneumonia (Hall-Stoodley et al., 2006; Hoa et al., 2009; Sanderson et al., 2006). Several studies have proved that endolysins are effective to disperse biofilms and kill the bacteria involved in biofilm formation (Shen, J. et al., 2013; Son et al., 2010). Due to the high activity of ClyX-1 on pneumococci *in vitro* and *in vivo*, ClyX-1 is a potential new source of antibiofilm therapy. ClyX-2 is the chimeric endolysin with a broad spectrum. Besides the anti-biofilm application, it may be used as an antimicrobial agent in the infections involved different bacteria. One example is bovine mastitis, which is a mammary gland infection in dairy cows causing the loss in milk production and quality. The mastitis pathogens, such as the GBS in the milk can lead to the infections in newborn babies (Ismail et al., 2011) and *S. uberis* causes 95% intramammary infections (Pedersen et al., 2003). ClyX-2 harboring the bactericidal activity against these two bacteria species and can be applied as the treatment of bovine mastitis as well as the biological disinfectant.

Adopting the Novel Design Method to Create Engineered Two-EAD Endolysins on Other Bacterial Species

The novel design to harness the synergy of two catalytic domains can be applied for chimeric endolysins on other bacterial species by changing the EADs for specific bonds. For example, the CHAP domain from LysK specifically cleaves the D-ala-gly

bonds in the staphylococcal PG, and the EAD from lysostaphin specifically cleavages a glycyl-glycine bond in staphylococci PG. Previously studies created a chimeric endolysin using these two EADs in a structure where both EADs are side by side at the N-terminus and the CBD is at the C-terminus (Becker et al., 2016). Although the chimeric endolysins displayed an advantage in not inducing resistance, the activity compared to parental endolysins did not improve. One explanation is that the tandemly linked EADs lose the flexibility to reach both substrates.

To further apply the novel design, we can generate a library of EADs with known cleavage specificities and CBDs with known host ranges. Then, randomly shuffle the EADs and CBDs based on the design that forces the CBD to be in the middle of two EADs. By doing so, we may generate the endolysins harboring high activity on more bacterial species.

Appendix A

Sequence Information for Constructs used in Dissertation-Related Studies

pBAD24::*plyC*

Insert Sequence (2213 nucleotides)

GAAGTAATTTCCATTCTTGAAAACGTCGCATGGTACTTACCAGTGCCAAAGAAACTG
CTAAATGTTTTAGCACAATTTAAAGAAATAGAAAATGAGGTAAAATCAAATGAGCAA
GATTAATGTAAACGTAGAAAATGTTTCTGGTGTACAAGGTTTCCTATTCCATACCGA
TGGAAAAGAAAGTTACGGTTATCGTGCTTTTATTAACGGAGTTGAAATTGGTATTAA
AGACATTGAAACCGTACAAGGATTTCAACAAATTATACCGTCTATCAATATTAGTAA
GTCTGATGTAGAGGCTATCAGAAAGGCTATGAAAAAGTAATGATTGAGGAGTGGGTC
AAGCACCCCTCCCTCAATTACTATATAAGTAGTTATGGCAGGGTGAAAAACTCTAAA
GGTTTAATAATGAAACAACACATATGCAATGGTTATAAGCGAATTAAATTAGTAAAG
GACGGTATAAAAAAGAATTACTATGTTCATCGCTTAGTTGCAGAAACATTCATACCT
AAACTACATGTTGACTATGTTGTACATCATATTGACCATGATAAACTAAACAACTGG
GTACATAACTTAGAATGGTGTCATTATCAAACTAACCTATTATATGAAAGGGAGAAT
TTATTTAATGAGTAAGAAGTATACACAACAACAATACGAAAAATATTTAGCACAACC
AGCAAATAACACATTTGGGTTATCACCTCAACAGGTTGCTGATTGGTTTATGGGTCA
AGCTGGTGCTAGGCCTGTTATTAACTCGTATGGGGTAAATGCTAGTAATTTAGTATC
AACGTACATACCTAAAATGCAGGAATACGGTGTATCATATACACTATTCTTAATGTA
TACTGTCTTTGAGGGAGGCGGCGCAGGTAATTGGATTAATCATTACATGTACGATAC
GGGGTCTAATGGATTAGAGTGTTTGGAACACGATTTACAATACATACATGGCGTCTG
GGAAACTTATTTTCCACCAGCTTTATCTGCGCCAGAATGTTACCCAGCTACGGAAGA
TAACGCAGGTGCTTTAGATAGATTTTATCAATCGCTACCAGGCCGAACATGGGGTGA
TGTTATGATACCTAGTACAATGGCTGGTAATGCTTGGGTATGGGCTTATAACTATTG
TGTTAACAACCAAGGGGCTGCCCCATTAGTTTACTTTGGCAATCCATACGATAGTCA
AATTGATAGCTTGCTTGCAATGGGAGCTGACCCGTTTACAGGTGGTTCAATTACAGG
TGATGGAAAAAATCCTAGTGTTGGCACTGGGAATGCTACCGTTTCTGCTAGCTCGGA
AGCTAACAGAGAGAAGTTAAAGAAAGCCCTAACAGATTTATTCAACAACAACCTAGA
ACATCTATCAGGTGAATTCTACGGTAACCAAGTGTTGAATGCTATGAAATACGGCAC
TATCCTGAAATGTGATTTAACAGATGACGGACTTAATGCCATTCTTCAATTAATAGC
TGATGTTAACTTACAGACTAACCCTAACCCAGACAAACCGACCGTTAAATCACCAGG
TCAAAACGATTTAGGGTCGGGGTCTGATAGAGTTGCAGCAAACTTAGCCAATGCACA
GGCGCAAGTCGGTAAGTATATTGGTGACGGTCAATGTTATGCTTGGGTTGGTTGGTG
GTCAGCTAGGGTATGTGGTTATTCTATTTCATACTCAACAGGTGACCCAATGCTACC
GTTAATTGGTGATGGTATGAACGCTCATTCTATCCATCTTGGTTGGGATTGGTCAAT
CGCAAATACTGGTATTGTTAACTACCCAGTTGGTACTGTTGGACGCAAGGAAGATTT
GAGAGTCGGCGCGATATGGTGCGCTACAGCATTCTCTGGCGCTCCGTTTTATACAGG

ACAATACGGCCATACTGGTATCATTGAAAGCTGGTCAGATACTACCGTTACAGTCTT
AGAACAAAACATTTTAGGGTCACCAGTTATACGCAGCACCTATGACCTTAACACATT
CCTATCAACACTAACTGGTTTGATAACATTTAAATAAAAAAGAAGAGACTGTAAAGT
CTCTTTTCTTATTTTATAATGACGTTATTAACAACTGTGTTATTAATCATGTCACTT
TCTTTGTGCCATAACCTTACACCTGCTTCAAACAAAGCTCTTAACATATTCATATGC
CCAGTGTCTACGTTAGGAAGAGTCCATATTCCCTTGAATTGAACCCA

Protein Sequence (Holoenzyme is 1032 aa, 113.11 kDa)

PlyCB (71 aa in monomer, 7.86 kDa)

MSKINVNVENVSGVQGFLFHTDGKESYGYRAFINGVEIGIKDIETVQGFQQIIPSIN
ISKSDVEAIRKAMKK*

PlyCA (464 aa, 50.37 kDa)

MSKKYTQQQYEKYLAQPANNTFGLSPQQVADWFMGQAGARPVINSYGVNASNLVSTY
IPKMQEYGVSYTLFLMYTVFEGGGAGNWINHYMYDTGSNGLECLEHDLQYIHGVWET
YFPPALSAPECYPATEDNAGALDRFYQSLPGRTWGDVMIPSTMAGNAWVWAYNYCVN
NQGAAPLVYFGNPYDSQIDSLLAMGADPFTGGSITGDGKNPSVGTGNATVSASSEAN
REKLKKALTDLFNNNLEHLSGEFYGNQVLNAMKYGTILKCDLTDDGLNAILQLIADV
NLQTNPNPDKPTVKSPGQNDLGSGSDRVAANLANAQAQVGKYIGDGQCYAWVGWWSA
RVCGYSISYSTGDPMLPLIGDGMNAHSIHLGWDWSIANTGIVNYPVGTVGRKEDLRV
GAIWCATAFSGAPFYTGQYGHTGIIESWSDTTVTVLEQNILGSPVIRSTYDLNTFLS
TLTGLITFK

pBAD24::*plyCA*

Insert Sequence (1398 nucleotides)

ATGAGTAAGAAGTATACACAACAACAATACGAAAAATATTTAGCACAACCAGCAAAT
AACACATTTGGGTTATCACCTCAACAGGTTGCTGATTGGTTTATGGGTCAAGCTGGT
GCTAGGCCTGTTATTAACTCGTATGGGGTAAATGCTAGTAATTTAGTATCAACGTAC
ATACCTAAAATGCAGGAATACGGTGTATCATATACACTATTCTTAATGTATACTGTC
TTTGAGGGAGGCGGCGCAGGTAATTGGATTAATCATTACATGTACGATACGGGGTCT
AATGGATTAGAGTGTTTGGAACACGATTTACAATACATACATGGCGTCTGGGAAACT
TATTTTCCACCAGCTTTATCTGCGCCAGAATGTTACCCAGCTACGGAAGATAACGCA
GGTGCTTTAGATAGATTTTATCAATCGCTACCAGGCCGAACATGGGGTGATGTTATG
ATACCTAGTACAATGGCTGGTAATGCTTGGGTATGGGCTTATAACTATTGTGTTAAC
AACCAAGGGGCTGCCCCATTAGTTTACTTTGGCAATCCATACGATAGTCAAATTGAT
AGCTTGCTTGCAATGGGAGCTGACCCGTTTACAGGTGGTTCAATTACAGGTGATGGA
AAAAATCCTAGTGTTGGCACTGGGAATGCTACCGTTTCTGCTAGCTCGGAAGCTAAC
AGAGAGAAGTTAAAGAAAGCCCTAACAGATTTATTCAACAACAACCTAGAACATCTA
TCAGGTGAATTCTACGGTAACCAAGTGTTGAATGCTATGAAATACGGCACTATCCTG
AAATGTGATTTAACAGATGACGGACTTAATGCCATTCTTCAATTAATAGCTGATGTT
AACTTACAGACTAACCCTAACCCAGACAAACCGACCGTTCAATCACCAGGTCAAAAC
GATTTAGGGTCGGGGTCTGATAGAGTTGCAGCAAACTTAGCCAATGCACAGGCGCAA
GTCGGTAAGTATATTGGTGACGGTCAATGTTATGCTTGGGTTGGTTGGTGGTCAGCT
AGGGTATGTGGTTATTCTATTTCATACTCAACAGGTGACCCAATGCTACCGTTAATT
GGTGATGGTATGAACGCTCATTCTATCCATCTTGGTTGGGATTGGTCAATCGCAAAT
ACTGGTATTGTTAACTACCCAGTTGGTACTGTTGGACGCAAGGAAGATTTGAGAGTC
GGCGCGATATGGTGCGCTACAGCATTCTCTGGCGCTCCGTTTTATACAGGACAATAC
GGCCATACTGGTATCATTGAAAGCTGGTCAGATACTACCGTTACAGTCTTAGAACAA
AACATTTTAGGGTCACCAGTTATACGCAGCACCTATGACCTTAACACATTCCTATCA
ACACTAACTGGTTTGATAACATTTAAATAA

Protein Sequence (464 aa, 50.37 kDa)

MSKKYTQQQYEKYLAQPANNTFGLSPQQVADWFMGQAGARPVINSYGVNASNLVSTY
IPKMQEYGVSYTLFLMYTVFEGGGAGNWINHYMYDTGSNGLECLEHDLQYIHGVWET
YFPPALSAPECYPATEDNAGALDRFYQSLPGRTWGDVMIPSTMAGNAWVWAYNYCVN
NQGAAPLVYFGNPYDSQIDSLLAMGADPFTGGSITGDGKNPSVGTGNATVSASSEAN
REKLKKALTDLFNNNLEHLSGEFYGNQVLNAMKYGTILKCDLTDDGLNAILQLIADV
NLQTNPNPDKPTVKSPGQNDLGSGSDRVAANLANAQAQVGKYIGDGQCYAWVGWWSA
RVCGYSISYSTGDPMLPLIGDGMNAHSIHLGWDWSIANTGIVNYPVGTVGRKEDLRV
GAIWCATAFSGAPFYTGQYGHTGIIESWSDTTVTVLEQNILGSPVIRSTYDLNTFLS
TLTGLITFK

pBAD24::*cpl-1*

Insert Sequence (1038 nucleotides)

ATGGTTAAAAAGAATGATTTATTTGTAGATGTTTCAAGTCACAACGGTTACGATATA
ACAGGTATCTTGGAGCAAATGGGAACAACTAACACCATCATTAAAATTTCTGAAAGT
ACGACCTATTTAAACCCTTGCTTGTCTGCTCAAGTGGAGCAGTCAAACCCTATTGGC
TTTTATCACTTCGCACGCTTTGGCGGAGACGTAGCAGAAGCCGAAAGAGAAGCGCAG
TTTTTCCTTGACAACGTGCCTATGCAAGTTAAATACCTTGTATTGGACTACGAGGAC
GACCCAAGCGGAGACGCACAAGCGAACACTAACGCATGCTTACGCTTTATGCAGATG
ATTGCTGACGCTGGATATAAACCTATTTATTATAGTTATAAACCGTTTACACATGAT
AATGTGGACTATCAGCAAATCCTTGCACAGTTCCCTAATTCTCTATGGATTGCAGGC
TATGGCTTAAACGATGGTACAGCTAACTTTGAATACTTCCCAAGCATGGACGGGATA
AGATGGTGGCAGTATTCTAGTAACCCGTTTGACAAGAATATTGTACTGTTAGACGAT
GAAGAAGACGACAAGCCAAAGACCGCTGGAACGTGGAAACAAGACAGCAAGGGGTGG
TGGTTCAGACGAAACAATGGCAGTTTCCCTTATAATAAATGGGAAAAAATCGGTGGT
GTGTGGTACTACTTCGATAGTAAAGGATATTGCTTAACGAGCGAATGGCTCAAAGAT
AATGAAAAATGGTACTACCTCAAGGACAACGGCGCAATGGCGACTGGTTGGGTGCTA
GTCGGGTCAGAGTGGTATTATATGGACGATTCAGGCGCTATGGTTACTGGTTGGGTC
AAGTATAAGAATAACTGGTACTATATGACAAATGAACGTGGTAACATGGTTTCTAAT
GAATTTATTAAGTCTGGAAAAGGTTGGTATTTCATGAACACAAACGGAGAGCTTGCA
GACAATCCAAGTTTCACGAAAGAACCAGACGGGCTTATAACCGTAGCACATCATCAT
CATCACCATTAA

Protein Sequence (464 aa, 50.37 kDa)

MVKKNDLFVDVSSHNGYDITGILEQMGTTNTIIKISESTTYLNPCLSAQVEQSNPIG
FYHFARFGGDVAEAEREAQFFLDNVPMQVKYLVLDYEDDPSGDAQANTNACLRFMQM
IADAGYKPIYYSYKPFTHDNVDYQQILAQFPNSLWIAGYGLNDGTANFEYFPSMDGI
RWWQYSSNPFDKNIVLLDDEEDDKPKTAGTWKQDSKGWWFRRNNGSFPYNKWEKIGG
VWYYFDSKGYCLTSEWLKDNEKWYYLKDNGAMATGWVLVGSEWYYMDDSGAMVTGWV
KYKNNWYYMTNERGNMVSNEFIKSGKGWYFMNTNGELADNPSFTKEPDGLITVAHHH
HHH*

pBAD24::*plySs2*

Insert Sequence (756 nucleotides)

ATGACCACCGTTAATGAAGCCCTGAATAATGTTCGTGCACAGGTTGGTAGCGGTGTT
AGCGTTGGTAATGGTGAATGTTATGCACTGGCAAGCTGGTATGAACGTATGATTAGT
CCGGATGCAACCGTTGGTCTGGGTGCCGGTGTTGGTTGGGTTAGCGGTGCAATTGGT
GATACCATTAGCGCAAAAAACATTGGCAGCAGCTATAATTGGCAGGCAAATGGTTGG
ACCGTTAGCACCAGCGGTCCGTTTAAAGCAGGTCAGATTGTTACCCTGGGTGCAACA
CCGGGTAATCCGTATGGTCATGTTGTTATTGTTGAAGCCGTTGATGGTGATCGTCTG
ACCATTCTGGAACAGAATTATGGTGGTAAACGTTATCCGGTGCGTAACTATTATTCA
GCAGCAAGCTATCGTCAGCAGGTTGTTCATTATATCACCCCTCCGGGTACAGTTGCA
CAGAGCGCACCGAATCTGGCAGGTAGCCGTAGCTATCGTGAAACCGGCACCATGACC
GTTACCGTTGATGCACTGAATGTTCGTCGTGCACCGAATACCAGCGGTGAAATTGTT
GCAGTGTATAAACGTGGTGAGAGCTTCGATTATGATACCGTGATTATTGATGTGAAC
GGTTATGTTTGGGTGAGCTATATTGGTGGTTCAGGCAAACGTAATTATGTTGCAACC
GGTGCCACCAAAGATGGTAAACGCTTTGGTAATGCATGGGGCACCTTTAAACATCAT
CATCATCATCATTAA

Protein Sequence (464 aa, 50.37 kDa)

MTTVNEALNNVRAQVGSGVSVGNGECYALASWYERMISPDATVGLGAGVGWVSGAIG
DTISAKNIGSSYNWQANGWTVSTSGPFKAGQIVTLGATPGNPYGHVVIVEAVDGDRL
TILEQNYGGKRYPVRNYYSAASYRQQVVHYITPPGTVAQSAPNLAGSRSYRETGTMT
VTVDALNVRRAPNTSGEIVAVYKRGESFDYDTVIIDVNGYVWVSYIGGSGKRNYVAT
GATKDGKRFGNAWGTFKHHHHHH*

pET28a(+)::*clyX-1*

Insert Sequence (1539 nucleotides)

ATGAGTAAGAAGTATACACAACAACAATACGAAAAATATTTAGCACAACCAGCAAAT
AACACATTTGGGTTATCACCTCAACAGGTTGCTGATTGGTTTATGGGTCAAGCTGGT
GCTAGGCCTGTTATTAACTCGTATGGGGTAAATGCTAGTAATTTAGTATCAACGTAC
ATACCTAAAATGCAGGAATACGGTGTATCATATACACTATTCTTAATGTATACTGTC
TTTGAGGGAGGCGGCGCAGGTAATTGGATTAATCATTACATGTACGATACGGGGTCT
AATGGATTAGAGTGTTTGGAACACGATTTACAATACATACATGGCGTCTGGGAAACT
TATTTTCCACCAGCTTTATCTGCGCCAGAATGTTACCCAGCTACGGAAGATAACGCA
GGTGCTTTAGATAGATTTTATCAATCGCTACCAGGCCGAACATGGGGTGATGTTATG
ATACCTAGTACAATGGCTGGTAATGCTTGGGTATGGGCTTATAACTATTGTGTTAAC
AACCAAGGGGCTGCCCCATTAGTTTACTTTGGCAATCCATACGATAGTCAAATTGAT
AGCTTGCTTGCAATGGGAGCTGACCCGTTTACAGGTGGTTCAATTATGGAAGAAGAC
GACAAGCCAAAGACCGCTGGAACGTGGAAACAAGACAGCAAGGGGTGGTGGTTCAGA
CGAAACAATGGCAGTTTCCCTTATAATAAATGGGAAAAAATCGGTGGTGTGTGGTAC
TACTTCGATAGTAAAGGATATTGCTTAACGAGCGAATGGCTCAAAGATAATGAAAAA
TGGTACTACCTCAAGGACAACGGCGCAATGGCGACTGGTTGGGTGCTAGTCGGGTCA
GAGTGGTATTATATGGACGATTCAGGCGCTATGGTTACTGGTTGGGTCAAGTATAAG
AATAACTGGTACTATATGACAAATGAACGTGGTAACATGGTTTCTAATGAATTTATT
AAGTCTGGAAAAGGTTGGTATTTCATGAACACAAACGGAGAGCTTGCAGACAATCCA
AGTTTCACGAAAGAACCAGACGGGCTTATAACCGTAGCAGGGTCTGATAGAGTTGCA
GCAAACTTAGCCAATGCACAGGCGCAAGTCGGTAAGTATATTGGTGACGGTCAATGT
TATGCTTGGGTTGGTTGGTGGTCAGCTAGGGTATGTGGTTATTCTATTTCATACTCA
ACAGGTGACCCAATGCTACCGTTAATTGGTGATGGTATGAACGCTCATTCTATCCAT
CTTGGTTGGGATTGGTCAATCGCAAATACTGGTATTGTTAACTACCCAGTTGGTACT
GTTGGACGCAAGGAAGATTTGAGAGTCGGCGCGATATGGTGCGCTACAGCATTCTCT
GGCGCTCCGTTTTATACAGGACAATACGGCCATACTGGTATCATTGAAAGCTGGTCA
GATACTACCGTTACAGTCTTAGAACAAAACATTTTAGGGTCACCAGTTATACGCAGC
ACCTATGACCTTAACACATTCCTATCAACACTAACTGGTTTGATAACATTTAAATAA

Protein Sequence (512 aa, 57.28 kDa)

MSKKYTQQQYEKYLAQPANNTFGLSPQQVADWFMGQAGARPVINSYGVNASNLVSTY
IPKMQEYGVSYTLFLMYTVFEGGGAGNWINHYMYDTGSNGLECLEHDLQYIHGVWET
YFPPALSAPECYPATEDNAGALDRFYQSLPGRTWGDVMIPSTMAGNAWVWAYNYCVN
NQGAAPLVYFGNPYDSQIDSLLAMGADPFTGGSIMEEDDKPKTAGTWKQDSKGWWFR
RNNGSFPYNKWEKIGGVWYYFDSKGYCLTSEWLKDNEKWYYLKDNGAMATGWVLVGS
EWYYMDDSGAMVTGWVKYKNNWYYMTNERGNMVSNEFIKSGKGWYFMNTNGELADNP
SFTKEPDGLITVAGSDRVAANLANAQAQVGKYIGDGQCYAWVGWWSARVCGYSISYS
TGDPMLPLIGDGMNAHSIHLGWDWSIANTGIVNYPVGTVGRKEDLRVGAIWCATAFS
GAPFYTGQYGHTGIIESWSDTTVTVLEQNILGSPVIRSTYDLNTFLSTLTGLITFK*

Template	Primer	Sequence (5'>3')
pBAD24::*plyCA*	XS49	CGCATATGAGTAAGAAGTATACACA
	XS107	GTCGTCTTCTTCCATAATTGAACCACCTGT
pBAD24::*cpl-1*	XS106	ACAGGTGGTTCAATTATGGAAGAAGACGAC
	XS109	AACTCTATCAGACCCTGCTACGGTTATAAG
pBAD24::*plyCA*	XS108	CTTATAACCGTAGCAGGGTCTGATAGAGTT
	XS2	CGGGATCCTTATTTAAATGTTATCAAACC

Notes

GyH ($PlyCA_{1-205}$), Cpl-1 $CBD_{(191-339)}$ and CHAP ($PlyCA_{309-465}$), fused via 2 round of SOE PCR cloned into NdeI/BamHI sites of pET28a(+)

pET28a(+)::*clyX-1 Linkers*

Insert Sequence (1677 nucleotides)

ATGAGTAAGAAGTATACACAACAACAATACGAAAAATATTTAGCACAACCAGCAAAT
AACACATTTGGGTTATCACCTCAACAGGTTGCTGATTGGTTTATGGGTCAAGCTGGT
GCTAGGCCTGTTATTAACTCGTATGGGGTAAATGCTAGTAATTTAGTATCAACGTAC
ATACCTAAAATGCAGGAATACGGTGTATCATATACACTATTCTTAATGTATACTGTC
TTTGAGGGAGGCGGCGCAGGTAATTGGATTAATCATTACATGTACGATACGGGGTCT
AATGGATTAGAGTGTTTGGAACACGATTTACAATACATACATGGCGTCTGGGAAACT
TATTTTCCACCAGCTTTATCTGCGCCAGAATGTTACCCAGCTACGGAAGATAACGCA
GGTGCTTTAGATAGATTTTATCAATCGCTACCAGGCCGAACATGGGGTGATGTTATG
ATACCTAGTACAATGGCTGGTAATGCTTGGGTATGGGCTTATAACTATTGTGTTAAC
AACCAAGGGGCTGCCCCATTAGTTTACTTTGGCAATCCATACGATAGTCAAATTGAT
AGCTTGCTTGCAATGGGAGCTGACCCGTTTACAGGTGGTTCAATTACAGGTGATGGA
AAAAATCCTAGTGTTGGCACTGGGAATGCTACCGTTTCTGCTAGCTCGGAATGTACA
ATGGAAGAAGACGACAAGCCAAAGACCGCTGGAACGTGGAAACAAGACAGCAAGGGG
TGGTGGTTCAGACGAAACAATGGCAGTTTCCCTTATAATAAATGGGAAAAAATCGGT
GGTGTGTGGTACTACTTCGATAGTAAAGGATATTGCTTAACGAGCGAATGGCTCAAA
GATAATGAAAAATGGTACTACCTCAAGGACAACGGCGCAATGGCGACTGGTTGGGTG
CTAGTCGGGTCAGAGTGGTATTATATGGACGATTCAGGCGCTATGGTTACTGGTTGG
GTCAAGTATAAGAATAACTGGTACTATATGACAAATGAACGTGGTAACATGGTTTCT
AATGAATTTATTAAGTCTGGAAAAGGTTGGTATTTCATGAACACAAACGGAGAGCTT
GCAGACAATCCAAGTTTCACGAAAGAACCAGACGGGCTTATAACCGTAGCACTGCAG
CAGACTAACCCTAACCCAGACAAACCGACCGTTAAATCACCAGGTCAAAACGATTTA
GGGTCGGGGTCTGATAGAGTTGCAGCAAACTTAGCCAATGCACAGGCGCAAGTCGGT
AAGTATATTGGTGACGGTCAATGTTATGCTTGGGTTGGTTGGTGGTCAGCTAGGGTA
TGTGGTTATTCTATTTCATACTCAACAGGTGACCCAATGCTACCGTTAATTGGTGAT
GGTATGAACGCTCATTCTATCCATCTTGGTTGGGATTGGTCAATCGCAAATACTGGT
ATTGTTAACTACCCAGTTGGTACTGTTGGACGCAAGGAAGATTTGAGAGTCGGCGCG
ATATGGTGCGCTACAGCATTCTCTGGCGCTCCGTTTTATACAGGACAATACGGCCAT
ACTGGTATCATTGAAAGCTGGTCAGATACTACCGTTACAGTCTTAGAACAAAACATT
TTAGGGTCACCAGTTATACGCAGCACCTATGACCTTAACACATTCCTATCAACACTA
ACTGGTTTGATAACATTTAAATAA

Protein Sequence (558 aa, 61.83 kDa)

MSKKYTQQQYEKYLAQPANNTFGLSPQQVADWFMGQAGARPVINSYGVNASNLVSTY
IPKMQEYGVSYTLFLMYTVFEGGGAGNWINHYMYDTGSNGLECLEHDLQYIHGVWET
YFPPALSAPECYPATEDNAGALDRFYQSLPGRTWGDVMIPSTMAGNAWVWAYNYCVN
NQGAAPLVYFGNPYDSQIDSLLAMGADPFTGGSITGDGKNPSVGTGNATVSASSECT
MEEDDKPKTAGTWKQDSKGWWFRRNNGSFPYNKWEKIGGVWYYFDSKGYCLTSEWLK
DNEKWYYLKDNGAMATGWVLVGSEWYYMDDSGAMVTGWVKYKNNWYYMTNERGNMVS
NEFIKSGKGWYFMNTNGELADNPSFTKEPDGLITVALQQTNPNPDKPTVKSPGQNDL
GSGSDRVAANLANAQAQVGKYIGDGQCYAWVGWWSARVCGYSISYSTGDPMLPLIGD
GMNAHSIHLGWDWSIANTGIVNYPVGTVGRKEDLRVGAIWCATAFSGAPFYTGQYGH
TGIIESWSDTTVTVLEQNILGSPVIRSTYDLNTFLSTLTGLITFK*

Template	Primer	Sequence (5'>3')
pBAD24::*plyCA*	XS49	CGCATATGAGTAAGAAGTATACACA
	XS132	TGTCGTCTTCTTCCATTTCCGAGCTAGCAGAAAC
pBAD24::*cpl-1*	XS131	TTCTGCTAGCTCGGAAATGGAAGAAGACGACAAG
	XS134	GGTTAGGGTTAGTCTGTGCTACGGTTATAAGCCC
pBAD24::*plyCA*	XS133	GCTTATAACCGTAGCACAGACTAACCCTAACCCA
	XS2	CGGGATCCTTATTTAAATGTTATCAAACC

Notes

GyH with linker ($PlyCA_{1-227}$), Cpl-1 $CBD_{(191-339)}$ and CHAP with linker ($PlyCA_{287-465}$), fused via 2 round of SOE PCR cloned into NdeI/BamHI sites of pET28a(+)

pET28a(+)::*clyX-2*

Insert Sequence (1401 nucleotides)

ATGAGTAAGAAGTATACACAACAACAATACGAAAAATATTTAGCACAACCAGCAAAT
AACACATTTGGGTTATCACCTCAACAGGTTGCTGATTGGTTTATGGGTCAAGCTGGT
GCTAGGCCTGTTATTAACTCGTATGGGGTAAATGCTAGTAATTTAGTATCAACGTAC
ATACCTAAAATGCAGGAATACGGTGTATCATATACACTATTCTTAATGTATACTGTC
TTTGAGGGAGGCGGCGCAGGTAATTGGATTAATCATTACATGTACGATACGGGGTCT
AATGGATTAGAGTGTTTGGAACACGATTTACAATACATACATGGCGTCTGGGAAACT
TATTTTCCACCAGCTTTATCTGCGCCAGAATGTTACCCAGCTACGGAAGATAACGCA
GGTGCTTTAGATAGATTTTATCAATCGCTACCAGGCCGAACATGGGGTGATGTTATG
ATACCTAGTACAATGGCTGGTAATGCTTGGGTATGGGCTTATAACTATTGTGTTAAC
AACCAAGGGGCTGCCCCATTAGTTTACTTTGGCAATCCATACGATAGTCAAATTGAT
AGCTTGCTTGCAATGGGAGCTGACCCGTTTACAGGTGGTTCAATTGGTACCATGCCT
CCGGGTACAGTTGCACAGAGCGCACCGAATCTGGCAGGTAGCCGTAGCTATCGTGAA
ACCGGCACCATGACCGTTACCGTTGATGCACTGAATGTTCGTCGTGCACCGAATACC
AGCGGTGAAATTGTTGCAGTGTATAAACGTGGTGAGAGCTTCGATTATGATACCGTG
ATTATTGATGTGAACGGTTATGTTTGGGTGAGCTATATTGGTGGTTCAGGCAAACGT
AATTATGTTGCAACCGGTGCCACCAAAGATGGTAAACGCTTTGGTAATGCATGGGGC
ACCTTTAAAACTAGTGGGTCTGATAGAGTTGCAGCAAACTTAGCCAATGCACAGGCG
CAAGTCGGTAAGTATATTGGTGACGGTCAATGTTATGCTTGGGTTGGTTGGTGGTCA
GCTAGGGTATGTGGTTATTCTATTTCATACTCAACAGGTGACCCAATGCTACCGTTA
ATTGGTGATGGTATGAACGCTCATTCTATCCATCTTGGTTGGGATTGGTCAATCGCA
AATACTGGTATTGTTAACTACCCAGTTGGTACTGTTGGACGCAAGGAAGATTTGAGA
GTCGGCGCGATATGGTGCGCTACAGCATTCTCTGGCGCTCCGTTTTATACAGGACAA
TACGGCCATACTGGTATCATTGAAAGCTGGTCAGATACTACCGTTACAGTCTTAGAA
CAAAACATTTTAGGGTCACCAGTTATACGCAGCACCTATGACCTTAACACATTCCTA
TCAACACTAACTGGTTTGATAACATTTAAATAA

Protein Sequence (466 aa, 50.68 kDa)

MSKKYTQQQYEKYLAQPANNTFGLSPQQVADWFMGQAGARPVINSYGVNASNLVSTY
IPKMQEYGVSYTLFLMYTVFEGGGAGNWINHYMYDTGSNGLECLEHDLQYIHGVWET
YFPPALSAPECYPATEDNAGALDRFYQSLPGRTWGDVMIPSTMAGNAWVWAYNYCVN
NQGAAPLVYFGNPYDSQIDSLLAMGADPFTGGSIGTMPPGTVAQSAPNLAGSRSYRE
TGTMTVTVDALNVRRAPNTSGEIVAVYKRGESFDYDTVIIDVNGYVWVSYIGGSGKR
NYVATGATKDGKRFGNAWGTFKTSGSDRVAANLANAQAQVGKYIGDGQCYAWVGWWS
ARVCGYSISYSTGDPMLPLIGDGMNAHSIHLGWDWSIANTGIVNYPVGTVGRKEDLR
VGAIWCATAFSGAPFYTGQYGHTGIIESWSDTTVTVLEQNILGSPVIRSTYDLNTFL
STLTGLITFK*

Template	Primer	Sequence (5'>3')
pBAD24::*plyCA*	XS49	CGCATATGAGTAAGAAGTATACACA
	XS125	ACTGTACCCGGAGGCATAATTGAACCACCTGT
pBAD24::*cpl-1*	XS124	ACAGGTGGTTCAATTATGCCTCCGGGTACAGT
	XS127	AACTCTATCAGACCCTTTAAAGGTGCCCCATG
pBAD24::*plyCA*	XS126	CATGGGGCACCTTTAAAGGGTCTGATAGAGTT
	XS2	CGGGATCCTTATTTAAATGTTATCAAACC

Notes

GyH ($PlyCA_{1-205}$), PlySs2 $CBD_{(148-245)}$ and CHAP ($PlyCA_{309-465}$), fused via 2 round of SOE PCR cloned into NdeI/BamHI sites of pET28a(+)

pET28a(+)::*GyH_cpl-1CBD*

Insert Sequence (1065 nucleotides)

```
ATGAGTAAGAAGTATACACAACAACAATACGAAAAATATTTAGCACAACCAGCAAAT
AACACATTTGGGTTATCACCTCAACAGGTTGCTGATTGGTTTATGGGTCAAGCTGGT
GCTAGGCCTGTTATTAACTCGTATGGGGTAAATGCTAGTAATTTAGTATCAACGTAC
ATACCTAAAATGCAGGAATACGGTGTATCATATACACTATTCTTAATGTATACTGTC
TTTGAGGGAGGCGGCGCAGGTAATTGGATTAATCATTACATGTACGATACGGGGTCT
AATGGATTAGAGTGTTTGGAACACGATTTACAATACATACATGGCGTCTGGGAAACT
TATTTTCCACCAGCTTTATCTGCGCCAGAATGTTACCCAGCTACGGAAGATAACGCA
GGTGCTTTAGATAGATTTTATCAATCGCTACCAGGCCGAACATGGGGTGATGTTATG
ATACCTAGTACAATGGCTGGTAATGCTTGGGTATGGGCTTATAACTATTGTGTTAAC
AACCAAGGGGCTGCCCCATTAGTTTACTTTGGCAATCCATACGATAGTCAAATTGAT
AGCTTGCTTGCAATGGGAGCTGACCCGTTTACAGGTGGTTCAATTATGGAAGAAGAC
GACAAGCCAAAGACCGCTGGAACGTGGAAACAAGACAGCAAGGGGTGGTGGTTCAGA
CGAAACAATGGCAGTTTCCCTTATAATAAATGGGAAAAAATCGGTGGTGTGTGGTAC
TACTTCGATAGTAAAGGATATTGCTTAACGAGCGAATGGCTCAAAGATAATGAAAAA
TGGTACTACCTCAAGGACAACGGCGCAATGGCGACTGGTTGGGTGCTAGTCGGGTCA
GAGTGGTATTATATGGACGATTCAGGCGCTATGGTTACTGGTTGGGTCAAGTATAAG
AATAACTGGTACTATATGACAAATGAACGTGGTAACATGGTTTCTAATGAATTTATT
AAGTCTGGAAAAGGTTGGTATTTCATGAACACAAACGGAGAGCTTGCAGACAATCCA
AGTTTCACGAAAGAACCAGACGGGCTTATAACCGTAGCATAA
```

Protein Sequence (354 aa, 40.27 kDa)

```
MSKKYTQQQYEKYLAQPANNTFGLSPQQVADWFMGQAGARPVINSYGVNASNLVSTY
IPKMQEYGVSYTLFLMYTVFEGGGAGNWINHYMYDTGSNGLECLEHDLQYIHGVWET
YFPPALSAPECYPATEDNAGALDRFYQSLPGRTWGDVMIPSTMAGNAWVWAYNYCVN
NQGAAPLVYFGNPYDSQIDSLLAMGADPFTGGSIMEEDDKPKTAGTWKQDSKGWWFR
RNNGSFPYNKWEKIGGVWYYFDSKGYCLTSEWLKDNEKWYYLKDNGAMATGWVLVGS
EWYYMDDSGAMVTGWVKYKNNWYYMTNERGNMVSNEFIKSGKGWYFMNTNGELADNP
SFTKEPDGLITVA*
```

Template	Primer	Sequence (5'>3')
pET28a(+)::*clyX-1*	XS49	CGCATATGAGTAAGAAGTATACACA
	XS204	CGGGATCCTTATGCTACGGTTATAAGCCCGTC

Notes

GyH (PlyCA$_{1\text{-}205}$) and Cpl-1 CBD$_{(191\text{-}339)}$, amplified using pET28a(+)::*clyX-1* as template, cloned into NdeI/BamHI sites of pET28a(+)

pET28a(+)::*cpl-1_CHAP*

Insert Sequence (924 nucleotides)

ATGGAAGAAGACGACAAGCCAAAGACCGCTGGAACGTGGAAACAAGACAGCAAGGGG
TGGTGGTTCAGACGAAACAATGGCAGTTTCCCTTATAATAAATGGGAAAAAATCGGT
GGTGTGTGGTACTACTTCGATAGTAAAGGATATTGCTTAACGAGCGAATGGCTCAAA
GATAATGAAAAATGGTACTACCTCAAGGACAACGGCGCAATGGCGACTGGTTGGGTG
CTAGTCGGGTCAGAGTGGTATTATATGGACGATTCAGGCGCTATGGTTACTGGTTGG
GTCAAGTATAAGAATAACTGGTACTATATGACAAATGAACGTGGTAACATGGTTTCT
AATGAATTTATTAAGTCTGGAAAAGGTTGGTATTTCATGAACACAAACGGAGAGCTT
GCAGACAATCCAAGTTTCACGAAAGAACCAGACGGGCTTATAACCGTAGCAGGGTCT
GATAGAGTTGCAGCAAACTTAGCCAATGCACAGGCGCAAGTCGGTAAGTATATTGGT
GACGGTCAATGTTATGCTTGGGTTGGTTGGTGGTCAGCTAGGGTATGTGGTTATTCT
ATTTCATACTCAACAGGTGACCCAATGCTACCGTTAATTGGTGATGGTATGAACGCT
CATTCTATCCATCTTGGTTGGGATTGGTCAATCGCAAATACTGGTATTGTTAACTAC
CCAGTTGGTACTGTTGGACGCAAGGAAGATTTGAGAGTCGGCGCGATATGGTGCGCT
ACAGCATTCTCTGGCGCTCCGTTTTATACAGGACAATACGGCCATACTGGTATCATT
GAAAGCTGGTCAGATACTACCGTTACAGTCTTAGAACAAAACATTTTAGGGTCACCA
GTTATACGCAGCACCTATGACCTTAACACATTCCTATCAACACTAACTGGTTTGATA
ACATTTAAATAA

Protein Sequence (307 aa, 34.58 kDa)

MEEDDKPKTAGTWKQDSKGWWFRRNNGSFPYNKWEKIGGVWYYFDSKGYCLTSEWLK
DNEKWYYLKDNGAMATGWVLVGSEWYYMDDSGAMVTGWVKYKNNWYYMTNERGNMVS
NEFIKSGKGWYFMNTNGELADNPSFTKEPDGLITVAGSDRVAANLANAQAQVGKYIG
DGQCYAWVGWWSARVCGYSISYSTGDPMLPLIGDGMNAHSIHLGWDWSIANTGIVNY
PVGTVGRKEDLRVGAIWCATAFSGAPFYTGQYGHTGIIESWSDTTVTVLEQNILGSP
VIRSTYDLNTFLSTLTGLITFK*

Template	Primer	Sequence (5'>3')
pET28a(+)::*clyX-1*	XS205	CGCATATGGAAGAAGACGACAAGCCA
	XS2	CGGGATCCTTATTTAAATGTTATCAAACC

Notes

Cpl-1 $CBD_{(191-339)}$ and CHAP ($PlyCA_{309-465}$), amplified using pET28a(+)::*clyX-1* as template, cloned into NdeI/BamHI sites of pET28a(+)

pET28a(+)::*clyX-3*

Insert Sequence (1491 nucleotides)

ATGGTTAAAAAGAATGATTTATTTGTAGATGTTTCAAGTCACAACGGTTACGATATA
ACAGGTATCTTGGAGCAAATGGGAACAACTAACACCATCATTAAAATTTCTGAAAGT
ACGACCTATTTAAACCCTTGCTTGTCTGCTCAAGTGGAGCAGTCAAACCCTATTGGC
TTTTATCACTTCGCACGCTTTGGCGGAGACGTAGCAGAAGCCGAAAGAGAAGCGCAG
TTTTTCCTTGACAACGTGCCTATGCAAGTTAAATACCTTGTATTGGACTACGAGGAC
GACCCAAGCGGAGACGCACAAGCGAACACTAACGCATGCTTACGCTTTATGCAGATG
ATTGCTGACGCTGGATATAAACCTATTTATTATAGTTATAAACCGTTTACACATGAT
AATGTGGACTATCAGCAAATCCTTGCACAGTTCCCTAATTCTCTATGGATTGCAGGC
TATGGCTTAAACGATGGTACAGCTAACTTTGAATACTTCCCAAGCATGGACGGGATA
AGATGGTGGCAGTATTCTAGTAACCCGTTTGACAAGAATATTGTACTGTTAGACGAT
GAAGAAGACGACAAGCCAAAGACCGCTGGAACGTGGAAACAAGACAGCAAGGGGTGG
TGGTTCAGACGAAACAATGGCAGTTTCCCTTATAATAAATGGGAAAAAATCGGTGGT
GTGTGGTACTACTTCGATAGTAAAGGATATTGCTTAACGAGCGAATGGCTCAAAGAT
AATGAAAAATGGTACTACCTCAAGGACAACGGCGCAATGGCGACTGGTTGGGTGCTA
GTCGGGTCAGAGTGGTATTATATGGACGATTCAGGCGCTATGGTTACTGGTTGGGTC
AAGTATAAGAATAACTGGTACTATATGACAAATGAACGTGGTAACATGGTTTCTAAT
GAATTTATTAAGTCTGGAAAAGGTTGGTATTTCATGAACACAAACGGAGAGCTTGCA
GACAATCCAAGTTTCACGAAAGAACCAGACGGGCTTATAACCGTAGCAGGGTCTGAT
AGAGTTGCAGCAAACTTAGCCAATGCACAGGCGCAAGTCGGTAAGTATATTGGTGAC
GGTCAATGTTATGCTTGGGTTGGTTGGTGGTCAGCTAGGGTATGTGGTTATTCTATT
TCATACTCAACAGGTGACCCAATGCTACCGTTAATTGGTGATGGTATGAACGCTCAT
TCTATCCATCTTGGTTGGGATTGGTCAATCGCAAATACTGGTATTGTTAACTACCCA
GTTGGTACTGTTGGACGCAAGGAAGATTTGAGAGTCGGCGCGATATGGTGCGCTACA
GCATTCTCTGGCGCTCCGTTTTATACAGGACAATACGGCCATACTGGTATCATTGAA
AGCTGGTCAGATACTACCGTTACAGTCTTAGAACAAAACATTTTAGGGTCACCAGTT
ATACGCAGCACCTATGACCTTAACACATTCCTATCAACACTAACTGGTTTGATAACA
TTTAAATAA

Protein Sequence (496 aa, 56.07 kDa)

MVKKNDLFVDVSSHNGYDITGILEQMGTTNTIIKISESTTYLNPCLSAQVEQSNPIG
FYHFARFGGDVAEAEREAQFFLDNVPMQVKYLVLDYEDDPSGDAQANTNACLRFMQM
IADAGYKPIYYSYKPFTHDNVDYQQILAQFPNSLWIAGYGLNDGTANFEYFPSMDGI
RWWQYSSNPFDKNIVLLDDEEDDKPKTAGTWKQDSKGWWFRRNNGSFPYNKWEKIGG
VWYYFDSKGYCLTSEWLKDNEKWYYLKDNGAMATGWVLVGSEWYYMDDSGAMVTGWV
KYKNNWYYMTNERGNMVSNEFIKSGKGWYFMNTNGELADNPSFTKEPDGLITVAGSD
RVAANLANAQAQVGKYIGDGQCYAWVGWWSARVCGYSISYSTGDPMLPLIGDGMNAH
SIHLGWDWSIANTGIVNYPVGTVGRKEDLRVGAIWCATAFSGAPFYTGQYGHTGIIE
SWSDTTVTVLEQNILGSPVIRSTYDLNTFLSTLTGLITFK*

Template	Primer	Sequence (5'>3')
pBAD24::*cpl-1*	XS206	CDCATATGGTTAAAAAGAATGATTTAT
pBAD24::*plyCA*	XS109	AACTCTATCAGACCCTGCTACGGTTATAAG
	XS108	CTTATAACCGTAGCAGGGTCTGATAGAGTT
	XS2	CGGGATCCTTATTTAAATGTTATCAAACC

Notes

Cpl-1 full length and CHAP ($PlyCA_{309-465}$), fused via 2 round of SOE PCR cloned into NdeI/BamHI sites of pET28a(+)

pET28a(+)::*clyX-4*

Insert Sequence (1401 nucleotides)

ATGACCACCGTTAATGAAGCCCTGAATAATGTTCGTGCACAGGTTGGTAGCGGTGTT
AGCGTTGGTAATGGTGAATGTTATGCACTGGCAAGCTGGTATGAACGTATGATTAGT
CCGGATGCAACCGTTGGTCTGGGTGCCGGTGTTGGTTGGGTTAGCGGTGCAATTGGT
GATACCATTAGCGCAAAAAACATTGGCAGCAGCTATAATTGGCAGGCAAATGGTTGG
ACCGTTAGCACCAGCGGTCCGTTTAAAGCAGGTCAGATTGTTACCCTGGGTGCAACA
CCGGGTAATCCGTATGGTCATGTTGTTATTGTTGAAGCCGTTGATGGTGATCGTCTG
ACCATTCTGGAACAGAATTATGGTGGTAAACGTTATCCGGTGCGTAACTATTATTCA
GCAGCAAGCTATCGTCAGCAGGTTGTTCATTATATCACCCCTCCGGGTACAGTTGCA
CAGAGCGCACCGAATCTGGCAGGTAGCCGTAGCTATCGTGAAACCGGCACCATGACC
GTTACCGTTGATGCACTGAATGTTCGTCGTGCACCGAATACCAGCGGTGAAATTGTT
GCAGTGTATAAACGTGGTGAGAGCTTCGATTATGATACCGTGATTATTGATGTGAAC
GGTTATGTTTGGGTGAGCTATATTGGTGGTTCAGGCAAACGTAATTATGTTGCAACC
GGTGCCACCAAAGATGGTAAACGCTTTGGTAATGCATGGGGCACCTTTAAAATGGTT
AAAAAGAATGATTTATTTGTAGATGTTTCAAGTCACAACGGTTACGATATAACAGGT
ATCTTGGAGCAAATGGGAACAACTAACACCATCATTAAAATTTCTGAAAGTACGACC
TATTTAAACCCTTGCTTGTCTGCTCAAGTGGAGCAGTCAAACCCTATTGGCTTTTAT
CACTTCGCACGCTTTGGCGGAGACGTAGCAGAAGCCGAAAGAGAAGCGCAGTTTTTC
CTTGACAACGTGCCTATGCAAGTTAAATACCTTGTATTGGACTACGAGGACGACCCA
AGCGGAGACGCACAAGCGAACACTAACGCATGCTTACGCTTTATGCAGATGATTGCT
GACGCTGGATATAAACCTATTTATTATAGTTATAAACCGTTTACACATGATAATGTG
GACTATCAGCAAATCCTTGCACAGTTCCCTAATTCTCTATGGATTGCAGGCTATGGC
TTAAACGATGGTACAGCTAACTTTGAATACTTCCCAAGCATGGACGGGATAAGATGG
TGGCAGTATTCTAGTAACCCGTTTGACAAGAATATTGTACTGTTAGACGATGAAGAA
GACGACAAGCCAAAGACCGCTGGAACGTGGAAACAAGACAGCAAGGGGTGGTGGTTC
AGACGAAACAATGGCAGTTTCCCTTATTAA

Protein Sequence (456 aa, 51.30 kDa)

MTTVNEALNNVRAQVGSGVSVGNGECYALASWYERMISPDATVGLGAGVGWVSGAIG
DTISAKNIGSSYNWQANGWTVSTSGPFKAGQIVTLGATPGNPYGHVVIVEAVDGDRL
TILEQNYGGKRYPVRNYYSAASYRQQVVHYITPPGTVAQSAPNLAGSRSYRETGTMT
VTVDALNVRRAPNTSGEIVAVYKRGESFDYDTVIIDVNGYVWVSYIGGSGKRNYVAT
GATKDGKRFGNAWGTFKMVKKNDLFVDVSSHNGYDITGILEQMGTTNTIIKISESTT
YLNPCLSAQVEQSNPIGFYHFARFGGDVAEAEREAQFFLDNVPMQVKYLVLDYEDDP
SGDAQANTNACLRFMQMIADAGYKPIYYSYKPFTHDNVDYQQILAQFPNSLWIAGYG
LNDGTANFEYFPSMDGIRWWQYSSNPFDKNIVLLDDEEDDKPKTAGTWKQDSKGWWF
RRNNGSFPY*

Template	Primer	Sequence (5'>3')
pBAD24:: *plySs2*	XS190	CGCATATGACCACCGTTAATGAAGCCCT
	XS193	AAATCATTCTTTTTAACCATTTTAAAGGTGCCCCATGCAT
pBAD24:: *cpl-1*	XS194	ATGCATGGGGCACCTTTAAAATGGTTAAAAAGAATGATTT
	XS195	CGGGATCCTTAATAAGGGAAACTGCCATTGT

Notes

PlySs2 full length and Cpl-1 EAD (Cpl-$1_{1\text{-}190}$), fused via 1 round of SOE PCR cloned into NdeI/BamHI sites of pET28a(+)

pBAD24::*plyCB*$_{D40A}$

Insert Sequence (246 nucleotides)

ATGCATCATCACCATCACCACGGTAGCGGTAGCAAGATTAATGTAAACGTAGAAAAT
GTTTCTGGTGTACAAGGTTTCCTATTCCATACCGATGGAAAAGAAAGTTACGGTTAT
CGTGCTTTTATTAACGGAGTTGAAATTGGTATTGCGGACATTGAAACCGTACAAGGA
TTTCAACAAATTATACCGTCTATCAATATTAGTAAGTCTGATGTAGAGGCTATCAGA
AAGGCTATGAAAAAGTAA

Protein Sequence (81aa, 8.956kDa)

MHHHHHHGSGSKINVNVENVSGVQGFLFHTDGKESYGYRAFINGVEIGIADETVQGF
QQIIPSINISKSDVEAIRKAMKK*

Template	Primer	Sequence (5'>3')
pBAD24::*plyCB*	XS33	[Phos]-GTTGAAATTGGTATT**GCG**GACATTGAAACCGTA

Notes

Site-direct mutagenesis of the 40th amino acid from lysine to alanine; N-terminal 6 His-tag.

pBAD24::*plyCB*$_{D41A}$

Insert Sequence (246 nucleotides)

ATGCATCATCACCATCACCACGGTAGCGGTAGCAAGATTAATGTAAACGTAGAAAAT
GTTTCTGGTGTACAAGGTTTCCTATTCCATACCGATGGAAAAGAAAGTTACGGTTAT
CGTGCTTTTATTAACGGAGTTGAAATTGGTATTAAAGCGATTGAAACCGTACAAGGA
TTTCAACAAATTATACCGTCTATCAATATTAGTAAGTCTGATGTAGAGGCTATCAGA
AAGGCTATGAAAAAGTAA

Protein Sequence (81 aa, 8.96 kDa)

MHHHHHHGSGSKINVNVENVSGVQGFLFHTDGKESYGYRAFINGVEIGIKAIETVQG
FQQIIPSINISKSDVEAIRKAMKK*

Template	Primer	Sequence (5'>3')
pBAD24::*plyCB*	XS34	[Phos]-GAAATTGGTATTAAA**GCG**ATTGAAACCGTACAA

Notes

Site-direct mutagenesis of the 41st amino acid from aspartic acid to alanine; N-terminal 6 His-tag.

pBAD24::*plyCB*$_{E43A}$

Insert Sequence (246 nucleotides)

ATGCATCATCACCATCACCACGGTAGCGGTAGCAAGATTAATGTAAACGTAGAAAAT
GTTTCTGGTGTACAAGGTTTCCTATTCCATACCGATGGAAAAGAAAGTTACGGTTAT
CGTGCTTTTATTAACGGAGTTGAAATTGGTATTAAAGACATTGCGACCGTACAAGGA
TTTCAACAAATTATACCGTCTATCAATATTAGTAAGTCTGATGTAGAGGCTATCAGA
AAGGCTATGAAAAAGTAA

Protein Sequence (81 aa, 8.97 kDa)

MHHHHHHGSGSKINVNVENVSGVQGFLFHTDGKESYGYRAFINGVEIGIKDIATVQG
FQQIIPSINISKSDVEAIRKAMKK*

Template	Primer	Sequence (5'>3')
pBAD24::*plyCB*	XS35	[Phos]-GGTATTAAAGACATT**GCG**ACCGTACAAGGATTT

Notes

Site-direct mutagenesis of the 43rd amino acid from glutamic acid to alanine; N-terminal 6 His-tag.

pBAD24::*plyCB*$_{D40A:K41A}$

Insert Sequence (246 nucleotides)

ATGCATCATCACCATCACCACGGTAGCGGTAGCAAGATTAATGTAAACGTAGAAAAT
GTTTCTGGTGTACAAGGTTTCCTATTCCATACCGATGGAAAAGAAAGTTACGGTTAT
CGTGCTTTTATTAACGGAGTTGAAATTGGTATTGCGGCGATTGAAACCGTACAAGGA
TTTCAACAAATTATACCGTCTATCAATATTAGTAAGTCTGATGTAGAGGCTATCAGA
AAGGCTATGAAAAAGTAA

Protein Sequence (81 aa, 8.91 kDa)

MHHHHHHGSGSKINVNVENVSGVQGFLFHTDGKESYGYRAFINGVEIGIAAIETVQG
FQQIIPSINISKSDVEAIRKAMKK*

Template	Primer	Sequence (5'>3')
pBAD24::*plyCB*	XS30	[Phos]-GTTGAAATTGGTATT**GCGGCG**ATTGAAACCGTACAA

Notes

Site-direct mutagenesis of the 40th amino acid lysine and the 41st amino acid aspartic acid to alanine; N-terminal 6 His-tag.

pBAD24::*plyCB* $^{K40A\ E43A}$ (pBAD24::*plyCBm*)

Insert Sequence (246 nucleotides)

ATGCATCATCACCATCACCACGGTAGCGGTAGCAAGATTAATGTAAACGTAGAAAAT
GTTTCTGGTGTACAAGGTTTCCTATTCCATACCGATGGAAAAGAAAGTTACGGTTAT
CGTGCTTTTATTAACGGAGTTGAAATTGGTATTGCGGACATTGCGACCGTACAAGGA
TTTCAACAAATTATACCGTCTATCAATATTAGTAAGTCTGATGTAGAGGCTATCAGA
AAGGCTATGAAAAAGTAA

Protein Sequence (81 aa, 8.89 kDa)

MHHHHHHGSGSKINVNVENVSGVQGFLFHTDGKESYGYRAFINGVEIGIADIATVQG
FQQIIPSINISKSDVEAIRKAMKK*

Template	Primer	Sequence (5'>3')
pBAD24:: *plyCB*	XS31	[Phos]-GTTGAAATTGGTATT**GCG**GACATT**GCG**ACCGTACAAGGATTT

Notes

Site-direct mutagenesis of the 40th amino acid lysine and the 43rd amino acid glutamic acid to alanine; N-terminal 6 His-tag.

pBAD24::*plyCB*$_{D41A\ E43A}$

Insert Sequence (246 nucleotides)

ATGCATCATCACCATCACCACGGTAGCGGTAGCAAGATTAATGTAAACGTAGAAAAT
GTTTCTGGTGTACAAGGTTTCCTATTCCATACCGATGGAAAAGAAAGTTACGGTTAT
CGTGCTTTTATTAACGGAGTTGAAATTGGTATTAAAGCGATTGCGACCGTACAAGGA
TTTCAACAAATTATACCGTCTATCAATATTAGTAAGTCTGATGTAGAGGCTATCAGA
AAGGCTATGAAAAAGTAA

Protein Sequence (81 aa, 8.91 kDa)

MHHHHHHGSGSKINVNVENVSGVQGFLFHTDGKESYGYRAFINGVEIGIKAIATVQG
FQQIIPSINISKSDVEAIRKAMKK*

Template	Primer	Sequence (5'>3')
pBAD24:: *plyCB*	XS32	[Phos]-GAAATTGGTATTAAA**GCG**ATT**GCG**ACCGTACAAGGATTT

Notes

Site-direct mutagenesis of the 41st amino acid aspartic acid and 43rd amino acid glutamic acid to alanine; N-terminal 6 His-tag.

pBAD24::*plyCB*$_{K40A\ D41A\ E43A}$

Insert Sequence (246 nucleotides)

ATGCATCATCACCATCACCACGGTAGCGGTAGCAAGATTAATGTAAACGTAGAAAAT
GTTTCTGGTGTACAAGGTTTCCTATTCCATACCGATGGAAAAGAAAGTTACGGTTAT
CGTGCTTTTATTAACGGAGTTGAAATTGGTATTGCGGCGATTGCGACCGTACAAGGA
TTTCAACAAATTATACCGTCTATCAATATTAGTAAGTCTGATGTAGAGGCTATCAGA
AAGGCTATGAAAAAGTAA

Protein Sequence (81 aa, 8.85 kDa)

MHHHHHHGSGSKINVNVENVSGVQGFLFHTDGKESYGYRAFINGVEIGIAAIATVQG
FQQIIPSINISKSDVEAIRKAMKK*

Template	Primer	Sequence (5'>3')
pBAD24:: *plyCB*	XS29	[Phos]-GTTGAAATTGGTATT**GCGGCG**ATT**GCG**ACCGTACAAGGATTT

Notes

Site-direct mutagenesis of 40th amino acid lysine, the 41st amino acid aspartic acid and 43th amino acid glutamic acid to alanine; N-terminal 6 His-tag.

pBAD24::*PlyCB2m*

Insert Sequence (468 nucleotides)

ATGCATCATCACCATCACCACGGTAGCGGTAGCAAGATTAATGTAAACGTAGAAAAT
GTTTCTGGTGTACAAGGTTTCCTATTCCATACCGATGGAAAAGAAAGTTACGGTTAT
CGTGCTTTTATTAACGGAGTTGAAATTGGTATTGCGGACATTGCGACCGTACAAGGA
TTTCAACAAATTATACCGTCTATCAATATTAGTAAGTCTGATGTAGAGGCTATCAGA
AAGGCTATGAAAAAGTCTAGAATGAGCAAGATTAATGTAAACGTAGAAAATGTTTCT
GGTGTACAAGGTTTCCTATTCCATACCGATGGAAAAGAAAGTTACGGTTATCGTGCT
TTTATTAACGGAGTTGAAATTGGTATTGCGGACATTGCGACCGTACAAGGATTTCAA
CAAATTATACCGTCTATCAATATTAGTAAGTCTGATGTAGAGGCTATCAGAAAGGCT
ATGAAAAAGTAA

Protein Sequence (155 aa, 16.99 kDa)

MHHHHHHGSGSKINVNVENVSGVQGFLFHTDGKESYGYRAFINGVEIGIADIATVQG
FQQIIPSINISKSDVEAIRKAMKKSRMSKINVNVENVSGVQGFLFHTDGKESYGYRA
FINGVEIGIADIATVQGFQQIIPSINISKSDVEAIRKAMKK*

Template	Primer	Sequence (5'>3')
pBAD24::*plyCBm*	XS130	CGGAATTCATTATGCATCATCACCATCACCACGGTAG
	XS114	CGTCTAGACTTTTTCATAGCCTTTC
	XS115	CGTCTAGAATGAGCAAGATTAATGTAAAC
	XS116	CGGTCGACTTACTTTTTCATAGCCTTTC

Notes

An additional *plyCBm* gene cloned into XbaI/SalI sites of pBAD24::*plyCBm-N'6His*;

N-terminal 6 His-tag.

pBAD24::*plyCBq*

Insert Sequence (912 nucleotides)

ATGCATCATCACCATCACCACGGTAGCGGTAGCAAGATTAATGTAAACGTAGAAAAT
GTTTCTGGTGTACAAGGTTTCCTATTCCATACCGATGGAAAAGAAAGTTACGGTTAT
CGTGCTTTTATTAACGGAGTTGAAATTGGTATTGCGGACATTGCGACCGTACAAGGA
TTTCAACAAATTATACCGTCTATCAATATTAGTAAGTCTGATGTAGAGGCTATCAGA
AAGGCTATGAAAAAGTCTAGAATGAGCAAGATTAATGTAAACGTAGAAAATGTTTCT
GGTGTACAAGGTTTCCTATTCCATACCGATGGAAAAGAAAGTTACGGTTATCGTGCT
TTTATTAACGGAGTTGAAATTGGTATTGCGGACATTGCGACCGTACAAGGATTTCAA
CAAATTATACCGTCTATCAATATTAGTAAGTCTGATGTAGAGGCTATCAGAAAGGCT
ATGAAAAAGGTCGACATGAGCAAGATTAATGTAAACGTAGAAAATGTTTCTGGTGTA
CAAGGTTTCCTATTCCATACCGATGGAAAAGAAAGTTACGGTTATCGTGCTTTTATT
AACGGAGTTGAAATTGGTATTGCGGACATTGCGACCGTACAAGGATTTCAACAAATT
ATACCGTCTATCAATATTAGTAAGTCTGATGTAGAGGCTATCAGAAAGGCTATGAAA
AAGTCTAGAATGAGCAAGATTAATGTAAACGTAGAAAATGTTTCTGGTGTACAAGGT
TTCCTATTCCATACCGATGGAAAAGAAAGTTACGGTTATCGTGCTTTTATTAACGGA
GTTGAAATTGGTATTGCGGACATTGCGACCGTACAAGGATTTCAACAAATTATACCG
TCTATCAATATTAGTAAGTCTGATGTAGAGGCTATCAGAAAGGCTATGAAAAAGTAA

Protein Sequence (330 aa, 33.16 kDa)

MHHHHHHGSGSKINVNVENVSGVQGFLFHTDGKESYGYRAFINGVEIGIADIATVQG
FQQIIPSINISKSDVEAIRKAMKKSRMSKINVNVENVSGVQGFLFHTDGKESYGYRA
FINGVEIGIADIATVQGFQQIIPSINISKSDVEAIRKAMKKVDMSKINVNVENVSGV
QGFLFHTDGKESYGYRAFINGVEIGIADIATVQGFQQIIPSINISKSDVEAIRKAMK
KSRMSKINVNVENVSGVQGFLFHTDGKESYGYRAFINGVEIGIADIATVQGFQQIIP
SINISKSDVEAIRKAMKK*

Template	Primer	Sequence (5'>3')
pBAD24::*PlyCB2m*	XS130	CGGAATTCATTATGCATCATCACCATCACCACGGTAG
	XS117	CGGTCGACCTTTTTCATAGCCTTTC
	XS118	CGGTCGACATGAGCAAGATTAATGTAAAC
	XS119	CGCTGCAGTTACTTTTTCATAGCCTTTC

Notes

An additional *PlyCB2m* gene cloned into SalI/PstI sites of pBAD24::*PlyCB2m-N'6His*; N-terminal 6 His-tag.

pET28a(+)::*Amidase*$_{Pal}$*_CBm*

Insert Sequence (738 nucleotides)

```
ATGGGAGTCGATATTGAAAAAGGCGTTGCGTGGATGCAGGCCCGAAAGGGTCGAGTA
TCTTATAGCATGGACTTTCGAGACGGTCCTGATAGCTATGACTGCTCAAGTTCTATG
TACTATGCTCTCCGCTCAGCCGGAGCTTCAAGTGCTGGATGGGCAGTCAATACTGAG
TACATGCACGCATGGCTTATTGAAAACGGTTATGAACTAATTAGTGAAAATGCTCCG
TGGGATGCTAAACGAGGCGACATCTTCATCTGGGGACGCAAAGGTGCTAGCGCAGGC
GCTGGAGGTCATACAGGGATGTTCATTGACAGTGATAACATCATTCACTGCAACTAC
GCCTACGACGGAATTTCCGTCAACGACCACGATGAGCGTTGGTACTATGCAGGTCAA
CCTTACTACTACGTCTATCGCTTGACTAACGCAAATGCTCAACCGGCTGAGAAGAAA
CTTGGCTGGCAGAAAGATGCTACTGGTTTCTGGTACGCTCGAGCAAACGGAACTTAT
CCAAAAATGAGCAAGATTAATGTAAACGTAGAAAATGTTTCTGGTGTACAAGGTTTC
CTATTCCATACCGATGGAAAAGAAAGTTACGGTTATCGTGCTTTTATTAACGGAGTT
GAAATTGGTATTGCGGACATTGCGACCGTACAAGGATTTCAACAAATTATACCGTCT
ATCAATATTAGTAAGTCTGATGTAGAGGCTATCAGAAAGGCTATGAAAAAGTAA
```

Protein Sequence (245 aa, 27.35 kDa)

```
MGVDIEKGVAWMQARKGRVSYSMDFRDGPDSYDCSSSMYYALRSAGASSAGWAVNTE
YMHAWLIENGYELISENAPWDAKRGDIFIWGRKGASAGAGGHT
GMFIDSDNIIHCNYAYDGISVNDHDERWYYAGQPYYYVYRLTNANAQPAEKKLGWQK
DATGFWYARANGTYPKMSKINVNVENVSGVQGFLFHTDGKESYGYRAFINGVEIGIA
DIATVQGFQQIIPSINISKSDVEAIRKAMKK*
```

Template	Primer	Sequence (5'>3')
pBAD24::*pal*	XS58	CGCATATGGGAGTCGATATTGAAAA
	XS62	TTTACATTAATCTTGCTCATTTTTGGATAAGTTCCGTTTG
pBAD24::*plyCBm*	XS53	CAAACGGAACTTATCCAAAAATGAGCAAGATTAATGTAAA
	XS56	CGGGATCCTTACTTTTTCATAGCCTTTC

Notes

Amidase$_{Pal}$ with its linker (Pal$_{1-149}$) and PlyCBm fragments, fused via SOE PCR cloned into NdeI/BamHI sites of pET28a(+).

pET28a(+)::*Amidase$_{PlyG}$_CBm*

Insert sequence (708 nucleotides)

```
ATGGGTAGCATGGAAATCCAGAAAAAACTGGTTGATCCGAGCAAATATGGCACCAAA
TGTCCGTATACCATGAAACCGAAATATATCACCGTGCACAACACCTATAATGATGCA
CCGGCAGAAAATGAAGTGAGCTATATGATTAGCAACAACAACGAGGTGAGCTTTCAT
ATTGCCGTGGATGATAAAAAAGCCATTCAGGGTATTCCGCTGGAACGTAATGCATGG
GCATGTGGTGATGGTAATGGTAGCGGTAATCGTCAGAGCATTAGCGTTGAAATCTGC
TATAGTAAAAGCGGTGGTGATCGTTATTACAAAGCCGAAGATAATGCCGTTGATGTT
GTTCGTCAGCTGATGAGCATGTATAACATTCCGATTGAAAATGTGCGTACCCATCAG
AGCTGGTCAGGTAAATATTGTCCGCATCGTATGCTGGCCGAAGGTCGTTGGGGTGCA
TTTATTCAGAAAGTGAAAAATGGTAATGTGGCAATGAGCAAGATTAATGTAAACGTA
GAAAATGTTTCTGGTGTACAAGGTTTCCTATTCCATACCGATGGAAAAGAAAGTTAC
GGTTATCGTGCTTTTATTAACGGAGTTGAAATTGGTATTGCGGACATTGCGACCGTA
CAAGGATTTCAACAAATTATACCGTCTATCAATATTAGTAAGTCTGATGTAGAGGCT
ATCAGAAAGGCTATGAAAAAGTAA
```

Protein Sequence (235 aa, 26.17 kDa)

```
MGSMEIQKKLVDPSKYGTKCPYTMKPKYITVHNTYNDAPAENEVSYMISNNNEVSFH
IAVDDKKAIQGIPLERNAWACGDGNGSGNRQSISVEICYSKSGGDRYYKAEDNAVDV
VRQLMSMYNIPIENVRTHQSWSGKYCPHRMLAEGRWGAFIQKVKNGNVAMSKINVNV
ENVSGVQGFLFHTDGKESYGYRAFINGVEIGIADIATVQGFQQIIPSINISKSDVEA
IRKAMKK*
```

Template	Primer	Sequence (5'>3')
pBAD24::*plyG*	XS57	CGCATATGGGTAGCATGGAAATCCAGAA
	XS61	TTTACATTAATCTTGCTCATTGCCACATTACCATTTTTCA
pBAD24::*plyCBm*	XS52	TGAAAAATGGTAATGTGGCAATGAGCAAGATTAATGTAAA
	XS56	CGGGATCCTTACTTTTTCATAGCCTTTC

Notes

Amidase$_{PlyG}$ with its linker (PlyG$_{1-172}$) and PlyCBm fragments, fused via SOE PCR cloned into NdeI/BamHI sites of pET28a(+).

pET28a(+)::*CHAP_CBm*

Insert Sequence (693 nucleotides)

ATGGGGTCTGATAGAGTTGCAGCAAACTTAGCCAATGCACAGGCGCAAGTCGGTAAG
TATATTGGTGACGGTCAATGTTATGCTTGGGTTGGTTGGTGGTCAGCTAGGGTATGT
GGTTATTCTATTTCATACTCAACAGGTGACCCAATGCTACCGTTAATTGGTGATGGT
ATGAACGCTCATTCTATCCATCTTGGTTGGGATTGGTCAATCGCAAATACTGGTATT
GTTAACTACCCAGTTGGTACTGTTGGACGCAAGGAAGATTTGAGAGTCGGCGCGATA
TGGTGCGCTACAGCATTCTCTGGCGCTCCGTTTTATACAGGACAATACGGCCATACT
GGTATCATTGAAAGCTGGTCAGATACTACCGTTACAGTCTTAGAACAAAACATTTTA
GGGTCACCAGTTATACGCAGCACCTATGACCTTAACACATTCCTATCAACACTAACT
GGTTTGATAACATTTAAAATGAGCAAGATTAATGTAAACGTAGAAAATGTTTCTGGT
GTACAAGGTTTCCTATTCCATACCGATGGAAAAGAAAGTTACGGTTATCGTGCTTTT
ATTAACGGAGTTGAAATTGGTATTGCGGACATTGCGACCGTACAAGGATTTCAACAA
ATTATACCGTCTATCAATATTAGTAAGTCTGATGTAGAGGCTATCAGAAAGGCTATG
AAAAAGTAA

Protein Sequence (230 aa, 24.89 kDa)

MGSDRVAANLANAQAQVGKYIGDGQCYAWVGWWSARVCGYSISYSTGDPMLPLIGDG
MNAHSIHLGWDWSIANTGIVNYPVGTVGRKEDLRVGAIWCATA
FSGAPFYTGQYGHTGIIESWSDTTVTVLEQNILGSPVIRSTYDLNTFLSTLTGLITF
KMSKINVNVENVSGVQGFLFHTDGKESYGYRAFINGVEIGIADIATVQGFQQIIPSI
NISKSDVEAIRKAMKK*

Template	Primer	Sequence (5'>3')
pBAD24::*plyC*	XS1	CGCATATGGGGTCTGATAGAGTT
	XS59	TTTACATTAATCTTGCTCATTTTAAATGTTATCAAC
	XS50	GTTTGATAACATTTAAAATGAGCAAGATTAATGTAAA
pBAD24::*plyCBm*	XS56	CGGGATCCTTACTTTTTCATAGCCTTTC

Notes

CHAP ($PlyCA_{309-465}$) and PlyCBm fragments, fused via SOE PCR cloned into

NdeI/BamHI sites of pET28a(+)

pET28a(+)::*GyH_CBm*

Insert Sequence (843 nucleotides)

ATGAGTAAGAAGTATACACAACAACAATACGAAAAATATTTAGCACAACCAGCAAAT
AACACATTTGGGTTATCACCTCAACAGGTTGCTGATTGGTTTATGGGTCAAGCTGGT
GCTAGGCCTGTTATTAACTCGTATGGGGTAAATGCTAGTAATTTAGTATCAACGTAC
ATACCTAAAATGCAGGAATACGGTGTATCATATACACTATTCTTAATGTATACTGTC
TTTGAGGGAGGCGGCGCAGGTAATTGGATTAATCATTACATGTACGATACGGGGTCT
AATGGATTAGAGTGTTTGGAACACGATTTACAATACATACATGGCGTCTGGGAAACT
TATTTTCCACCAGCTTTATCTGCGCCAGAATGTTACCCAGCTACGGAAGATAACGCA
GGTGCTTTAGATAGATTTTATCAATCGCTACCAGGCCGAACATGGGGTGATGTTATG
ATACCTAGTACAATGGCTGGTAATGCTTGGGTATGGGCTTATAACTATTGTGTTAAC
AACCAAGGGGCTGCCCCATTAGTTTACTTTGGCAATCCATACGATAGTCAAATTGAT
AGCTTGCTTGCAATGGGAGCTGACCCGTTTACAGGTGGTTCAATTATGAGCAAGATT
AATGTAAACGTAGAAAATGTTTCTGGTGTACAAGGTTTCCTATTCCATACCGATGGA
AAAGAAAGTTACGGTTATCGTGCTTTTATTAACGGAGTTGAAATTGGTATTGCGGAC
ATTGCGACCGTACAAGGATTTCAACAAATTATACCGTCTATCAATATTAGTAAGTCT
GATGTAGAGGCTATCAGAAAGGCTATGAAAAAGTAA

Protein Sequence (277 aa, 30.58 kDa)

MSKKYTQQQYEKYLAQPANNTFGLSPQQVADWFMGQAGARPVINSYGVNASNLVSTY
IPKMQEYGVSYTLFLMYTVFEGGGAGNWINHYMYDTGSNGLECLEHDLQYIHGVWET
YFPPALSAPECYPATEDNAGALDRFYQSLPGRTWGDVMIPSTMAGNAWVWAYNYCVN
NQGAAPLVYFGNPYDSQIDSLLAMGADPFTGGSIMSKINVNVENVSGVQGFLFHTDG
KESYGYRAFINGVEIGIADIATVQGFQQIIPSINISKSDVEAIRKAMKK*

Template	Primer	Sequence (5'>3')
pBAD24:: *plyC*	XS49	CGCATATGAGTAAGAAGTATACACA
	XS60	TTTACATTAATCTTGCTCATAATTGAACCACCTGTAAACG
pBAD24:: *plyCBm*	XS51	CGTTTACAGGTGGTTCAATTATGAGCAAGATTAATGTAAA
	XS56	CGGGATCCTTACTTTTTCATAGCCTTTC

Notes

GyH ($PlyCA_{1-205}$) and PlyCBm fragments, fused via SOE PCR cloned into

NdeI/BamHI sites of pET28a(+).

pET28a(+)::*CHAPK_CBm*

Insert Sequence (828 nucleotides)

ATGGCAAAAACCCAGGCCGAAATTAACAAACGTCTGGATGCATATGCCAAAGGCACC
GTTGATAGCCCGTATCGTGTTAAAAAAGCAACCAGCTATGATCCGAGCTTTGGTGTT
ATGGAAGCCGGTGCAATTGATGCAGATGGTTATTATCATGCACAGTGCCAGGATCTG
ATTACCGATTATGTTCTGTGGCTGACCGATAACAAAGTTCGTACCTGGGGTAATGCA
AAAGATCAGATTAAACAGAGCTATGGCACGGGCTTTAAAATCCATGAAAATAAACCG
AGCACCGTGCCGAAAAAAGGTTGGATTGCAGTTTTTACCAGCGGTAGCTATGAACAG
TGGGGTCATATTGGTATTGTTTATGATGGTGGTAACACCAGCACCTTTACCATTCTG
GAACAGAATTGGAATGGCTACGCAAACAAAAAACCGACCAAACGTGTGGATAACTAT
TATGGTCTGACCCACTTTATTGAGATTCCGGTTAAAGCAGGCACCACCGTGAAAAAA
GAAACCGCAAAAAAAAGCGCAAGCAAAACACCGGCACCGAAAAAGAAAGCAACCCTG
AAAGTTAGCAAAAACCACATCAACTACACCATGGATAAAATGAGCAAGATTAATGTA
AACGTAGAAAATGTTTCTGGTGTACAAGGTTTCCTATTCCATACCGATGGAAAAGAA
AGTTACGGTTATCGTGCTTTTATTAACGGAGTTGAAATTGGTATTGCGGACATTGCG
ACCGTACAAGGATTTCAACAAATTATACCGTCTATCAATATTAGTAAGTCTGATGTA
GAGGCTATCAGAAAGGCTATGAAAAAGTAA

Protein Sequence (275 aa, 30.58 kDa)

MAKTQAEINKRLDAYAKGTVDSPYRVKKATSYDPSFGVMEAGAIDADGYYHAQCQDL
ITDYVLWLTDNKVRTWGNAKDQIKQSYGTGFKIHENKPSTVPKKGWIAVFTSGSYEQ
WGHIGIVYDGGNTSTFTILEQNWNGYANKKPTKRVDNYYGLTHFIEIPVKAGTTVKK
ETAKKSASKTPAPKKKATLKVSKNHINYTMDKMSKINVNVENVSGVQGFLFHTDGKE
SYGYRAFINGVEIGIADIATVQGFQQIIPSINISKSDVEAIRKAMKK*

Template	Primer	Sequence (5'>3')
pBAD24:: *lysK*	XS27	CGGCTAGCATGGCAAAAACCCAGGCCGAA
	XS63	TTTACATTAATCTTGCTCATTTTATCCATGGTGTAGTTGA
pBAD24:: *plyCBm*	XS54	TCAACTACACCATGGATAAAATGAGCAAGATTAATGTAAA
	XS56	CGGGATCCTTACTTTTTCATAGCCTTTC

Notes

CHAPK with its linker ($LysK_{1-197}$) and PlyCBm fragments, fused via SOE PCR

cloned into NheI/BamHI sites of pET28a(+).

pET28a(+)::*CHAPS_CBm*

Insert Sequence (684 nucleotides)

ATGCTGAATAATGTTCGTGCACAGGTTGGTAGCGGTGTTAGCGTTGGTAATGGTGAA
TGTTATGCACTGGCAAGCTGGTATGAACGTATGATTAGTCCGGATGCAACCGTTGGT
CTGGGTGCCGGTGTTGGTTGGGTTAGCGGTGCAATTGGTGATACCATTAGCGCAAAA
AACATTGGCAGCAGCTATAATTGGCAGGCAAATGGTTGGACCGTTAGCACCAGCGGT
CCGTTTAAAGCAGGTCAGATTGTTACCCTGGGTGCAACACCGGGTAATCCGTATGGT
CATGTTGTTATTGTTGAAGCCGTTGATGGTGATCGTCTGACCATTCTGGAACAGAAT
TATGGTGGTAAACGTTATCCGGTGCGTAACTATTATTCAGCAGCAAGCTATCGTCAG
CAGGTTGTTCATTATATCACCCCTCCGGGTACAGTTGCACAGAGCGCACCGAATCTG
GCAGGTAGCATGAGCAAGATTAATGTAAACGTAGAAAATGTTTCTGGTGTACAAGGT
TTCCTATTCCATACCGATGGAAAAGAAAGTTACGGTTATCGTGCTTTTATTAACGGA
GTTGAAATTGGTATTGCGGACATTGCGACCGTACAAGGATTTCAACAAATTATACCG
TCTATCAATATTAGTAAGTCTGATGTAGAGGCTATCAGAAAGGCTATGAAAAAGTAA

Protein Sequence (227 aa, 24.05 kDa)

MLNNVRAQVGSGVSVGNGECYALASWYERMISPDATVGLGAGVGWVSGAIGDTISAK
NIGSSYNWQANGWTVSTSGPFKAGQIVTLGATPGNPYGHVVIVEAVDGDRLTILEQN
YGGKRYPVRNYYSAASYRQQVVHYITPPGTVAQSAPNLAGSMSKINVNVENVSGVQG
FLFHTDGKESYGYRAFINGVEIGIADIATVQGFQQIIPSINISKSDVEAIRKAMKK*

Template	Primer	Sequence (5'>3')
pBAD24::*plySs2*	XS9	CGCATATGCTGAATAATGTTCGTGCA
	XS64	TTTACATTAATCTTGCTCATGCTACCTGCCAGATTCGGTG
pBAD24::*plyCBm*	XS55	CACCGAATCTGGCAGGTAGCATGAGCAAGATTAATGTAAA
	XS56	CGGGATCCTTACTTTTTCATAGCCTTTC

Notes

CHAPS with its linker (PlySs2$_{1\text{-}166}$) and PlyCBm fragments, fused via SOE PCR cloned into NdeI/BamHI sites of pET28a(+).

pET28a(+)::*plyCA_CBm*

Insert Sequence (1616 nucleotides)

ATGAGTAAGAAGTATACACAACAACAATACGAAAAATATTTAGCACAACCAGCAAAT
AACACATTTGGGTTATCACCTCAACAGGTTGCTGATTGGTTTATGGGTCAAGCTGGT
GCTAGGCCTGTTATTAACTCGTATGGGGTAAATGCTAGTAATTTAGTATCAACGTAC
ATACCTAAAATGCAGGAATACGGTGTATCATATACACTATTCTTAATGTATACTGTC
TTTGAGGGAGGCGGCGCAGGTAATTGGATTAATCATTACATGTACGATACGGGGTCT
AATGGATTAGAGTGTTTGGAACACGATTTACAATACATACATGGCGTCTGGGAAACT
TATTTTCCACCAGCTTTATCTGCGCCAGAATGTTACCCAGCTACGGAAGATAACGCA
GGTGCTTTAGATAGATTTTATCAATCGCTACCAGGCCGAACATGGGGTGATGTTATG
ATACCTAGTACAATGGCTGGTAATGCTTGGGTATGGGCTTATAACTATTGTGTTAAC
AACCAAGGGGCTGCCCCATTAGTTTACTTTGGCAATCCATACGATAGTCAAATTGAT
AGCTTGCTTGCAATGGGAGCTGACCCGTTTACAGGTGGTTCAATTACAGGTGATGGA
AAAAATCCTAGTGTTGGCACTGGGAATGCTACCGTTTCTGCTAGCTCGGAAGCTAAC
AGAGAGAAGTTAAAGAAAGCCCTAACAGATTTATTCAACAACAACCTAGAACATCTA
TCAGGTGAATTCTACGGTAACCAAGTGTTGAATGCTATGAAATACGGCACTATCCTG
AAATGTGATTTAACAGATGACGGACTTAATGCCATTCTTCAATTAATAGCTGATGTT
AACTTACAGACTAACCCTAACCCAGACAAACCGACCGTTCAATCACCAGGTCAAAAC
GATTTAGGGTCGGGGTCTGATAGAGTTGCAGCAAACTTAGCCAATGCACAGGCGCAA
GTCGGTAAGTATATTGGTGACGGTCAATGTTATGCTTGGGTTGGTTGGTGGTCAGCT
AGGGTATGTGGTTATTCTATTTCATACTCAACAGGTGACCCAATGCTACCGTTAATT
GGTGATGGTATGAACGCTCATTCTATCCATCTTGGTTGGGATTGGTCAATCGCAAAT
ACTGGTATTGTTAACTACCCAGTTGGTACTGTTGGACGCAAGGAAGATTTGAGAGTC
GGCGCGATATGGTGCGCTACAGCATTCTCTGGCGCTCCGTTTTATACAGGACAATAC
GGCCATACTGGTATCATTGAAAGCTGGTCAGATACTACCGTTACAGTCTTAGAACAA
AACATTTTAGGGTCACCAGTTATACGCAGCACCTATGACCTTAACACATTCCTATCA
ACACTAACTGGTTTGATAACATTTAAATAAATGAGCAAGATTAATGTAAACGTAGAA
AATGTTTCTGGTGTACAAGGTTTCCTATTCCATACCGATGGAAAAGAAAGTTACGGT
TATCGTGCTTTTATTAACGGAGTTGAAATTGGTATTGCGGACATTGCGACCGTACAA
GGATTTCAACAAATTATACCGTCTATCAATATTAGTAAGTCTGATGTAGAGGCTATC
AGAAAGGCTATGAAAAAGTAA

Protein Sequence (465 aa, 50.49 kDa)

MSKKYTQQQYEKYLAQPANNTFGLSPQQVADWFMGQAGARPVINSYGVNASNLVSTY
IPKMQEYGVSYTLFLMYTVFEGGGAGNWINHYMYDTGSNGLECLEHDLQYIHGVWET
YFPPALSAPECYPATEDNAGALDRFYQSLPGRTWGDVMIPSTMAGNAWVWAYNYCVN
NQGAAPLVYFGNPYDSQIDSLLAMGADPFTGGSITGDGKNPSVGTGNATVSASSEAN
REKLKKALTDLFNNNLEHLSGEFYGNQVLNAMKYGTILKCDLTDDGLNAILQLIADV
NLQTNPNPDKPTVQSPGQNDLGSGSDRVAANLANAQAQVGKYIGDGQCYAWVGWWSA
RVCGYSISYSTGDPMLPLIGDGMNAHSIHLGWDWSIANTGIVNYPVGTVGRKEDLRV
GAIWCATAFSGAPFYTGQYGHTGIIESWSDTTVTVLEQNILGSPVIRSTYDLNTFLS
TLTGLITFKMSKINVNVENVSGVQGFLFHTDGKESYGYRAFINGVEIGIADIATVQG
FQQIIPSINISKSDVEAIRKAMKK*

Template	Primer	Sequence (5'>3')
pBAD24:: *plyC*	XS49	CGCATATGAGTAAGAAGTATACACA
	XS59	TTTACATTAATCTTGCTCATTTTAAATGTTATCAAC
	XS50	GTTTGATAACATTTAAAATGAGCAAGATTAATGTAAA
pBAD24:: *plyCBm-N'6His*	XS56	CGGGATCCTTACTTTTTCATAGCCTTTC

Notes

PlyCA and PlyCBm fragments, fused via SOE PCR cloned into NdeI/BamHI sites of pET28a(+).

pET28a(+)::*CHAP_CBd*

Insert Sequence (909 nucleotides)

ATGGGGTCTGATAGAGTTGCAGCAAACTTAGCCAATGCACAGGCGCAAGTCGGTAAG
TATATTGGTGACGGTCAATGTTATGCTTGGGTTGGTTGGTGGTCAGCTAGGGTATGT
GGTTATTCTATTTCATACTCAACAGGTGACCCAATGCTACCGTTAATTGGTGATGGT
ATGAACGCTCATTCTATCCATCTTGGTTGGGATTGGTCAATCGCAAATACTGGTATT
GTTAACTACCCAGTTGGTACTGTTGGACGCAAGGAAGATTTGAGAGTCGGCGCGATA
TGGTGCGCTACAGCATTCTCTGGCGCTCCGTTTTATACAGGACAATACGGCCATACT
GGTATCATTGAAAGCTGGTCAGATACTACCGTTACAGTCTTAGAACAAAACATTTTA
GGGTCACCAGTTATACGCAGCACCTATGACCTTAACACATTCCTATCAACACTAACT
GGTTTGATAACATTTAAAATGAGCAAGATTAATGTAAACGTAGAAAATGTTTCTGGT
GTACAAGGTTTCCTATTCCATACCGATGGAAAAGAAAGTTACGGTTATCGTGCTTTT
ATTAACGGAGTTGAAATTGGTATTGCGGACATTGCGACCGTACAAGGATTTCAACAA
ATTATACCGTCTATCAATATTAGTAAGTCTGATGTAGAGGCTATCAGAAAGGCTATG
AAAAAGATGAGCAAGATTAATGTAAACGTAGAAAATGTTTCTGGTGTACAAGGTTTC
CTATTCCATACCGATGGAAAAGAAAGTTACGGTTATCGTGCTTTTATTAACGGAGTT
GAAATTGGTATTGCGGACATTGCGACCGTACAAGGATTTCAACAAATTATACCGTCT
ATCAATATTAGTAAGTCTGATGTAGAGGCTATCAGAAAGGCTATGAAAAAGTAA

Protein Sequence (302 aa, 32.74 kDa)

MGSDRVAANLANAQAQVGKYIGDGQCYAWVGWWSARVCGYSISYSTGDPMLPLIGDG
MNAHSIHLGWDWSIANTGIVNYPVGTVGRKEDLRVGAIWCATAFSGAPFYTGQYGHT
GIIESWSDTTVTVLEQNILGSPVIRSTYDLNTFLSTLTGLITFKMSKINVNVENVSG
VQGFLFHTDGKESYGYRAFINGVEIGIADIATVQGFQQIIPSINISKSDVEAIRKAM
KKMSKINVNVENVSGVQGFLFHTDGKESYGYRAFINGVEIGIADIATVQGFQQIIPS
INISKSDVEAIRKAMKK*

Template	Primer	Sequence (5'>3')
pBAD24::*plyC*	XS1	CGCATATGGGGTCTGATAGAGTT
pBAD24::*PlyCB2m-N'6His*	XS59	TTTACATTAATCTTGCTCATTTTAAATGTTATCAAC
	XS51	GTTTGATAACATTTAAAATGAGCAAGATTAATGTAAA
	XS56	CGGGATCCTTACTTTTTCATAGCCTTTC

Notes

CHAP (PlyCA$_{309-465}$) and PlyCB2m fragments, fused via SOE PCR cloned into

NdeI/EcoRI sites of pET28a(+).

pET28a:: *plyC CHAP*

Insert Sequence (477 nucleotides)

ATGGGGTCTGATAGAGTTGCAGCAAACTTAGCCAATGCACAGGCGCAAGTCGGTAAG
TATATTGGTGACGGTCAATGTTATGCTTGGGTTGGTTGGTGGTCAGCTAGGGTATGT
GGTTATTCTATTTCATACTCAACAGGTGACCCAATGCTACCGTTAATTGGTGATGGT
ATGAACGCTCATTCTATCCATCTTGGTTGGGATTGGTCAATCGCAAATACTGGTATT
GTTAACTACCCAGTTGGTACTGTTGGACGCAAGGAAGATTTGAGAGTCGGCGCGATA
TGGTGCGCTACAGCATTCTCTGGCGCTCCGTTTTATACAGGACAATACGGCCATACT
GGTATCATTGAAAGCTGGTCAGATACTACCGTTACAGTCTTAGAACAAAACATTTTA
GGGTCACCAGTTATACGCAGCACCTATGACCTTAACACATTCCTATCAACACTAACT
GGTTTGATAACATTTAAATAA

Protein Sequence (158 aa, 17.6kDa)

MGSKRVAANLANAQAQVGKYIGDGQCYAWVGWWSARVCGYSISYSTGKPMLPLIGDG
MNAHSIHLGWDWSIANTGIVNYPVGTVGRKEDLRVGAIWCATAFSGAPFYTGQYGHT
GIIESWSDTTVTVLEQNILGSPVIRSTYDLNTFLSTLTGLITFK*

Template	Primer	Sequence (5'>3')
pBAD24:: *plyC*	XS1	CGCCATATGGGGTCTGATAGAGTT
	XS2	CGCGGATCCTTATTTAAATGTTATCAAACC

Notes

PlyC CHAP was cloned and inserted via NdeI/BamHI restriction enzyme sites into pET28a vector.

pET28a:: *plyC CHAP*$_{D311K\ D355K}$ (CHAP+1)

Insert Sequence (477 nucleotides)

ATGGGGTCTAAAAGAGTTGCAGCAAACTTAGCCAATGCACAGGCGCAAGTCGGTAAG
TATATTGGTGACGGTCAATGTTATGCTTGGGTTGGTTGGTGGTCAGCTAGGGTATGT
GGTTATTCTATTTCATACTCAACAGGTAAACCAATGCTACCGTTAATTGGTGATGGT
ATGAACGCTCATTCTATCCATCTTGGTTGGGATTGGTCAATCGCAAATACTGGTATT
GTTAACTACCCAGTTGGTACTGTTGGACGCAAGGAAGATTTGAGAGTCGGCGCGATA
TGGTGCGCTACAGCATTCTCTGGCGCTCCGTTTTATACAGGACAATACGGCCATACT
GGTATCATTGAAAGCTGGTCAGATACTACCGTTACAGTCTTAGAACAAAACATTTTA
GGGTCACCAGTTATACGCAGCACCTATGACCTTAACACATTCCTATCAACACTAACT
GGTTTGATAACATTTAAATAA

Protein Sequence (158 aa, 17.6 kDa)

MGSKRVAANLANAQAQVGKYIGDGQCYAWVGWWSARVCGYSISYSTGKPMLPLIGDG
MNAHSIHLGWDWSIANTGIVNYPVGTVGRKEDLRVGAIWCATAFSGAPFYTGQYGHT
GIIESWSDTTVTVLEQNILGSPVIRSTYDLNTFLSTLTGLITFK*

Template	Primer	Sequence (5'>3')
pET28a:: *plyC CHAP*	XS3	[Phos]- ATGGGGTCTAAAAGAGTTGCAGCAAAC
	XS4	[Phos]- TCATACTCAACAGGTAAACCAATGCTACCGTTA

Notes

Site-direct mutagenesis of 311th and the 355th aspartic acid of PlyCA to lysine.

pET28a:: *plyC CHAP*$_{D311K\ D355K\ D429A}$ (CHAP+2)

Insert Sequence (477 nucleotides)

ATGGGGTCTAAAAGAGTTGCAGCAAACTTAGCCAATGCACAGGCGCAAGTCGGTAAG
TATATTGGTGACGGTCAATGTTATGCTTGGGTTGGTTGGTGGTCAGCTAGGGTATGT
GGTTATTCTATTTCATACTCAACAGGTAAACCAATGCTACCGTTAATTGGTGATGGT
ATGAACGCTCATTCTATCCATCTTGGTTGGGATTGGTCAATCGCAAATACTGGTATT
GTTAACTACCCAGTTGGTACTGTTGGACGCAAGGAAGATTTGAGAGTCGGCGCGATA
TGGTGCGCTACAGCATTCTCTGGCGCTCCGTTTTATACAGGACAATACGGCCATACT
GGTATCATTGAAAGCTGGTCAGCGACTACCGTTACAGTCTTAGAACAAAACATTTTA
GGGTCACCAGTTATACGCAGCACCTATGACCTTAACACATTCCTATCAACACTAACT
GGTTTGATAACATTTAAATAA

Protein Sequence (158 aa, 17.6 kDa)

MGSKRVAANLANAQAQVGKYIGDGQCYAWVGWWSARVCGYSISYSTGKPMLPLIGDG
MNAHSIHLGWDWSIANTGIVNYPVGTVGRKEDLRVGAIWCATAFSGAPFYTGQYGHT
GIIESWSATTVTVLEQNILGSPVIRSTYDLNTFLSTLTGLITFK*

Template	Primer	Sequence (5'>3')
pET28a:: *plyC CHAP*$_{D311K\ D355K}$	XS8	[Phos]- ATTGAAAGCTGGTCAGCGACTACCGTTACAGTC

Notes

Site-directed mutagenesis of 311th and the 355th aspartic acid of PlyCA to lysine. Site-directed mutagenesis of 429th aspartic acid of PlyCA to alanine.

pET28a:: *plyC CHAP*$_{D311K\ D355K\ D363K}$ (CHAP+3)

Insert Sequence (477 nucleotides)

ATGGGGTCTAAAAGAGTTGCAGCAAACTTAGCCAATGCACAGGCGCAAGTCGGTAAG
TATATTGGTGACGGTCAATGTTATGCTTGGGTTGGTTGGTGGTCAGCTAGGGTATGT
GGTTATTCTATTTCATACTCAACAGGTAAACCAATGCTACCGTTAATTGGTAAAGGT
ATGAACGCTCATTCTATCCATCTTGGTTGGGATTGGTCAATCGCAAATACTGGTATT
GTTAACTACCCAGTTGGTACTGTTGGACGCAAGGAAGATTTGAGAGTCGGCGCGATA
TGGTGCGCTACAGCATTCTCTGGCGCTCCGTTTTATACAGGACAATACGGCCATACT
GGTATCATTGAAAGCTGGTCAGATACTACCGTTACAGTCTTAGAACAAAACATTTTA
GGGTCACCAGTTATACGCAGCACCTATGACCTTAACACATTCCTATCAACACTAACT
GGTTTGATAACATTTAAATAA

Protein Sequence (158 aa, 17.6 kDa)

MGSKRVAANLANAQAQVGKYIGDGQCYAWVGWWSARVCGYSISYSTGKPMLPLIGKG
MNAHSIHLGWDWSIANTGIVNYPVGTVGRKEDLRVGAIWCATAFSGAPFYTGQYGHT
GIIESWSDTTVTVLEQNILGSPVIRSTYDLNTFLSTLTGLITFK*

Template	Primer	Sequence (5'>3')
pET28a:: *plyC CHAP*$_{D311K\ D355K}$	XS5	[Phos]- CTACCGTTAATTGGTAAAGGTATGAACGCTCAT

Notes

Site-direct mutagenesis of 311th, 355th, and 363rd aspartic acid of PlyCA to lysine.

pET28a:: *plyC CHAP*$_{D311K\ D355K\ D363K\ D429A}$ (CHAP+4)

Insert Sequence (477 nucleotides)

ATGGGGTCTAAAAGAGTTGCAGCAAACTTAGCCAATGCACAGGCGCAAGTCGGTAAG
TATATTGGTGACGGTCAATGTTATGCTTGGGTTGGTTGGTGGTCAGCTAGGGTATGT
GGTTATTCTATTTCATACTCAACAGGTAAACCAATGCTACCGTTAATTGGTAAAGGT
ATGAACGCTCATTCTATCCATCTTGGTTGGGATTGGTCAATCGCAAATACTGGTATT
GTTAACTACCCAGTTGGTACTGTTGGACGCAAGGAAGATTTGAGAGTCGGCGCGATA
TGGTGCGCTACAGCATTCTCTGGCGCTCCGTTTTATACAGGACAATACGGCCATACT
GGTATCATTGAAAGCTGGTCAGCGACTACCGTTACAGTCTTAGAACAAAACATTTTA
GGGTCACCAGTTATACGCAGCACCTATGACCTTAACACATTCCTATCAACACTAACT
GGTTTGATAACATTTAAATAA

Protein Sequence (158 aa, 17.6 kDa)

MGSKRVAANLANAQAQVGKYIGDGQCYAWVGWWSARVCGYSISYSTGKPMLPLIGKG
MNAHSIHLGWDWSIANTGIVNYPVGTVGRKEDLRVGAIWCATAFSGAPFYTGQYGHT
GIIESWSATTVTVLEQNILGSPVIRSTYDLNTFLSTLTGLITFK*

Template	Primer	Sequence (5'>3')
pET28a:: *plyC CHAP*$_{D311K\ D355K\ D363K}$	XS8	[Phos]- ATTGAAAGCTGGTCAGCGACTACCGTTACAGTC

Notes

Site-directed mutagenesis of 311th, 355th and 363rd aspartic acid of PlyCA to lysine.

Site-directed mutagenesis of 429th aspartic acid of PlyCA to alanine.

pET28a:: *plyC CHAP*$_{D311K\ D355K\ D363K\ D429K}$ (CHAP+5)

Insert Sequence (477 nucleotides)

ATGGGGTCTAAAAGAGTTGCAGCAAACTTAGCCAATGCACAGGCGCAAGTCGGTAAG
TATATTGGTGACGGTCAATGTTATGCTTGGGTTGGTTGGTGGTCAGCTAGGGTATGT
GGTTATTCTATTTCATACTCAACAGGTAAACCAATGCTACCGTTAATTGGTAAAGGT
ATGAACGCTCATTCTATCCATCTTGGTTGGGATTGGTCAATCGCAAATACTGGTATT
GTTAACTACCCAGTTGGTACTGTTGGACGCAAGGAAGATTTGAGAGTCGGCGCGATA
TGGTGCGCTACAGCATTCTCTGGCGCTCCGTTTTATACAGGACAATACGGCCATACT
GGTATCATTGAAAGCTGGTCAAAAACTACCGTTACAGTCTTAGAACAAAACATTTTA
GGGTCACCAGTTATACGCAGCACCTATGACCTTAACACATTCCTATCAACACTAACT
GGTTTGATAACATTTAAATAA

Protein Sequence (158 aa, 17.6 kDa)

MGSKRVAANLANAQAQVGKYIGDGQCYAWVGWWSARVCGYSISYSTGKPMLPLIGKG
MNAHSIHLGWDWSIANTGIVNYPVGTVGRKEDLRVGAIWCATAFSGAPFYTGQYGHT
GIIESWSKTTVTVLEQNILGSPVIRSTYDLNTFLSTLTGLITFK*

Template	Primer	Sequence (5'>3')
pET28a:: *plyC CHAP*$_{D311K\ D355K\ D363K}$	XS6	[Phos]- ATTGAAAGCTGGTCAAAAACTACCGTTACAGTC

Notes

Site-direct mutagenesis of 311th, 355th, 363rd and 429th, aspartic acid of PlyCA to lysine.

pET28a:: *plyC CHAP*$_{D311K\ D355K\ D363K\ D429A\ D450K}$ (CHAP+6)

Insert Sequence (477 nucleotides)

ATGGGGTCTAAAAGAGTTGCAGCAAACTTAGCCAATGCACAGGCGCAAGTCGGTAAG
TATATTGGTGACGGTCAATGTTATGCTTGGGTTGGTTGGTGGTCAGCTAGGGTATGT
GGTTATTCTATTTCATACTCAACAGGTAAACCAATGCTACCGTTAATTGGTAAAGGT
ATGAACGCTCATTCTATCCATCTTGGTTGGGATTGGTCAATCGCAAATACTGGTATT
GTTAACTACCCAGTTGGTACTGTTGGACGCAAGGAAGATTTGAGAGTCGGCGCGATA
TGGTGCGCTACAGCATTCTCTGGCGCTCCGTTTTATACAGGACAATACGGCCATACT
GGTATCATTGAAAGCTGGTCAGCGACTACCGTTACAGTCTTAGAACAAAACATTTTA
GGGTCACCAGTTATACGCAGCACCTATAAACTTAACACATTCCTATCAACACTAACT
GGTTTGATAACATTTAAATAA

Protein Sequence (158 aa, 17.6 kDa)

MGSKRVAANLANAQAQVGKYIGDGQCYAWVGWWSARVCGYSISYSTGKPMLPLIGKG
MNAHSIHLGWDWSIANTGIVNYPVGTVGRKEDLRVGAIWCATAFSGAPFYTGQYGHT
GIIESWSATTVTVLEQNILGSPVIRSTYKLNTFLSTLTGLITFK*

Template	Primer	Sequence (5'>3')
pET28a:: *plyC CHAP*$_{D311K\ D355K\ D363K\ D429A}$	XS7	[Phos]- ATACGCAGCACCTATAAACTTAACACATTCCTA

Notes

Site-directed mutagenesis of 311th, 355th, 363rd , and 450th aspartic acid of PlyCA to lysine. Site-directed mutagenesis of 429th aspartic acid of PlyCA to alanine.

pET28a:: *plyC CHAP*$_{D311K\ D355K\ D363K\ D429K\ D450K}$ (CHAP+7)

Insert Sequence (477 nucleotides)

ATGGGGTCTAAAAGAGTTGCAGCAAACTTAGCCAATGCACAGGCGCAAGTCGGTAAG
TATATTGGTGACGGTCAATGTTATGCTTGGGTTGGTTGGTGGTCAGCTAGGGTATGT
GGTTATTCTATTTCATACTCAACAGGTAAACCAATGCTACCGTTAATTGGTAAAGGT
ATGAACGCTCATTCTATCCATCTTGGTTGGGATTGGTCAATCGCAAATACTGGTATT
GTTAACTACCCAGTTGGTACTGTTGGACGCAAGGAAGATTTGAGAGTCGGCGCGATA
TGGTGCGCTACAGCATTCTCTGGCGCTCCGTTTTATACAGGACAATACGGCCATACT
GGTATCATTGAAAGCTGGTCAAAAACTACCGTTACAGTCTTAGAACAAAACATTTTA
GGGTCACCAGTTATACGCAGCACCTATAAACTTAACACATTCCTATCAACACTAACT
GGTTTGATAACATTTAAATAA

Protein Sequence (158 aa, 17.6 kDa)

MGSKRVAANLANAQAQVGKYIGDGQCYAWVGWWSARVCGYSISYSTGKPMLPLIGKG
MNAHSIHLGWDWSIANTGIVNYPVGTVGRKEDLRVGAIWCATAFSGAPFYTGQYGHT
GIIESWSKTTVTVLEQNILGSPVIRSTYKLNTFLSTLTGLITFK*

Template	Primer	Sequence (5'>3')
pET28a:: *plyC CHAP*$_{D311K\ D355K\ D363K\ D450K}$	XS6	[Phos]- ATTGAAAGCTGGTCAAAAACTACCGTTACAGTC

Notes

Site-directed mutagenesis of 311th, 355th, 363rd, 429th, and 450th aspartic acid of PlyCA to lysine.

Appendix B

List of Bacterial Strains used in Dissertation-Related Studies

Organism	Serotype	Strain	ATCC	Source*	Notes
Bacillus cereus			4342	2	
Enterococcus faecalis		JH2-2		5	
Enterococcus faecalis		EF-1		5	Van^R
Enterococcus faecalis		EF-17		5	Van^R
Enterococcus faecalis		EF-24		5	
Enterococcus faecalis		EF-25		5	
Enterococcus faecium		EFSK2		5	Van^R
Enterococcus faecium		EFSK16		5	Van^R
Enterococcus faecium		EFSK33		5	Van^R
Group E streptococci	2	K131	123191	1	Group E streptococcus
Staphylococcus aureus		NRS385		6	MRSA, MDR, USA500
Staphylococcus aureus		NRS14		6	VISA
Streptococcus agalactiae	Type III	A909		1	Group B streptococcus
Streptococcus agalactiae	Type IA	A349		1	Group B streptococcus
Streptococcus agalactiae	Type IB	A934		1	Group B streptococcus
Streptococcus dysagalactiae subs.equisimilis			21597	2	Group C streptococcus
Streptococcus equi			9528	2	Group C streptococcus
Streptococcus equi subs.zooepidemicus			700400	2	Group C streptococcus
Streptococcus mutans	Type c	10449		2	
Streptococcus mutans	Type c		25175	2	
Streptococcus mutans	Type e	LM7		2	
Streptococcus pneumoniae	11	DCC1811		5	
Streptococcus pneumoniae	15	DCC1476		5	
Streptococcus pneumoniae	23F (Sp23-1)	DCC1420		5	
Streptococcus pneumoniae	19	DCC1355		5	
Streptococcus pneumoniae	14 (Sp14-3)	DCC1494		5	
Streptococcus pneumoniae	6	DCC1850		5	
Streptococcus pneumoniae	14	DCC1490		5	
Streptococcus pneumoniae	3	DCC1714		5	
Streptococcus pneumoniae	9V (Sp9-3)	DCC1335		5	
Streptococcus pneumoniae	Derived from D39	R36A		5	Capsule free strain.
Streptococcus pneumoniae	Derived from R36A	R6		5	Capsule free strain.
Streptococcus pneumoniae		765		5	
Streptococcus pneumoniae		#8		5	
Streptococcus pneumoniae		763		5	
Streptococcus pneumoniae	2	D39		5	

Streptococcus pneumoniae	4	TIGR 4		5	
Streptococcus pneumoniae	18	GB2017		5	
Streptococcus pneumoniae	1	AR620		5	
Streptococcus pneumoniae	10	GB2163		5	
Streptococcus pneumoniae	4	GB2092		5	
Streptococcus pneumoniae	5	AR314		5	
Streptococcus pneumoniae	Derived from R6	Lyt4.4		5	LytA is non-functional
Streptococcus pyogenes		MGAS315		1	Group A streptococcus
Streptococcus pyogenes	M6	D471		1	Group A streptococcus
Streptococcus pyogenes	A-variant strain	A486		1	Group A streptococcus
Streptococcus rattus		BHT		4	
Streptococcus suis		7-3008-2		7	
Streptococcus uberis			BAA-854	2	
Streptococcus uberis			700407	2	
Streptococcus uberis			27958	2	
Streptococus sobrinus		6715		4	

*1. Vincent Fischetti, Rockefeller University; 2. ATCC; 3. Paul Kolenbrander, NIH; 4. Burton Rosan, University of Pennsylvania; 5. Alexandar Tomasz, Rockefeller University; 6. NARSA; 7. Randy Shirbroun, Newport Labs, Worthington, MN.

Appendix C

List of Published, Submitted and Planned Co-Authored Manuscripts

- **Shang, X.,** and Nelson, D.C. Contributions of Net Charge on the PlyC Endolysin CHAP Domain. In preparation.
- **Shang, X.,** Kelman, Z., Schiel, J.E., Schmelcher, M., Etobayeva, I., Nelson, D.C. (2019) A Novel Design of Exploit the Synergy of PlyC Catalytic Domains. In preparation.
- **Shang, X**., Blanco Medina, M.A., Nelson, D.C. (2019) Creation of Monomeric Cell Binding Domain of Bacteriophage Endolysin PlyC. In preparation.
- Harhala, M., Nelson, D. C., Miernikiewicz, P., Heselpoth, R. D., Brzezicka, B., Majewska, J., Linden, S. B., **Shang, X.**, Szymczak, A., Lecion, D., Marek-Bukowiec, K., Kłak, M., Wojciechowicz, B., Lahutta, K., Konieczny, A., and Dąbrowska, K. (2018). Safety Studies of Pneumococcal Endolysins Cpl-1 and Pal. *Viruses*, *10*(11), 638. doi:10.3390/v10110638
- Yang, H., Bi, Y., **Shang, X**., Wang, M., Linden, S.B., Li, Y., Li, Y., Nelson, D.C. and Wei, H., (2016). Antibiofilm activities of a novel chimeolysin against *Streptococcus mutans* under physiological and cariogenic conditions. *Antimicrobial agents and chemotherapy*, *60*(12), pp.7436-7443.
- Roelofs, K. G., Jones, C. J., Helman, S. R., **Shang, X**., Orr, M. W., Goodson, J. R., and Lee, V. T. (2015). Systematic identification of cyclic-di-GMP binding proteins in *Vibrio cholerae* reveals a novel class of cyclic-di-GMP-binding ATPases associated with type II secretion systems. *PLoS Pathog*, *11*(10), e1005232.

Bibliography

Abdul Rahman, N., Parks, D. H., Vanwonterghem, I., Morrison, M., Tyson, G. W., & Hugenholtz, P. (2015). A Phylogenomic Analysis of the Bacterial Phylum Fibrobacteres. *Front Microbiol, 6*, 1469. doi:10.3389/fmicb.2015.01469

Abdullahi, O., Karani, A., Tigoi, C. C., Mugo, D., Kungu, S., Wanjiru, E., Jomo, J., Musyimi, R., Lipsitch, M., & Scott, J. A. (2012). The prevalence and risk factors for pneumococcal colonization of the nasopharynx among children in Kilifi District, Kenya. *PLoS One, 7*(2), e30787. doi:10.1371/journal.pone.0030787

Andersson, D. I., & Hughes, D. (2010). Antibiotic resistance and its cost: is it possible to reverse resistance? *Nat Rev Microbiol, 8*(4), 260-271. doi:10.1038/nrmicro2319

Becker, S. C., Dong, S., Baker, J. R., Foster-Frey, J., Pritchard, D. G., & Donovan, D. M. (2009). LysK CHAP endopeptidase domain is required for lysis of live staphylococcal cells. *FEMS Microbiol Lett, 294*(1), 52-60. doi:10.1111/j.1574-6968.2009.01541.x

Becker, S. C., Foster-Frey, J., & Donovan, D. M. (2008). The phage K lytic enzyme LysK and lysostaphin act synergistically to kill MRSA. *FEMS Microbiol Lett, 287*(2), 185-191. doi:10.1111/j.1574-6968.2008.01308.x

Becker, S. C., Roach, D. R., Chauhan, V. S., Shen, Y., Foster-Frey, J., Powell, A. M., Bauchan, G., Lease, R. A., Mohammadi, H., Harty, W. J., Simmons, C., Schmelcher, M., Camp, M., Dong, S., Baker, J. R., Sheen, T. R., Doran, K. S., Pritchard, D. G., Almeida, R. A., Nelson, D. C., Marriott, I., Lee, J. C., & Donovan, D. M. (2016). Triple-acting lytic enzyme treatment of drug-resistant and intracellular *Staphylococcus aureus*. *Sci Rep, 6*, 25063. doi:10.1038/srep25063

Blair, J. M., Webber, M. A., Baylay, A. J., Ogbolu, D. O., & Piddock, L. J. (2015). Molecular mechanisms of antibiotic resistance. *Nat Rev Microbiol, 13*(1), 42-51. doi:10.1038/nrmicro3380

Blazquez, B., Fresco-Taboada, A., Iglesias-Bexiga, M., Menendez, M., & Garcia, P. (2016). PL3 amidase, a tailor-made lysin constructed by domain shuffling with potent killing activity against pneumococci and related species. *Front Microbiol, 7*, 1156. doi:10.3389/fmicb.2016.01156

Boiesen, P., Bendahl, P. O., Anagnostaki, L., Domanski, H., Holm, E., Idvall, I., Johansson, S., Ljungberg, O., Ringberg, A., Ostberg, G., & Ferno, M. (2000). Histologic grading in breast cancer--reproducibility between seven pathologic departments. South Sweden Breast Cancer Group. *Acta Oncol, 39*(1), 41-45.

Bonnet, R. (2004). Growing group of extended-spectrum beta-lactamases: the CTX-M enzymes. *Antimicrob Agents Chemother, 48*(1), 1-14.

Borysowski, J., Weber-Dabrowska, B., & Gorski, A. (2006). Bacteriophage endolysins as a novel class of antibacterial agents. *Exp Biol Med (Maywood), 231*(4), 366-377.

Braun, J. S., Sublett, J. E., Freyer, D., Mitchell, T. J., Cleveland, J. L., Tuomanen, E. I., & Weber, J. R. (2002). Pneumococcal pneumolysin and H(2)O(2) mediate

brain cell apoptosis during meningitis. *J Clin Invest, 109*(1), 19-27. doi:10.1172/JCI12035

Briers, Y., & Lavigne, R. (2015). Breaking barriers: expansion of the use of endolysins as novel antibacterials against Gram-negative bacteria. *Future Microbiol, 10*(3), 377-390. doi:10.2217/fmb.15.8

Briers, Y., Volckaert, G., Cornelissen, A., Lagaert, S., Michiels, C. W., Hertveldt, K., & Lavigne, R. (2007). Muralytic activity and modular structure of the endolysins of *Pseudomonas aeruginosa* bacteriophages phiKZ and EL. *Mol Microbiol, 65*(5), 1334-1344. doi:10.1111/j.1365-2958.2007.05870.x

Briers, Y., Walmagh, M., Van Puyenbroeck, V., Cornelissen, A., Cenens, W., Aertsen, A., Oliveira, H., Azeredo, J., Verween, G., Pirnay, J. P., Miller, S., Volckaert, G., & Lavigne, R. (2014). Engineered endolysin-based "Artilysins" to combat multidrug-resistant gram-negative pathogens. *MBio, 5*(4), e01379-01314. doi:10.1128/mBio.01379-14

Broendum, S. S., Buckle, A. M., & McGowan, S. (2018). Catalytic diversity and cell wall binding repeats in the phage encoded endolysins. *Mol Microbiol*. doi:10.1111/mmi.14134

Brook, I. (2013). Penicillin failure in the treatment of streptococcal pharyngo-tonsillitis. *Curr Infect Dis Rep, 15*(3), 232-235. doi:10.1007/s11908-013-0338-0

Brown, E. D., & Wright, G. D. (2016). Antibacterial drug discovery in the resistance era. *Nature, 529*(7586), 336-343. doi:10.1038/nature17042

Buist, G., Steen, A., Kok, J., & Kuipers, O. P. (2008). LysM, a widely distributed protein motif for binding to (peptido)glycans. *Mol Microbiol, 68*(4), 838-847. doi:10.1111/j.1365-2958.2008.06211.x

Bush, K., Jacoby, G. A., & Medeiros, A. A. (1995). A functional classification scheme for beta-lactamases and its correlation with molecular structure. *Antimicrob Agents Chemother, 39*(6), 1211-1233.

Carapetis, J. R., McDonald, M., & Wilson, N. J. (2005). Acute rheumatic fever. *Lancet, 366*(9480), 155-168. doi:10.1016/S0140-6736(05)66874-2

Carapetis, J. R., Steer, A. C., Mulholland, E. K., & Weber, M. (2005). The global burden of group A streptococcal diseases. *Lancet Infect Dis, 5*(11), 685-694. doi:10.1016/S1473-3099(05)70267-X

Cattoir, V. (2016). Mechanisms of Antibiotic Resistance. In J. J. Ferretti, D. L. Stevens, & V. A. Fischetti (Eds.), *Streptococcus pyogenes : Basic Biology to Clinical Manifestations*. Oklahoma City (OK).

Celia, L. K., Nelson, D., & Kerr, D. E. (2008). Characterization of a bacteriophage lysin (Ply700) from *Streptococcus uberis*. *Vet Microbiol, 130*(1-2), 107-117. doi:10.1016/j.vetmic.2007.12.004

Cheng, Q., Nelson, D., Zhu, S., & Fischetti, V. A. (2005). Removal of group B streptococci colonizing the vagina and oropharynx of mice with a bacteriophage lytic enzyme. *Antimicrob Agents Chemother, 49*(1), 111-117. doi:10.1128/AAC.49.1.111-117.2005

Cockeran, R., Durandt, C., Feldman, C., Mitchell, T. J., & Anderson, R. (2002). Pneumolysin activates the synthesis and release of interleukin-8 by human neutrophils in vitro. *J Infect Dis, 186*(4), 562-565. doi:10.1086/341563

Cole, C., & Gazewood, J. (2007). Diagnosis and treatment of impetigo. *Am Fam Physician, 75*(6), 859-864.

Cundell, D. R., Gerard, N. P., Gerard, C., Idanpaan-Heikkila, I., & Tuomanen, E. I. (1995). *Streptococcus pneumoniae* anchor to activated human cells by the receptor for platelet-activating factor. *Nature, 377*(6548), 435-438. doi:10.1038/377435a0

Cunningham, M. W. (2000). Pathogenesis of group A streptococcal infections. *Clin Microbiol Rev, 13*(3), 470-511.

Davies, S. B., & Di Girolamo, N. (2010). Corneal stem cells and their origins: significance in developmental biology. *Stem Cells Dev, 19*(11), 1651-1662. doi:10.1089/scd.2010.0201

DeHart, H. P., Heath, H. E., Heath, L. S., LeBlanc, P. A., & Sloan, G. L. (1995). The lysostaphin endopeptidase resistance gene (epr) specifies modification of peptidoglycan cross bridges in *Staphylococcus simulans* and *Staphylococcus aureus*. *Appl Environ Microbiol, 61*(4), 1475-1479.

Diez-Martinez, R., de Paz, H. D., Bustamante, N., Garcia, E., Menendez, M., & Garcia, P. (2013). Improving the lethal effect of cpl-7, a pneumococcal phage lysozyme with broad bactericidal activity, by inverting the net charge of its cell wall-binding module. *Antimicrob Agents Chemother, 57*(11), 5355-5365. doi:10.1128/AAC.01372-13

Diez-Martinez, R., De Paz, H. D., Garcia-Fernandez, E., Bustamante, N., Euler, C. W., Fischetti, V. A., Menendez, M., & Garcia, P. (2015). A novel chimeric phage lysin with high in vitro and in vivo bactericidal activity against *Streptococcus pneumoniae*. *J Antimicrob Chemother, 70*(6), 1763-1773. doi:10.1093/jac/dkv038

Djurkovic, S., Loeffler, J. M., & Fischetti, V. A. (2005). Synergistic killing of *Streptococcus pneumoniae* with the bacteriophage lytic enzyme Cpl-1 and penicillin or gentamicin depends on the level of penicillin resistance. *Antimicrob Agents Chemother, 49*(3), 1225-1228. doi:10.1128/AAC.49.3.1225-1228.2005

Donlan, R. M. (2008). Biofilms on central venous catheters: is eradication possible? *Curr Top Microbiol Immunol, 322*, 133-161.

Donovan, D. M., & Foster-Frey, J. (2008). LambdaSa2 prophage endolysin requires Cpl-7-binding domains and amidase-5 domain for antimicrobial lysis of streptococci. *FEMS Microbiol Lett, 287*(1), 22-33. doi:10.1111/j.1574-6968.2008.01287.x

Donovan, D. M., Foster-Frey, J., Dong, S., Rousseau, G. M., Moineau, S., & Pritchard, D. G. (2006). The cell lysis activity of the *Streptococcus agalactiae* bacteriophage B30 endolysin relies on the cysteine, histidine-dependent amidohydrolase/peptidase domain. *Appl Environ Microbiol, 72*(7), 5108-5112. doi:10.1128/AEM.03065-05

Douzi, B. (2017). Protein-Protein Interactions: Surface Plasmon Resonance. *Methods Mol Biol, 1615*, 257-275. doi:10.1007/978-1-4939-7033-9_21

Dy, R. L., Richter, C., Salmond, G. P., & Fineran, P. C. (2014). Remarkable mechanisms in microbes to resist phage infections. *Annu Rev Virol, 1*(1), 307-331. doi:10.1146/annurev-virology-031413-085500

Eicher, T., Cha, H. J., Seeger, M. A., Brandstatter, L., El-Delik, J., Bohnert, J. A., Kern, W. V., Verrey, F., Grutter, M. G., Diederichs, K., & Pos, K. M. (2012). Transport of drugs by the multidrug transporter AcrB involves an access and a deep binding pocket that are separated by a switch-loop. *Proc Natl Acad Sci U S A, 109*(15), 5687-5692. doi:10.1073/pnas.1114944109

Elder, B. L., Boraker, D. K., & Fives-Taylor, P. M. (1982). Whole-bacterial cell enzyme-linked immunosorbent assay for *Streptococcus sanguis* fimbrial antigens. *J Clin Microbiol, 16*(1), 141-144.

Entenza, J. M., Loeffler, J. M., Grandgirard, D., Fischetti, V. A., & Moreillon, P. (2005). Therapeutic effects of bacteriophage Cpl-1 lysin against *Streptococcus pneumoniae* endocarditis in rats. *Antimicrob Agents Chemother, 49*(11), 4789-4792. doi:10.1128/AAC.49.11.4789-4792.2005

Facklam, R. (2002). What happened to the streptococci: overview of taxonomic and nomenclature changes. *Clin Microbiol Rev, 15*(4), 613-630.

Fenton, M., Casey, P. G., Hill, C., Gahan, C. G., Ross, R. P., McAuliffe, O., O'Mahony, J., Maher, F., & Coffey, A. (2010). The truncated phage lysin CHAP(k) eliminates *Staphylococcus aureus* in the nares of mice. *Bioeng Bugs, 1*(6), 404-407. doi:10.4161/bbug.1.6.13422

Fischetti, V. A. (1991). Streptococcal M protein. *Sci Am, 264*(6), 58-65.

Fischetti, V. A. (2005). Bacteriophage lytic enzymes: novel anti-infectives. *Trends Microbiol, 13*(10), 491-496. doi:10.1016/j.tim.2005.08.007

Fischetti, V. A. (2008). Bacteriophage lysins as effective antibacterials. *Curr Opin Microbiol, 11*(5), 393-400. doi:10.1016/j.mib.2008.09.012

Fischetti, V. A. (2010). Bacteriophage endolysins: a novel anti-infective to control Gram-positive pathogens. *Int J Med Microbiol, 300*(6), 357-362. doi:10.1016/j.ijmm.2010.04.002

Fischetti, V. A. (2018). Development of phage lysins as novel therapeutics: a historical perspective. *Viruses, 10*(6). doi:10.3390/v10060310

Fischetti, V. A., Jones, K. F., & Scott, J. R. (1985). Size variation of the M protein in group A streptococci. *J Exp Med, 161*(6), 1384-1401.

Fischetti, V. A., Nelson, D., & Schuch, R. (2006). Reinventing phage therapy: are the parts greater than the sum? *Nat Biotechnol, 24*(12), 1508-1511. doi:10.1038/nbt1206-1508

Fischetti VA, Z. J., Gotschlich EC (1972). (1972). Physical, chemical and biological properties of Type 6 M-protein extracted with purified streptococcal phage-associated lysin. *Fifth International Symposium on Streptococcus pyogenes, ed Haverkorn MJ (Excerpta Medica, Amsterdam*, pp 26–36.

Garcia, J. L., Garcia, E., Arraras, A., Garcia, P., Ronda, C., & Lopez, R. (1987). Cloning, purification, and biochemical characterization of the pneumococcal bacteriophage Cp-1 lysin. *J Virol, 61*(8), 2573-2580.

Gargis, S. R., Heath, H. E., Heath, L. S., Leblanc, P. A., Simmonds, R. S., Abbott, B. D., Timkovich, R., & Sloan, G. L. (2009). Use of 4-sulfophenyl isothiocyanate labeling and mass spectrometry to determine the site of action of the streptococcolytic peptidoglycan hydrolase zoocin A. *Appl Environ Microbiol, 75*(1), 72-77. doi:10.1128/AEM.01647-08

Garvey, E. P., & Santi, D. V. (1986). Stable amplified DNA in drug-resistant Leishmania exists as extrachromosomal circles. *Science, 233*(4763), 535-540.
Gerstmans, H., Rodriguez-Rubio, L., Lavigne, R., & Briers, Y. (2016). From endolysins to Artilysin(R)s: novel enzyme-based approaches to kill drug-resistant bacteria. *Biochem Soc Trans, 44*(1), 123-128. doi:10.1042/BST20150192
Gilmer, D. B., Schmitz, J. E., Euler, C. W., & Fischetti, V. A. (2013). Novel bacteriophage lysin with broad lytic activity protects against mixed infection by *Streptococcus pyogenes* and methicillin-resistant *Staphylococcus aureus*. *Antimicrob Agents Chemother, 57*(6), 2743-2750. doi:10.1128/AAC.02526-12
Goodridge, L. D. (2004). Bacteriophage biocontrol of plant pathogens: fact or fiction? *Trends Biotechnol, 22*(8), 384-385. doi:10.1016/j.tibtech.2004.05.007
Grandgirard, D., Loeffler, J. M., Fischetti, V. A., & Leib, S. L. (2008). Phage lytic enzyme Cpl-1 for antibacterial therapy in experimental pneumococcal meningitis. *J Infect Dis, 197*(11), 1519-1522. doi:10.1086/587942
Grundling, A., Missiakas, D. M., & Schneewind, O. (2006). *Staphylococcus aureus* mutants with increased lysostaphin resistance. *J Bacteriol, 188*(17), 6286-6297. doi:10.1128/JB.00457-06
Gu, J., Xu, W., Lei, L., Huang, J., Feng, X., Sun, C., Du, C., Zuo, J., Li, Y., Du, T., Li, L., & Han, W. (2011). LysGH15, a novel bacteriophage lysin, protects a murine bacteremia model efficiently against lethal methicillin-resistant *Staphylococcus aureus* infection. *J Clin Microbiol, 49*(1), 111-117. doi:10.1128/JCM.01144-10
Guerois, R., Nielsen, J. E., & Serrano, L. (2002). Predicting changes in the stability of proteins and protein complexes: a study of more than 1000 mutations. *J Mol Biol, 320*(2), 369-387. doi:10.1016/S0022-2836(02)00442-4
Ha, E., Son, B., & Ryu, S. (2018). *Clostridium perfringens* Virulent Bacteriophage CPS2 and Its Thermostable Endolysin LysCPS2. *Viruses, 10*(5). doi:10.3390/v10050251
Hall-Stoodley, L., Hu, F. Z., Gieseke, A., Nistico, L., Nguyen, D., Hayes, J., Forbes, M., Greenberg, D. P., Dice, B., Burrows, A., Wackym, P. A., Stoodley, P., Post, J. C., Ehrlich, G. D., & Kerschner, J. E. (2006). Direct detection of bacterial biofilms on the middle-ear mucosa of children with chronic otitis media. *JAMA, 296*(2), 202-211. doi:10.1001/jama.296.2.202
Hammerschmidt, S., Talay, S. R., Brandtzaeg, P., & Chhatwal, G. S. (1997). SpsA, a novel pneumococcal surface protein with specific binding to secretory immunoglobulin A and secretory component. *Mol Microbiol, 25*(6), 1113-1124.
Hardie, J. M., & Whiley, R. A. (1997a). Classification and overview of the genera Streptococcus and Enterococcus. *Soc Appl Bacteriol Symp Ser, 26*, 1S-11S.
Hardie, J. M., & Whiley, R. A. (1997b). Classification and overview of the genera Streptococcus and Enterococcus. *J Appl Microbiol, 83*(S1), 1S-11S. doi:10.1046/j.1365-2672.83.s1.1.x
Harhala, M., Barylski, J., Huminska-Lisowska, K., Lecion, D., Wojciechowicz, J., Lahutta, K., Kus, M., Kropinski, A. M., Nowak, S., Nowicki, G., Hodyra-Stefaniak, K., & Dabrowska, K. (2018). Two novel temperate bacteriophages

infecting *Streptococcus pyogenes*: Their genomes, morphology and stability. *PLoS One, 13*(10), e0205995. doi:10.1371/journal.pone.0205995

Hermoso, J. A., Garcia, J. L., & Garcia, P. (2007). Taking aim on bacterial pathogens: from phage therapy to enzybiotics. *Curr Opin Microbiol, 10*(5), 461-472. doi:10.1016/j.mib.2007.08.002

Heselpoth, R. D., & Nelson, D. C. (2012). A new screening method for the directed evolution of thermostable bacteriolytic enzymes. *J Vis Exp*(69). doi:10.3791/4216

Heselpoth, R. D., Yin, Y., Moult, J., & Nelson, D. C. (2015). Increasing the stability of the bacteriophage endolysin PlyC using rationale-based FoldX computational modeling. *Protein Eng Des Sel, 28*(4), 85-92. doi:10.1093/protein/gzv004

Hirst, R. A., Sikand, K. S., Rutman, A., Mitchell, T. J., Andrew, P. W., & O'Callaghan, C. (2000). Relative roles of pneumolysin and hydrogen peroxide from *Streptococcus pneumoniae* in inhibition of ependymal ciliary beat frequency. *Infect Immun, 68*(3), 1557-1562.

Hoa, M., Syamal, M., Sachdeva, L., Berk, R., & Coticchia, J. (2009). Demonstration of nasopharyngeal and middle ear mucosal biofilms in an animal model of acute otitis media. *Ann Otol Rhinol Laryngol, 118*(4), 292-298. doi:10.1177/000348940911800410

Hoopes, J. T., Stark, C. J., Kim, H. A., Sussman, D. J., Donovan, D. M., & Nelson, D. C. (2009). Use of a bacteriophage lysin, PlyC, as an enzyme disinfectant against *Streptococcus equi*. *Appl Environ Microbiol, 75*(5), 1388-1394. doi:10.1128/AEM.02195-08

Horgan, M., O'Flynn, G., Garry, J., Cooney, J., Coffey, A., Fitzgerald, G. F., Ross, R. P., & McAuliffe, O. (2009). Phage lysin LysK can be truncated to its CHAP domain and retain lytic activity against live antibiotic-resistant staphylococci. *Appl Environ Microbiol, 75*(3), 872-874. doi:10.1128/AEM.01831-08

Horton, R. M., Cai, Z. L., Ho, S. N., & Pease, L. R. (1990). Gene splicing by overlap extension: tailor-made genes using the polymerase chain reaction. *Biotechniques, 8*(5), 528-535.

Huang, Y., Yang, H., Yu, J., & Wei, H. (2015). Molecular dissection of phage lysin PlySs2: integrity of the catalytic and cell wall binding domains is essential for its broad lytic activity. *Virol Sin, 30*(1), 45-51. doi:10.1007/s12250-014-3535-6

Hung, L. W., Kim, H. B., Murakami, S., Gupta, G., Kim, C. Y., & Terwilliger, T. C. (2013). Crystal structure of AcrB complexed with linezolid at 3.5 A resolution. *J Struct Funct Genomics, 14*(2), 71-75. doi:10.1007/s10969-013-9154-x

Ishii, S., Nagase, T., & Shimizu, T. (2002). Platelet-activating factor receptor. *Prostaglandins Other Lipid Mediat, 68-69*, 599-609.

Ismail, A. Q., Yeates, D. G., Marciano, A., Goldacre, M., & Anthony, M. (2011). Cow's milk and the emergence of group B streptococcal disease in newborn babies. *Neonatology, 100*(4), 404-408. doi:10.1159/000328700

Jado, I., Lopez, R., Garcia, E., Fenoll, A., Casal, J., Garcia, P., & Spanish Pneumococcal Infection Study, N. (2003). Phage lytic enzymes as therapy for

antibiotic-resistant *Streptococcus pneumoniae* infection in a murine sepsis model. *J Antimicrob Chemother, 52*(6), 967-973. doi:10.1093/jac/dkg485

Jun, S. Y., Jang, I. J., Yoon, S., Jang, K., Yu, K. S., Cho, J. Y., Seong, M. W., Jung, G. M., Yoon, S. J., & Kang, S. H. (2017). Pharmacokinetics and tolerance of the phage endolysin-based candidate drug SAL200 after a single intravenous administration among healthy volunteers. *Antimicrob Agents Chemother, 61*(6). doi:10.1128/AAC.02629-16

Jun, S. Y., Jung, G. M., Yoon, S. J., Choi, Y. J., Koh, W. S., Moon, K. S., & Kang, S. H. (2014). Preclinical safety evaluation of intravenously administered SAL200 containing the recombinant phage endolysin SAL-1 as a pharmaceutical ingredient. *Antimicrob Agents Chemother, 58*(4), 2084-2088. doi:10.1128/AAC.02232-13

Jun, S. Y., Jung, G. M., Yoon, S. J., Youm, S. Y., Han, H. Y., Lee, J. H., & Kang, S. H. (2016). Pharmacokinetics of the phage endolysin-based candidate drug SAL200 in monkeys and its appropriate intravenous dosing period. *Clin Exp Pharmacol Physiol, 43*(10), 1013-1016. doi:10.1111/1440-1681.12613

Kapoor, G., Saigal, S., & Elongavan, A. (2017). Action and resistance mechanisms of antibiotics: A guide for clinicians. *J Anaesthesiol Clin Pharmacol, 33*(3), 300-305. doi:10.4103/joacp.JOACP_349_15

Katz, V., & Bowes, W. A., Jr. (1988). Perinatal group B streptococcal infections across intact amniotic membranes. *J Reprod Med, 33*(5), 445-449.

Kohanski, M. A., Dwyer, D. J., & Collins, J. J. (2010). How antibiotics kill bacteria: from targets to networks. *Nat Rev Microbiol, 8*(6), 423-435. doi:10.1038/nrmicro2333

Kokai-Kun, J. F., Chanturiya, T., & Mond, J. J. (2009). Lysostaphin eradicates established *Staphylococcus aureus* biofilms in jugular vein catheterized mice. *J Antimicrob Chemother, 64*(1), 94-100. doi:10.1093/jac/dkp145

Kong, M., Shin, J. H., Heu, S., Park, J. K., & Ryu, S. (2017). Lateral flow assay-based bacterial detection using engineered cell wall binding domains of a phage endolysin. *Biosens Bioelectron, 96*, 173-177. doi:10.1016/j.bios.2017.05.010

Kong, M., Sim, J., Kang, T., Nguyen, H. H., Park, H. K., Chung, B. H., & Ryu, S. (2015). A novel and highly specific phage endolysin cell wall binding domain for detection of *Bacillus cereus*. *Eur Biophys J, 44*(6), 437-446. doi:10.1007/s00249-015-1044-7

Kotra, L. P., & Mobashery, S. (1999). Mechanistic and clinical aspects of beta-lactam antibiotics and beta-lactamases. *Arch Immunol Ther Exp (Warsz), 47*(4), 211-216.

Krause, R. M. (1957). Studies on bacteriophages of hemolytic streptococci. I. Factors influencing the interaction of phage and susceptible host cell. *J Exp Med, 106*(3), 365-384.

Kretzer, J. W., Lehmann, R., Schmelcher, M., Banz, M., Kim, K. P., Korn, C., & Loessner, M. J. (2007). Use of high-affinity cell wall-binding domains of bacteriophage endolysins for immobilization and separation of bacterial cells. *Appl Environ Microbiol, 73*(6), 1992-2000. doi:10.1128/AEM.02402-06

Krissinel, E., & Henrick, K. (2007). Inference of macromolecular assemblies from crystalline state. *J Mol Biol, 372*(3), 774-797. doi:10.1016/j.jmb.2007.05.022

Li, J., Kasper, D. L., Ausubel, F. M., Rosner, B., & Michel, J. L. (1997). Inactivation of the alpha C protein antigen gene, bca, by a novel shuttle/suicide vector results in attenuation of virulence and immunity in group B Streptococcus. *Proc Natl Acad Sci U S A, 94*(24), 13251-13256.

Linden, S. B., Zhang, H., Heselpoth, R. D., Shen, Y., Schmelcher, M., Eichenseher, F., & Nelson, D. C. (2015). Biochemical and biophysical characterization of PlyGRCS, a bacteriophage endolysin active against methicillin-resistant *Staphylococcus aureus*. *Appl Microbiol Biotechnol, 99*(2), 741-752. doi:10.1007/s00253-014-5930-1

Loeffler, J. M., Djurkovic, S., & Fischetti, V. A. (2003). Phage lytic enzyme Cpl-1 as a novel antimicrobial for pneumococcal bacteremia. *Infect Immun, 71*(11), 6199-6204.

Loeffler, J. M., & Fischetti, V. A. (2003). Synergistic lethal effect of a combination of phage lytic enzymes with different activities on penicillin-sensitive and -resistant *Streptococcus pneumoniae* strains. *Antimicrob Agents Chemother, 47*(1), 375-377.

Loeffler, J. M., Nelson, D., & Fischetti, V. A. (2001). Rapid killing of *Streptococcus pneumoniae* with a bacteriophage cell wall hydrolase. *Science, 294*(5549), 2170-2172. doi:10.1126/science.1066869

Loessner, M. J. (2005). Bacteriophage endolysins--current state of research and applications. *Curr Opin Microbiol, 8*(4), 480-487. doi:10.1016/j.mib.2005.06.002

Lood, R., Raz, A., Molina, H., Euler, C. W., & Fischetti, V. A. (2014). A highly active and negatively charged Streptococcus pyogenes lysin with a rare D-alanyl-L-alanine endopeptidase activity protects mice against streptococcal bacteremia. *Antimicrob Agents Chemother, 58*(6), 3073-3084. doi:10.1128/AAC.00115-14

Lopez, R., & Garcia, E. (2004). Recent trends on the molecular biology of pneumococcal capsules, lytic enzymes, and bacteriophage. *FEMS Microbiol Rev, 28*(5), 553-580. doi:10.1016/j.femsre.2004.05.002

Low, L. Y., Yang, C., Perego, M., Osterman, A., & Liddington, R. (2011). Role of net charge on catalytic domain and influence of cell wall binding domain on bactericidal activity, specificity, and host range of phage lysins. *J Biol Chem, 286*(39), 34391-34403. doi:10.1074/jbc.M111.244160

Lukacik, P., Barnard, T. J., & Buchanan, S. K. (2012). Using a bacteriocin structure to engineer a phage lysin that targets *Yersinia pestis*. *Biochem Soc Trans, 40*(6), 1503-1506. doi:10.1042/BST20120209

Macris, M. H., Hartman, N., Murray, B., Klein, R. F., Roberts, R. B., Kaplan, E. L., Horn, D., & Zabriskie, J. B. (1998). Studies of the continuing susceptibility of group A streptococcal strains to penicillin during eight decades. *Pediatr Infect Dis J, 17*(5), 377-381.

Matthews, B. W., & Remington, S. J. (1974). The three dimensional structure of the lysozyme from bacteriophage T4. *Proc Natl Acad Sci U S A, 71*(10), 4178-4182.

Mayer, B. J., Hamaguchi, M., & Hanafusa, H. (1988). Characterization of p47gag-crk, a novel oncogene product with sequence similarity to a putative modulatory domain of protein-tyrosine kinases and phospholipase C. *Cold Spring Harb Symp Quant Biol, 53 Pt 2*, 907-914.

Mayer, M. J., Garefalaki, V., Spoerl, R., Narbad, A., & Meijers, R. (2011). Structure-based modification of a *Clostridium difficile*-targeting endolysin affects activity and host range. *J Bacteriol, 193*(19), 5477-5486. doi:10.1128/JB.00439-11

Mayer, M. J., Payne, J., Gasson, M. J., & Narbad, A. (2010). Genomic sequence and characterization of the virulent bacteriophage phiCTP1 from Clostridium tyrobutyricum and heterologous expression of its endolysin. *Appl Environ Microbiol, 76*(16), 5415-5422. doi:10.1128/AEM.00989-10

McGowan, S., Buckle, A. M., Mitchell, M. S., Hoopes, J. T., Gallagher, D. T., Heselpoth, R. D., Shen, Y., Reboul, C. F., Law, R. H., Fischetti, V. A., Whisstock, J. C., & Nelson, D. C. (2012). X-ray crystal structure of the streptococcal specific phage lysin PlyC. *Proc Natl Acad Sci U S A, 109*(31), 12752-12757. doi:10.1073/pnas.1208424109

McIver, K. S., Heath, A. S., Green, B. D., & Scott, J. R. (1995). Specific binding of the activator Mga to promoter sequences of the emm and scpA genes in the group A streptococcus. *J Bacteriol, 177*(22), 6619-6624.

McNicholas, S., Potterton, E., Wilson, K. S., & Noble, M. E. (2011). Presenting your structures: the CCP4mg molecular-graphics software. *Acta Crystallogr D Biol Crystallogr, 67*(Pt 4), 386-394. doi:10.1107/S0907444911007281

Meroueh, S. O., Bencze, K. Z., Hesek, D., Lee, M., Fisher, J. F., Stemmler, T. L., & Mobashery, S. (2006). Three-dimensional structure of the bacterial cell wall peptidoglycan. *Proc Natl Acad Sci U S A, 103*(12), 4404-4409. doi:10.1073/pnas.0510182103

Mitchell, T. J. (2003). The pathogenesis of streptococcal infections: from tooth decay to meningitis. *Nat Rev Microbiol, 1*(3), 219-230. doi:10.1038/nrmicro771

Munita, J. M., & Arias, C. A. (2016). Mechanisms of Antibiotic Resistance. *Microbiol Spectr, 4*(2). doi:10.1128/microbiolspec.VMBF-0016-2015

Nakano, K., Lapirattanakul, J., Nomura, R., Nemoto, H., Alaluusua, S., Gronroos, L., Vaara, M., Hamada, S., Ooshima, T., & Nakagawa, I. (2007). *Streptococcus mutans* clonal variation revealed by multilocus sequence typing. *J Clin Microbiol, 45*(8), 2616-2625. doi:10.1128/JCM.02343-06

Nelson, D., Loomis, L., & Fischetti, V. A. (2001). Prevention and elimination of upper respiratory colonization of mice by group A streptococci by using a bacteriophage lytic enzyme. *Proc Natl Acad Sci U S A, 98*(7), 4107-4112. doi:10.1073/pnas.061038398

Nelson, D., Schuch, R., Chahales, P., Zhu, S., & Fischetti, V. A. (2006). PlyC: a multimeric bacteriophage lysin. *Proc Natl Acad Sci U S A, 103*(28), 10765-10770. doi:10.1073/pnas.0604521103

Nelson, D., Schuch, R., Zhu, S., Tscherne, D. M., & Fischetti, V. A. (2003). Genomic sequence of C1, the first streptococcal phage. *J Bacteriol, 185*(11), 3325-3332.

Nelson, D. C., Schmelcher, M., Rodriguez-Rubio, L., Klumpp, J., Pritchard, D. G., Dong, S., & Donovan, D. M. (2012). Endolysins as antimicrobials. *Adv Virus Res, 83*, 299-365. doi:10.1016/B978-0-12-394438-2.00007-4

Nomura, R., Yoneyama, R., Naka, S., Otsugu, M., Ogaya, Y., Hatakeyama, R., Morita, Y., Maruo, J., Matsumoto-Nakano, M., Yamada, O., & Nakano, K. (2017). The *in vivo* inhibition of oral biofilm accumulation and *Streptococcus mutans* by ceramic water. *Caries Res, 51*(1), 58-67. doi:10.1159/000452343

Nunes, S., Sa-Leao, R., Carrico, J., Alves, C. R., Mato, R., Avo, A. B., Saldanha, J., Almeida, J. S., Sanches, I. S., & de Lencastre, H. (2005). Trends in drug resistance, serotypes, and molecular types of *Streptococcus pneumoniae* colonizing preschool-age children attending day care centers in Lisbon, Portugal: a summary of 4 years of annual surveillance. *J Clin Microbiol, 43*(3), 1285-1293. doi:10.1128/JCM.43.3.1285-1293.2005

O'Flaherty, S., Coffey, A., Meaney, W., Fitzgerald, G. F., & Ross, R. P. (2005). The recombinant phage lysin LysK has a broad spectrum of lytic activity against clinically relevant staphylococci, including methicillin-resistant *Staphylococcus aureus*. *J Bacteriol, 187*(20), 7161-7164. doi:10.1128/JB.187.20.7161-7164.2005

Obeso, J. M., Martinez, B., Rodriguez, A., & Garcia, P. (2008). Lytic activity of the recombinant staphylococcal bacteriophage PhiH5 endolysin active against *Staphylococcus aureus* in milk. *Int J Food Microbiol, 128*(2), 212-218. doi:10.1016/j.ijfoodmicro.2008.08.010

Ohnuma, T., Onaga, S., Murata, K., Taira, T., & Katoh, E. (2008). LysM domains from *Pteris ryukyuensis* chitinase-A: a stability study and characterization of the chitin-binding site. *J Biol Chem, 283*(8), 5178-5187. doi:10.1074/jbc.M707156200

Oliveira, H., Melo, L. D., Santos, S. B., Nobrega, F. L., Ferreira, E. C., Cerca, N., Azeredo, J., & Kluskens, L. D. (2013). Molecular aspects and comparative genomics of bacteriophage endolysins. *J Virol, 87*(8), 4558-4570. doi:10.1128/JVI.03277-12

Oliveira, H., Thiagarajan, V., Walmagh, M., Sillankorva, S., Lavigne, R., Neves-Petersen, M. T., Kluskens, L. D., & Azeredo, J. (2014). A thermostable Salmonella phage endolysin, Lys68, with broad bactericidal properties against gram-negative pathogens in presence of weak acids. *PLoS One, 9*(10), e108376. doi:10.1371/journal.pone.0108376

Oliveira, I. C., Almeida, R. C., Hofer, E., & Almeida, P. F. (2012). Bacteriophage amplification assay for detection of Listeria spp. using virucidal laser treatment. *Braz J Microbiol, 43*(3), 1128-1136. doi:10.1590/S1517-838220120003000040

Oliveira, L. M., Gomes, R. A., Yang, D., Dennison, S. R., Familia, C., Lages, A., Coelho, A. V., Murphy, R. M., Phoenix, D. A., & Quintas, A. (2013). Insights into the molecular mechanism of protein native-like aggregation upon glycation. *Biochim Biophys Acta, 1834*(6), 1010-1022. doi:10.1016/j.bbapap.2012.12.001

Parks, T., Barrett, L., & Jones, N. (2015). Invasive streptococcal disease: a review for clinicians. *Br Med Bull, 115*(1), 77-89. doi:10.1093/bmb/ldv027

Pastagia, M., Euler, C., Chahales, P., Fuentes-Duculan, J., Krueger, J. G., & Fischetti, V. A. (2011). A novel chimeric lysin shows superiority to mupirocin for skin decolonization of methicillin-resistant and -sensitive *Staphylococcus aureus* strains. *Antimicrob Agents Chemother, 55*(2), 738-744. doi:10.1128/AAC.00890-10

Patterson, M. J. (1996). Streptococcus. In th & S. Baron (Eds.), *Medical Microbiology*. Galveston (TX).

Pearlman, M. (2003). Prevention of early-onset group B streptococcal disease in newborns. *Obstet Gynecol, 102*(2), 414-415; author reply 415.

Pedersen, L. H., Aalbaek, B., Rontved, C. M., Ingvartsen, K. L., Sorensen, N. S., Heegaard, P. M., & Jensen, H. E. (2003). Early pathogenesis and inflammatory response in experimental bovine mastitis due to *Streptococcus uberis*. *J Comp Pathol, 128*(2-3), 156-164.

Pfoh, E., Wessels, M. R., Goldmann, D., & Lee, G. M. (2008). Burden and economic cost of group A streptococcal pharyngitis. *Pediatrics, 121*(2), 229-234. doi:10.1542/peds.2007-0484

Phares, C. R., Lynfield, R., Farley, M. M., Mohle-Boetani, J., Harrison, L. H., Petit, S., Craig, A. S., Schaffner, W., Zansky, S. M., Gershman, K., Stefonek, K. R., Albanese, B. A., Zell, E. R., Schuchat, A., Schrag, S. J., & Active Bacterial Core surveillance/Emerging Infections Program, N. (2008). Epidemiology of invasive group B streptococcal disease in the United States, 1999-2005. *JAMA, 299*(17), 2056-2065. doi:10.1001/jama.299.17.2056

Plotka, M., Kaczorowska, A. K., Stefanska, A., Morzywolek, A., Fridjonsson, O. H., Dunin-Horkawicz, S., Kozlowski, L., Hreggvidsson, G. O., Kristjansson, J. K., Dabrowski, S., Bujnicki, J. M., & Kaczorowski, T. (2014). Novel highly thermostable endolysin from Thermus scotoductus MAT2119 bacteriophage Ph2119 with amino acid sequence similarity to eukaryotic peptidoglycan recognition proteins. *Appl Environ Microbiol, 80*(3), 886-895. doi:10.1128/AEM.03074-13

Poole, K. (2004). Resistance to beta-lactam antibiotics. *Cell Mol Life Sci, 61*(17), 2200-2223. doi:10.1007/s00018-004-4060-9

Pouliot, J. J., Thomson, M., Xie, M., Horton, J., Johnson, J., Krull, D., Mathis, A., Morikawa, Y., Parks, D., Peterson, R., Shimada, T., Thomas, E., Vamathevan, J., Van Horn, S., Xiong, Z., Hamatake, R., & Peat, A. J. (2015). Preclinical characterization and *in vivo* efficacy of GSK8853, a small-molecule inhibitor of the hepatitis C virus NS4B protein. *Antimicrob Agents Chemother, 59*(10), 6539-6550. doi:10.1128/AAC.00813-15

Pritchard, D. G., Dong, S., Baker, J. R., & Engler, J. A. (2004). The bifunctional peptidoglycan lysin of *Streptococcus agalactiae* bacteriophage B30. *Microbiology, 150*(Pt 7), 2079-2087. doi:10.1099/mic.0.27063-0

Pritchard, D. G., Dong, S., Kirk, M. C., Cartee, R. T., & Baker, J. R. (2007). LambdaSa1 and LambdaSa2 prophage lysins of *Streptococcus agalactiae*. *Appl Environ Microbiol, 73*(22), 7150-7154. doi:10.1128/AEM.01783-07

Rashel, M., Uchiyama, J., Ujihara, T., Uehara, Y., Kuramoto, S., Sugihara, S., Yagyu, K., Muraoka, A., Sugai, M., Hiramatsu, K., Honke, K., & Matsuzaki, S. (2007). Efficient elimination of multidrug-resistant *Staphylococcus aureus* by

cloned lysin derived from bacteriophage phi MR11. *J Infect Dis, 196*(8), 1237-1247. doi:10.1086/521305

Raz, A., Serrano, A., Lawson, C., Thaker, M., Alston, T., Bournazos, S., Ravetch, J. V., & Fischetti, V. A. (2017). Lysibodies are IgG Fc fusions with lysin binding domains targeting *Staphylococcus aureus* wall carbohydrates for effective phagocytosis. *Proc Natl Acad Sci U S A, 114*(18), 4781-4786. doi:10.1073/pnas.1619249114

Regulski, K., Courtin, P., Kulakauskas, S., & Chapot-Chartier, M. P. (2013). A novel type of peptidoglycan-binding domain highly specific for amidated D-Asp cross-bridge, identified in *Lactobacillus casei* bacteriophage endolysins. *J Biol Chem, 288*(28), 20416-20426. doi:10.1074/jbc.M112.446344

Resch, G., Moreillon, P., & Fischetti, V. A. (2011). A stable phage lysin (Cpl-1) dimer with increased antipneumococcal activity and decreased plasma clearance. *Int J Antimicrob Agents, 38*(6), 516-521. doi:10.1016/j.ijantimicag.2011.08.009

Ring, A., Braun, J. S., Nizet, V., Stremmel, W., & Shenep, J. L. (2000). Group B streptococcal beta-hemolysin induces nitric oxide production in murine macrophages. *J Infect Dis, 182*(1), 150-157. doi:10.1086/315681

Rodriguez-Rubio, L., Gutierrez, D., Martinez, B., Rodriguez, A., & Garcia, P. (2012). Lytic activity of LysH5 endolysin secreted by *Lactococcus lactis* using the secretion signal sequence of bacteriocin Lcn972. *Appl Environ Microbiol, 78*(9), 3469-3472. doi:10.1128/AEM.00018-12

Royet, J., & Dziarski, R. (2007). Peptidoglycan recognition proteins: pleiotropic sensors and effectors of antimicrobial defences. *Nat Rev Microbiol, 5*(4), 264-277. doi:10.1038/nrmicro1620

Sambrook, J., Maniatis, J., and Fritsch, E.F. . (1989). Molecular Cloning: A Laboratory Manuel. . *New York, USA: Cold Spring Harbor Laboratory Press*.

Sanderson, A. R., Leid, J. G., & Hunsaker, D. (2006). Bacterial biofilms on the sinus mucosa of human subjects with chronic rhinosinusitis. *Laryngoscope, 116*(7), 1121-1126. doi:10.1097/01.mlg.0000221954.05467.54

Sanz, J. M., Garcia, J. L., Laynez, J., Usobiaga, P., & Menendez, M. (1993). Thermal stability and cooperative domains of CPL1 lysozyme and its NH2- and COOH-terminal modules. Dependence on choline binding. *J Biol Chem, 268*(9), 6125-6130.

Sao-Jose, C. (2018). Engineering of phage-derived lytic enzymes: improving their potential as antimicrobials. *Antibiotics (Basel), 7*(2). doi:10.3390/antibiotics7020029

Sass, P., & Bierbaum, G. (2007). Lytic activity of recombinant bacteriophage phi11 and phi12 endolysins on whole cells and biofilms of *Staphylococcus aureus*. *Appl Environ Microbiol, 73*(1), 347-352. doi:10.1128/AEM.01616-06

Schleifer, K. H., & Kandler, O. (1972). Peptidoglycan types of bacterial cell walls and their taxonomic implications. *Bacteriol Rev, 36*(4), 407-477.

Schmelcher, M., Donovan, D. M., & Loessner, M. J. (2012). Bacteriophage endolysins as novel antimicrobials. *Future Microbiol, 7*(10), 1147-1171. doi:10.2217/fmb.12.97

Schmelcher, M., Powell, A. M., Camp, M. J., Pohl, C. S., & Donovan, D. M. (2015). Synergistic streptococcal phage lambdaSA2 and B30 endolysins kill streptococci in cow milk and in a mouse model of mastitis. *Appl Microbiol Biotechnol, 99*(20), 8475-8486. doi:10.1007/s00253-015-6579-0

Schmelcher, M., Shabarova, T., Eugster, M. R., Eichenseher, F., Tchang, V. S., Banz, M., & Loessner, M. J. (2010). Rapid multiplex detection and differentiation of Listeria cells by use of fluorescent phage endolysin cell wall binding domains. *Appl Environ Microbiol, 76*(17), 5745-5756. doi:10.1128/AEM.00801-10

Schmelcher, M., Tchang, V. S., & Loessner, M. J. (2011). Domain shuffling and module engineering of Listeria phage endolysins for enhanced lytic activity and binding affinity. *Microb Biotechnol, 4*(5), 651-662. doi:10.1111/j.1751-7915.2011.00263.x

Schubert, A., Zakikhany, K., Schreiner, M., Frank, R., Spellerberg, B., Eikmanns, B. J., & Reinscheid, D. J. (2002). A fibrinogen receptor from group B Streptococcus interacts with fibrinogen by repetitive units with novel ligand binding sites. *Mol Microbiol, 46*(2), 557-569.

Schuch, R., Lee, H. M., Schneider, B. C., Sauve, K. L., Law, C., Khan, B. K., Rotolo, J. A., Horiuchi, Y., Couto, D. E., Raz, A., Fischetti, V. A., Huang, D. B., Nowinski, R. C., & Wittekind, M. (2014). Combination therapy with lysin CF-301 and antibiotic is superior to antibiotic alone for treating methicillin-resistant *Staphylococcus aureus*-induced murine bacteremia. *J Infect Dis, 209*(9), 1469-1478. doi:10.1093/infdis/jit637

Schuch, R., Nelson, D., & Fischetti, V. A. (2002). A bacteriolytic agent that detects and kills *Bacillus anthracis*. *Nature, 418*(6900), 884-889. doi:10.1038/nature01026

Schuchat, A. (2001). Group B streptococcal disease: from trials and tribulations to triumph and trepidation. *Clin Infect Dis, 33*(6), 751-756. doi:10.1086/322697

Schymkowitz, J., Borg, J., Stricher, F., Nys, R., Rousseau, F., Serrano, L. (2005). The FoldX web server: an online force field. *Nucleic Acids Res, 33*(Web Server issue), W382-388. doi:10.1093/nar/gki387

Shah, N. B., & Duncan, T. M. (2014). Bio-layer interferometry for measuring kinetics of protein-protein interactions and allosteric ligand effects. *J Vis Exp*(84), e51383. doi:10.3791/51383

Sheehan, M. M., Garcia, J. L., Lopez, R., & Garcia, P. (1997). The lytic enzyme of the pneumococcal phage Dp-1: a chimeric lysin of intergeneric origin. *Mol Microbiol, 25*(4), 717-725.

Shen, J., Wang, F., Li, F., Housley, R., Carolan, H., Yasuda, I., Burrows, E., Binet, R., Sampath, R., Zhang, J., Allard, M. W., & Meng, J. (2013). Rapid identification and differentiation of non-O157 Shiga toxin-producing *Escherichia coli* using polymerase chain reaction coupled to electrospray ionization mass spectrometry. *Foodborne Pathog Dis, 10*(8), 737-743. doi:10.1089/fpd.2012.1469

Shen, Y., Barros, M., Vennemann, T., Gallagher, D. T., Yin, Y., Linden, S. B., Heselpoth, R. D., Spencer, D. J., Donovan, D. M., Moult, J., Fischetti, V. A., Heinrich, F., Losche, M., & Nelson, D. C. (2016). A bacteriophage endolysin that eliminates intracellular streptococci. *Elife, 5*. doi:10.7554/eLife.13152

Shen, Y., Koller, T., Kreikemeyer, B., & Nelson, D. C. (2013). Rapid degradation of *Streptococcus pyogenes* biofilms by PlyC, a bacteriophage-encoded endolysin. *J Antimicrob Chemother, 68*(8), 1818-1824. doi:10.1093/jac/dkt104

Shulman, S. T., & Tanz, R. R. (2010). Group A streptococcal pharyngitis and immune-mediated complications: from diagnosis to management. *Expert Rev Anti Infect Ther, 8*(2), 137-150. doi:10.1586/eri.09.134

Son, J. S., Lee, S. J., Jun, S. Y., Yoon, S. J., Kang, S. H., Paik, H. R., Kang, J. O., & Choi, Y. J. (2010). Antibacterial and biofilm removal activity of a podoviridae *Staphylococcus aureus* bacteriophage SAP-2 and a derived recombinant cell-wall-degrading enzyme. *Appl Microbiol Biotechnol, 86*(5), 1439-1449. doi:10.1007/s00253-009-2386-9

Spellerberg, B., Rozdzinski, E., Martin, S., Weber-Heynemann, J., Schnitzler, N., Lutticken, R., & Podbielski, A. (1999). Lmb, a protein with similarities to the LraI adhesin family, mediates attachment of *Streptococcus agalactiae* to human laminin. *Infect Immun, 67*(2), 871-878.

Sugai, M., Fujiwara, T., Ohta, K., Komatsuzawa, H., Ohara, M., & Suginaka, H. (1997). epr, which encodes glycylglycine endopeptidase resistance, is homologous to femAB and affects serine content of peptidoglycan cross bridges in *Staphylococcus capitis* and *Staphylococcus aureus*. *J Bacteriol, 179*(13), 4311-4318.

Sulakvelidze, A., Alavidze, Z., & Morris, J. G., Jr. (2001). Bacteriophage therapy. *Antimicrob Agents Chemother, 45*(3), 649-659. doi:10.1128/AAC.45.3.649-659.2001

Sullivan, A. M., Lakoma, M. D., Matsuyama, R. K., Rosenblatt, L., Arnold, R. M., & Block, S. D. (2007). Diagnosing and discussing imminent death in the hospital: a secondary analysis of physician interviews. *J Palliat Med, 10*(4), 882-893. doi:10.1089/jpm.2007.0189

Summers, W. C. (2011). In the beginning. *Bacteriophage, 1*(1), 50-51. doi:10.4161/bact.1.1.14070

Swift, S. M., Seal, B. S., Garrish, J. K., Oakley, B. B., Hiett, K., Yeh, H. Y., Woolsey, R., Schegg, K. M., Line, J. E., & Donovan, D. M. (2015). A thermophilic phage endolysin fusion to a *Clostridium perfringens*-specific cell wall binding domain creates an anti-clostridium antimicrobial with improved thermostability. *Viruses, 7*(6), 3019-3034. doi:10.3390/v7062758

Tenover, F. C. (2006). Mechanisms of antimicrobial resistance in bacteria. *Am J Infect Control, 34*(5 Suppl 1), S3-10; discussion S64-73. doi:10.1016/j.ajic.2006.05.219

Tolba, M., Minikh, O., Brovko, L. Y., Evoy, S., & Griffiths, M. W. (2010). Oriented immobilization of bacteriophages for biosensor applications. *Appl Environ Microbiol, 76*(2), 528-535. doi:10.1128/AEM.02294-09

Tuomanen, E., Liu, H., Hengstler, B., Zak, O., & Tomasz, A. (1985). The induction of meningeal inflammation by components of the pneumococcal cell wall. *J Infect Dis, 151*(5), 859-868.

Vargiu, A. V., & Nikaido, H. (2012). Multidrug binding properties of the AcrB efflux pump characterized by molecular dynamics simulations. *Proc Natl Acad Sci U S A, 109*(50), 20637-20642. doi:10.1073/pnas.1218348109

Vazquez, R., Domenech, M., Iglesias-Bexiga, M., Menendez, M., & Garcia, P. (2017). Csl2, a novel chimeric bacteriophage lysin to fight infections caused by Streptococcus suis, an emerging zoonotic pathogen. *Sci Rep, 7*(1), 16506. doi:10.1038/s41598-017-16736-0

Veiga-Crespo, P., Ageitos, J. M., Poza, M., & Villa, T. G. (2007). Enzybiotics: a look to the future, recalling the past. *J Pharm Sci, 96*(8), 1917-1924. doi:10.1002/jps.20853

Ventola, C. L. (2015). The antibiotic resistance crisis: part 1: causes and threats. *P T, 40*(4), 277-283.

Verani, J. R., & Schrag, S. J. (2010). Group B streptococcal disease in infants: progress in prevention and continued challenges. *Clin Perinatol, 37*(2), 375-392. doi:10.1016/j.clp.2010.02.002

Veronese, F. M., & Mero, A. (2008). The impact of PEGylation on biological therapies. *BioDrugs, 22*(5), 315-329. doi:10.2165/00063030-200822050-00004

Visweswaran, G. R., Dijkstra, B. W., & Kok, J. (2011). A minimum of three motifs is essential for optimal binding of pseudomurein cell wall-binding domain of *Methanothermobacter thermautotrophicus*. *PLoS One, 6*(6), e21582. doi:10.1371/journal.pone.0021582

Walcher, G., Stessl, B., Wagner, M., Eichenseher, F., Loessner, M. J., & Hein, I. (2010). Evaluation of paramagnetic beads coated with recombinant Listeria phage endolysin-derived cell-wall-binding domain proteins for separation of *Listeria monocytogenes* from raw milk in combination with culture-based and real-time polymerase chain reaction-based quantification. *Foodborne Pathog Dis, 7*(9), 1019-1024. doi:10.1089/fpd.2009.0475

Walencka, E., Sadowska, B., Rozalska, S., Hryniewicz, W., & Rozalska, B. (2005). Lysostaphin as a potential therapeutic agent for staphylococcal biofilm eradication. *Pol J Microbiol, 54*(3), 191-200.

Walker, M. J., Barnett, T. C., McArthur, J. D., Cole, J. N., Gillen, C. M., Henningham, A., Sriprakash, K. S., Sanderson-Smith, M. L., & Nizet, V. (2014). Disease manifestations and pathogenic mechanisms of Group A Streptococcus. *Clin Microbiol Rev, 27*(2), 264-301. doi:10.1128/CMR.00101-13

Walmagh, M., Briers, Y., dos Santos, S. B., Azeredo, J., & Lavigne, R. (2012). Characterization of modular bacteriophage endolysins from Myoviridae phages OBP, 201phi2-1 and PVP-SE1. *PLoS One, 7*(5), e36991. doi:10.1371/journal.pone.0036991

Walsh, S., Shah, A., & Mond, J. (2003). Improved pharmacokinetics and reduced antibody reactivity of lysostaphin conjugated to polyethylene glycol. *Antimicrob Agents Chemother, 47*(2), 554-558.

Wheeler, J., Holland, J., Terry, J. M., & Blainey, J. D. (1980). Production of group C streptococcus phage-associated lysin and the preparation of *Streptococcus*

pyogenes protoplast membranes. *J Gen Microbiol, 120*(1), 27-33. doi:10.1099/00221287-120-1-27

Wiegand, I., Hilpert, K., & Hancock, R. E. (2008). Agar and broth dilution methods to determine the minimal inhibitory concentration (MIC) of antimicrobial substances. *Nat Protoc, 3*(2), 163-175. doi:10.1038/nprot.2007.521

Withey, S., Cartmell, E., Avery, L. M., & Stephenson, T. (2005). Bacteriophages--potential for application in wastewater treatment processes. *Sci Total Environ, 339*(1-3), 1-18. doi:10.1016/j.scitotenv.2004.09.021

Wu, J. A., Kusuma, C., Mond, J. J., & Kokai-Kun, J. F. (2003). Lysostaphin disrupts *Staphylococcus aureus* and *Staphylococcus epidermidis* biofilms on artificial surfaces. *Antimicrob Agents Chemother, 47*(11), 3407-3414.

Yahiaoui, R. Y., den Heijer, C., van Bijnen, E. M., Paget, W. J., Pringle, M., Goossens, H., Bruggeman, C. A., Schellevis, F. G., Stobberingh, E. E., & Team, A. S. (2016). Prevalence and antibiotic resistance of commensal *Streptococcus pneumoniae* in nine European countries. *Future Microbiol, 11*, 737-744. doi:10.2217/fmb-2015-0011

Yang, H., Bi, Y., Shang, X., Wang, M., Linden, S. B., Li, Y., Li, Y., Nelson, D. C., & Wei, H. (2016). Antibiofilm activities of a novel chimeolysin against *Streptococcus mutans* under physiological and cariogenic conditions. *Antimicrob Agents Chemother, 60*(12), 7436-7443. doi:10.1128/AAC.01872-16

Yang, H., Linden, S. B., Wang, J., Yu, J., Nelson, D. C., & Wei, H. (2015). A chimeolysin with extended-spectrum streptococcal host range found by an induced lysis-based rapid screening method. *Sci Rep, 5*, 17257. doi:10.1038/srep17257

Young, R. (1992). Bacteriophage lysis: mechanism and regulation. *Microbiol Rev, 56*(3), 430-481.

Yu, J., Zhang, Y., Zhang, Y., Li, H., Yang, H., & Wei, H. (2016). Sensitive and rapid detection of *staphylococcus aureus* in milk via cell binding domain of lysin. *Biosens Bioelectron, 77*, 366-371. doi:10.1016/j.bios.2015.09.058

Zhang, H., Bao, H., Billington, C., Hudson, J. A., & Wang, R. (2012). Isolation and lytic activity of the Listeria bacteriophage endolysin LysZ5 against Listeria monocytogenes in soya milk. *Food Microbiol, 31*(1), 133-136. doi:10.1016/j.fm.2012.01.005